DOE/ID/01717-2

MASTER

DO NOT MICROFILM
COVER

New Mexico Energy Institute
at New Mexico State University

STATE-COUPLED LOW-TEMPERATURE GEOTHERMAL RESOURCE ASSESSMENT PROGRAM FISCAL YEAR 1980

FINAL TECHNICAL REPORT

August 1981

Work Performed under DOE Contract No. AS07-78ID01717

Prepared for the
Department of Energy
Division of Geothermal Energy

DISTRIBUTION OF THIS DOCUMENT IS UNLIMITED

DISCLAIMER

This report was prepared as an account of work sponsored by an agency of the United States Government. Neither the United States Government nor any agency Thereof, nor any of their employees, makes any warranty, express or implied, or assumes any legal liability or responsibility for the accuracy, completeness, or usefulness of any information, apparatus, product, or process disclosed, or represents that its use would not infringe privately owned rights. Reference herein to any specific commercial product, process, or service by trade name, trademark, manufacturer, or otherwise does not necessarily constitute or imply its endorsement, recommendation, or favoring by the United States Government or any agency thereof. The views and opinions of authors expressed herein do not necessarily state or reflect those of the United States Government or any agency thereof.

DISCLAIMER

Portions of this document may be illegible in electronic image products. Images are produced from the best available original document.

DOE/ID/01717-2
Distribution Category UC-66b

DOE/ID/01717--2

DE82 019755

STATE-COUPLED LOW-TEMPERATURE GEOTHERMAL-RESOURCE-ASSESSMENT PROGRAM, FISCAL YEAR 1980,

FINAL TECHNICAL REPORT

Edited by

Larry Icerman, Arlene Starkey, and Nora Trentman
New Mexico Energy Institute
at
New Mexico State University
Las Cruces, New Mexico

DISCLAIMER

This report was prepared as an account of work sponsored by an agency of the United States Government. Neither the United States Government nor any agency thereof, nor any of their employees, makes any warranty, express or implied, or assumes any legal liability or responsibility for the accuracy, completeness, or usefulness of any information, apparatus, product, or process disclosed, or represents that its use would not infringe privately owned rights. Reference herein to any specific commercial product, process, or service by trade name, trademark, manufacturer, or otherwise, does not necessarily constitute or imply its endorsement, recommendation, or favoring by the United States Government or any agency thereof. The views and opinions of authors expressed herein do not necessarily state or reflect those of the United States Government or any agency thereof.

DISTRIBUTION OF THIS DOCUMENT IS UNLIMITED

August, 1981

NOTICE

This report was prepared to document work sponsored by the United States government. Neither the Unites States nor its agent, the United States Energy Research and Development Administration, nor any federal employees, nor any of their contractors, subcontractors or their employees, makes any warranty, express or implied, or assumes any legal liability or responsibility for the accuracy, completeness, or usefulness of any information, apparatus, product or process disclosed, or represents that its use would not infringe privately owned rights.

FOREWORD

This report summarizes the results of low-temperature geothermal energy resource assessment efforts in New Mexico during the period from May 15, 1979, through June 14, 1980, under the sponsorship of the U.S. Department of Energy (Contract DE-AS07-78ID01717). The research program was administered by the New Mexico Energy Institute at New Mexico State University and the research was conducted by university faculty members at New Mexico State University, the University of New Mexico, and the New Mexico Institute of Mining and Technology.

The report is divided into seven chapters, which correspond to the tasks delineated in the above contract. This work extends the knowledge of low-temperature geothermal reservoirs in New Mexico with the potential for direct heating applications. The research effort focused on compiling basic geothermal data throughout selected areas in New Mexico in a format suitable for direct transfer to the U.S. Geological Survey and the National Oceanic and Atmospheric Administration for inclusion in the GEOTHERM data file and for preparation of New Mexico low-temperature geothermal resources maps. Funding from the United States Geological Survey, the National Science Foundation, and the State of New Mexico Energy and Minerals Department supported work from which some data compiled in this research effort were taken.

TABLE OF CONTENTS

LIST OF FIGURES

LIST OF TABLES

Chapter 1

Magnetic, Gravity, Seismic-Refraction, and Seismic-Reflection Profiles across the Las Alturas Geothermal Anomaly, New Mexico*

Introduction

The Las Alturas Geothermal Anomaly lies a few kilometers southeast of the city of Las Cruces and immediately west of Tortugas Mountain in central Dona Ana County, New Mexico (see Figure 1-1). It is situated centrally in the southern Rio Grande Rift system at the eastern margin of the Basin and Range Province.

As described by Seager (1975), three major stages are recognized in the Cenozoic tectonic evolution of the area:

1. Laramide Uplift: The deeply eroded structurally-highest folds of this uplift approximately underlie the present course of the Rio Grande.

2. Eocene-Oligocene andesite and rhyolite vulcanism: These silicic volcanic sequences overlie the eroded Laramide uplifts and basins. Immediately east of the anomaly area is Tortugas Mountain, an uplifted block of Paleozoic limestone which is thought to be a remnant part of the rim of the Organ Caldera (Seager and Brown 1978). The caldera is described as a "trap-door" type; 16 to 19 km in diameter and hinged along its northern margin extending east to the Organ Mountains. Two sheets of ash-flow tuff (up to 600-m thick), the Cueva tuff and the Cox Ranch tuff, (Dunham 1935; Seager and Brown 1978), have spread beyond the caldera boundaries and are considered to be representative of the eruption prior to the major cauldron subsidence.

*The principal authors of Chapter 1 are Timothy R. Dicey, Graduate Assistant, Department of Physics, New Mexico State University and Dr. Paul Morgan, Staff Scientist, Lunar and Planetary Institute, Houston, Texas.

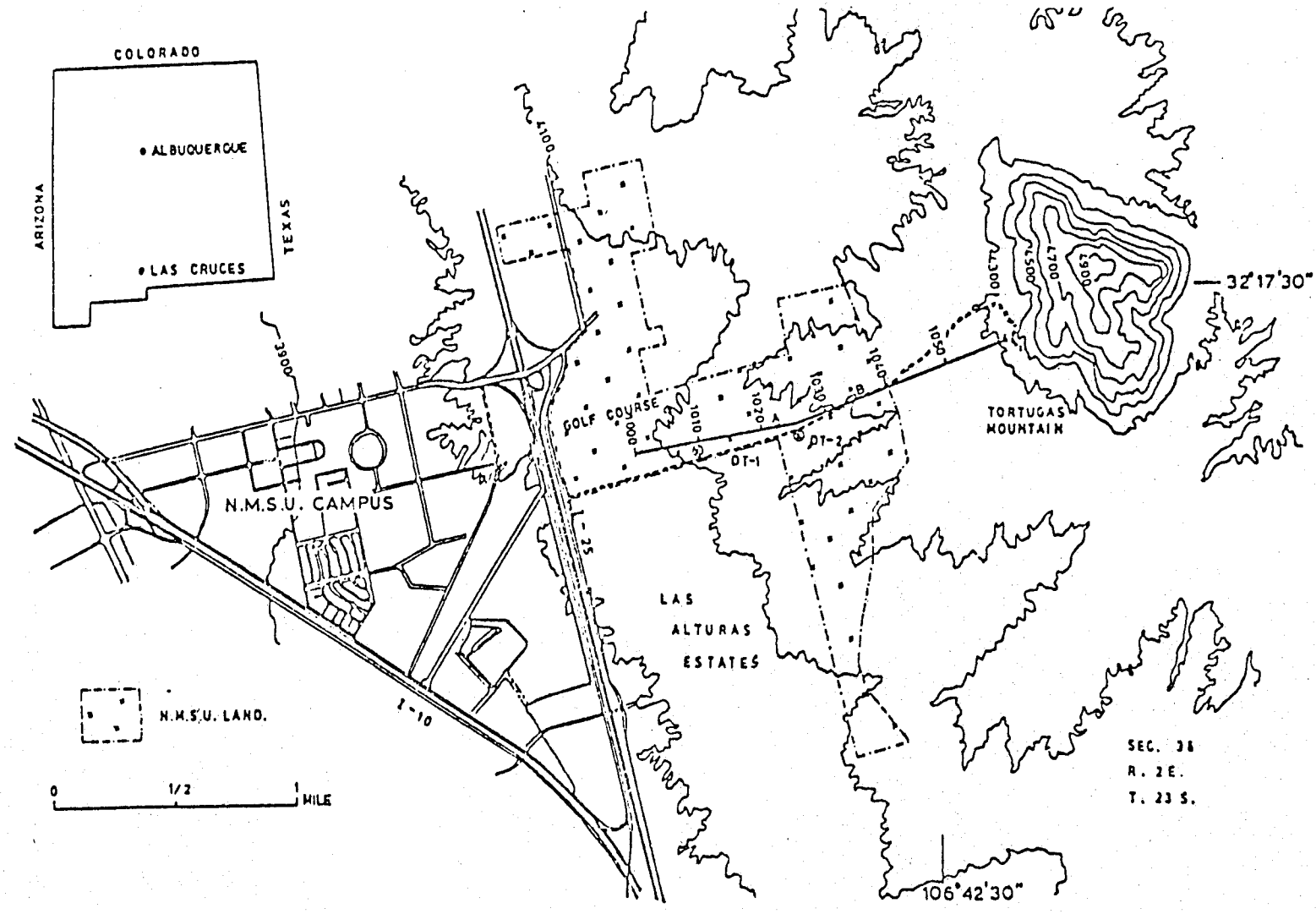

Figure 1-1. Index map of Las Cruces, New Mexico, including the NMSU campus and the Las Alturas area. Also shown is the profile along which the magnetic, gravity, seismic-refraction, and seismic-reflection profiles were recorded.

One of the sheets of the Cueva tuff has been K-Ar dated at 32 m.y. (million years). Another 2150 m (7000 ft) of ash-flow tuff later erupted (which was the cause of the cauldron subsidence) and was contained by the walls of the caldera. Because no major unconformities have been recognized throughout the sequence, the date of 32 m.y. (mid-Oligocene) is thought to be representative of the whole structure. Furthermore, the Organ Batholith which appears to have intruded the caldera on its eastern margin is also dated at 32 m.y. and has been interpreted to be probably the magma chamber from which the caldera volcanics erupted. It has been uplifted by block faulting on the rim of the caldera during the Rio Grande Rift movements.

3. Late Tertiary block faulting: 26 m.y. marked the transition to active rifting shown by a halting of the silicic vulcanism. After a period of quiescence, alkali olivine basalts appeared around 13 m.y. Ramberg and Smithson (1975) suggest that bidirectional-fault patterns may be inherited from pre-existing structural grains. This rifting has created local basins separated by ranges which have now been partly buried in their own debris. The Organ Mountains are representative of the late Tertiary fault block that extends north-south for over 160 km. Uplift has been principally along the boundary fault on the eastern side of the block. Gravity and topographical data indicate a total throw of more than 3000 m. Piedmont scarps indicate movement has continued into the late Quaternary.

The area of the geothermal anomaly is characterized by valley-fill deposits which increase in depth away from Tortugas Mountain (King and Hawley 1975). There is no surface manifestation of the anomaly; it was discovered by accident in the 1960's when water wells encountered temperatures of 45°C around 100 m.

The Las Cruces area is a zone of unusually high heat flow as compared to adjacent Basin and Range and High Plains areas (Cook et al. 1979; Reiter et al. 1979). A prominent north-to-northwest trend of high geochemical temperatures passes through the Las Alturas area (Swanberg 1979) and follows what is thought to be a fault as indicated by gravity surveys in the region. Both the silica and the Na-K-Ca geothermometers indicate temperatures around 150°C (Swanberg 1975).

Previous surface exploration work includes an electrical resistivity (dipole-dipole) survey and subsequent two-dimensional modeling (Jiracek and Gerety 1978). This work not only shows a low-resistivity layer interpreted to be the geothermal reservoir but indicates the presence of a high-resistivity barrier to the east, possibly a fault striking north to northeast. It is considered that this fault may be a primary structural control governing the rising hot water.

Six shallow (approximately 30-m) and two deep (approximately 300-m) holes have been drilled across the Las Alturas Anomaly (see Figure 1-1). The maximum water temperature measured in the DT-1 well at a depth of 300 m (975 ft) was 63°C (Morgan et al. 1979).

The gravity, magnetic, seismic-refraction and seismic-reflection profiling which is the subject of this report is an attempt to delineate structure related to the geothermal anomaly.

Field Techniques

The four geophysical exploration techniques were recorded along the same profile to enable direct comparison between the data sets. The profile was an approximately east-west traverse from a kilometer east of Interstate 10 to the

base of Tortugas Mountain, such that it intersected the two deep well sites (DT-1 and DT-2) and also lay approximately perpendicular to the strike of the suspected fault(s). The traverse was chained and pegged at 46-m intervals (150 ft) with pegs numbered from 1000 in the west to 1058 in the east. The boundary between New Mexico State University (NMSU) and Bureau of Land Management (BLM) land cuts across the line at peg 1040 (see Figure 1-1).

Magnetic Survey

The total magnetic field at each peg on the line was measured with a proton precession magnetometer using a standard "looping" technique to correct for drift in the data. Field data were recorded to within ± 1 gamma.

Gravity Survey

Measurements of the vertical component of gravity were recorded at each peg using a La Coste Romberg gravimeter. The base station was the corner of the police station on Picacho Avenue where there is a gravity base reference station. A "looping" technique was used (see Figure 1-2) to ensure accurate drift corrections might be applied to the data. Field data were recorded to an accuracy of ± 0.01 mgal.

Seismic-Refraction Survey

Data were recorded on a six-channel engineering seismograph with an analogue paper recorder. All data were recorded without filters on the input data. It was necessary to vary the gain on each channel so as to offset the differential intensity of arrivals with respect to varying shotpoint-geophone station distance. At each spread location, each geophone was buried 0.3 m (1

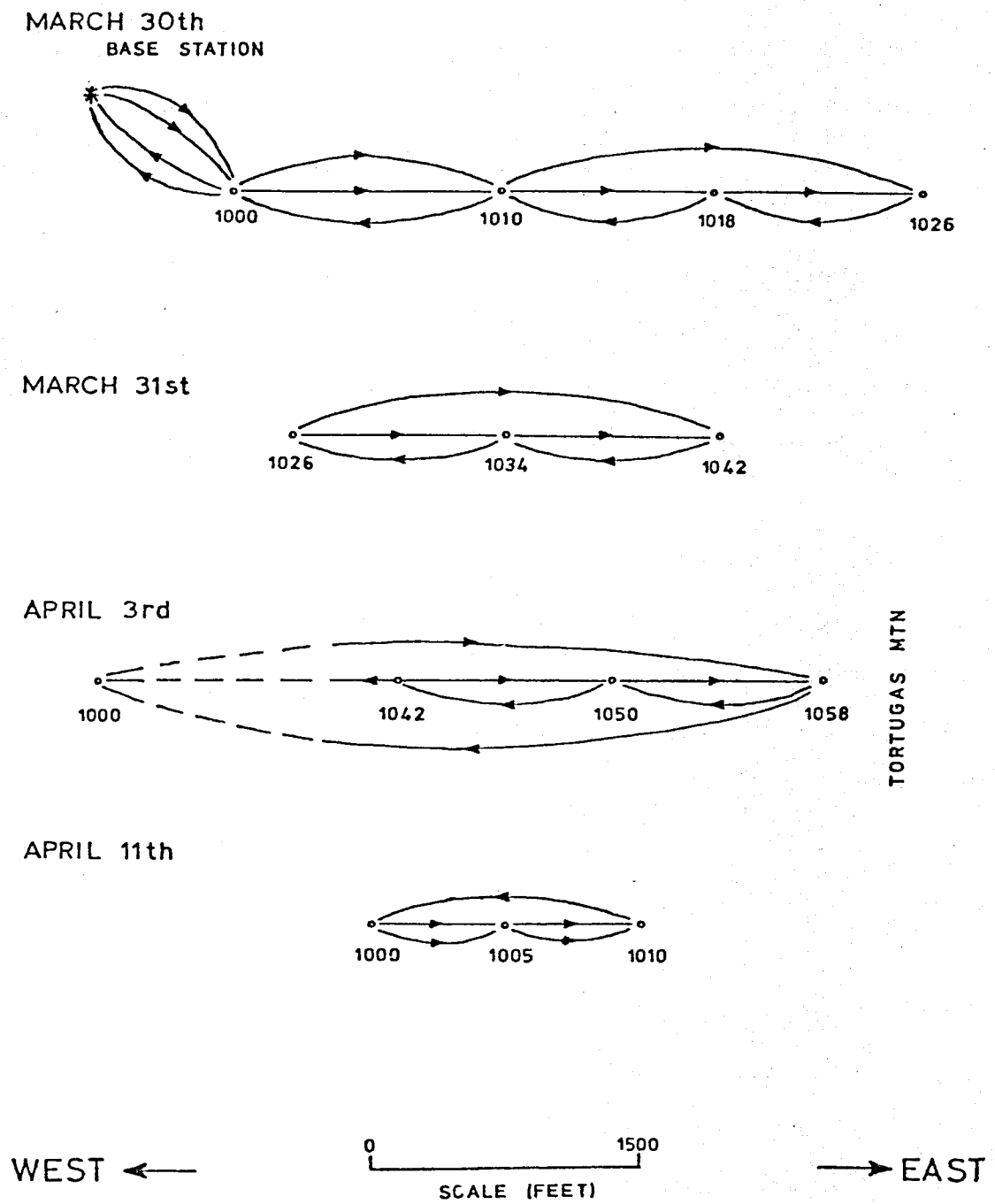

Figure 1-2. Gravity-looping diagram displaying the mode field measurements that were recorded to enable accurate calculations of drift.

ft) beneath the surface to maximize geophone-ground coupling and to reduce ambient (particularly wind) noise. Charges varied from one detonator to a four-hole pattern totaling six sticks of 65-percent Powerdyne dynamite (3 lbs). Charges were tamped in a 1 to 1.33 m (3 to 4 ft) deep hole dug with a post-hole digger. The maximum charge per hole was 1 lb of dynamite, as any greater charge caused cratering. Thus, for large offsets (up to 523 m [1700 ft]), a pattern charge of simultaneously detonated charges in up to four holes was used.

The second mode of recording was designed to record arrivals from as deep a refractor as possible. A geophone spread with 15.4-m spacing (50 ft) was located between pegs 1023 and 1025. Recordings were made from shotpoints with progressively greater offsets east of the spread, 15.4 m (50 ft) to 523 m (1700 ft). A similar set of data was recorded in the reverse sense in that the spread was located at 1033 to 1035 and shotpoints recorded with progressively greater offsets to the west (see Figure 1-3).

Uphole Survey

First arrivals from charges (1 detonator of 0.25 lbs dynamite) detonated at 10-m intervals (32.5 ft) down each deep well (DT-1 and DT-2) were recorded on the engineering seismograph by a linear spread of equally-spaced 15-m geophones (48.75 ft) laid in an easterly direction away from each well site. A complete set of recordings for all 10-m positions (30 ft) was not recorded due to hole collapse.

Seismic-Reflection Survey

Five Sprengnether DR 100 digital cassette magnetic tape recorders and associated amplifiers were used, each at one geophone station. Each

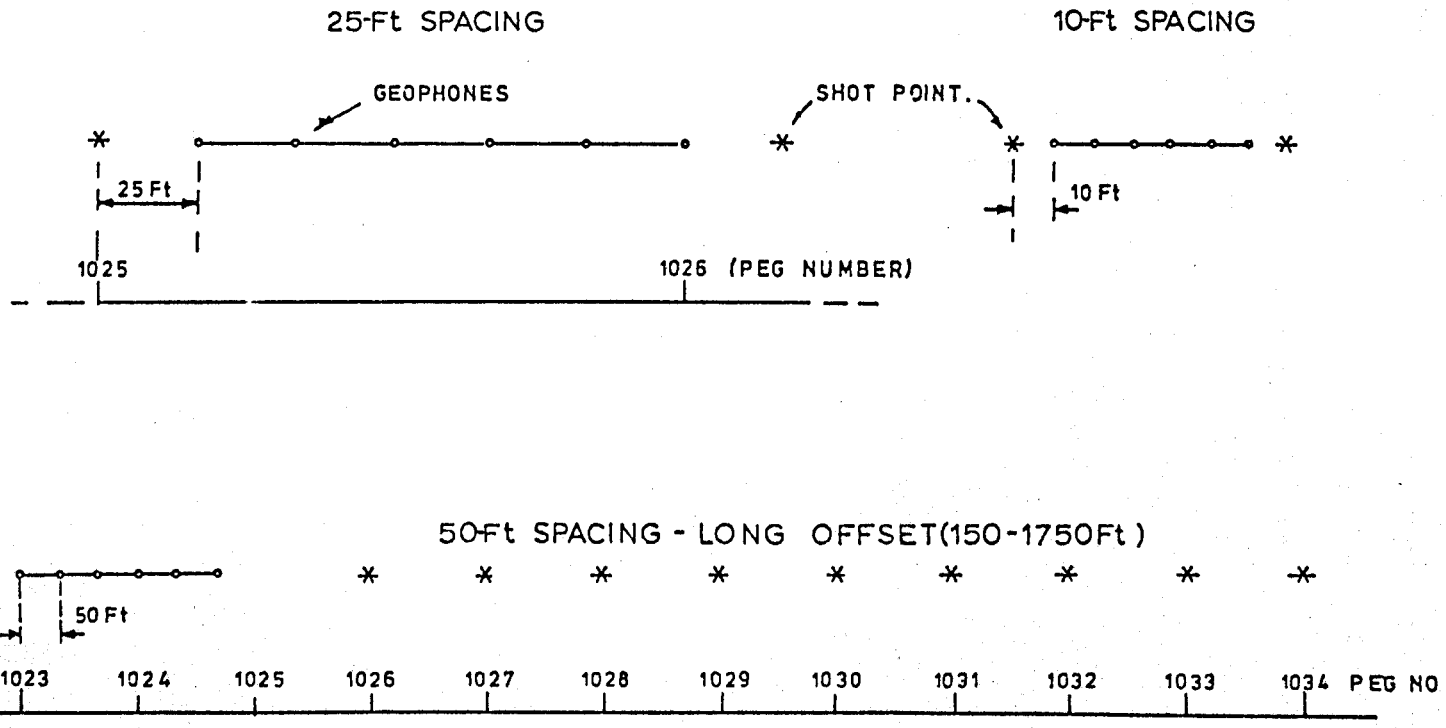

Figure 1-3. Geophone array and shotpoint location diagram for the refraction survey.

instrument recorded both vertical and horizontal motions (perpendicular to the line--north being positive direction). The geophones used were those used for the refraction survey. Recording parameters for the instruments were deduced empirically to optimize "triggering" and make the signal to noise ratio a maximum. The instrument settings were as follows:

Gain ---------- 78 dB.

Hi-cut filter ---------- 30 Hz

Low-cut filter ---------- Out

Signal Duration --------- 5 secs

Ratio ---------- 12 dB. triggering parameter

Short-term average ------ 1 sec } triggering parameters

Long-term average ------- 100 secs }

Sample rate ---------- 2 channels, each at 100 sample/sec

Each instrument has an internal clock which was synchronized before each day's recording, first visually using a WWV radio, and then via a correction computed later by comparison of the clock pulses and those recorded directly from a WWVB radio.

Geophones were buried 0.3 to 0.5 m (1 to 1.5 ft) beneath the surface to maximize the geophone-ground coupling and also to minimize the ambient noise which might otherwise be high enough to trigger the instruments.

Charge sizes were from 0.33 lb to 1 lb in a single well, tamped in a 1.00 to 1.33 m (3 to 4 ft) deep hole dug with a post-hole digger or shovel. An MEQ analogue smoked paper drum recorder (Sprengnether MEQ 800) with a geophone (and attenuating circuitry) was used to record the shot time. The shot recorded was also synchronized using the WWV and WWVB radios. The geophone was placed on the surface over the charge; the delay from the charge to the

geophone at the surface was assumed constant and negligible for the whole survey.

Each geophone station spread (named Z, O, A, B, C, D, E and F) consisted of the five instruments with a separation of 46.2 m (150 ft). Up to eleven shots were fired into the spread from each direction. Recording was carried out between 5:30 a.m. and 7:30 a.m. so that no interference from the gravel pit located to the northeast and any noise from Interstate 10 would be at a minimum.

The only instrument problem encountered was with the WWVB radio which intermittently reduced the amplitude of its output signal to a random noise. Because this problem was not completely detectable in the field, it is suggested that for future studies the WWVB signal be monitored by a portable oscilloscope when being recorded as part of the clock correction procedure.

If any future reflection recording is to be attempted, it would be recommended that a low-cut or small-range band reject (possibly "notch") filter be placed in series with the input before recording to attenuate the low-frequency groundroll and leave unaffected any relatively higher frequency reflections.

Processing and Data Reduction

Magnetic Data

The raw field data were corrected for drift and plotted against distance (peg number). Also plotted was a centered three-point moving average of the data to smooth local, near-surface, short wavelength perturbations (see Figure 1-4).

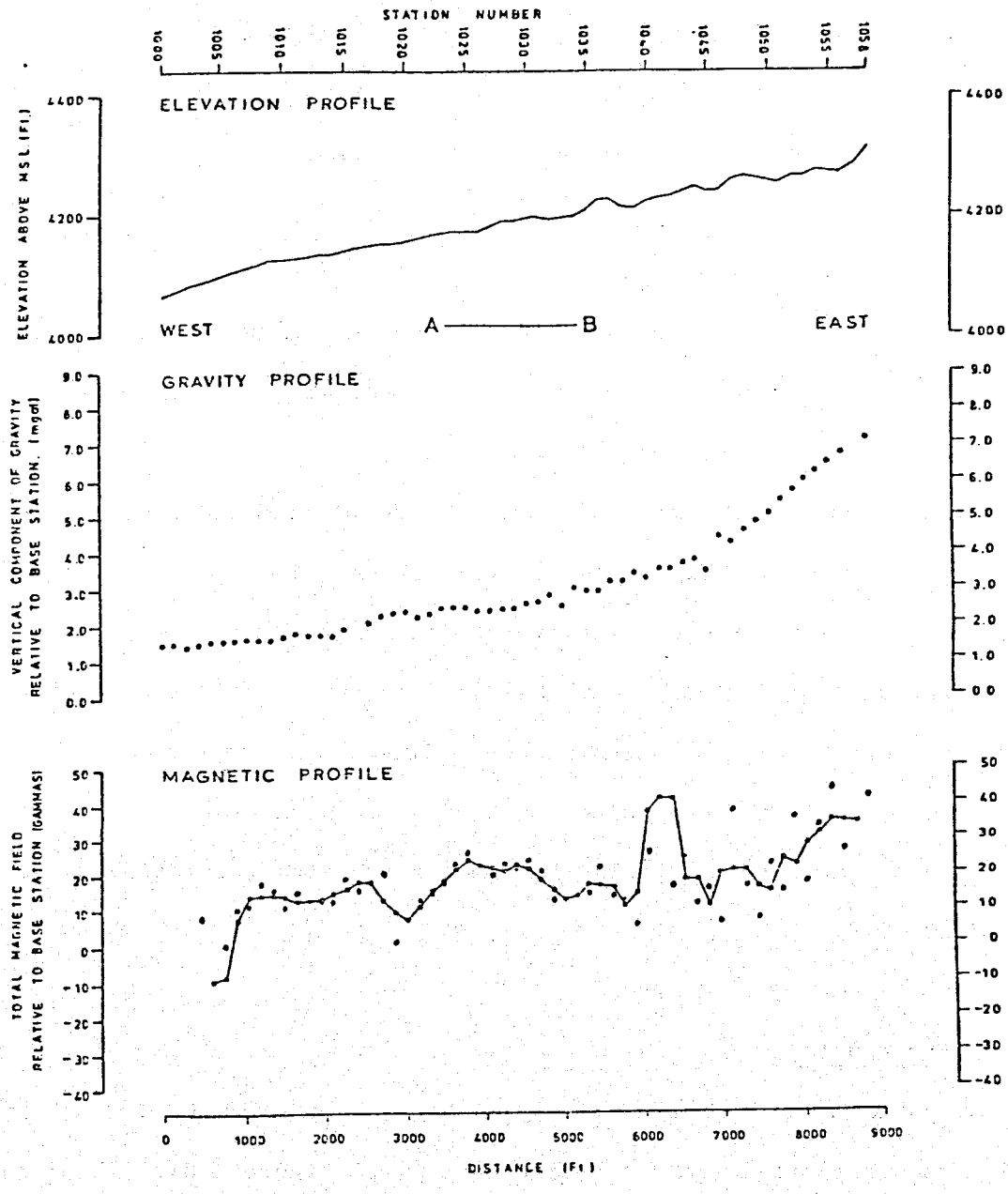

Figure 1-4. Elevation, magnetic, and gravity profiles. A-B denotes area as marked on Figure 1-6 where the long offset seismic-refraction data were recorded.

Gravity Data

The raw field data were corrected for instrument and tidal drift. Free Air and Bouguer corrections (with a density of 2.67 gms-cm^3) were also applied to the data. No terrain, latitude, or regional corrections were applied. The resulting data were plotted against distance (peg number).

For ease of comparison, the gravity, magnetic, and elevation profiles were plotted above each other (see Figure 1-4).

Seismic-Refraction Data

The field data are on ultraviolet sensitive paper, which is very sensitive to overexposure. Each field record was labeled and picked the time of the first arrivals of each channel.

The data from the shorter spreads were plotted on a time-distance graph for each record (see Figure 1-5). Velocities and depths were calculated from these graphs using one- or two-layer weathering computations.

The first-arrival times of the long offset records were also plotted but with the shot- and geophone-station positions interchanged (see Figure 1-6). Velocities and depths were also computed from these plots.

A diagram correlating all the results from the refraction survey is shown in Figure 1-7.

Uphole Data

The first-arrival times for the geophone nearest ($\sim$ 2 m [6 ft]) to the well top was plotted against charge depth (see Figure 1-8). The first-arrival times for all 6 traces were plotted against charge depth in the form of a Meisner diagram (see Figure 1-9). Both plots show data from the west well, DT-2, to a depth of 90 m displayed vertically above data from DT-1 profiling

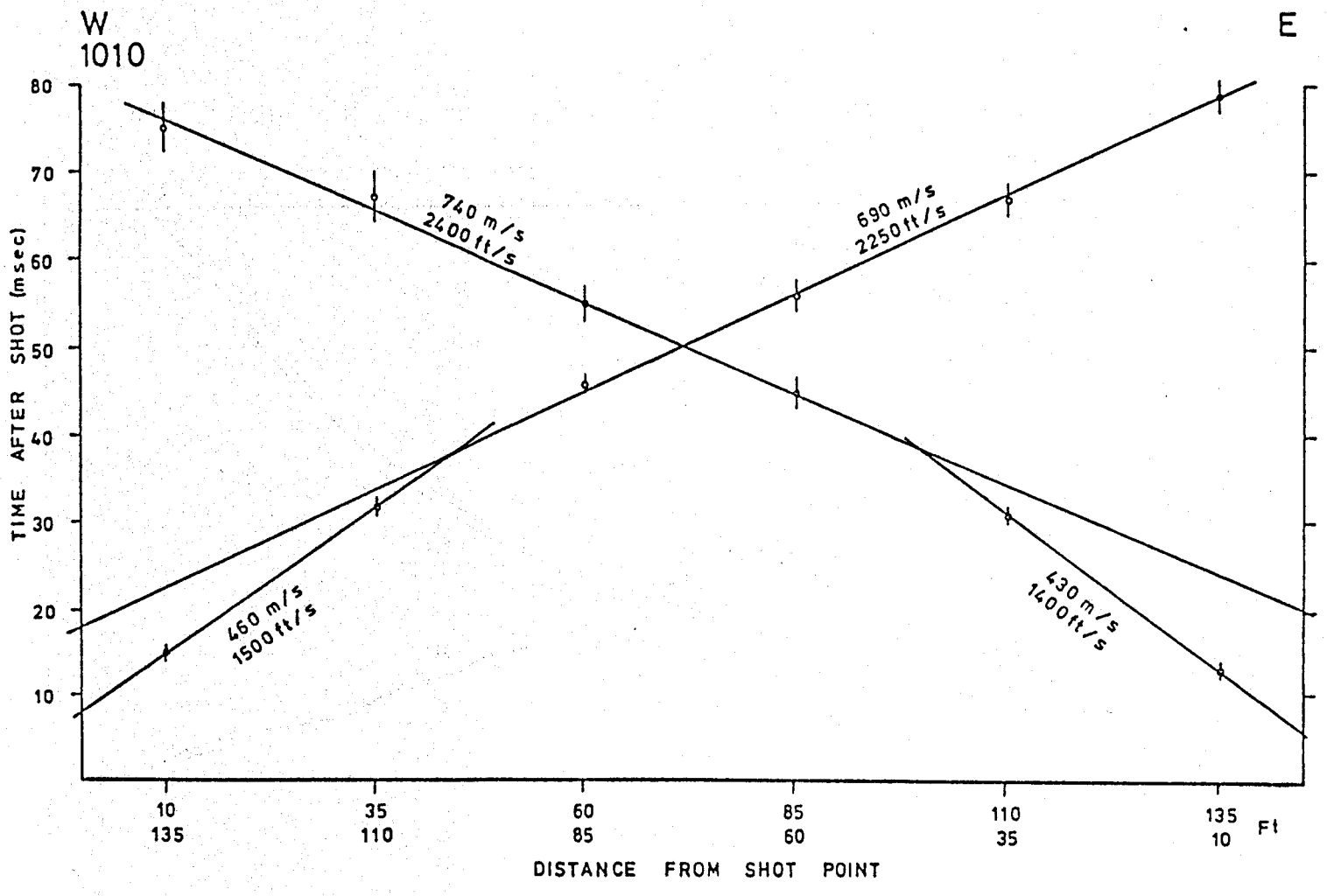

Figure 1-5. Example of time-distance plot as used for delineation of near-surface weathering layers.

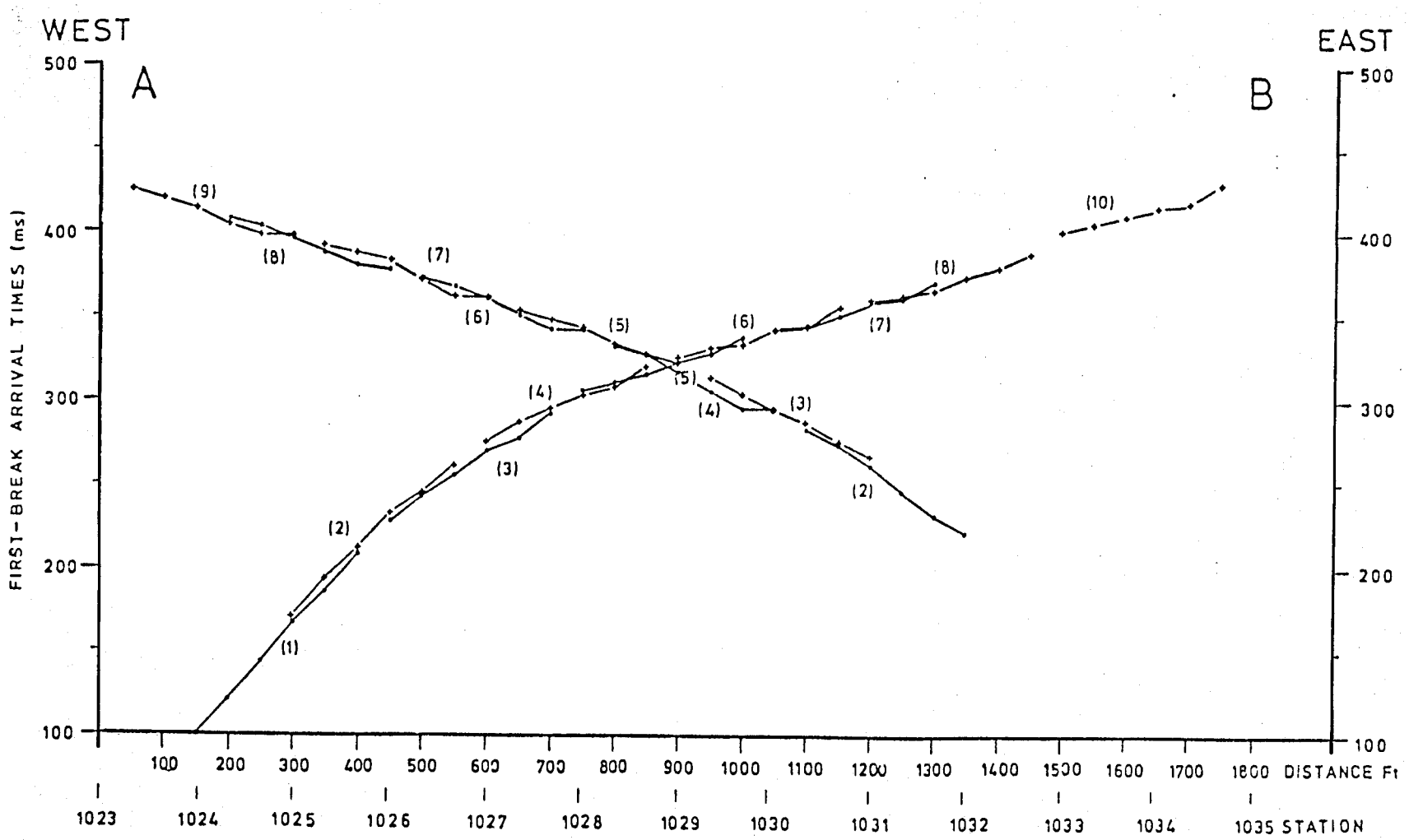

Figure 1-6. Time-distance plot of long offset-refraction survey recording. A-B is indicated on Figure 1-4 for comparison.

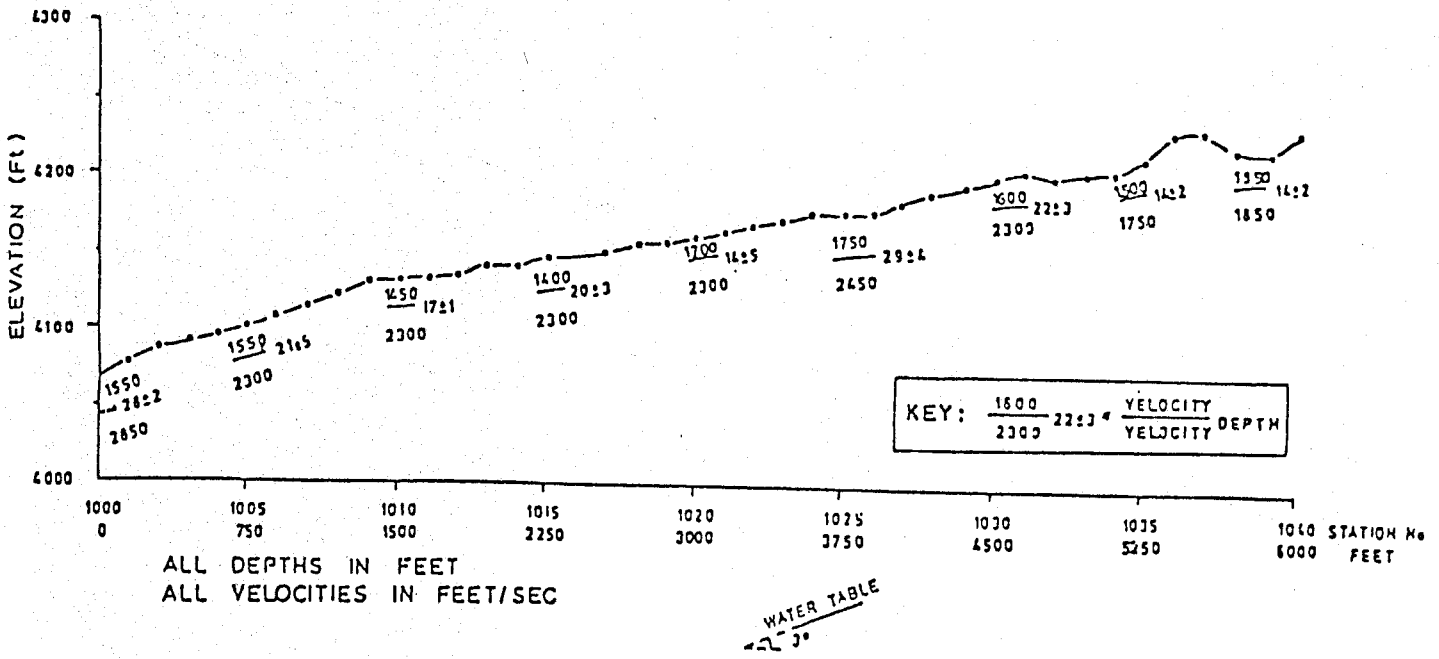

Figure 1-7. Display of results of the seismic-refraction survey.

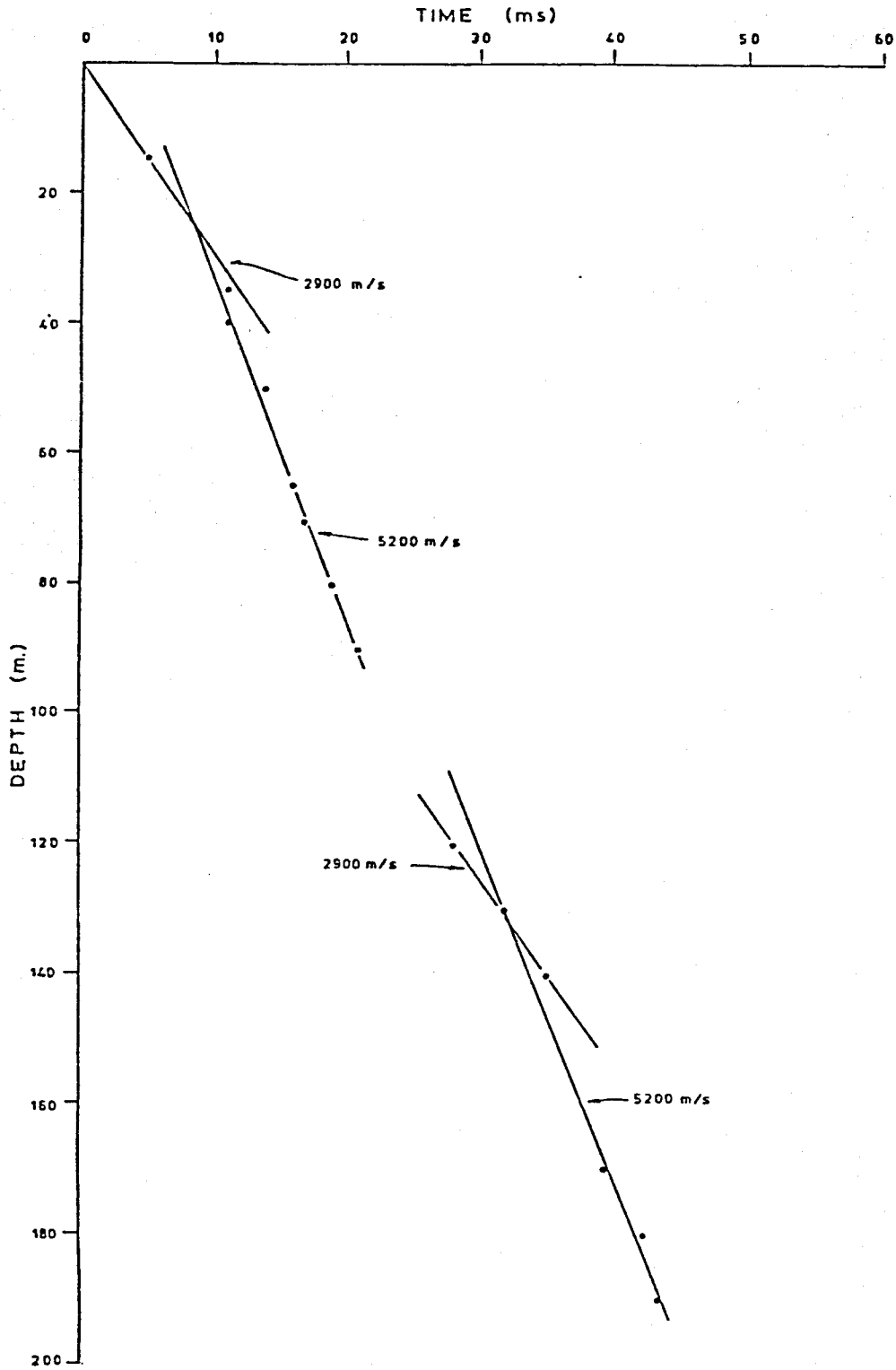

Figure 1-8. Plot of time versus depth of the first arrivals recorded at the geophone station nearest the hole and compiled from uphole-survey data. The velocities shown represent the vertical seismic velocity in the material adjacent to the well.

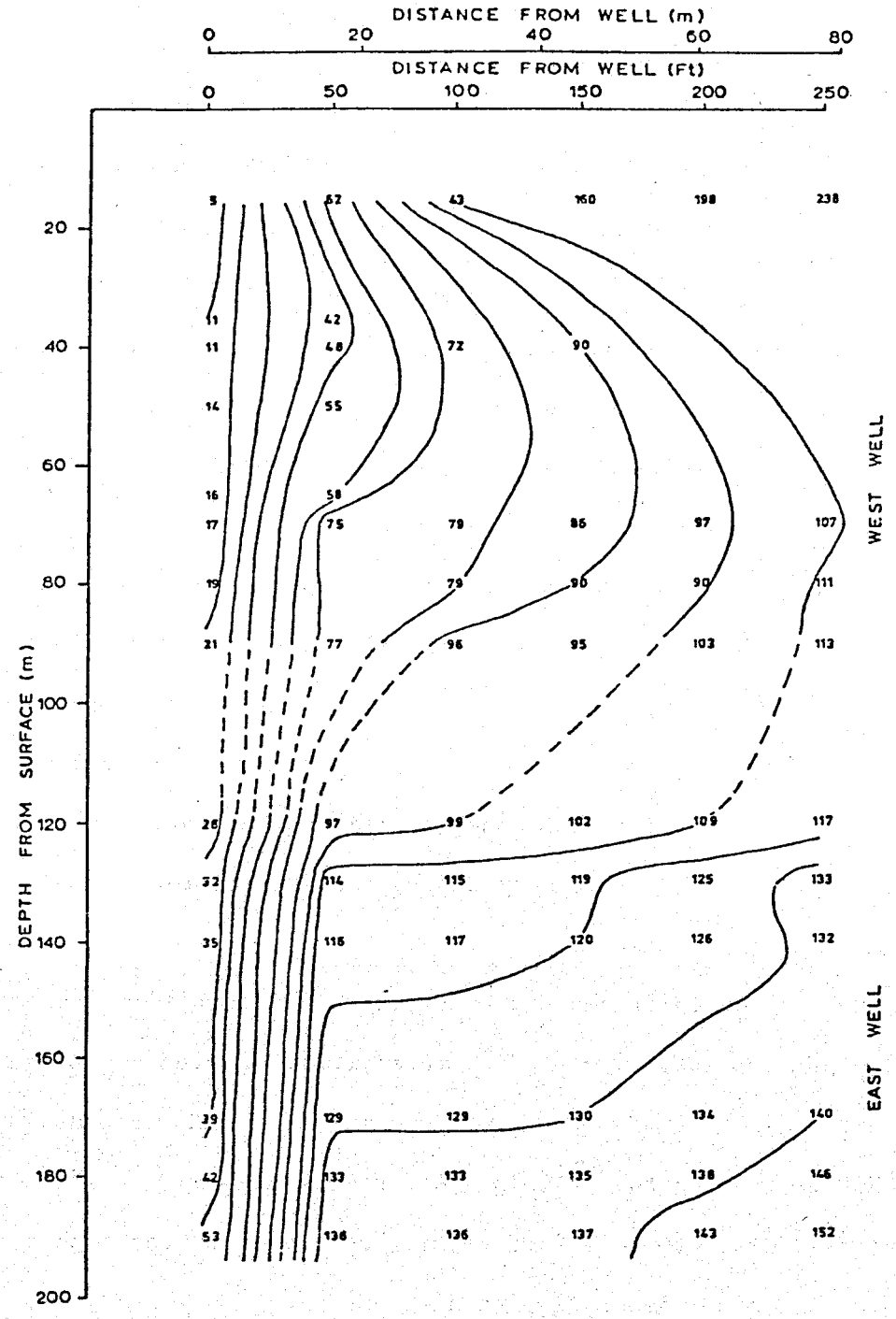

Figure 1-9. Meisner diagram compiled from the uphole data of the two deep wells. Points plotted are in meters (m) and 10-m contours are shown. The bunching contours between the geophone stations next to the well and at a distance of 18 m (50 ft) indicate a high-velocity medium is present (see Figure 1-8).

depths of 120 m to 190 m. The Meisner diagram was contoured with 10-m intervals.

Seismic-Reflection Data

The data from each day's recording were read onto a PDP 11/60 computer and via a suite of data handling programs, the raw data were copied onto disc, edited for unwanted events, and each event cropped to the same time length. The data were then printed on the plotter and finally the output copied onto a tape suitable for use on an Amdahl 470 version 5 computer. The raw field data and the edited data were copied onto separate tapes and filed. The output tape was taken to the Amdahl and the traces plotted sequentially. These plots were grouped by instrument recordings for each day.

A display of the total shooting-recording configuration is shown in Figure 1-10. Figures 1-11 through 1-15 are displays of the shotpoints recorded for each instrument as a function of day recorded and position on the line. With this information, a display of recorded information (trace name) as a function of common-depth point (positioned half-way between shotpoint and geophone station at an arbitrary depth) and shotpoint-geophone station offset was drawn (see Figure 1-16).

There were up to eleven shotpoints recorded from each direction (east and west) by each spread. For each configuration of eleven shots recorded by a particular spread, it is possible to compile eleven records of five traces each. However, using the principle of "reversible ray paths" these data could be grouped together to form five records of eleven traces each. The principal advantages of this mode of display are:

1. There are more traces on each record; thus, reflections present may be picked and their movement computed more accurately with eleven traces than with five.

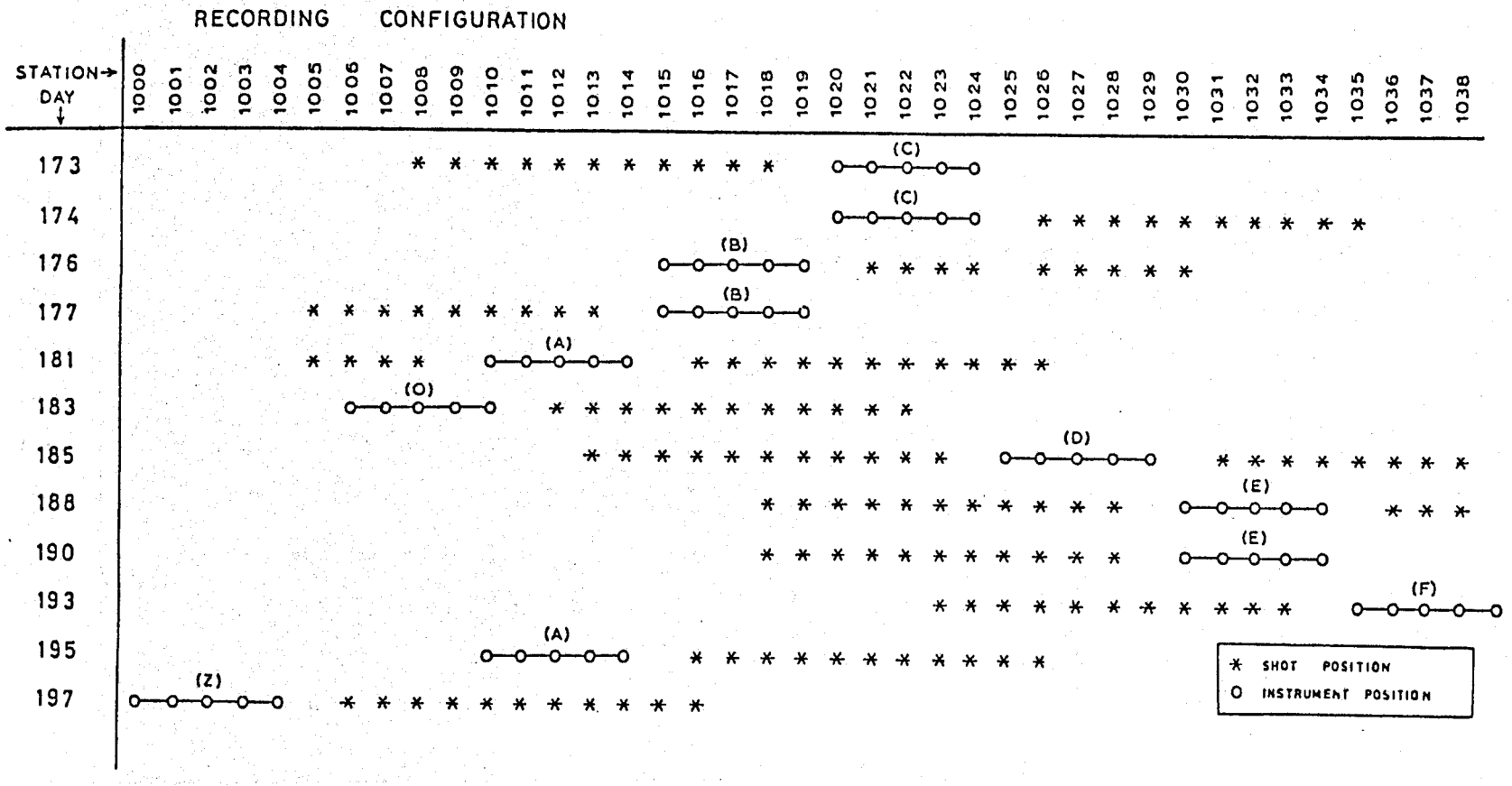

Figure 1-10. Display of shotpoint-geophone station seismic-refraction recording configuration.

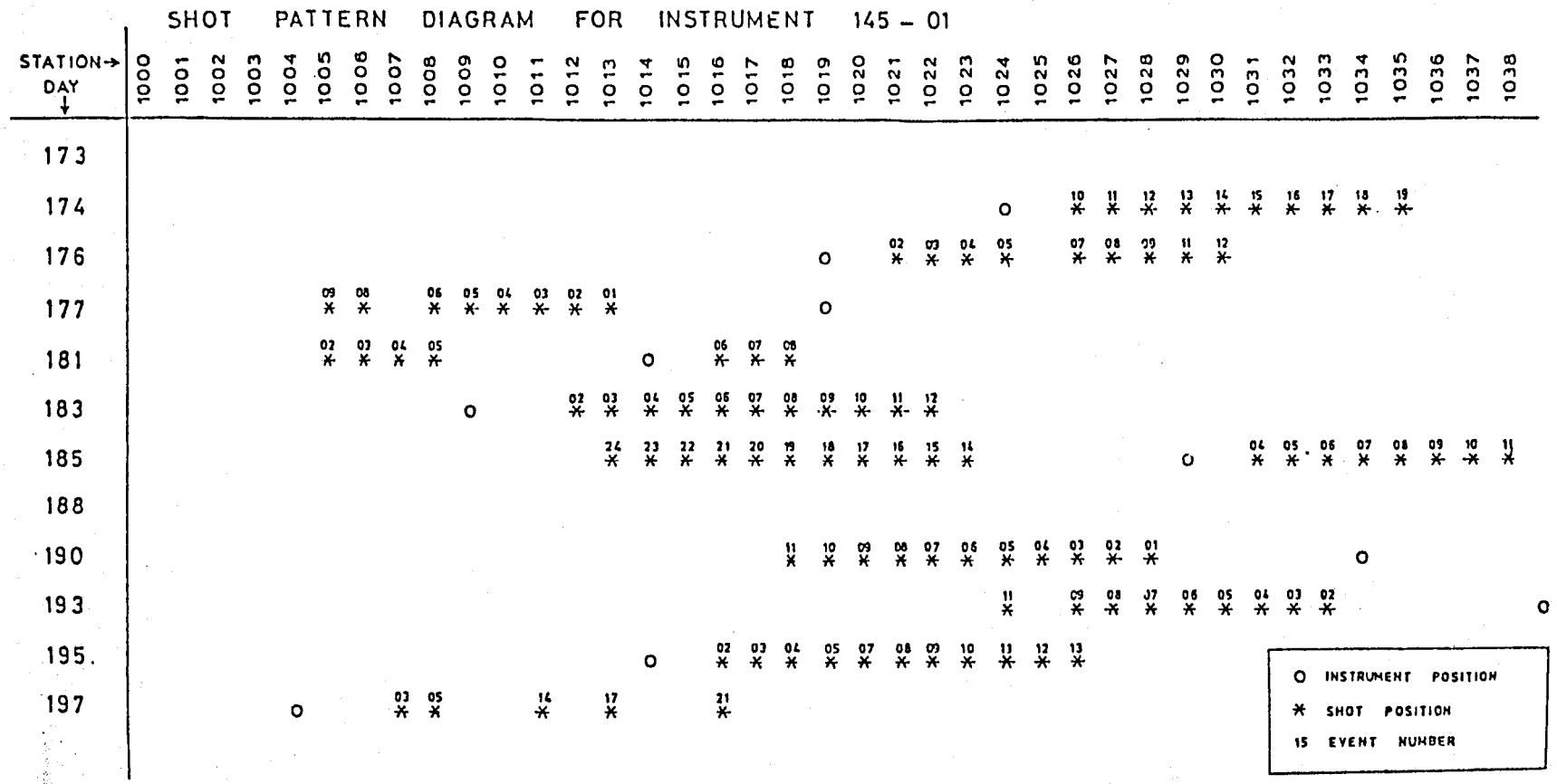

Figure 1-11. Display of shotpoint-geophone station seismic-reflection recording configuration for instrument 145-01.

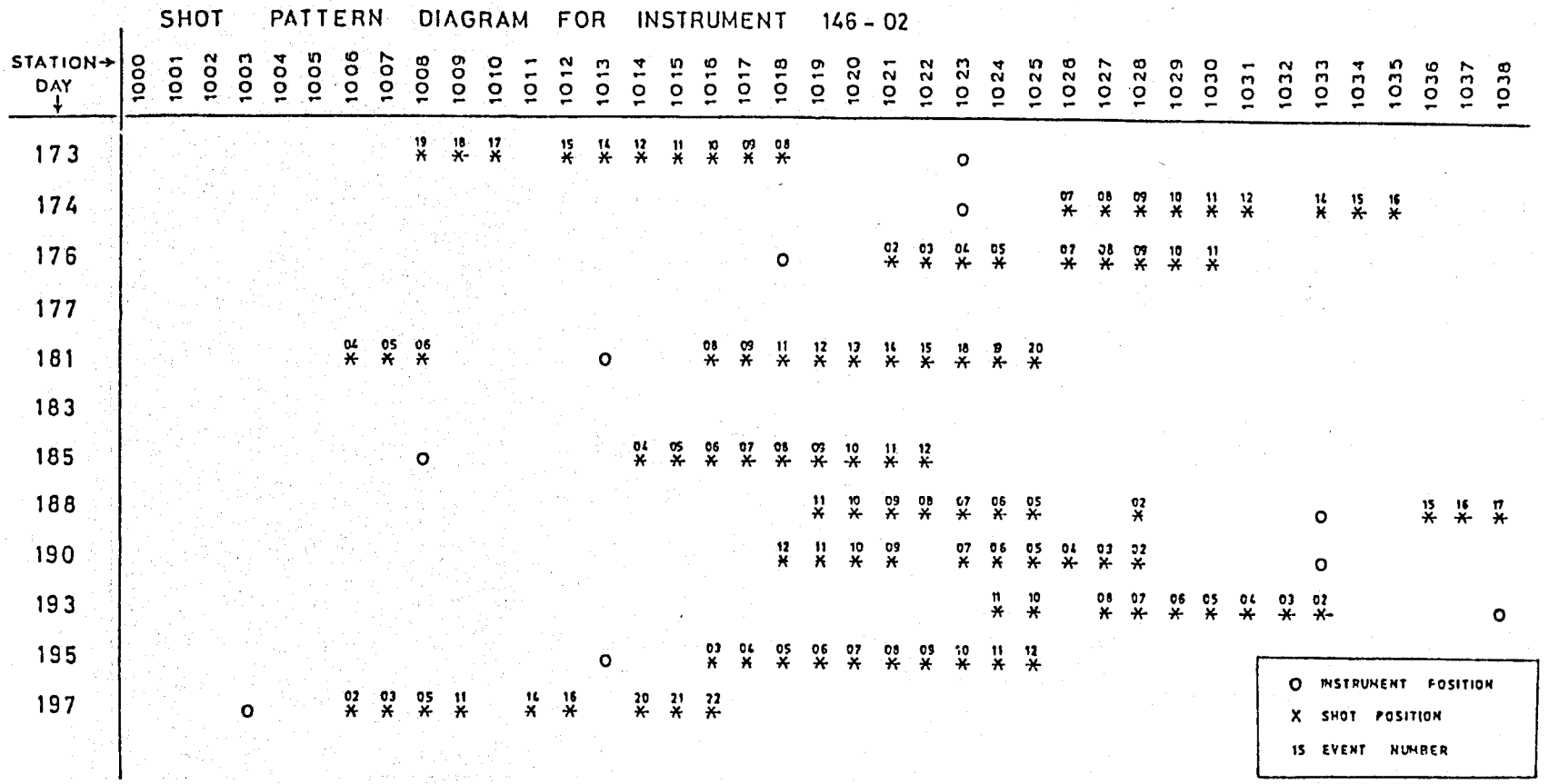

Figure 1-12. Display of shotpoint-geophone station seismic-reflection recording configuration for instrument 146-02.

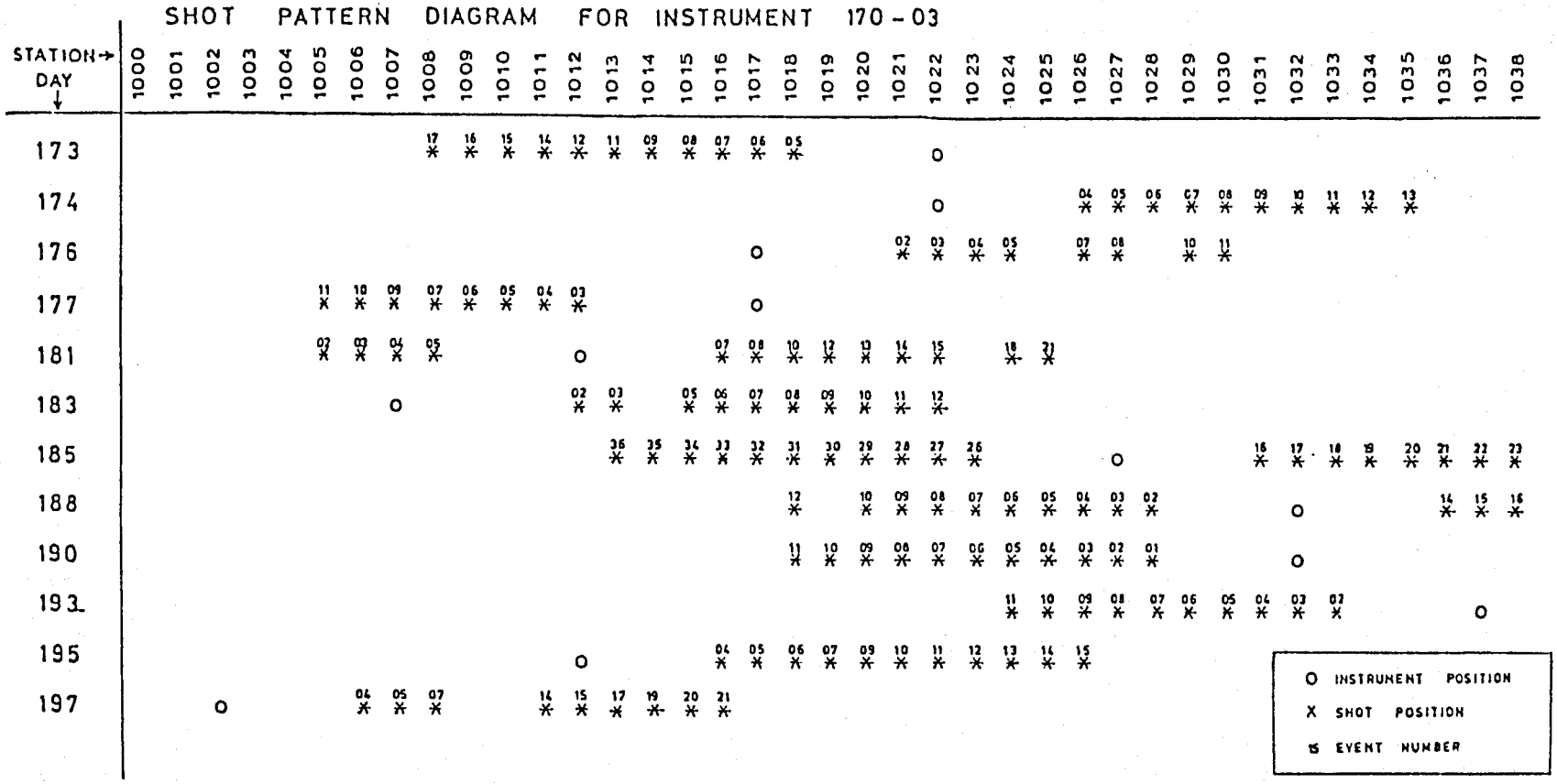

Figure 1-13. Display of shotpoint-geophone station seismic-reflection recording configuration for instrument 170-03.

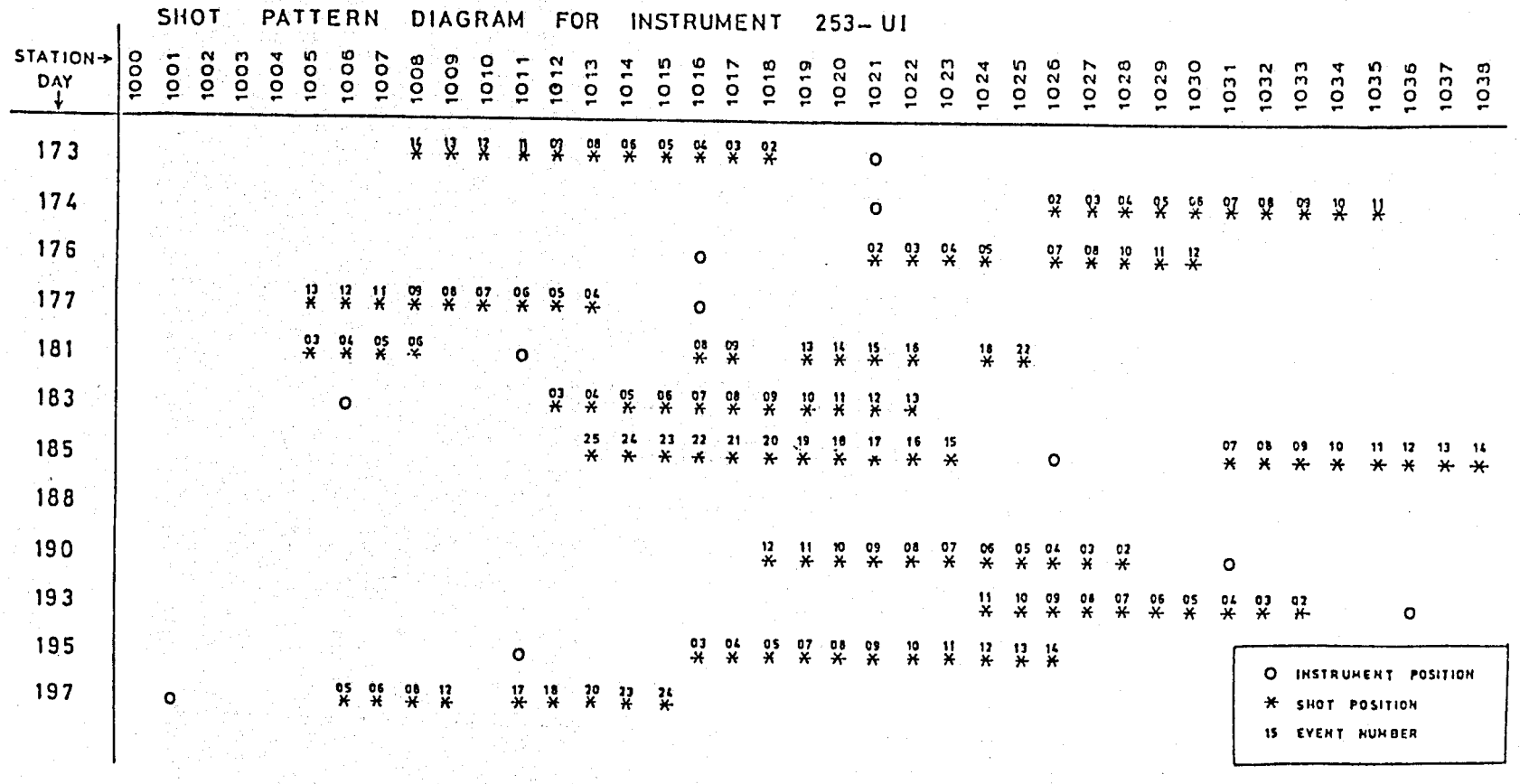

Figure 1-14. Display of shotpoint-geophone station seismic-reflection recording configuration for instrument 253 U1.

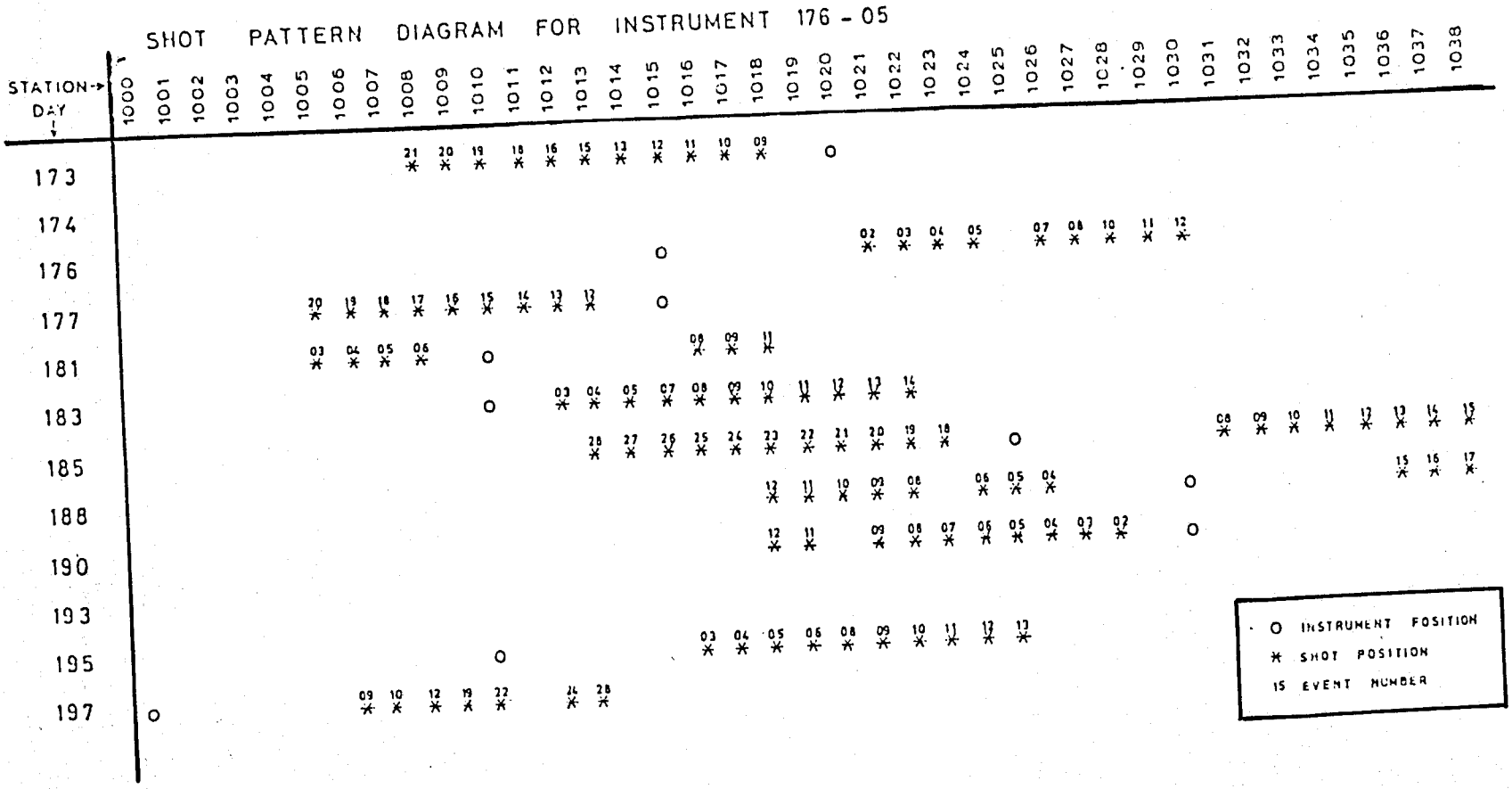

Figure 1-15. Display of shotpoint-geophone station seismic-reflection recording configuration for instrument 176-05.

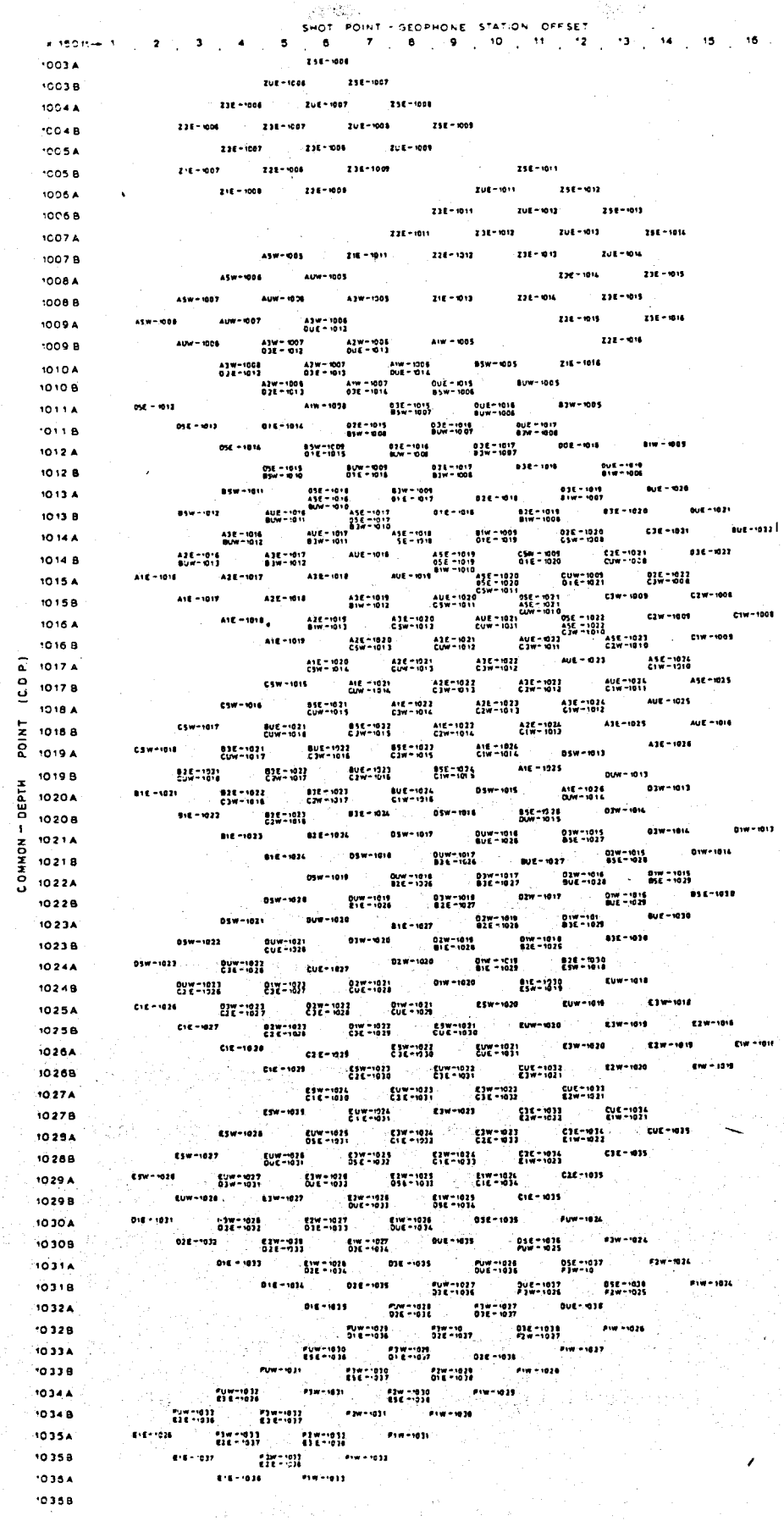

Figure 1-16. Data coverage plot of common-depth point versus shotpoint-geophone station offset.

2. There is a smaller quantity of individual data.

To be able to compile these records, the shot time relative to the individual traces must be known. Because of the problems encountered with the WWVB radio, these could not be computed directly with any certainty on approximately 30 percent of the traces, and not at all on approximately 20 percent of the traces.

From the results of the refraction survey, a table of predicted first-arrival times versus shotpoint instrument offset was computed (see Table 1-1). Because of the velocity contrast between the refracting medium and the material above, the refracted arrivals are of a high enough intensity to be observed on all traces up to the greatest offset. Hence, this method of compiling the eleven trace records was accurately completed. Nine examples from different parts of the line are displayed in Figures 1-17 through 1-25.

Reflections were picked from the records with the aid of a graticule overlay, plotted to show the predicted normal moveout (NMO), and calculated using velocities from the refraction data. Normal moveout is the geophysical effect of increasing arrival times of reflected data due to the lateral increase of the shotpoint-geophone station distance.

Refraction data were used to construct static corrections for each instrument and shot position. However, these corrections only accounted for the gradual increase in elevation for that part of the line recorded on, and so, by using an inclined datum, these corrections would not need to be applied to the data (see Table 1-2).

From Figure 1-16, traces were chosen for specific shotpoint-geophone station offsets and compiled into sections with offsets of: 140 m (450 ft), (see Figure 1-26); 185 m (600 ft), (see Figure 1-27); 275 m (900 ft), (see Figure 1-28); 370 m (1200 ft), (see Figure 1-29); and 555 m (1800 ft), (see Figure 1-30). Groundroll (surface or Rayleigh waves) were the most

Table 1-1. Predicted first-break times derived from the seismic-refraction data.

Shotpoint-Instrument Offset (m)	(ft)	First-Break Time (secs)
92.3	(300)	0.125
138.5	(450)	0.188
184.6	(600)	0.250
230.8	(750)	0.287
276.9	(900)	0.302
323.1	(1050)	0.317
269.2	(1200)	0.333
415.4	(1350)	0.348
461.5	(1500)	0.363
507.7	(1650)	0.378
583.8	(1800)	0.394
600.0	(1950)	0.409
646.2	(2100)	0.424
692.3	(2250)	0.440
738.5	(2400)	0.455

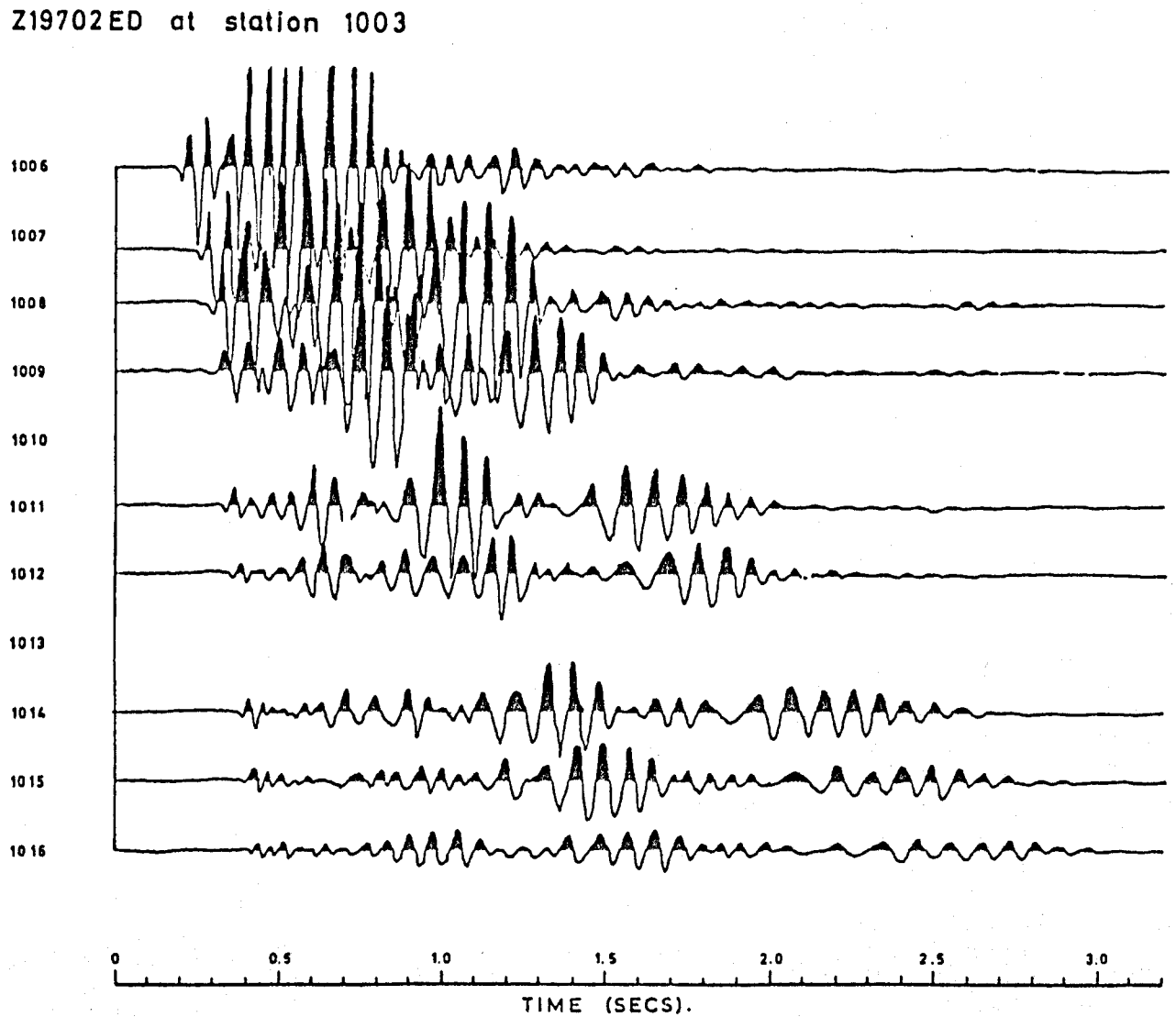

Figure 1-17. Record section with increasing shotpoint-geophone station offset (station 1003).

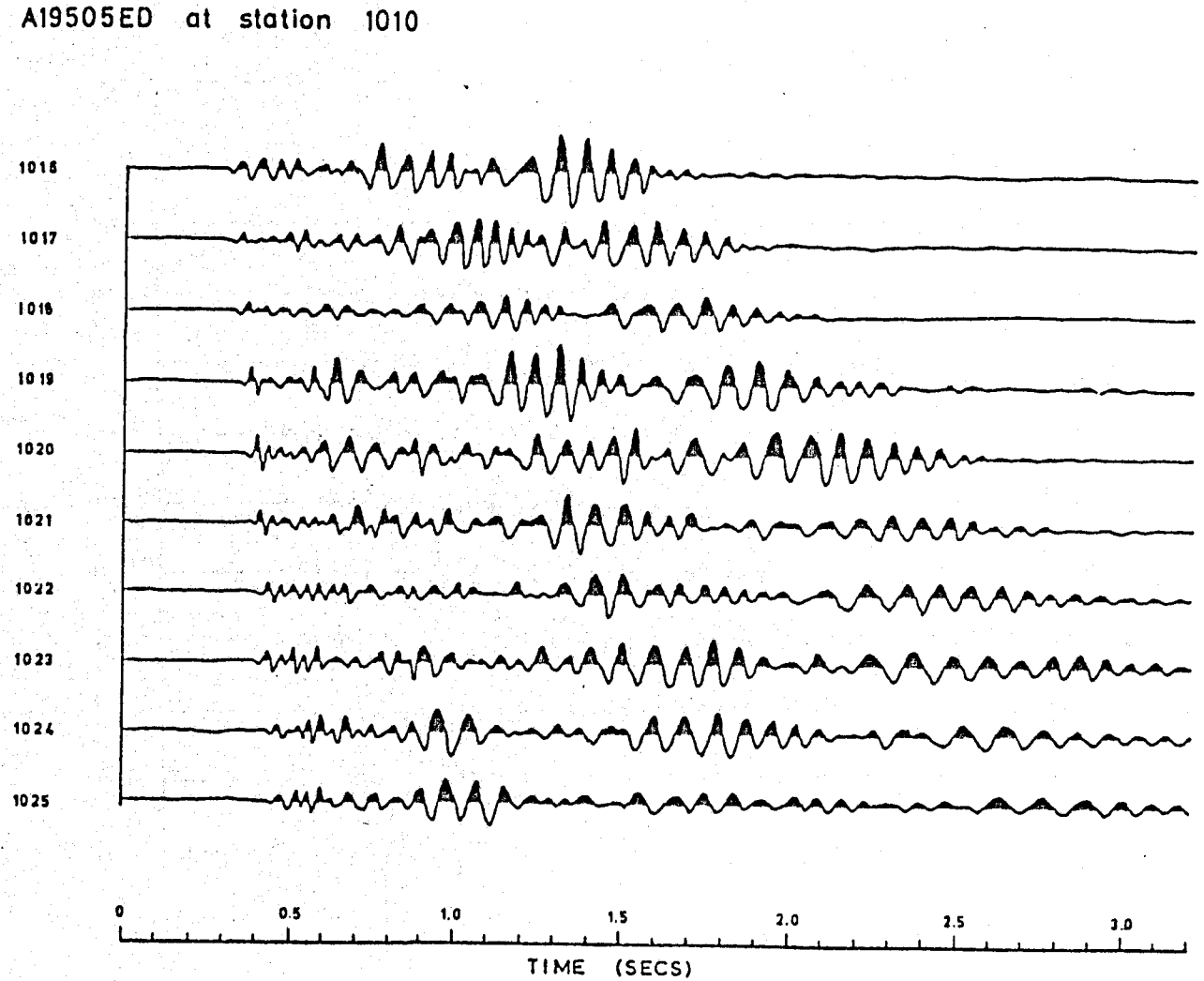

Figure 1-18. Record section with increasing shotpoint-geophone station offset (station 1010).

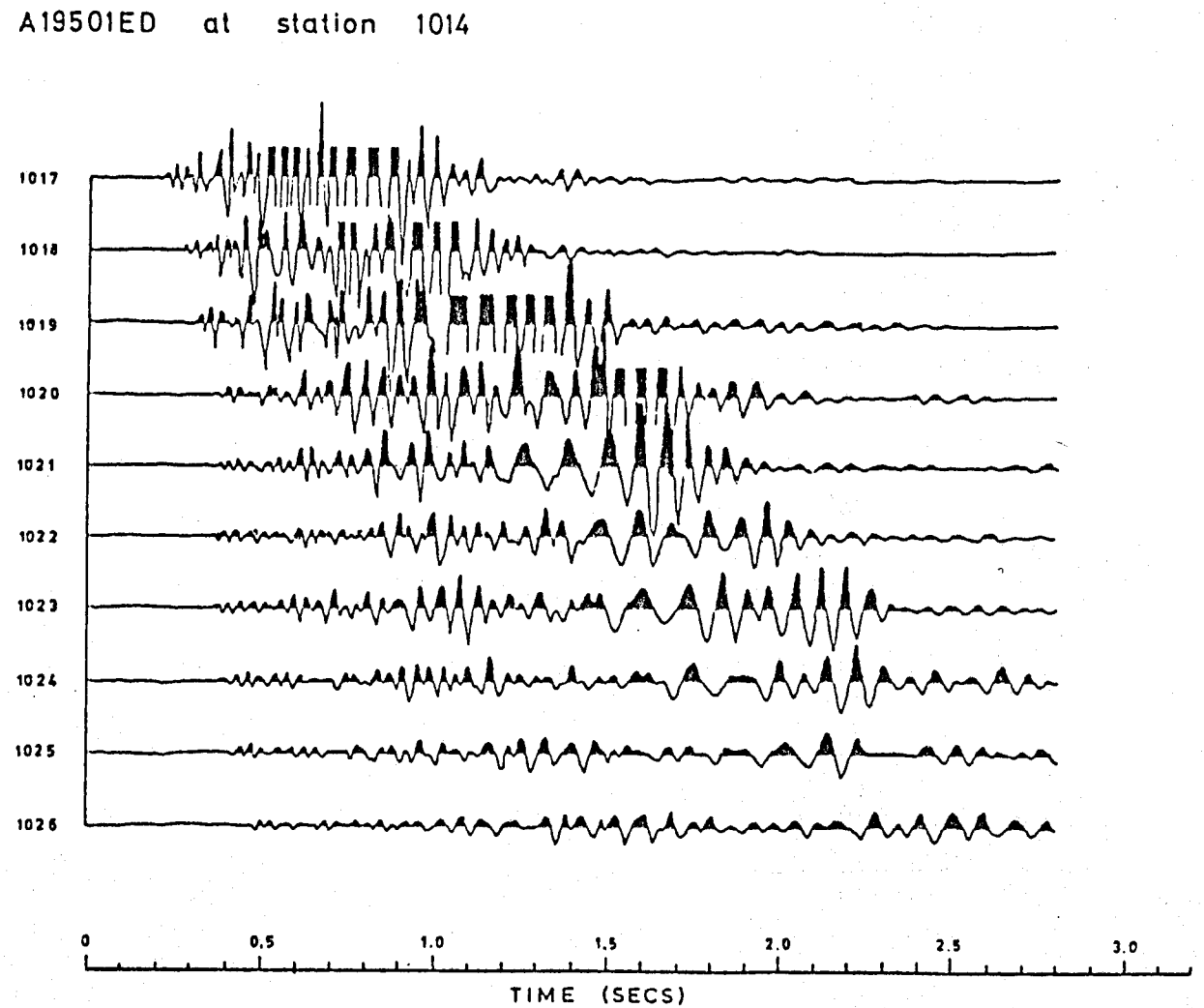

Figure 1-19. Record section with increasing shotpoint-geophone station offset (station 1014).

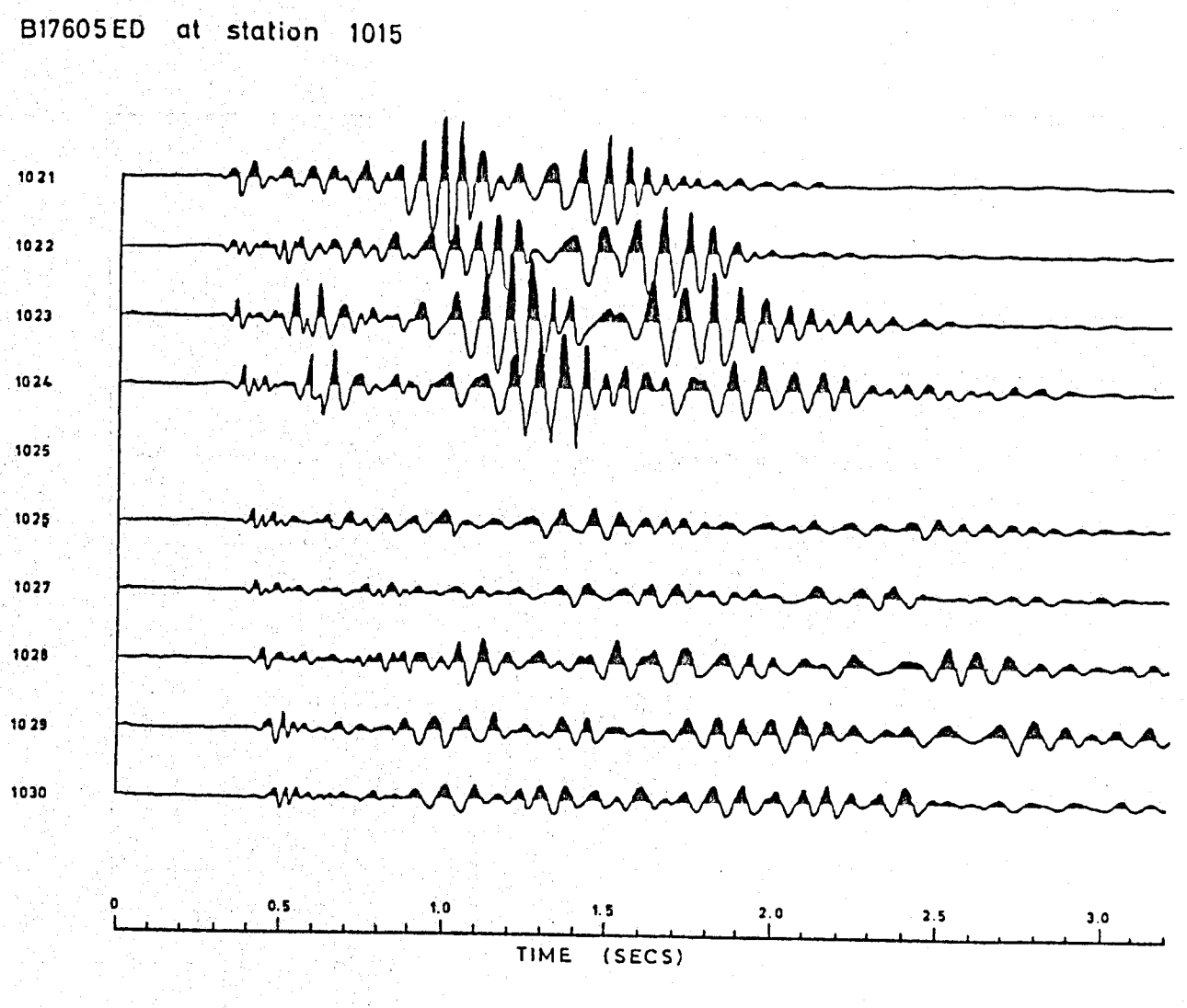

Figure 1-20. Record section with increasing shotpoint-geophone offset (station 1015).

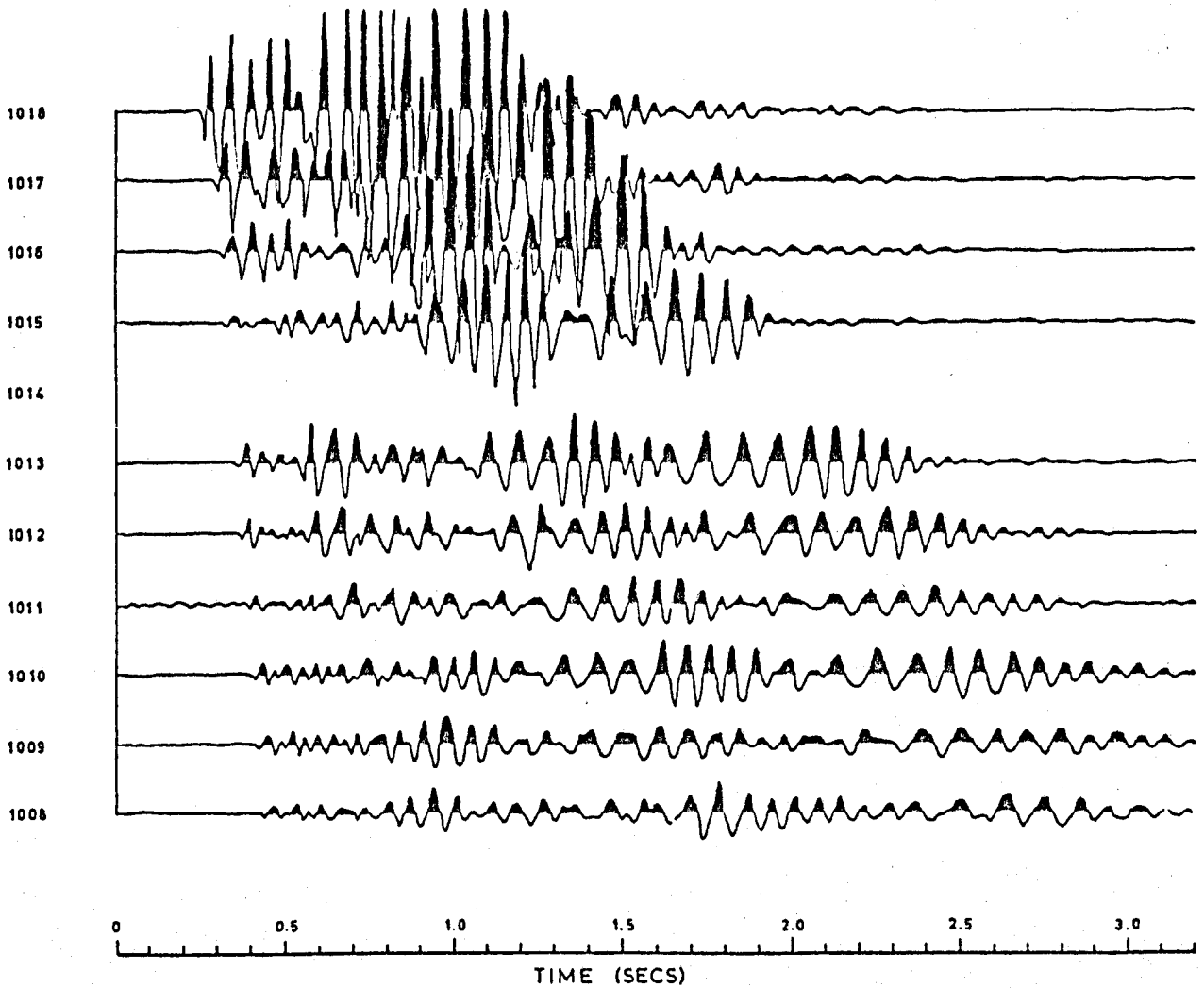

Figure 1-21. Record section with increasing shotpoint-geophone station offset (station 1022).

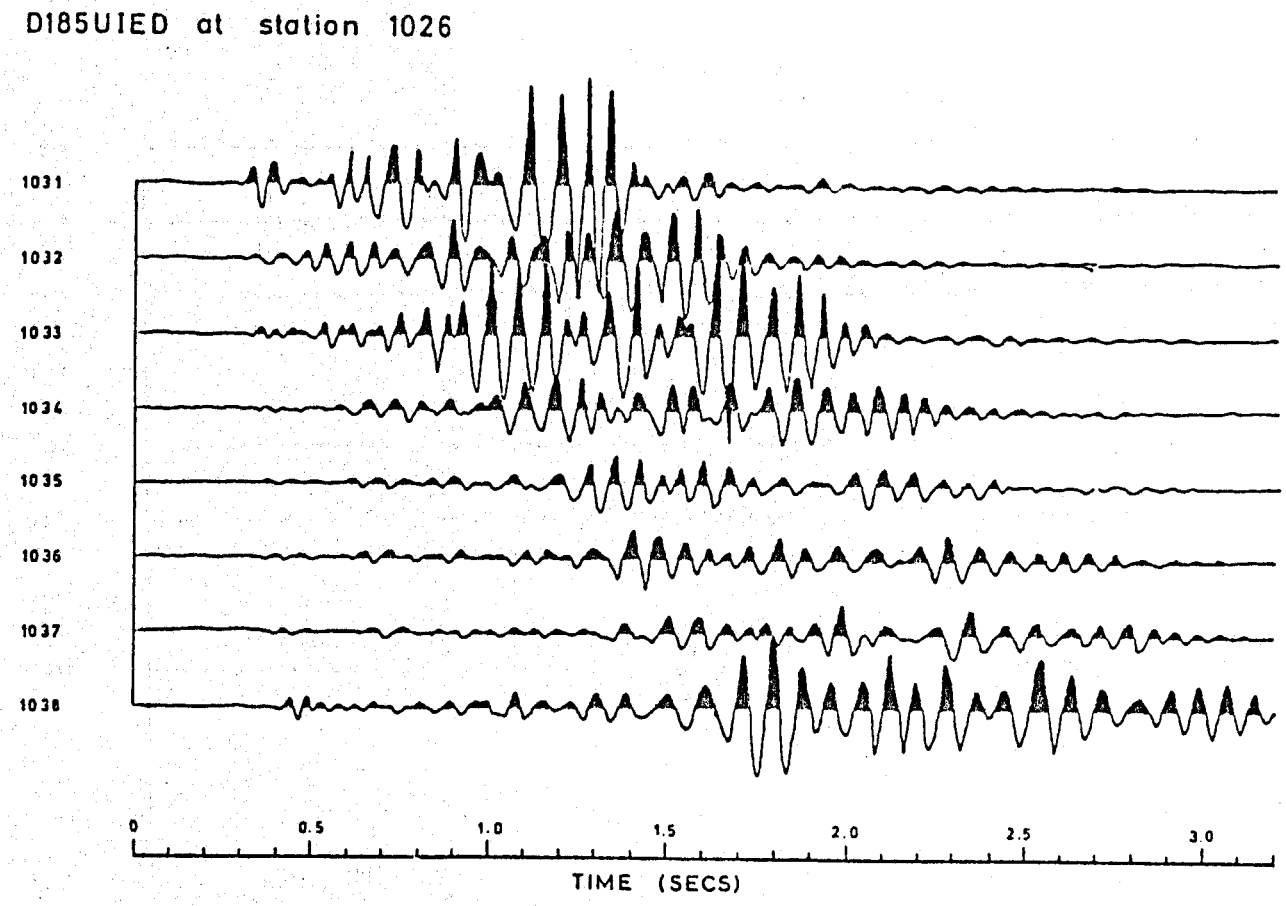

Figure 1-22. Record section with increasing shotpoint-geophone station offset (station 1026).

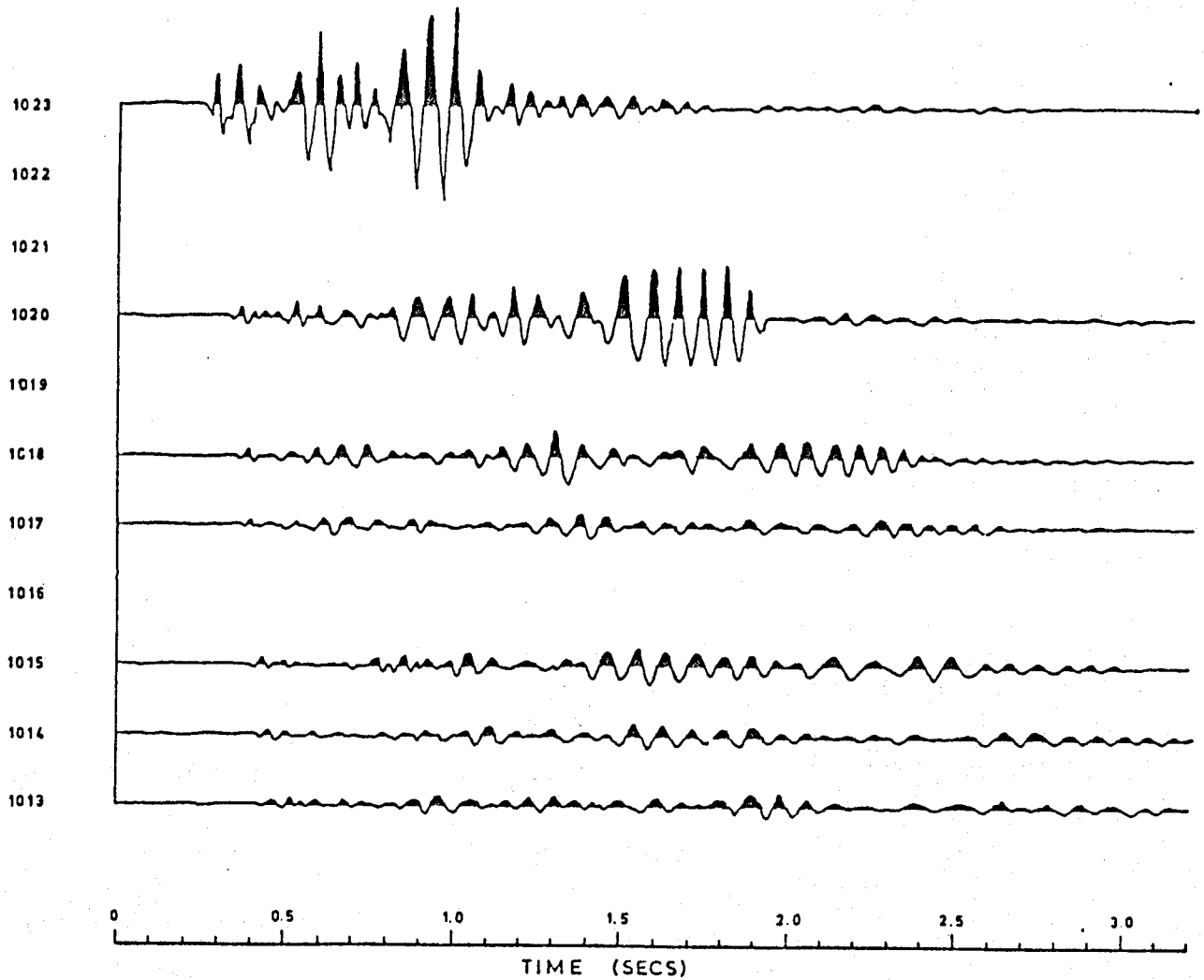

Figure 1-23. Record section with increasing shotpoint-geophone station offset (station 1027).

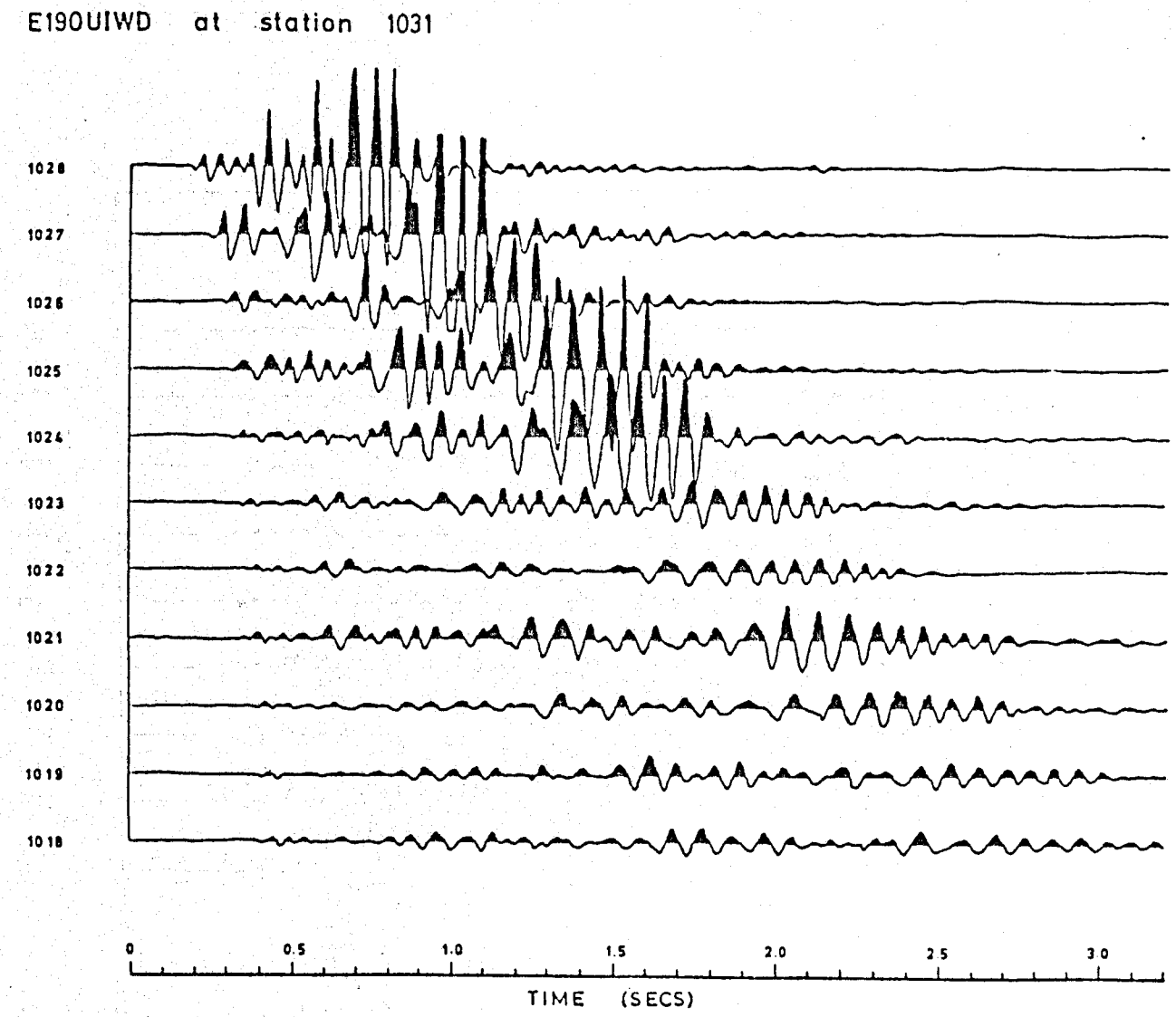

Figure 1-24. Record section with increasing shotpoint-geophone station offset (station 1031).

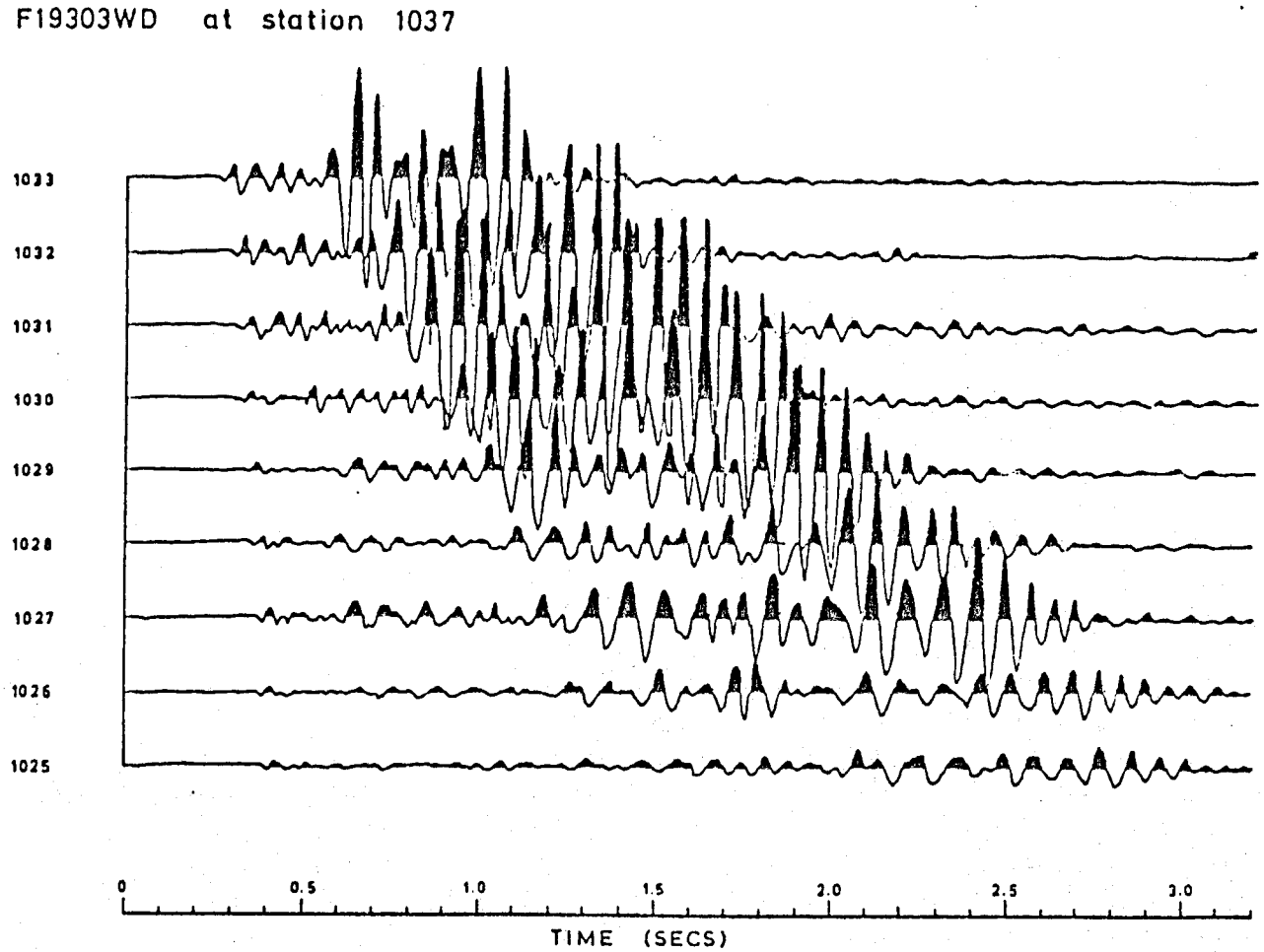

Figure 1-25. Record section with increasing shotpoint-geophone station offset (station 1037).

Table 1-2. Table of static corrections.

Station	Elevation above m.s.l. (ft)	Difference of Elevation from Datum Plane (ft)	Static Correction 2400 ft/s Upper Maximum Velocity (sec)	
1000	4067	-20.6	0.009	0.013
1001	4077	-14.1	0.006	0.009
1002	4086	- 8.6	0.004	0.006
1003	4088	-10.1	0.004	0.007
1004	4094	- 7.5	0.003	0.005
1005	4100	- 5.0	0.002	0.003
1006	4106	- 2.5	0.001	0.002
1007	4112	0	0	0
1008	4119	3.5	-0.001	-0.002
1009	4127	8.0	-0.003	-0.005
1010	4127	4.5	-0.002	-0.003
1011	4130	4.1	-0.002	-0.003
1012	4132	2.6	-0.001	-0.002
1013	4139	6.1	-0.002	-0.004
1014	4138	1.6	-0.001	-0.001
1015	4143	3.1	-0.001	-0.002
1016		(1.6)	-0.001	-0.001
1017	4148	1.2	-0.001	-0.001
1018	4153	2.7	-0.001	-0.002
1019	4154	0.2	0	0
1020	4158	0.7	0	0
1021	4161	0.2	0	0
1022	4166	1.7	-0.001	-0.001
1023	4169	1.2	-0.001	-0.001
1024	4174	2.8	-0.001	-0.002
1025	4173	1.7	-0.001	-0.001
1026	4173	- 5.2	0.002	0.003
1027	4182	- 0.7	0	0
1028	4188	0	0	0
1029	4199	2.3	-0.001	-0.001
1030	4197	4.8	-0.002	-0.003
1031	4201	5.4	-0.002	-0.003
1032	4198	- 1.1	0.001	0.001
1033	4200	- 2.6	0.001	0.002
1034	4201	- 5.1	0.002	0.003
1035	4210	0.4	0	0
1036	4227	13.0	-0.006	-0.009
1037	4228	11.5	-0.005	-0.008
1038	4216	- 4.0	0.002	0.003
1039	4215	- 8.5	0.004	0.006
1040	4277	0	0	0

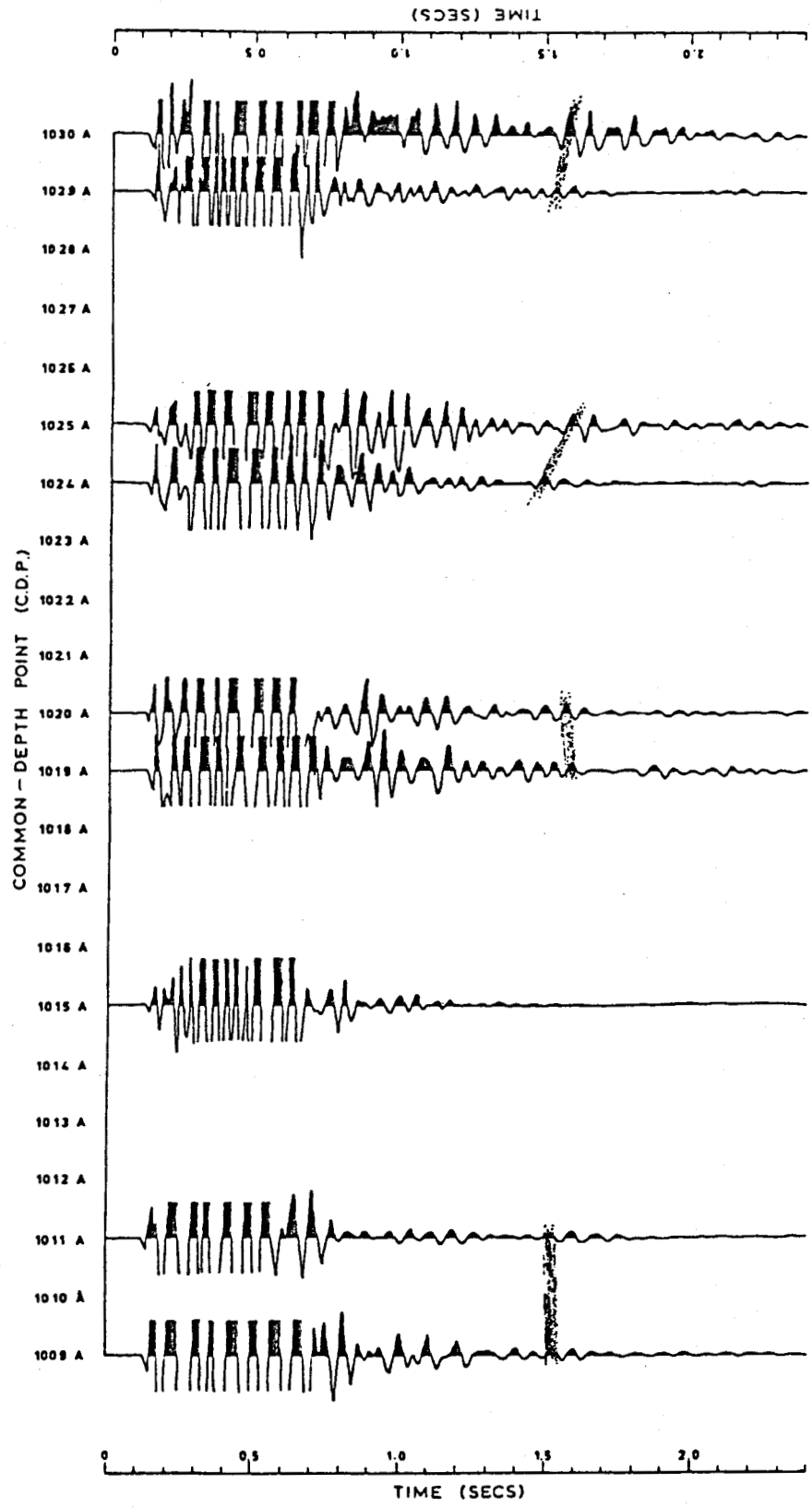

Figure 1-26. Two-peg offset section (92 m or 300 ft).

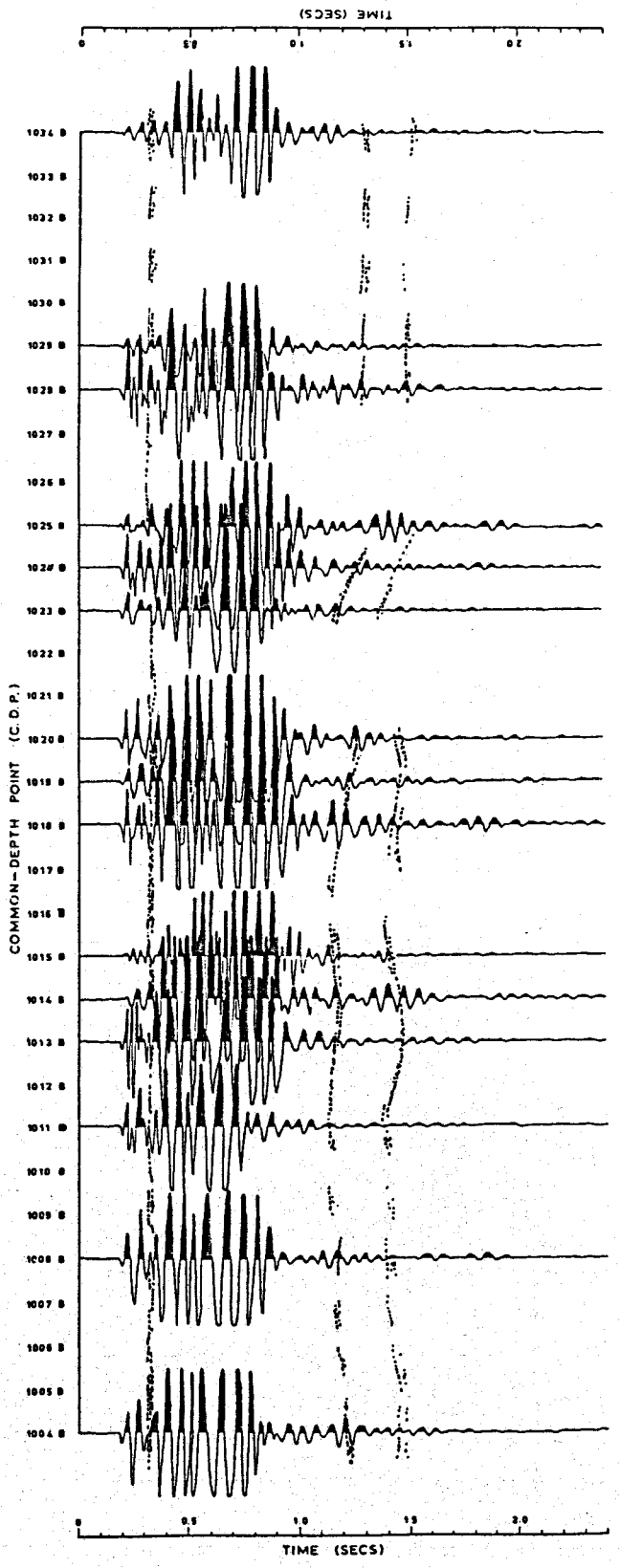

Figure 1-27. Three-peg offset section (140 m or 450 ft).

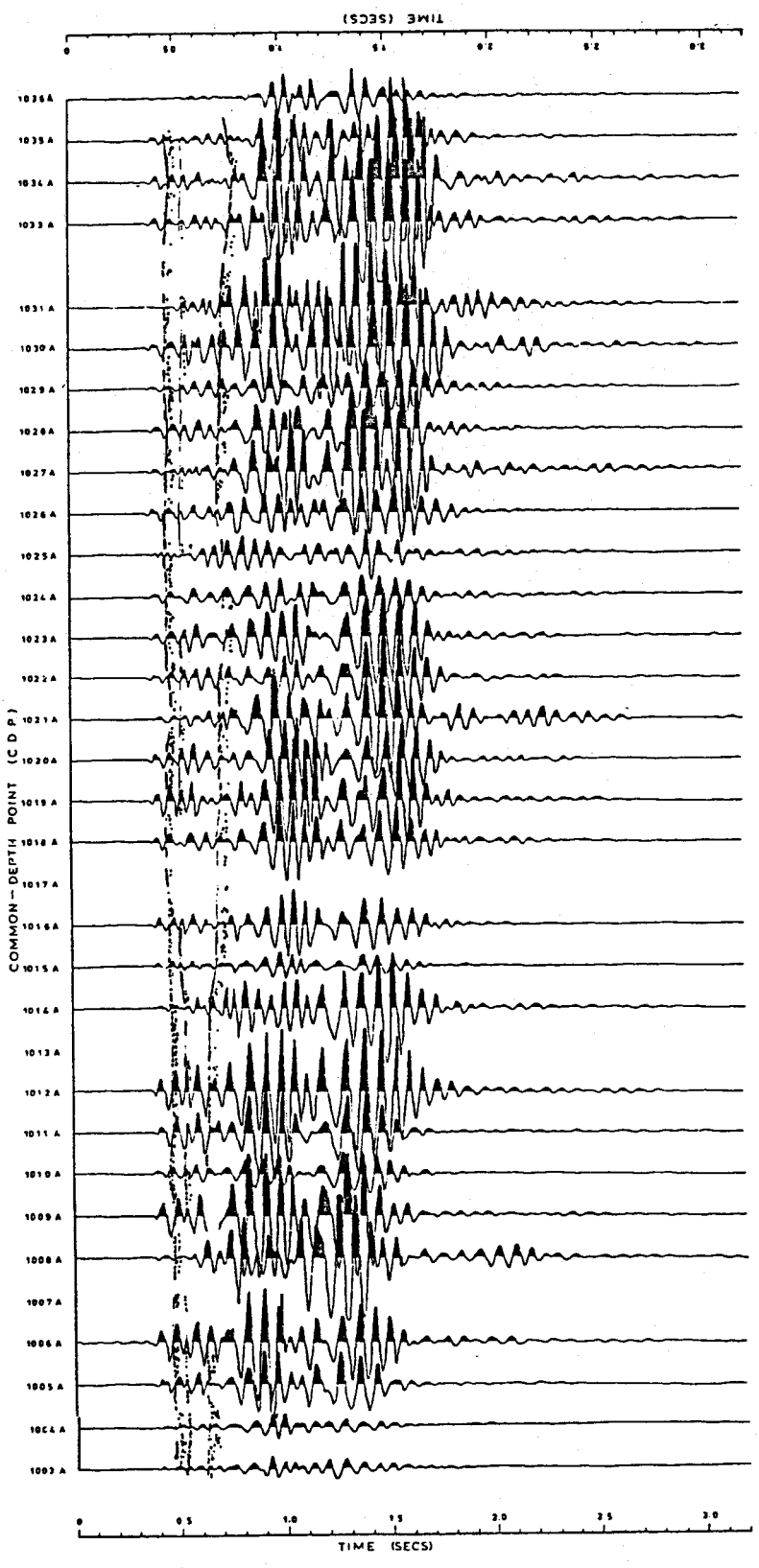

Figure 1-28. Six-peg offset section (280 m or 900 ft).

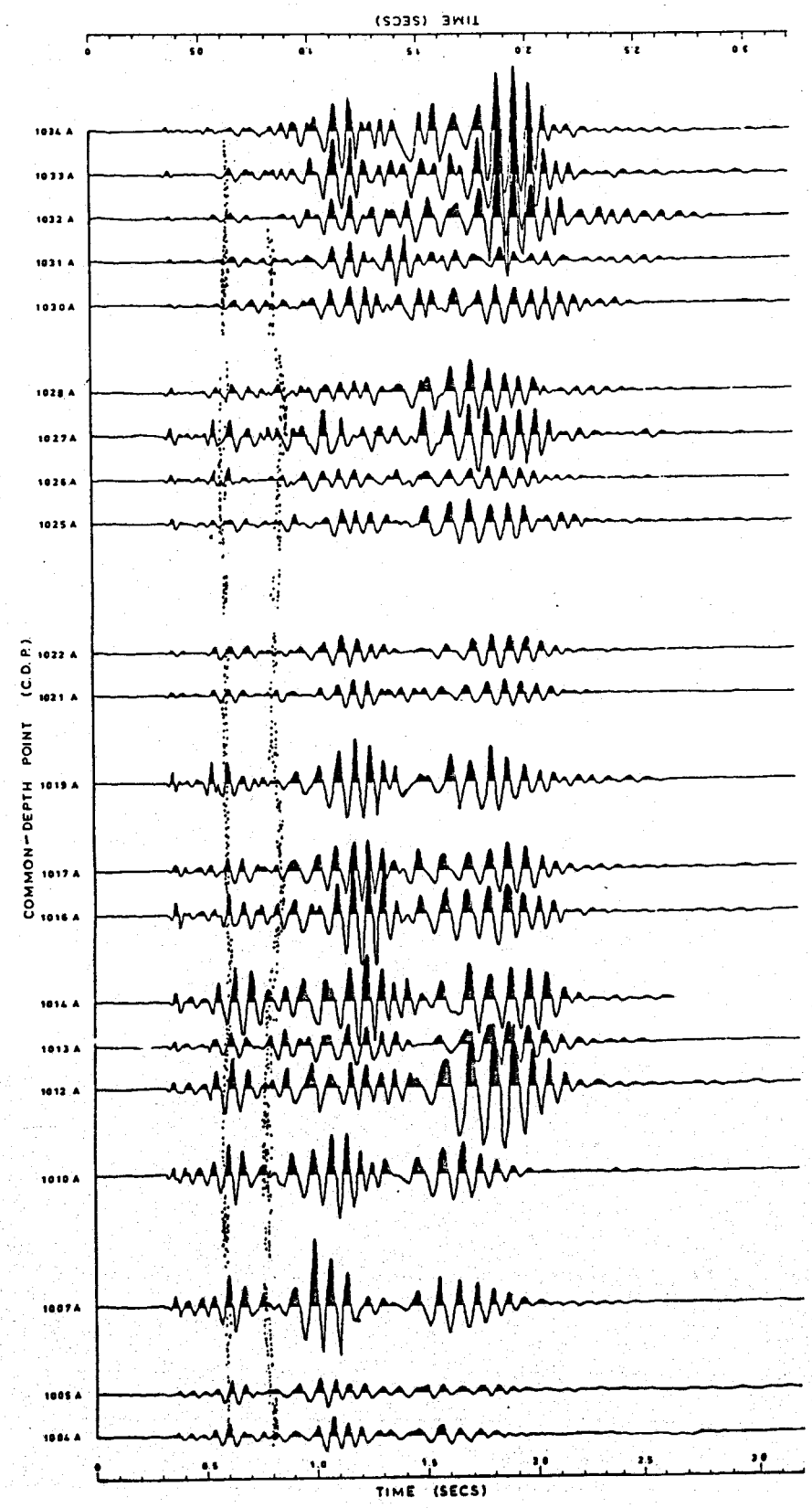

Figure 1-29. Eight-peg offset section (370 m or 1200 ft).

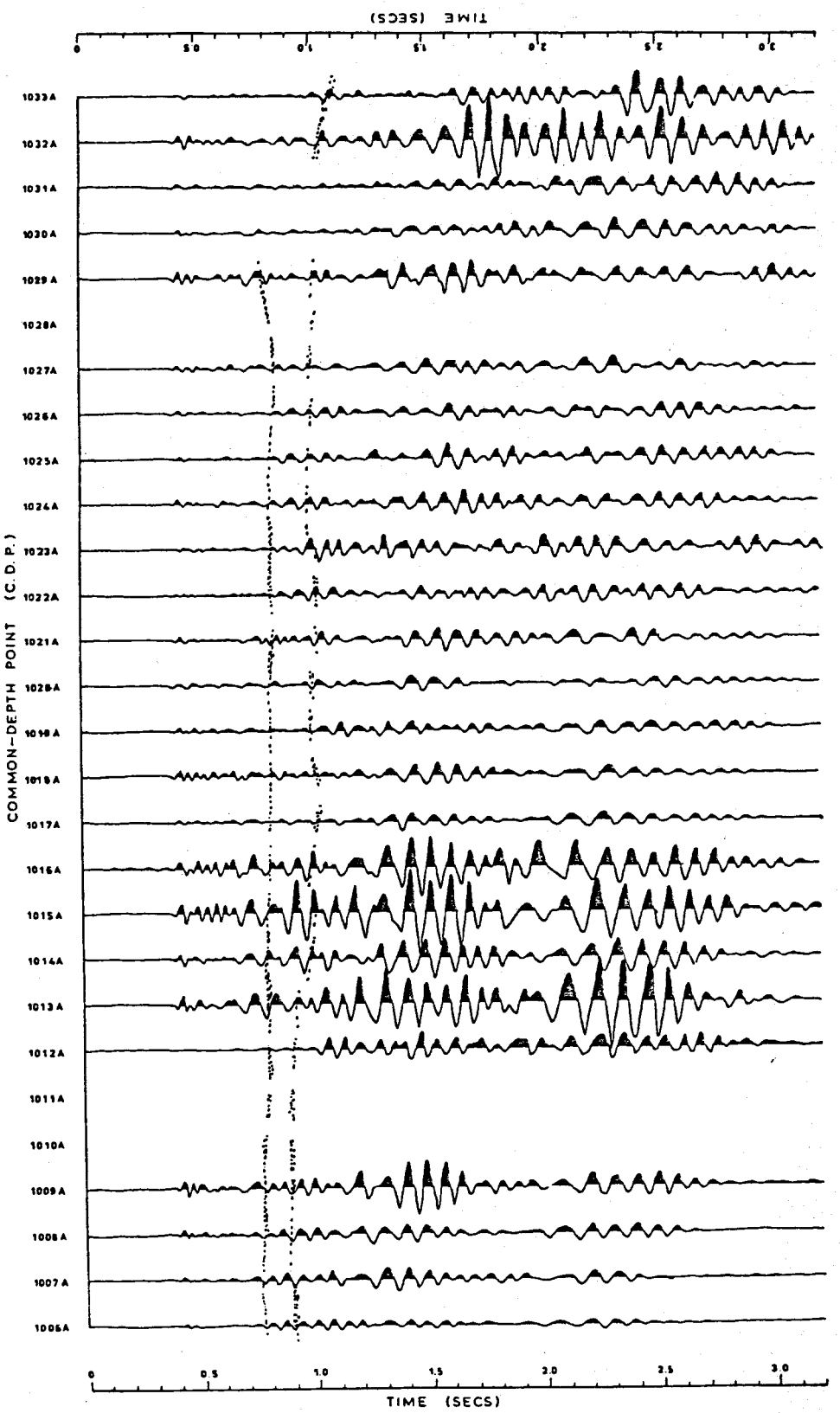

Figure 1-30. Twelve-peg offset section (550 m or 1800 ft).

prominently recorded event; thus, obliterating reflection information at different times on the records. Therefore, the choice of offset for a particular section was governed by the position of the groundroll with respect to the time window of interest.

The data from the logs of the two deep wells DT-1 and DT-2 were used with velocities from the refraction data to predict the position of reflections shallower than 300 m (1000 ft) (see Figure 1-31). These predictions were plotted onto the graticule to assist in picking of reflection events from the records.

Reflection events picked from the sections were collected together (after moveout corrections had been applied) and plotted to give a final section for the profile (see Figure 1-32). Comparison traces were picked from the common-depth point offset diagram (see Figure 1-16) for the same common-depth point (see Figure 1-33).

Results

Magnetic and Gravity

Displays of the elevation, magnetic, and gravity profiles are shown in Figure 1-4.

Seismic-Refraction Survey

A correlation of the results from the survey is shown in Figure 1-7. The maximum observable depth was limited by a high velocity "stringer" at a depth associated with the top of the water table. Although refracted first arrivals might be recorded using shot offsets greater than those of this survey, not only would the instrumentation and increased offset limit the quality of the arrivals observed due to probable lateral changes in lithology, but

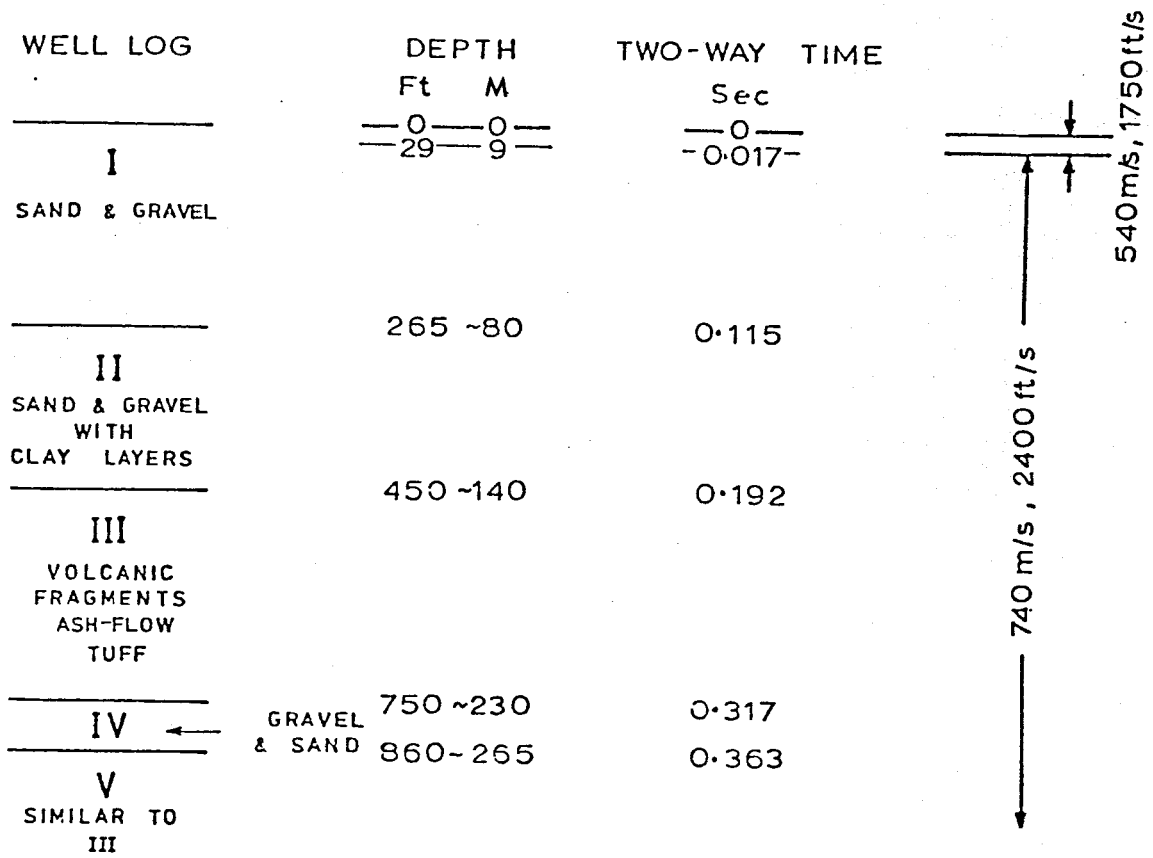

Figure 1-31. Diagram of well log and velocity model used to calculate reflected arrival times from each interface.

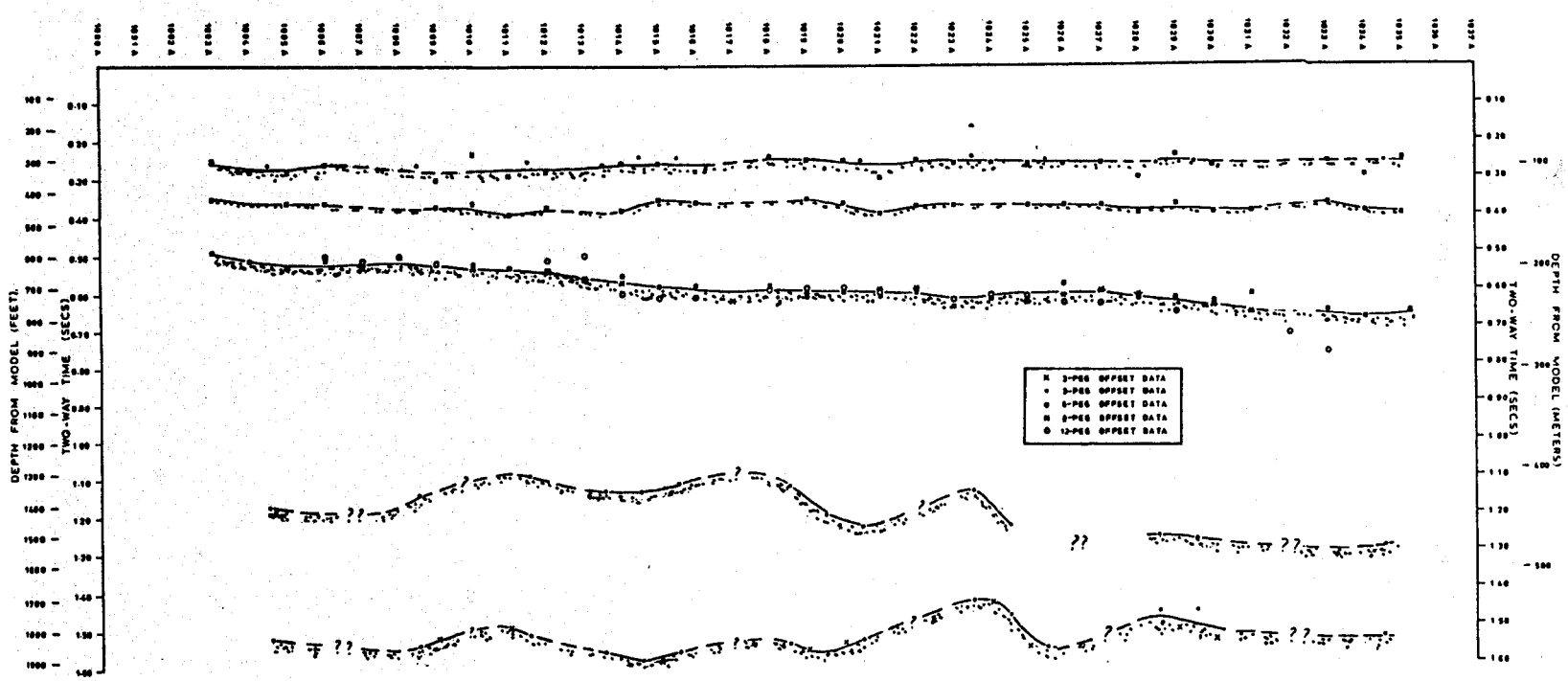

Figure 1-32. Common-depth point time depth section.

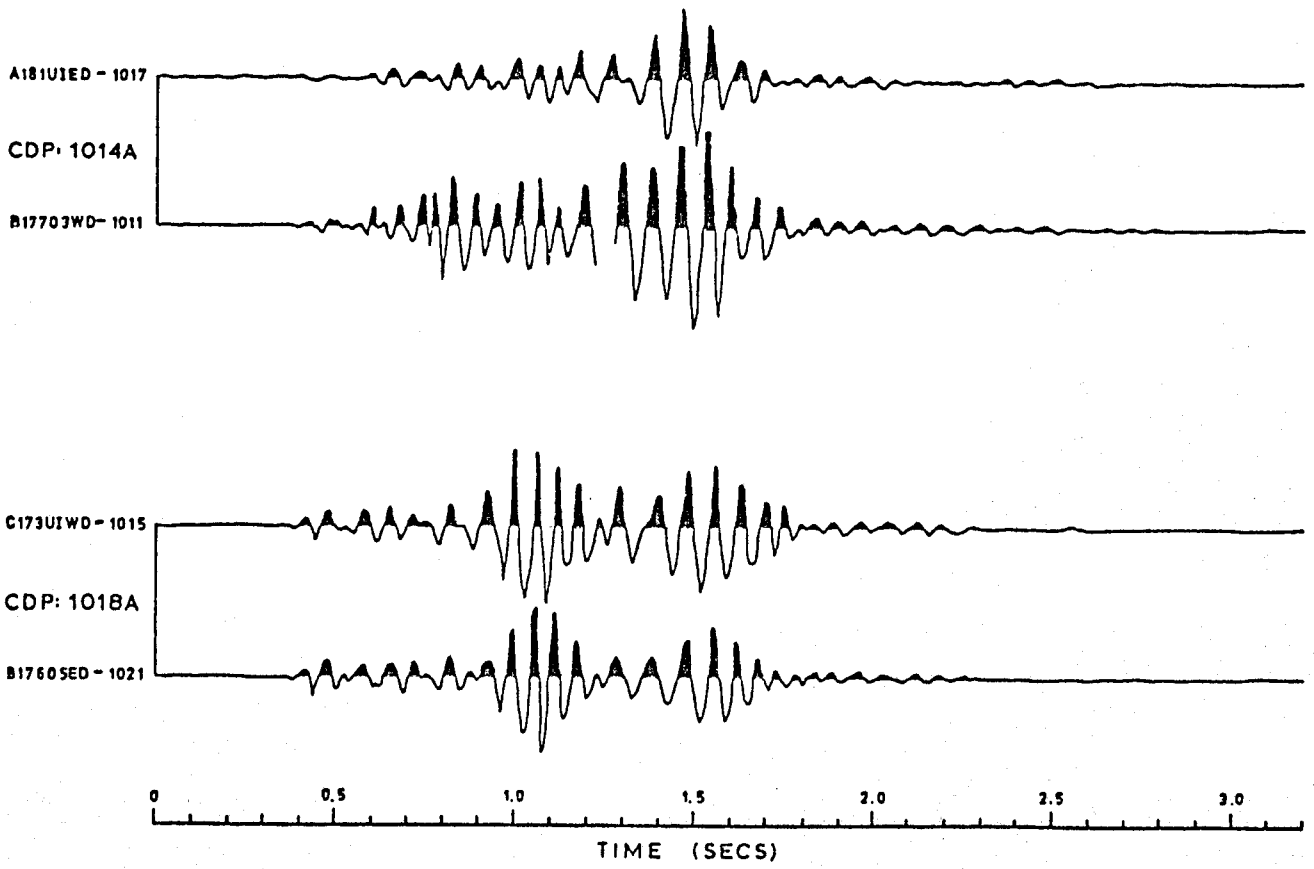

Figure 1-33. Trace comparisons for equal common-depth point and offset.

interpretation of such results would be a major problem. The results of the uphole survey are displayed in the Meisner diagram (see Figure 1-9) and in the time-depth plot for the near trace to the well (see Figure 1-8).

Seismic-Reflection Survey

The construction of the common-depth point (CDP) section for each offset (see Figures 1-26 through 1-30) has been described in the section on processing and data reduction. Reflected arrivals were traced by comparison of signal character from station to station on each CDP section. The reflected events were corrected for normal moveout (with velocities from the model) and plotted onto a final CDP section versus time. Between 0.7 seconds and 1.10 seconds, it was impossible to distinguish any reflected events because groundroll had dominated all other input data on all offset sections. The depth scales (in meters and feet) are intended as an indication of depth and are not to be used as a direct translation to be applied to each point plotted.

Interpretation of Results

Magnetic Survey

The profile of the magnetic data shows considerable short wavelength information which must be due to near-surface lateral variations in the concentration of detrital magnetic minerals. The 25- to 30-gamma amplitude anomaly to the east is completely due to one very high point and is thus also supposed to be of local origin.

Between stations 1015 and 1025 (0.7 km to 1.15 km from the western end of the profile), there is an anomaly which most probably relates to distinct

lithologic structure. No quantitative analysis of this anomaly has been attempted because only one profile was recorded.

Gravity Survey

The profile of the vertical component of gravity, after drift, Free Air, and Bouguer corrections were applied, was plotted above the magnetic profile to aid direct comparison. The profile shows a rapid gradient to the east which must be interpreted as the thickening of low-density, probably poorly-consolidated sediments to the west. Immediately east of the profile, the Paleozoic limestone of Tortugas Mountain rises above the sediments.

Between stations 1013 and 1022 (0.60 km and 1.02 km from the western end of the profile), there is a "step" of approximately 0.9 mgal in the otherwise relatively flat profile. This anomaly, although probably of deeper origin than that shown on the magnetic profile, is possibly of a similar genetic origin as indicated by its spatial coincidence.

Uphole Survey

The data displayed in the time-depth plot and the Meisner diagram indicate a high-velocity region near to the well site. This high velocity of 5200 m/sec (17,200 ft/sec) is approximately the P-wave velocity of steel; thus, it is interpreted to be representative of the steel casing in the well, although there are other slower velocities that are apparent.

Seismic-Refraction Survey

Four layers were differentiated by the refraction data:

1. A thin intermittent surface "weathering" layer of velocity 250 m/s (800 ft/sec). The thickness of this layer varied between not being detectable to 2 m (6 ft).

2. A weathering layer with velocity between 420 m/s (1350 ft/s) and 540 m/s (1750 ft/s) and a depth between 4.5 m (14 ft) and 9 m (29 ft), variable over the lateral extent of the profile.

3. A layer which is probably poorly consolidated with a velocity of between 540 m/s (1750 ft/s) and 880 m/sec (2950 ft/s). This layer extends down to a depth of 80 m (260 ft) as calculated from the long offset data.

4. At 80 m (260 ft), a high-velocity material with a velocity of 2900 m/s (9400 ft/s) and with an indeterminable depth. The layer may not be very thick, but refracts all energy along its upper interface because of the high-velocity contrast with the material above. By recording charges detonated in opposite directions, the dip of this interface was calculated to be approximately 3° to the horizontal on the element of line observed. This layer is interpreted to be a cementation (caliche) layer initially associated with the water table.

Seismic-Reflection Survey

The display of common-depth point (CDP) and two-way time (and depth as predicted by the model) shows five distinct reflections. Because of the presence of groundroll any reflections between 0.7 seconds and 1.10 seconds could not be distinguished. Some of the reflectors, notably that at 0.6 seconds, could be delineated on several CDP sections with different offsets. All the reflected events picked have been corrected for normal moveout (NMO) before being plotted on this display; thus, the coincidence of points on those reflectors for various offsets indicated a good agreement of the data with the model velocities used for the NMO corrections. The various features are as follows:

1. The most shallow reflector discernible is that associated with the water table. As was shown by the refraction-survey results, there is a high-velocity material with a velocity of 2900 m/sec (9400 ft/s) and with a calculated depth of that of the water table. This layer has been interpreted not to be of any great thickness and to be representative of a cementation layer (caliche). The reflected arrivals were not easily differentiated due to change in character and were weak in amplitude. The large scatter in the points plotted is attributed to the different ray path involved (for different offsets) encountering local lateral inhomogeneities, most predominantly present in the near-surface material. It is noted that the dip calculated from the refraction data is not evident in the CDP-time depth sections.

2. The reflector with a two-way time of 0.40 seconds is best differentiated on the 6-peg section (280 m or 900 ft). An event may picked on the 8-peg (370 m or 1200 ft) and the 12-peg (550 m or 1800 ft) sections. However, neither of the latter two picked events correspond to any interface as predicted from the well logs and the velocity model.

3. The reflector, as best differentiated by 3 sections, has a two-way time which is from 0.50 seconds in the west to 0.68 seconds in the east. At well site DT-1, this reflection would correspond to a layer (or possible lens) of gravel and sand. Possibly this reflection is not a single reflector but several lenses of sand and gravel along the length of the profile.

4. Reflection with two-way time varying from 1.15 seconds in the west to 1.30 seconds in the east has a minimum of 1.10 seconds and maximum of 1.30 seconds; it shows not only a general dip to the east but a rapidly varying two-way time.

5. The reflection signifying the deepest recorded event varies markedly from 1.40 seconds to 1.55 seconds. As compared to the reflection above, there is no apparent dip towards the east. This reflection has been interpreted to be the upper interface of the Paleozoic limestone of which Tortugas Mountain is an upthrust block.

6. The two deep reflections apparently have a similar character. However, such large dips, as have been interpolated between plots of these reflections, are of an order (30° to 40°) so that direct interpretation of an interface without any consideration to migration appears to be an over-simplification. However, it is supposed that these interfaces are broken by faulting.

7. The two shallow reflections appear to be parallel to the surface. However, the reflector interpreted to be the upper interface of a layer (or lens) of gravel and sand dips towards the east implying a thickening of the volcanic-fragment layer towards the east. The possibility that this apparent dip is due to an eastward lateral increase of velocity has been considered and, if true, would require a velocity at the eastern end of the profile of 2500 m/s (8000 ft/s) from the water table down to this interface.

8. It is further noted that although the 1.20-second reflector has a similar dip to that of the sand and gravel lens; the limestone interface appears to have no general dip. Further, as previously stated, reflected arrivals for the 0.60-second reflector as picked from various offset-CDP sections show good coincidence and, if there was a marked increase in velocity towards the east, application of a single velocity for the NMO corrections would produce an increasing difference in reflection time which was not observed.

9. If the apparent easterly dip is a true representation of interface inclination, then it may be conjectured that an interface between the 0.60-second reflector and the 1.10-second reflector may be the western structural control for geothermally-heated water which has risen via faulting in the Paleozoic limestone.

Summary

Five velocity interfaces have been delineated from the seismic-reflection data, the deepest of which has been interpreted to be the Paleozoic limestone. The anomalies as indicated by the magnetic and gravity profiles have no direct correlation with the five reflected events and are thus considered to have a deeper origin, although it is quite possible that the magnetic anomaly may be created by a lateral change of magnetic mineral content in the ash-flow tuff.

Further exploration work would involve a more detailed (higher resolution) seismic-reflection survey using larger charge size, geophone patterns (to both enhance signal and attenuate groundroll), and more sensitive equipment.

This survey recorded a profile in only two dimensions. To justify results from a higher resolution survey would necessitate the recording of an areal grid of profile to delineate three-dimentional structures.

Conclusions with Respect to the Geothermal Anomaly

The seismic-reflection data show that there is no major faulting above 300 m (1000 ft); thus, the rise of hot water in the portion of the geothermal anomaly penetrated by test hole DT-1 must be a pore- or microfracture-controlled flow, as opposed to a major fracture-controlled flow. A dip in the third reflector from approximately 180 m (600 ft) in the west to 245 m (800 ft) in the east possibly exerts structural control on the westerly

lateral migration of the hot water away from the local peak in the geothermal anomaly. Consistent with this hypothesis, temperatures in a second test hole, DT-2, decrease significantly beneath this reflector (Morgan et al. 1979). The depth of the maximum temperature in DT-2, 50.8°C (123°F) at 160 m (525 ft) is just below the second reflector, which is interpreted as the top of the first volcanic layer, indicating the lateral water flow is somehow confined primarily within the volcanic layer.

In contrast to the apparent continuity of the three shallow reflectors, significant offsets are indicated in the two deeper reflectors, the greatest of which is coincident with the peak of the shallow temperature anomaly at the DT-1 well site. These offsets are thought to be fault controlled, with downthrows of the order of 30 m (100 ft) to the east, and possibly represent minor antithetic faults related to the major normal fault on the western margin of Tortugas Mountain, downthrown to the west, which has been delineated by Seager and Brown (1978) and Jiracek and Gerety (1978). From the information available, the fault indicated by the reflection data beneath the DT-1 site is the structural feature most likely to act as a conduit along which the hot water of the geothermal anomaly ascends from depth. Other faults in the area, including the westward-dipping western marginal fault of Tortugas Mountain, may also act as conduits for ascending hot water. The shallow temperature gradient data (Morgan et al. 1979) indicate that, at least locally, the relatively minor fault beneath the DT-1 site acts as the dominant conduit for the geothermal anomaly.

Although sufficient gravity data are not available for a rigorous analysis to be made, the magnitude of the gravity decrease westwards from Tortugas Mountain across the geothermal anomaly is consistent with the depth of the deepest reflector, 550 to 580 m (1800 to 1900 ft), being the top of the

downfaulted surface of the Paleozoic limestone, which outcrops at Tortugas Mountain. Extensive water flow through solution cavities controlled by joint and fault planes in limestone beds is very common. If limestone beds do underlie Las Alturas, they would probably provide extensive channels for both lateral and vertical flow of hot water into the Las Alturas Geothermal Anomaly. This potential factor should be considered very carefully before deep exploitation of the Las Alturas anomaly is attempted.

References

Cook, F. A., McCullar, D. B., Decker, E. R., and Smithson, S. B., 1979, Crustal structure and evolution of the southern Rio Grande Rift, in Riecker, R. E., ed., Rio Grande Rift, Tectonics and magmatism: American Geophysical Union, Washington, D.C., p. 195-208.

Dunham, K. C., 1935, Geology of the Organ Mountains, New Mexico: New Mexico Bureau of Mines and Mineral Resources, Bulletin 11, 272 pp.

Jiracek, G. R., and Gerety, M. T., 1978, Comparisons of surface and down-hole resistivity mapping of geothermal reservoirs in New Mexico: Geothermal Resources Council, Transactions, v. 2, p. 335-336.

King, W. E., and Hawley, J. W., 1975, Geology and groundwater resources of the Las Cruces area, New Mexico, in 26th Field Conference Guidebook: New Mexico Geological Society, p. 195-204.

Morgan, P., Swanberg, C. A., and Lohse, R. L., 1979, Borehole temperature studies of the Las Alturas Geothermal Anomaly, New Mexico: Geothermal Resources Council, Transactions, v. 3, p. 279-288.

Ramberg, I. B., and Smithson, S. B., 1975, Gridded fault patterns in a late Cenozoic and Paleozoic continental rift: Geology, v. 3, p. 201-205.

Reiter, M., Shearer, C., and Edwards, C. L., 1979, Geothermal anomalies along the Rio Grande Rift in New Mexico: Geology, v. 6, p. 85-88.

Seager, W. R., 1975, Cenozoic tectonic evolution of the Las Cruces area, New Mexico, in 26th Field Conference Guidebook: New Mexico Geological Society, p. 241-250.

Seager, W. R. and Brown, L. F., 1978, The Organ Caldera: New Mexico Geological Society, Special Publication 7, p. 139-149.

Swanberg, C. A., 1975, Detection of geothermal components in groundwaters of Dona Ana County, Southern Rio Grande Rift, in 26th Field Conference Guidebook, New Mexico Geological Society, p. 175-180.

Swanberg, C. A., 1979, Chemistry of thermal and non-thermal groundwaters in the Rio Grande Rift and adjacent tectonic provinces, in Riecker, R. E. ed., Rio Grande Rift, Tectonics and magmatism: American Geophysical Union, Washington, D.C., p. 279-288.

Chapter 2

Seismic, Water Analyses, and Hydrology Studies in the Socorro Area

Part 1

Seismic Measurements of the Tertiary Fill in the Rio Grande Depression West of Socorro, New Mexico*

Introduction

An area between Socorro Mountain and the main New Mexico Tech campus has been suggested as a drill site to explore for geothermal waters to heat buildings at New Mexico Tech. The target of the geothermal exploration is a possible aquifer within the lower Popotosa Formation. A 400-m to 800-m thick aquitard in the upper Popotosa Formation would separate any aquifer in the lower Popotosa from the main Rio Grande aquifer (Chamberlin, personal communication 1979). Detailed information on the Tertiary structure and stratigraphy in the Socorro area can be found in Chapin et al. (1978a; 1978b).

The economic feasibility of heating the campus with geothermal waters hinges to a large extent on the depth of the resource. If a production well has to be drilled through several kilometers of Tertiary fill, the cost of the well could far exceed any long-term economic gains from the project. The purpose of the seismic study was to determine the depth to the aquitard using active reflection and refraction techniques.

*The principal authors of Chapter 2, Part 1 are Dr. Allan Sanford and Dr. William Schlue of the Geoscience Department, New Mexico Institute of Mining and Technology.

Seismic Velocities from Sonic Well Logs

As an aid to interpreting the seismic data, sonic logs for three wells drilled in the Albuquerque Basin were examined. These logs showed ideal conditions for generation of reflections and large velocity changes (up to about 500 m/sec) in a short distance throughout the Tertiary section, but particularly in the first 500 m from the surface.

Inasmuch as seismic reflection or refraction data cannot reveal the velocity detail of the sonic logs, the latter were smoothed by eye and the linear velocity function

$$V = V_o \quad aZ \quad ,$$

where V_o = velocity of water-saturated rock near the surface and

$$a = \frac{dV}{dz} \quad ,$$

was fitted to the resulting velocity values. Plots of the velocity functions for the three wells are given in Figure 2-1. Note that the velocity function for the Shell #1 Santa Fe differs little from those for the other two wells even though the depth to Cretaceous is markedly different in the two cases. Thus, it appears it would be difficult to establish whether one were in the upper or lower part of the Tertiary fill on the basis of observed velocities alone.

Seismic Reflection and Refraction Data

The line along which seismic-reflection and refraction data were obtained is shown in Figure 2-2. The line extends from the base of Socorro Mountain to the northwest fringe of the main New Mexico Tech campus in a S76E direction. Two sets of data were analyzed, consisting of recordings made by the senior author in 1957 and 1958 and recordings obtained in the summer of 1979. Although the principal purpose of the 1957 and 1958 work

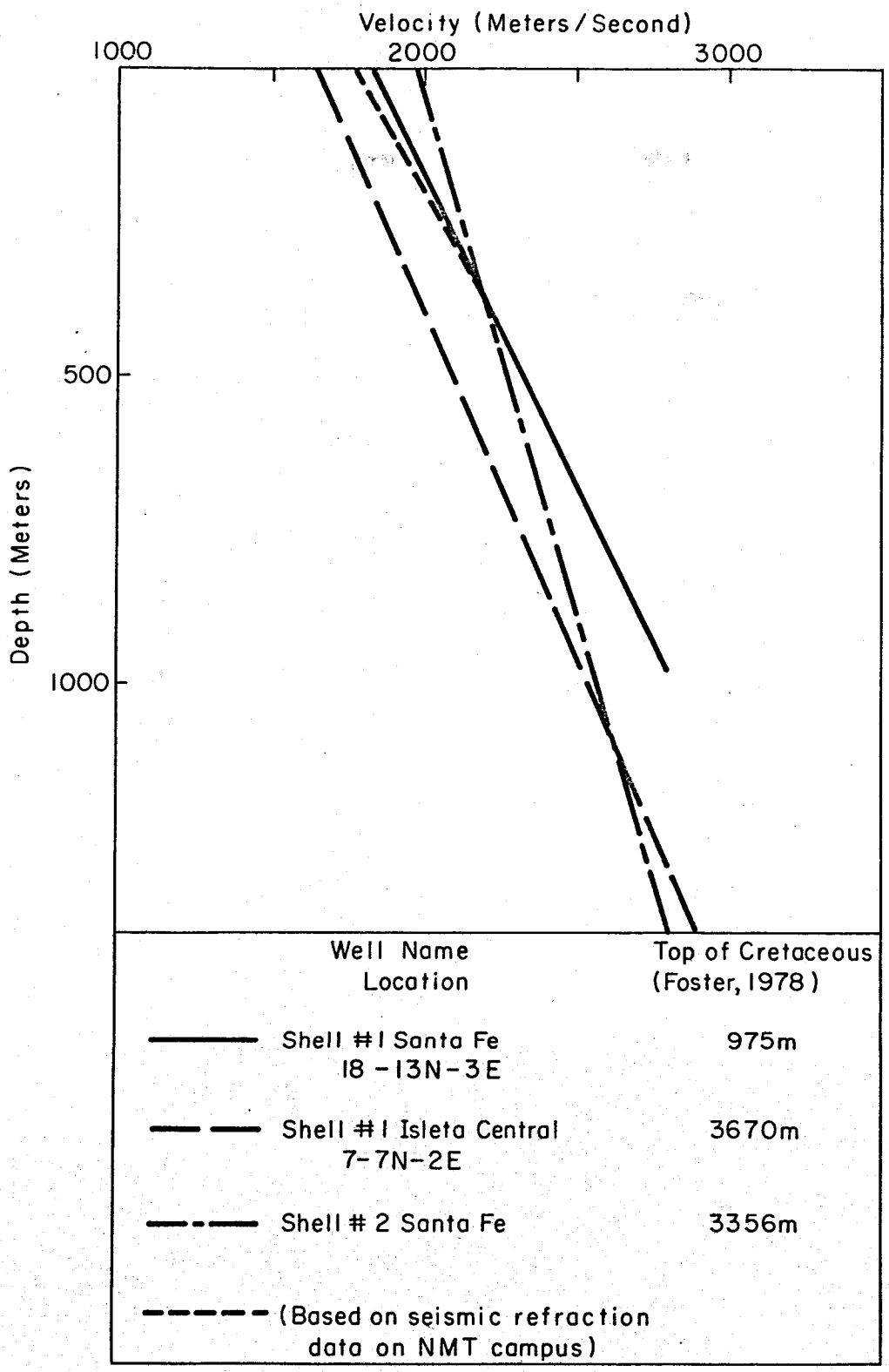

Figure 2-1. Linear velocity functions for Tertiary sedimentary rocks in the Rio Grande Rift. The linear increases in velocity with depth are based on sonic logs of exploratory drill holes in the Albuquerque Basin and seismic-refraction shooting in the Socorro Basin along the line shown in Figure 2-2.

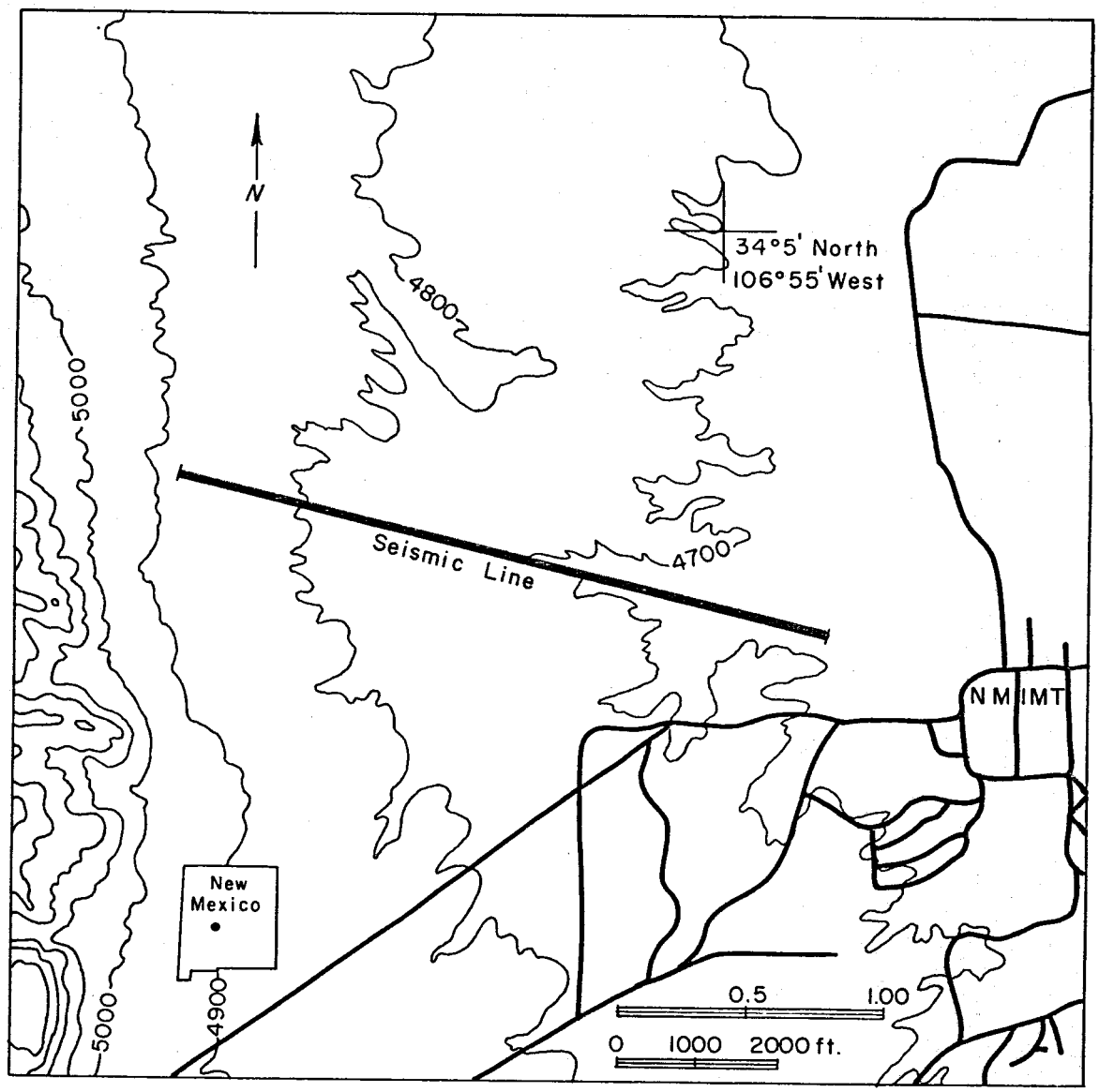

Figure 2-2. Map showing the line along which seismic-reflection and seismic-refraction measurements were made.

was to define the depth and properties of the shallow Rio Grande aquifer, an attempt was made to obtain information on deeper structure by shooting both a 2500-m unreversed refraction profile and some spreads for reflections. A description of procedures used in the 1957 and 1958 work along with an analysis of the data relevant to the depth and properties of the shallow aquifer is given by Ibrahim (1962).

No attempt was made to interpret the 1957-1958 seismic data for deeper structure until 1979. Re-examination and analysis of these data revealed definite shallow reflections (at depths up to $\sim$ 400 m) on the west end of the line and probable deep reflections on the east end of the line. Depths and velocities based on the shallow reflections are plotted on the western end of the cross section shown in Figure 2-3. The lengths of the lines shown for these and other reflections on the cross section correspond to approximately the subsurface extent of the reflecting velocity discontinuity.

The depths of the reflections on the east end of the line are great relative to the spread length, and therefore average velocities to the discontinuities cannot be calculated. The depth shown to the top and bottom of the zone of reflectors is based on the velocity function

$$v = 1.8 \text{ (km/sec)} + 1.0 \text{ (1/sec)} \; Z \text{ (km)} \quad ,$$

which is close to the average function for the well velocity data shown in Figure 2-1. The observed moveout on the reflections indicates that the reflectors cannot have dips in excess of about 5 degrees to the west or east.

The apparent velocities observed on the long unreversed refraction profile were used to obtain the velocity function

$$v = 1.77 \text{ (km/sec)} + 1.14 \text{ (1/sec)} \; Z \text{ (km)} \quad .$$

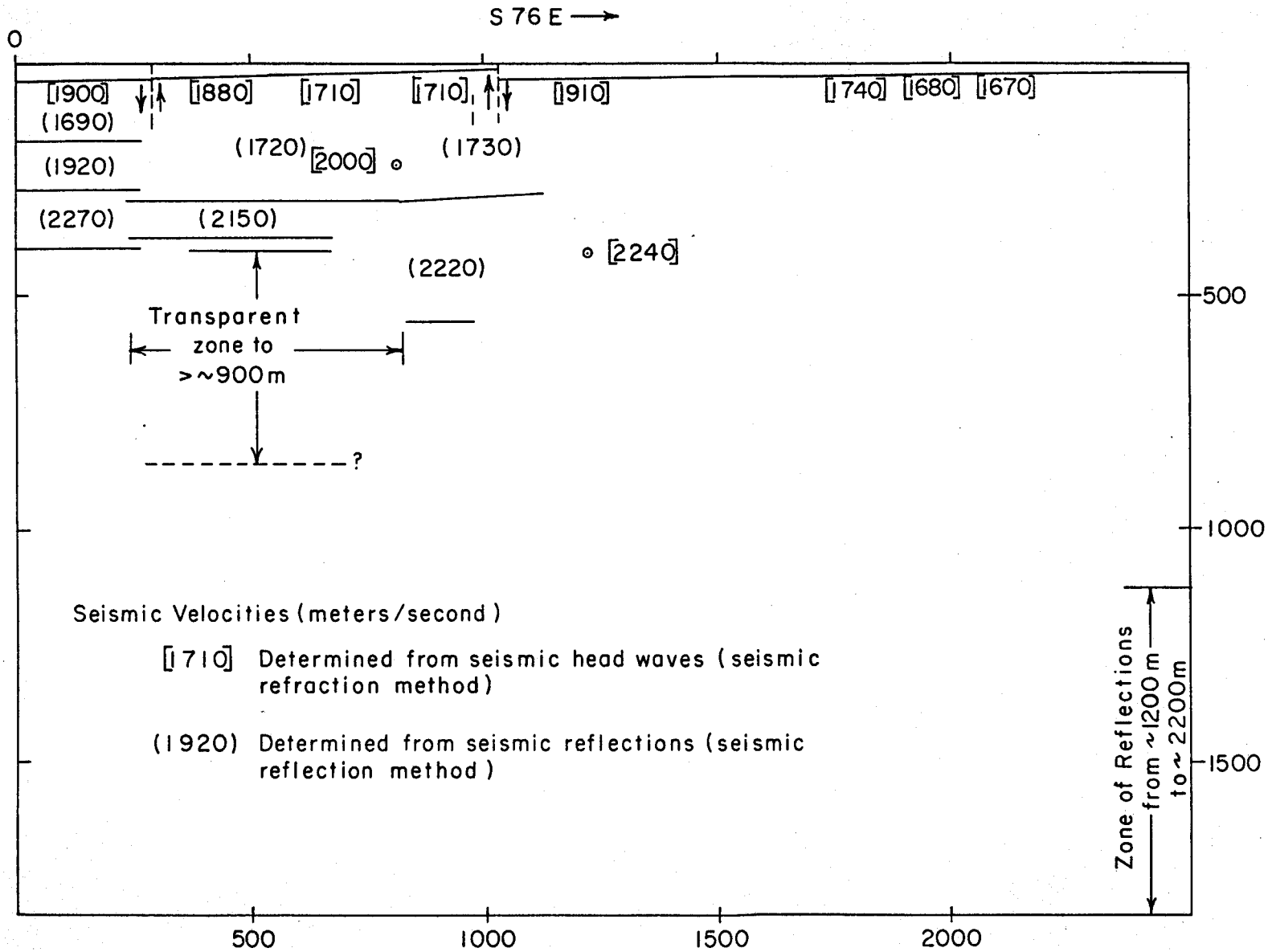

Figure 2-3. Cross section along the seismic profile showing velocities and discontinuities detected within the Tertiary fill.

The fit of the relation to the observations is not good along the entire length of the refraction profile because of rapid changes in the velocity at shallow depths (< 400 m). The velocity function indicates that the seismic energy recorded at the end of the profile (2500 m from the shot) reached a maximum velocity of 2.24 km/sec at a depth of 410 m. As shown in Figure 2-2, the velocity function from the refraction data is similar to those obtained from the sonic well logs.

To expand upon and confirm the results of the earlier seismic work, observations were made along the same line in the summer of 1979 with a new 12-channel seismograph. The instrument, a Geometrics ES 1210, allows stacking of seismic signals in the field. The field procedure was to record shorts located 312.5 m from a 275-m spread of 12 geophones. Shots and spreads were positioned to give equal amounts of moveout information to the east and to the west as well as continuous subsurface coverage. A final record was obtained by stacking the seismic signals from four separate 0.5-pound TNT explosions that were located in trenches (∿1 m x 1 m x 7 m) at right angles to the line. The standard record length was 0.5 secs at a sampling rate of 0.5 msecs. A delay of 0.3 secs was used, inasmuch as the near-surface structure and velocity were known from refraction shooting along the line in 1957 and 1958 (Ibrahim 1962). The reason for the large shot offset (312.5 m) was to avoid severe interference between surface waves and shallow reflections.

The depths and velocities calculated from some of the observed reflections in the 1979 survey are shown in Figure 2-3. The main purpose of the analysis was to obtain velocities, and thus no attempt was made to establish precisely the beginning of a reflection event even if this were possible. Thus, the depths of reflectors shown on the section should not

be interpreted as the depth to a particular geologic horizon nor should the offset in horizons between the 1957-58 and 1979 results be interpreted as fault displacements. Actually, the results of both seismic surveys indicate a fairly large number of reflecting horizons within 500 m of the surface. Those shown in Figure 2-3 were selected because of their clarity and continuity which allowed the best determination of velocity.

Discussion and Conclusions

The detailed seismic-refraction data on shallow structure revealed two faults offsetting the surface layer; the one located about 1 km from the west end of the line was the best defined (Ibrahim 1962). Neither fault has an obvious surface expression but John Hawley (personal communication 1979) believes there is geomorphic evidence for several recent faults in the area between the main New Mexico Tech campus and the mountain front to the west. The importance of these observations of recent faulting is that a deep drill hole may penetrate recent faults even if located away from the mountain front.

The velocities obtained from analyses of the seismic-refraction and reflection data to depths of a little over 500 m are characteristic of Tertiary fill, although it would be difficult to ascertain position in the Tertiary section from this information alone. However, it appears that the absence of a large dip on the reflectors does indicate that the aquitard lies below the deepest observed reflections. On the basis of extensive geologic mapping in the Socorro area, Chamberlin (personal communication 1979) believes that the aquitard should have westward dips from 10 to 20 degrees. The largest dips possible on the deep reflections appears to be about 5 degrees, either west or east. Thus, the

seismic data suggest that the aquitard must lie at depths greater than 2200 m.

Assuming a minimum thickness of 400 m for the aquitard, the target aquifer in the lower Popotosa is at a depth of at least 2600 m. This result is compatible with interpretations of gravity data (Sanford 1968; Heckert, unpublished interpretation of gravity data in the Socorro area) in same area as the seismic measurements.

Acknowledgements

Student assistants who made contributions to this seismic study were Francois Nguene, Becky Petzinger, Del Byrd, Bob Will, Dan Wilder and Tim Wallace.

References

Chamberlin, R. M., 1979, Personal communication, New Mexico Bureau of Mines and Mineral Resources, Socorro, New Mexico.

Chapin, C. E., Chamberlin, R. M., and Hawley, J. W., 1978a, Socorro to Rio Salado, in Hawley, J.W., compiler, Guidebook to Rio Grande Rift in New Mexico and Colorado: New Mexico Bureau of Mines and Mineral Resources, Circular 163, p. 121-134.

Chapin, C. E., Chamberlin, R. M., Osburn, G. R., White, D. W., and Sanford, A. R., 1978b, Exploration framework of the Socorro geothermal area, New Mexico: New Mexico Geologic Society, Special Publication 7, p. 115-129.

Hawley, J. W., 1979, Personal communication, New Mexico Bureau of Mines and Mineral Resources, Socorro, New Mexico.

Ibrahim, A-B. K., 1962, Relation between compressional wave velocity and aquifer porosity: New Mexico Institute of Mining and Technology, M.S. thesis, 59 pp.

Sanford, A. R., 1968, Gravity survey in central Socorro County, New Mexico: New Mexico Bureau of Mines and Mineral Resources, Circular 91, 13 pp.

Part 2

Geothermal Data Availability for Computer Simulation in the Socorro Peak KGRA, Socorro County, New Mexico*

Introduction

On the basis of the presence of several thermal springs (32°C or 90°F) which issue from the mountain front to the west of Socorro, New Mexico, the U. S. Geological Survey designated a 362-square kilometer (140-square mile) area in the Socorro area as the Socorro Peak Known Geothermal Resource Area (KGRA) in 1976. Supporting evidence for existence of a geothermal resource comes from geophysical studies which show anomalously high-heat flows in the area of Socorro Peak, as high as 11.7 heat-flow units (HFU) (Reiter et al. 1975; Reiter and Smith 1977; Sanford 1977b).

It is possible that the source of heat in the Socorro Peak KGRA is a magma body which is presently intruding the crust in the vicinity of the KGRA. This magma body has been studied over a period of years by Sanford and his students at New Mexico Tech (Sanford and Long 1965; Sanford et al. 1973; Sanford 1977a, 1977b; Caravella 1976; Rinehart 1976; Shuleski 1976; Fischer 1977; Sanford 1977a; Shuleski et al. 1977; Rinehart et al. 1979). Their interpretations of microearthquake seismograms have led to the mapping of five shallow (3- to 5-km or 1.9- to 3.1-mi) dike-like magma bodies to the south of Socorro Peak and of an extensive midcrustal (20-km or 12.4-mi depth) sill-like magma body. Leveling studies by Reilinger and Oliver (1976) and Reilinger et al. (1979) document a modern uplift over the proposed magma body.

*The principal authors of Chapter 2, Part 2 are David B. Hawkins, Graduate Research Assistant, and Daniel B. Stephens, Assistant Professor of Hydrology, New Mexico Institute of Mining and Technology.

Several recent geological studies have shed considerable light on the nature of the rocks which make up the Socorro Peak geothermal reservoir, notably those of Chapin et al. (1978) and Chamberlin (1980). As a result of these studies of the structure and stratigraphy in the Socorro area in conjunction with interpretation of geophysical data, Chapin et al. (1978) proposed the existence of a "leaky lineament" trending northeast-southwest through the KGRA. This "leaky lineament" is composed of a transverse shear zone which may allow the upward leakage of magma forming the bodies which have been located by geophysical techniques.

Most of the studies mentioned above on the Socorro Peak area are specific in nature. Our purpose here is to synthesize portions of previous studies which could be used as inputs to a hydrogeothermal computer simulation in the Socorro Peak KGRA. Such information would include identification of basin geometry, hydrologic and thermal properties of geologic units, sources of groundwater recharge and discharge, and chemical characteristics of the geothermal fluids. Where no information for these categories was available specifically from the Socorro area, data were collected from areas outside the KGRA which were interpreted as having similar hydrogeothermal properties.

Deep Subsurface Features

One of the most important requirements in designing a computer simulation of a flow system is the location of geologic features which control fluid movement within the geothermal system. To date, interpretation in the subsurface is based mostly on studies of tectonic setting, microearthquakes, seismic reflection, gravity, and land elevation changes.

The Socorro Peak KGRA is located within the Rio Grande Rift zone where the rift transects the northeastern edge of the Datil-Mogollon volcanic field of Oligocene to early Miocene age (Chapin et al. 1978). The Rio Grande Rift is a major north-trending structure formed by an east-west crustal extension beginning between about 25 and 29 m.y. ago and continuing to the present (Chapin and Seager 1975).

To the north of Socorro the rift consists of linked north-trending structural depressions and to the south of Socorro near Las Cruces, New Mexico, the rift merges in a complex way with the Basin and Range Province. In this area, the Socorro-Lemitar mountains and the Chupadera Mountains comprise intergraben horst blocks which separate the La Jencia Basin (which includes the Snake Ranch Flats) to the west from the Rio Grande Valley to the east (see Figure 2-4). These intergraben horsts were formed relatively late in the history of the rift, about 9 to 10 m.y. ago (Chapin and Seager 1975). The only other location along the rift at which a similar development of horsts through several thousand feet of Cenozoic fill is known to occur is at Las Cruces, New Mexico (Sanford, Mott, Shuleski, Rinehart, Caravella, Ward, and Wallace 1977).

Within the KGRA, microearthquake studies suggest the presence of an extensive magma body in the crust at a depth of about 18 to 20 kilometers (11.2 to 12.4 mi) (Sanford, in Chapin et al. 1978; Sanford, Mott, Shuleski, Rinehart, Caravella, Ward, and Wallace 1977). Similar studies delineate a number of smaller and shallower magma bodies south of the deeper intrusion at depths of as little as 2.5 km (1.6 miles) (Sanford, Rinehart, Shuleski, and Johnston 1977) (see Figure 2-5). High temperature gradients and high heat flows measured in boreholes in the Socorro Mountains suggest that these shallow bodies may be interpreted as a geothermal heat source (Reiter and Smith 1977; Sanford 1977b).

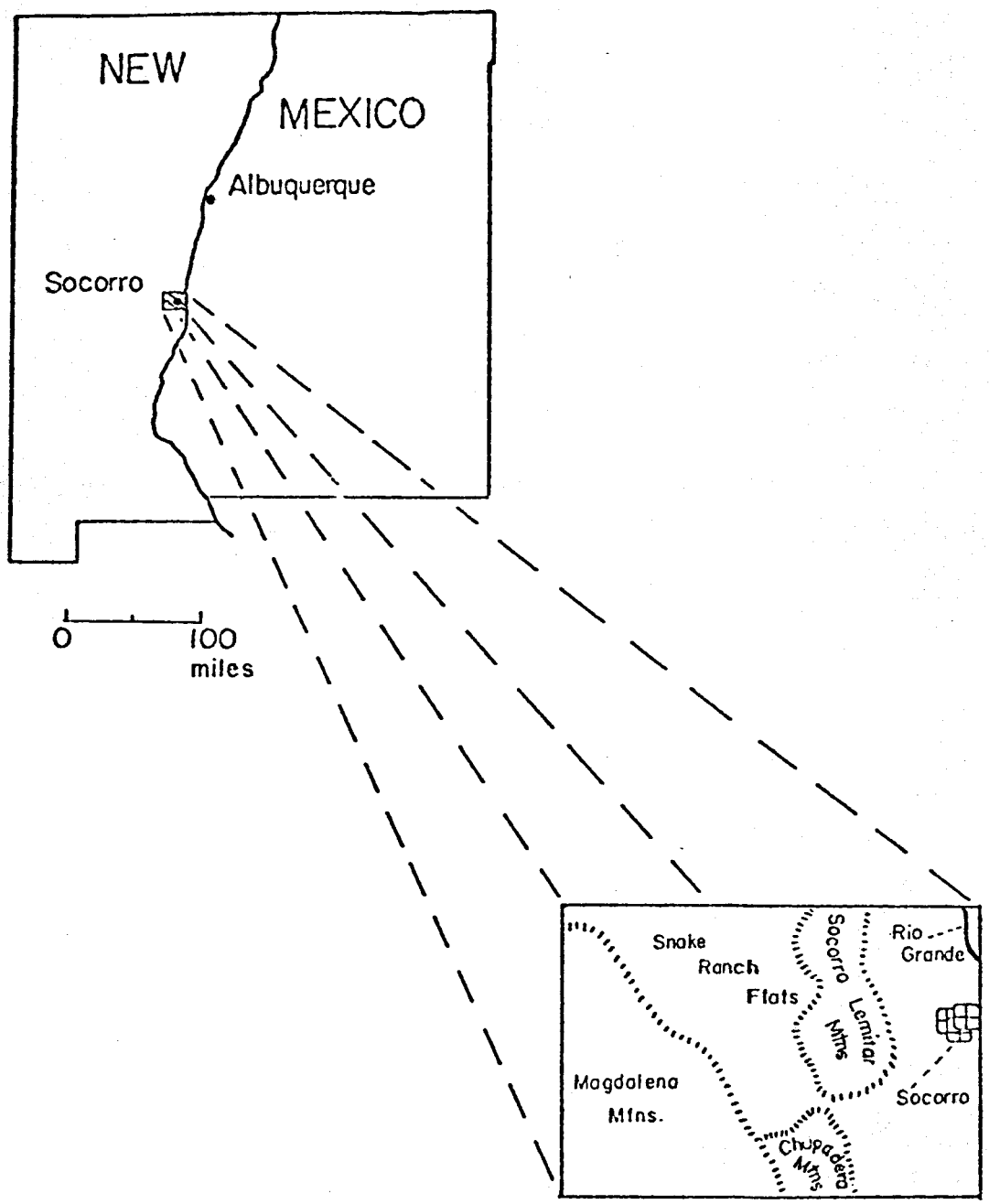

Figure 2-4. Location of the study area (Gross and Wilcox 1980).

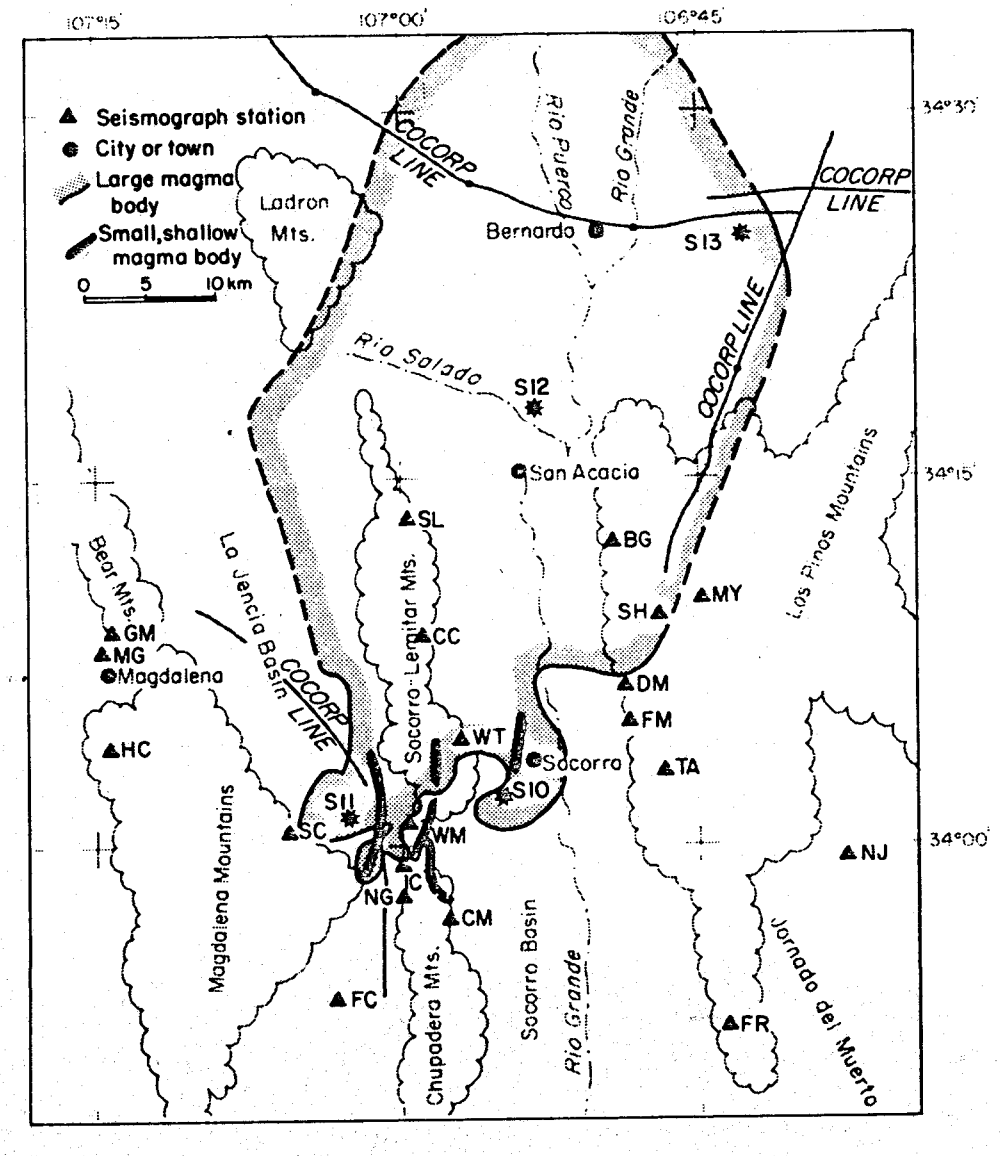

Figure 2-5. Geographical extent of the extensive magma body. A solid line indicates that the boundary is closely defined; a dashed line denotes some uncertainty of its location. Positions of the Consortium on Continental Reflection Profiling (COCORP) lines and the shallow magma bodies are also shown (Sanford 1978).

Large scale seismic-reflection studies carried out by the Consortium on Continental Reflection Profiling (COCORP) also suggest the presence of the extensive magma body (Brown et al. 1979). Interpretation of the COCORP results indicates that the magma body was intruded after the main episodes of rift faulting and thus could be quite recent (Brown et al. 1979). In fact, Reilinger et al. (1979) have noted a topographic uplift of 20 cm (7.9 in) between 1911 and 1951 about 25 km (15.5 mi) north of Socorro. This uplift may indicate that the magma body is presently intruding at midcrustal depths.

The COCORP has carried out several deep seismic-reflection surveys in the vicinity of the Socorro Peak KGRA (Brown et al. 1979). One line has been run in the vicinity of the southern end of the La Jencia Basin (see Figure 2-5), and the data from this profile could be useful in defining the thickness and extent of the hydrogeologic units.

A detailed gravity survey covering parts of the Rio Grande depression and adjacent areas in Socorro County was performed by Sanford (1968). This gravity survey shows that the Rio Grande Valley in the Socorro area is actually made up of three linked structural depressions (see Figure 2-6). The two structural depressions which lie to the east of the Socorro-Lemitar mountains are asymmetrical. Their western margin appears to be a high-angle normal fault with a displacement of as much as 4 km (2.5 mi). The eastern margins of these depressions rise much more gradually, possibly indicating the presence of step faulting (Sanford 1978). From the gravity survey, the La Jencia Basin appears to be more symmetrical than the Rio Grande Valley, but with comparable structural relief. Sanford (1968) constructed gravity profiles based on a suite of rocks which included a complete Mesozoic section. However, according to Chamberlin (1980), the Mesozoic section is probably missing and therefore the profiles computed by Sanford may be inaccurate.

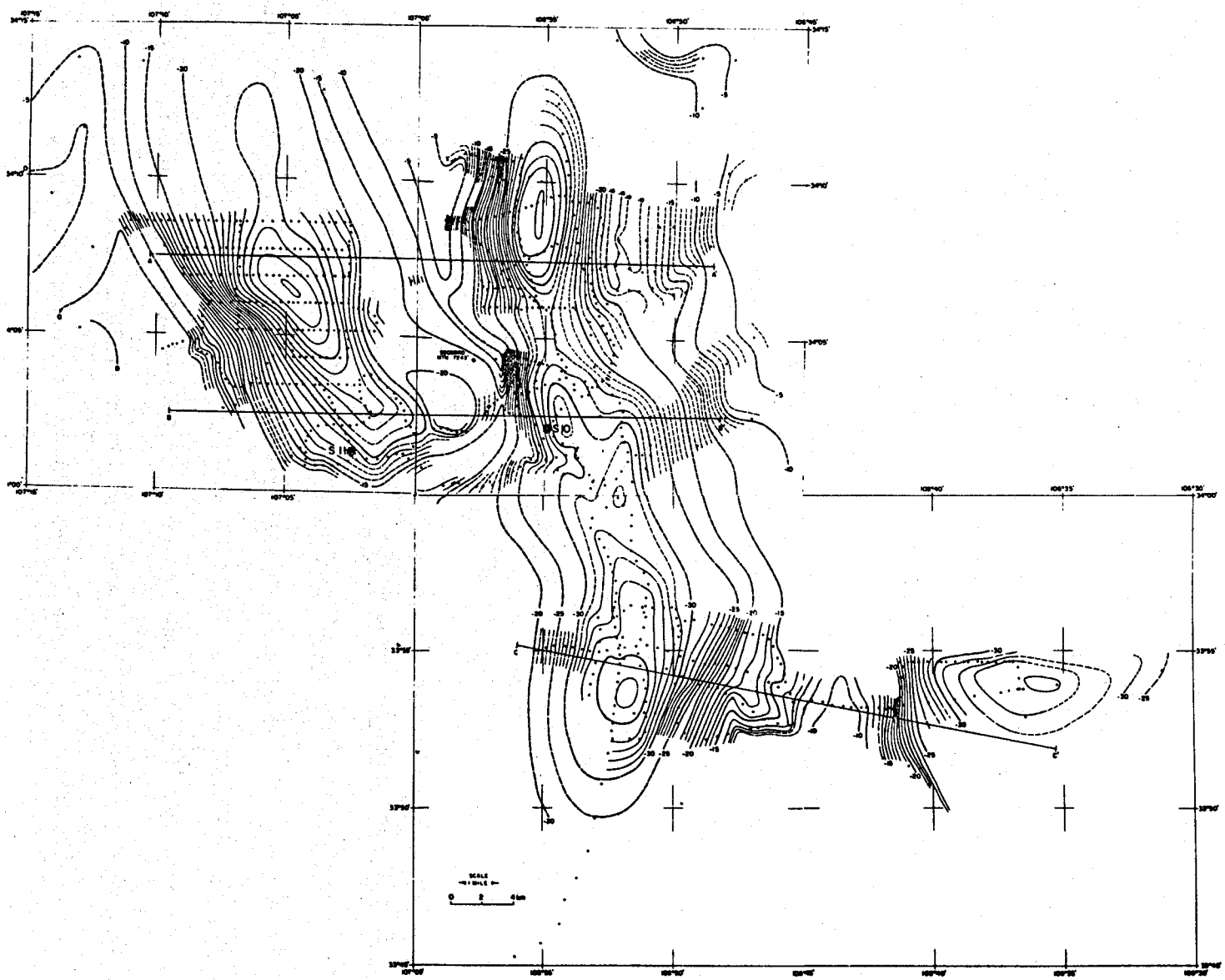

Figure 2-6. Bouguer gravity map of the Socorro area; terrain and regional corrections have been applied (Sanford 1968).

Sanford (personal communication 1980) indicates that reinterpretation of the gravity profiling in light of the presently available geological data would probably produce a significant increase in the depth of the post-Mesozoic valley-fill sediments which would consist primarily of rocks of the Santa Fe Group. Based on the original model proposed by Sanford (1968), there are at least 305 m (1000 ft) of Santa Fe valley fill present. Gross and Wilcox (1980) performed some calculations which indicate that if the entire Mesozoic section is missing, the thickness of the Santa Fe Group in the La Jencia Basin may be as much as 1000 m (3300 ft).

Another method of delineating the geometry of the geological units comprising the geothermal system is analyses of samples from deep drill holes. Such studies have been undertaken in the area of interest by various private companies involved in exploration for geothermal energy. Unfortunately, the results of the core analyses are proprietary and are not available to the public (Chapin, personal communication 1980). Exploratory drilling of deep-core holes has been proposed by a number of private companies (Chapin, personal communication 1980).

Geologic Units and Material Properties

There have been a number of geologic studies and surface mapping projects which have been carried out in the immediate vicinity of the Socorro Peak KGRA, notably those of Lasky (1932); Miesch (1956); Waldron (1956); Debrine et al. (1963); Smith (1963); Lowell (1967); Burton (1971); Bruning (1973); Machette (1977); Osburn (1977); and Chamberlin (1980). Useful summaries of much of these data may be found in reports by Chapin et al. (1974, 1975, and 1978) and Chapin and Seager (1975).

Probably the most comprehensive and up-to-date work dealing with the rocks of the Socorro Peak geothermal reservoir system is that of Chamberlin (1980). These geological interpretations and those of Chapin et al. (1978) are used here to outline the geological units within the geothermal system. For a detailed description of the geologic structure and stratigraphy of the Socorro Peak KGRA, refer to the study by Chamberlin (1980).

The rocks of the Socorro Peak KGRA are composed of a complex series of depositional units. Precambrian metamorphic rocks and Paleozoic sediments are overlain by ash-flow tuffs and flows of varying compositions vented from a nearby chain of Oligocene cauldrons. Because of their depositional environment, these volcanic units vary considerably in thickness. During the Miocene, a broad, early-rift depression in the Socorro area called the Popotosa Basin was being filled by heterolithic mudflow deposits, fanglomerates, playa mudstones, and minor interbedded basalt flows. Numerous rhyodacite to high-silica rhyolite domes and tuffs erupted in the Socorro Peak area 12 m.y. to seven m.y. ago onto the playa floor of the Popotosa Basin. The floor of the Popotosa Basin was disrupted by rift faulting and epeirogenic uplift seven to four m.y. ago to form the modern Lemitar-Socorro mountains. Some basaltic eruption occurred to the southwest of Socorro Peak as recently as four m.y. ago. Erosion of the modern highlands in the area led to the deposition in the Rio Grande Basin of the Sierra Ladrones Formation consisting of intertonguing fluvial sands and piedmont gravels (Chamberlin 1980). A simplified geologic map of the area is shown in Figure 2-7 and a composite stratigraphic column of the Socorro Peak area is shown in Figure 2-8.

Fractures developed in rocks in the study area as a result of at least three major tectonic events: (1) the formation, collapse, and resurgence of the Socorro Cauldron; (2) faulting due to movement along the transverse shear

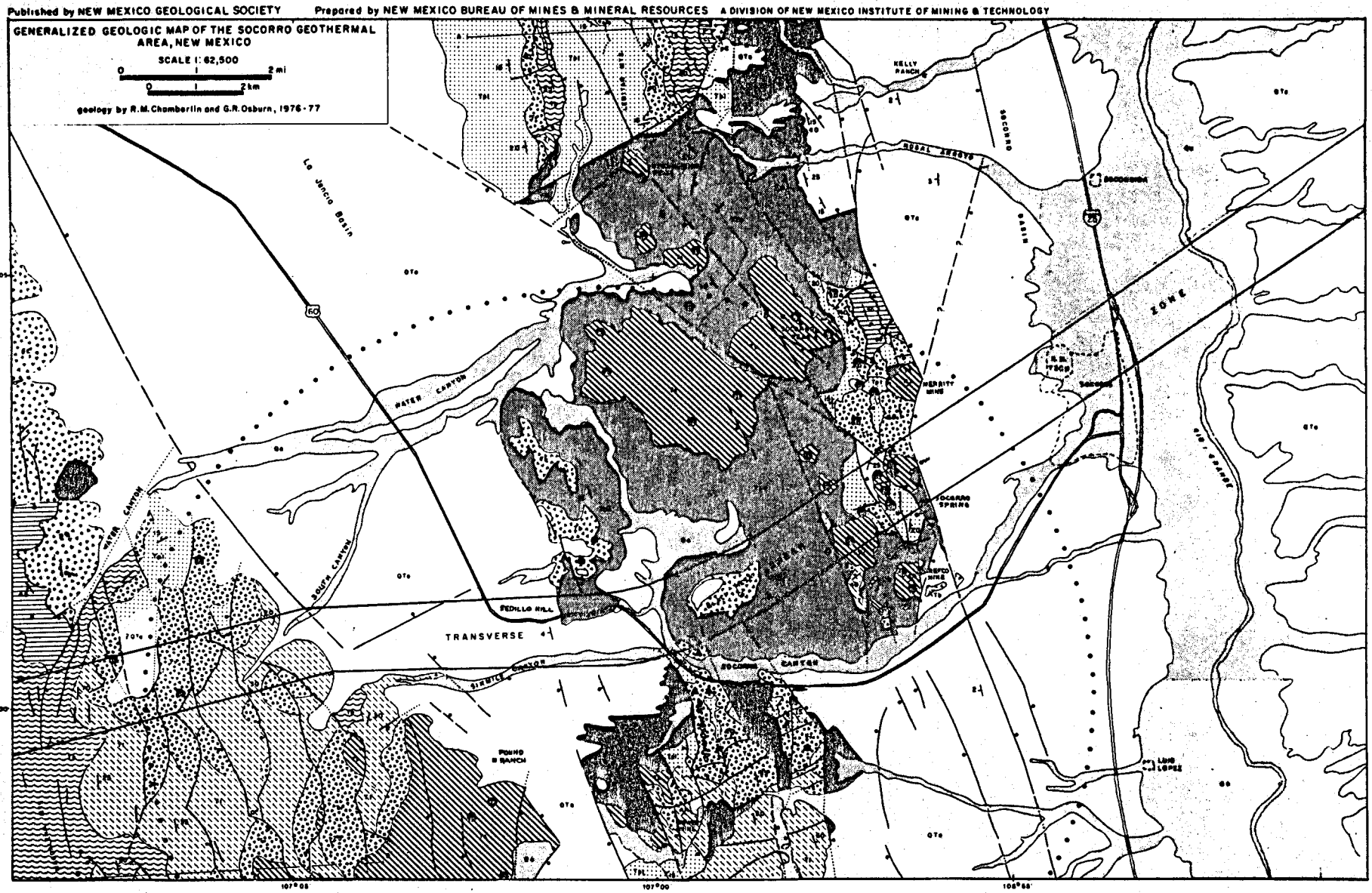

Figure 2-7. Generalized geologic map of the Socorro geothermal area, Socorro, New Mexico (geology by R. M. Chamberlin and G. R. Osburn). See following page for legend.

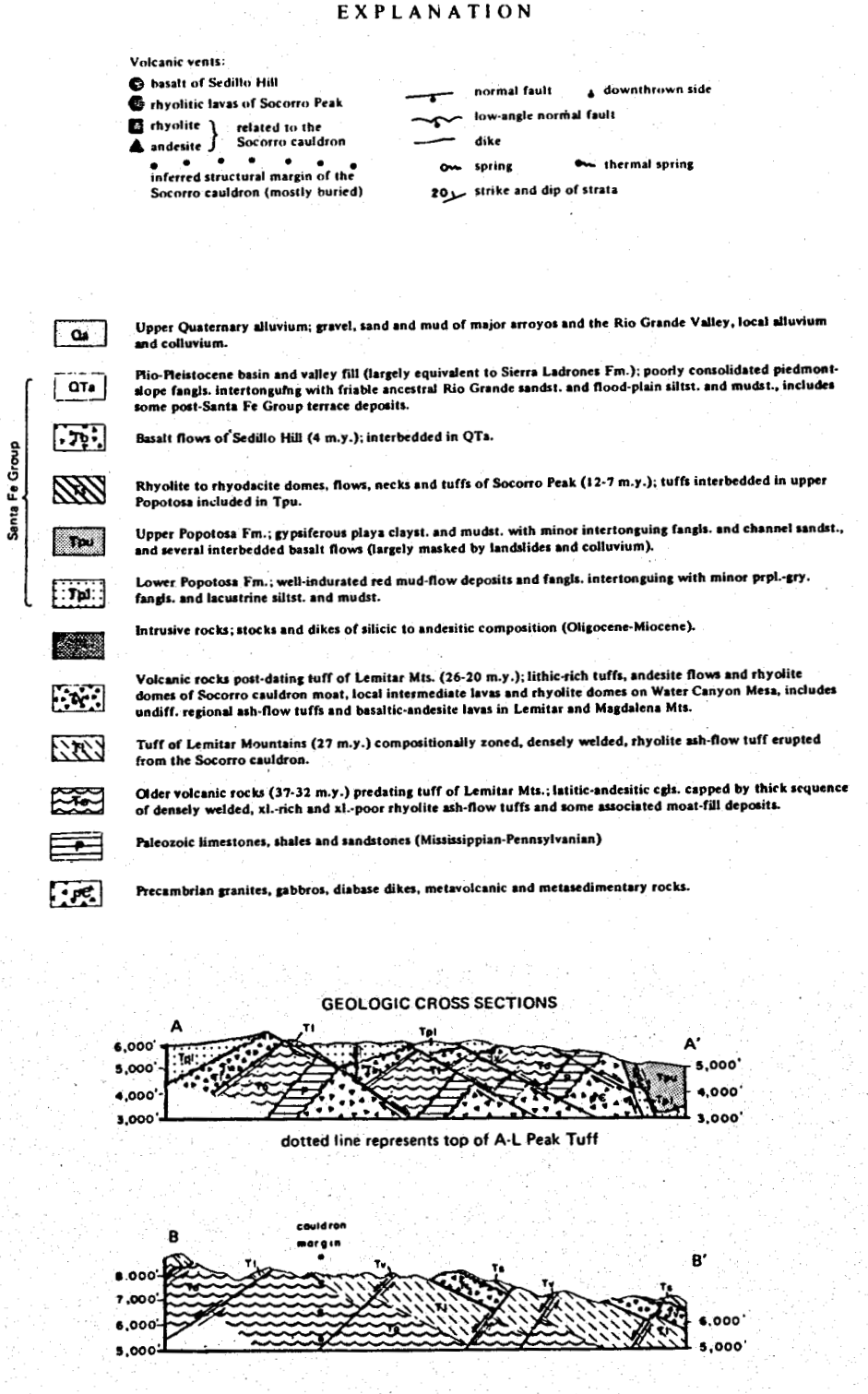

Figure 2-7. (continued).

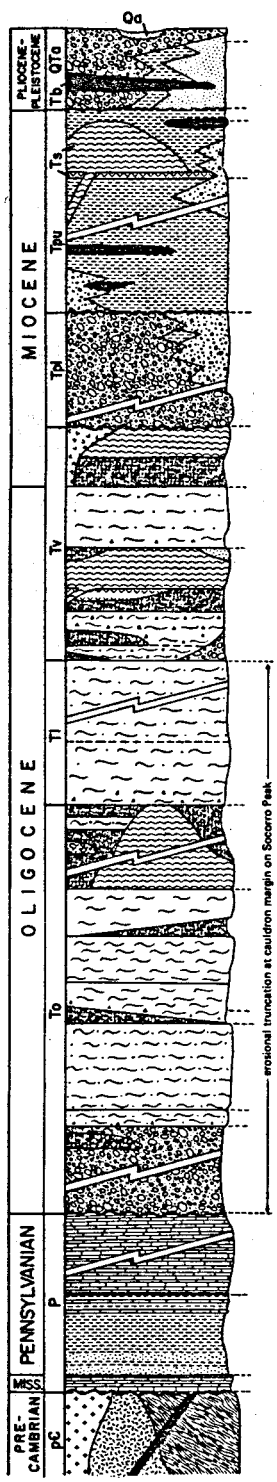

Post Santa Fe Alluvium: (0-50', 15 m) ALLUVIUM, SLUMP BLOCKS, and COLLUVIUM: inset deposits of gravel, sand, & mud along the Rio Grande & its tributaries. Fan, piedmont-slope and playa deposits of La Jencia bolson. Extensive slump & colluvial deposits on slopes around Socorro Pk., Strawberry Pk., & Black Mesa mantle mudstones of upper Popotosa Fm.

Sierra Ladrones Formation: (0-1000', 305 m) PIEDMONT-SLOPE, RIVER CHANNEL and FLOOD PLAIN DEPOSITS, and BASALT FLOWS: buff to pale-rd., poorly indur., fangl. w/ mixed clasts of all major rock types shed off present highlands. Fangl. intertongue w/ lt.-gry., friable, well-sorted, fn.-med.-grd. sands of ancestral Rio Grande. Flood plain deposits are rd. & grn. mudst. & siltst. Basalt of Sedillo Hill (4 m.y.) underlies piedmont-slope facies & overlaps ancestral Rio Grande sands & piedmont facies near Grefco mine.

Rhyolite of Socorro Peak: 7-12 m.y. (0-800', 244 m) SILICIC DOMES, FLOWS, and TUFFS: pale-rd.-gry. to lt.-gry. rhyolite & rd.-brn. to lt.-gry. rhyodacite flow-banded lavas, domes, necks, & tuffs. Tuffs interbedded w/ clayst. of upper Popotosa at Socorro Spring, of Blue Canyon, Kelly Ranch (12 m.y.), and N. of Sedillo Hill.

Upper Popotosa Formation: (0-2500', 762 m) CLAYSTONES, MUDSTONES, SILTSTONES, SANDSTONES, CONGLOMERATES, and BASALT FLOWS: Dk.-rd.-maroon gyp. playa clayst. & mudst. w/ thn. bds. of yel.-brn. to grn.-gry. clayst. North of Strawberry Pk., playa deposits intertongue w/ buff, cgl. ss w/ hydro. altered clasts derived from Magdalena area. At Grefco mine, mudst. intertongue w/ pale-rd. cgls. derived from E. of Rio Grande and w/ perlite-rich cgls. shed from Grefco dome. Basalt flows interbedded w/ playa deposits near Pound Ranch, Strawberry Pk., & Hwy. 60.

Lower Popotosa Formation: (0-1500', 457 m) MUDFLOW DEPOSITS, FANGLOMERATES, and minor LACUSTRINE DEPOSITS: rd.-brn., v. well-indur., heterolithic, crs. cgls. w/ abun. clasts of underlying volc. units & locally grading downward into ancient colluvial breccias. Gry. siltst., mudst., & thn. fresh-water ls. intertongue w/ lt.-gry. to prpl.-gry. cgl. ss. in Socorro Pk.-Blue Canyon area. Facies relationships reflect late-stage topography of Socorro caldera.

Lavas of Water Canyon Mesa: 20 m.y. (0-600', 183 m) INTERMEDIATE to SILICIC LAVAS and TUFFS: rd. silicic lavas & tuffs underlain by intermed., dk.-gry. to dk.-rd.-brn., dense lavas; intruded and overlain by flow-banded wht. rhyolite domes & flows.

Tuff of South Canyon: 26 m.y. (0-600', 183 m) ASH-FLOW TUFFS: multiple-flow, simple cooling unit of rhyolite ash-flow tuffs. Lower zone of lt.-gry., poorly to densely welded, xl.-poor tuff w/ "botryoidal" pumice & lithic-rich lenses. Upper zone of med.-gry. to prpl.-gry., mod. to densely welded, mod. xl.-rich tuff w/ chatoyant sanidine & euhedral qtz.

Unit of Luis Lopez: (0-2000', 610 m) ASH-FLOW TUFFS, ANDESITE LAVAS, RHYOLITE DOMES and TUFFS, minor LANDSLIDE DEPOSITS and TUFFACEOUS SANDSTONES. Moat fill of Socorro cauldron. Lt.-gry., pumiceous, lithic-rich, poorly welded, rhyolite ash-flow tuffs intertongue w/ andesite flows, vent agglomerates, & minor andesitic laharic breccias. Pale-rd., orng.-rd., & lt.-gry. flow-banded rhyolite lavas, domes and tuffs cap sequence. Contemporaneous tongue of La Jara Peak Basaltic Andesite (0-800', 244 m) in Lemitar Mts.

Tuff of Lemitar Mountains: 27 m.y. (0-400', 122 m outflow; 700-2900', 213-884 m cauldron) ASH-FLOW TUFFS: multiple-flow, comp. zoned, simple to compound cooling unit of densely welded tuff. Lt.-gry. to pale-rd., xl.-poor lower member 200-800 ft. (61-244 m) thk. in Socorro cauldron but only locally present as thn. lenses on outflow sheet. Md.-rd., xl.-rich, qtz.- & biotite-rich, 2-feld. upper member 0-400 ft (122 m) outflow facies, 350-2900 ft (107-884 m) cauldron facies. Contact sharply gradational & welded. Xl.-rich clots common at top. Lithic-rich zones w/ Precambrian & andesite clasts widespread S. of Tower mine.

Unit of Sixmile Canyon: (0-2000', 610 m) ANDESITE to BASALTIC ANDESITE LAVAS, RHYOLITE LAVAS and DOMES, ASH-FLOW TUFFS, LAHARIC BRECCIAS, and SANDSTONES: post-collapse fill of Sawmill Canyon cauldron. Drk.-gry. mafic lavas intertongue with & surround other rock types. Heterolithic breccias along cauldron walls. Contemporaneous tongue of La Jara Peak Basaltic Andesite (0-500', 152 m) in Lemitar Mts.

A-L Peak Tuff: 32 m.y. (0-700', 213 m outflow; 2000+', 610+ m cauldron) ASH-FLOW TUFFS: composite sheet w/ basal gray-massive, middle flow-banded, & upper pinnacles members. All densely welded, xl.-poor, l-feld., rhyolite, ash-flow tuffs. Sources are Mt. Withington, Magdalena, & Sawmill Canyon cauldrons. Tongue of La Jara Peak Basaltic Andesite (0-200', 61 m) usually separates flow-banded & pinnacles members.

Lava Flows: (0-300', 91 m) ANDESITE to BASALTIC ANDESITE: unnamed tongue of dense prpl.-rd. flows locally present in SW Lemitar Mts.

Hells Mesa Tuff: 32-33 m.y. (0-500', 152 m outflow; 3000+', 915 m cauldron) ASH-FLOW TUFFS: rhyolite, multiple-flow, simple cooling unit, densely welded, xl.-rich, qtz.-rich, 2-feld., mass. tuffs. Pk. to rd.-brn. when fresh, gry. when propyl. altered. Weathers to blocky bldrs. Basal tuffs similar to tuff of Granite Mtn.; abrupt increase in qtz. 10-25 ft above base.

Spears Formation – tuff of Granite Mountain: (0-100', 30 m) ASH-FLOW TUFFS: qtz.-latite, multiple-flow, simple cooling unit, densely welded, xl.-rich, lithic-rich, qtz.-poor, mass. tuffs; rd.-brn. when fresh, dk.-grn.-gry. when propyl. altered.

Spears Formation – volcaniclastic unit: 37-33 m.y. (0-1500', 457 m) CONGLOMERATES, MUDFLOW DEPOSITS, SANDSTONES, LAVAS, and ASH-FLOW TUFFS: volcaniclastic apron of latite to andesite comp., becomes coarser & contains more volc. units up & to south.

Madera Limestone: (500-1500', 152-457m) LIMESTONES: thk., homo. sequence of gry. to blk. micrites w/ a few thn. bds. of med.-crs.-gnd. qtz. ss. Up. 200-300 ft (61-91 m) is rd., grn., & gry. micrites grading up. into arkosic bds. of Abo Fm. Nodular micrites abun. throughout.

Sandia Formation: (550-650', 168-198 m) SHALES, QUARTZITES, and LIMESTONES: gry. to blk., sdy., carb. sh. and siltst. w/ thn. bds. of gry. to brn., med.-crs.-gnd. qtz. ss. (abun. near base) & gry., med.-gnd. micritic ls. (gradational w/ Madera).

Kelly Limestone: (0-90', 27 m) LIMESTONE: lt.-gry., med.-crs.-gnd., thk.-bdd. crinoidal biosparrites.
Caloso Formation: (0-30', 9 m) LIMESTONES and CONGLOMERATES: basal arkosic cgl. overlain by gry., mass., sdy. or pbly. micrites.

Basement: ARGILLITES, QUARTZITES, VOLCANIC and PLUTONIC ROCKS: thk. sequence of low-grade metased. & metavolc. rocks intruded by granitic & gabbroic plutons, & diabase dikes.

Figure 2-8. Complete stratigraphic column of the Socorro area. Thickness of units are not to scale (Chapin et al. 1978).

zone related to the northeast-trending Morenci Lineament; and (3) horst and graben-type faulting relating to the formation of the Rio Grande Rift zone (Chamberlin 1980; Chapin et al. 1978). An additional possible source of fracturing of the rock matrix is jointing due to cooling of the welded ash-flow tuffs and lavas.

In attempting to model the geothermal system, basic rock properties must be quantified. These parameters include permeability, storage coefficient, porosity, compressibility, thermal conductivity, specific heat, and density. Unfortunately, very little specific information on the physical parameters of the rocks actually present in the Socorro Peak KGRA is known. For this reason, the existing literature must be used to provide physical parameters for the general rock types which are thought to be present in the geothermal system. Unfortunately, this approach has some limitations. For instance, many of the physical parameters presented in the literature were determined in the laboratory from experiments on small rock samples. The parameters determined from such a small sample may not actually be representative of the macroscopic properties of rocks in the geological environment. Another closely associated problem is that rocks under high-confining pressures or high heat may exhibit properties which differ significantly from rocks of similar lithologies which are not exposed to these conditions. Nonetheless, physical parameters reported in the literature provide a useful starting point for model calibration.

Precambrian Basement Rocks

Rocks of Precambrian age presumably underlie the entire geothermal system and are presumed to define a lower boundary of the groundwater flow system. In some places, Precambrian rocks have been displaced upward by faulting and presently are very near the surface (see Figure 2-7; Sanford, 1968, Figure 8;

Chamberlin, 1980, cross sections G-G' and H-H'). The principal surface exposures of rocks of Precambrian age are located on the eastern side of the Lemitar Mountains and on the eastern side of the Magdalena Mountains from Water Canyon north to Magdalena (Waldron 1956). Outcrops of Precambrian rocks in the Lemitar Mountains include porphyritic granites, biotite gneisses, and low-grade metasedimentary argillites and quartzites intruded by feldspathic and basic dikes (Waldron 1956; Chapin et al. 1978). Precambrian metasediments such as argillities are common in the Water Canyon area. Granites are exposed at the north end of the Magdalena Mountains.

In general, the crystalline Precambrian rocks have unfavorable aquifer properties except where extensively fractured or weathered. A well in the Magdalena Mountains (T.3.S, R.3.W, Sec. 10) is reported to produce groundwater from a weathered granite zone (Waldron 1956). Tables 2-1 through 2-6 present some physical parameters of rocks presumed to be similar to those Precambrian rocks present in the Socorro Peak KGRA.

An estimate of the specific storage coefficient, S_s, of rocks similar to those of the Precambrian in the Socorro Peak geothermal system may be obtained from the equation

$$S_s = \rho g(\alpha + n\beta),$$

where ρ = density of water, g = acceleration of gravity, α = compressibility of rock, n = porosity of rock, and β = compressibility of water. If $\rho \cong 1000$ kg/m^3, $g \cong 9.8$ m/s^2, $\alpha = 1.56 \times 10^{-10}$ ms^2/kg (granite @ 0 kb pressure) to 1.76×10^{-11} ms^2/kg (granite @ 9 kb pressure) (values from Brace 1965; as given in Table 2-1), $n = 0.00013$ to 0.011 (maximum and minimum values from Table 2-5 in Brace 1965), and $\beta = 4.4 \times 10^{-10}$ ms^2/kg, S_s ranges from 1.73×10^{-7} m^{-1} to 1.58×10^{-6} m^{-1}.

Table 2-1. Volume compressibility of crystalline rocks.

Lithology	Pressure	Volume Compressibility Enclosed (cm^2/dyne)	Volume Compressibility Unenclosed (cm^2/dyne)	Reference	Comments
	(Kg/cm^2)				
Granite, Quincy,	0	75.6	19.2	Zisman 1933	Laboratory experiments on cores. NOTE: This is only a sampling of the values available. For a more comprehensive treatment, which is beyond the scope of this work, see Birch 1966.
(from 100 ft	120	40.2	18.5	"	
depth in quarry)	600	25.3	16.7	"	
Granite, Quincy,	0	89.9	21.1	"	"
(from 275 ft	120	50.8		"	"
depth in quarry)	600	25.0		"	"
Granite, Rockport	0	91.7	19.5	"	"
	120	50.4	18.7	"	"
	600	26.6		"	"
	(bars)				
Granite, Westerly	2,000	-	21.2	Birch 1942	"
	10,000	-	18.2	"	"
Granite, Stone Mountain	2,000	-	20.6	"	"
	10,000	-	18.2	"	"
Granite, Washington	2,000	-	22.3	"	"
	10,000	-	18.2	"	"
Granite, Stone Mountain	2,000	-	20.6	"	"
	10,000	-	18.2	"	"
	(kbars)				
Granite	0	15.6	-	Brace 1965	Volume compressibility of jacketed samples measured by electric resistance strain gauges.
	9	.76		"	

Table 2-2. Thermal conductivity of crystalline rocks.

Lithology	Temperature (°C)	Thermal Conductivity at One Atmosphere (mcal/sec-cm-°C)	Reference	Comments
Granite			Birch and Clark 1940	NOTE: For more complete listing of values, see Clark 1966.
Barre, Vermont	0	6.66		
	50	6.25	"	Experiments were conducted on rock disks in the laboratory.
	100	5.90	"	
	200	5.50	"	
Westerly, R.I.	0	5.80	"	"
	50	5.60	"	"
	100	5.42	"	"
	200	5.12	"	"
Granite, Rockport, Massachusetts	0	8.4	"	"
	50	7.8	"	"
	100	7.2	"	"
	200	6.5	"	"
	300	5.9	"	"
Granite gneiss parallel to foliation	0	7.42	"	"
	100	6.58	"	"
perpendicular to foliation	0	5.17	"	"
	100	4.82	"	"
Crystalline rock complex (including granite, gneissic granite, amphibolite, granodiorite gneiss)	0	5.43 - 9.08	Sibbit, Dodson, Tester 1979	From laboratory experiments performed on 14 drill cores (maximum depth 2929 m) drilled into Precambrian rock in the Jemez Mountains of New Mexico.
	50	5.20 - 8.30	"	
	100	5.03 - 7.66	"	
	150	4.89 - 7.16	"	
	200	4.76 - 6.74	"	
	250	4.65 - 6.40	"	

Table 2-2. (continued).

Lithology	Temperature (°C)	Thermal Conductivity at One Atmosphere (mcal/sec-cm-°C)	Reference	Comments
Granite		7.86 - 10.34	Lundstrom and Stille 1978	Determined in situ by filling a borehole with warm water and measuring the temperature decrease as a function of time.
Gneiss		5.4	Combs 1980	Mean of 38 samples.
Granite		6.9	"	Mean of 27 samples.
Granodiorite		5.1	"	Mean of 17 samples.
Diorite		4.9	"	Mean of 10 samples.
Quartzitic sandstone parallel to bedding	0	13.6	Birch and Clark 1940	Experiments were conducted on rock disks in the laboratory.
	100	10.6	"	
	200	9.0	"	"
perpendicular to bedding	0	13.1	"	"
	100	10.3	"	"
	200	8.7	"	"
Slate perpendicular to bedding	0	4.6	"	"
	100	4.2	"	"
	200	4.1	"	"
Diabase	0	5.04 - 5.62	"	"
	100	5.01 - 5.35	"	"
	200	5.03 - 5.37	"	"
	300	5.03	"	"
	400	5.06	"	"
Gabbro	0	4.75 - 5.55	"	"
	100	4.75 - 5.25	"	"
	200	4.76 - 5.13	"	"
	300	4.78	"	"
	400	4.81	"	"

Table 2-3. Specific heat of crystalline rocks.

Lithology	Temperature (°C)	Specific Heat (cal/g-°C)	Reference	Comments
Granite	0	0.155 - 0.191	Goranson 1942	Computed from data on constituent minerals.
	200	0.227	"	"
	400	0.256 - 0.260	"	"
	800	0.270 - 0.332	"	"
Granodiorite	0	0.167	"	"
	200	0.232	"	"
	400	0.258	"	"
	800	0.279	"	"
Diabase	0	0.167	"	"
	200	0.208	"	"
	400	0.234	"	"
	800	0.284	"	"
	1200	0.325	"	"
Gabbro	0	0.172	"	"
	200	0.236	"	"
	400	0.263	"	"
	800	0.282	"	"
Gneiss	0	0.177	"	"
	200	0.241	"	"
Slate	0	0.170	"	"
	200	0.239	"	"
	400	0.263	"	"
	800	0.287	"	"
Quartzite	0	0.167	"	"
	200	0.232	"	"
	400	0.270	"	"
	800	0.279	"	"
	1200	0.318	"	"

Table 2-4. Density of crystalline rocks.

Lithology	No. of Samples	Density (g/cm^3) Mean	Range	Reference	Comments
					NOTE: For additional values, see Daly et al. 1966.
Gneiss (Precambrian Grenville Formation)	25	2.85	2.70 - 3.06	Bean 1953	Laboratory experiments on fresh, unweathered samples from outcrops.
Quartzite (Precambrian Grenville Formation)	1	2.62			
Granite and Syenite (Precambrian)	11	2.70	2.63 - 2.79	"	"
Anorthosite (Precambrian)	3	2.72	2.68 - 2.75	"	"
Gabbro (Precambrian)	3	2.97	2.91 - 3.04	"	"
Slate (Taconic Sequence)	17	2.81	2.72 - 2.84	"	"
Phyllite (Nassau Formation of Taconic Sequence	1	2.82	2.72 - 2.84	"	"
Precambrian rock assemblage in Green Mountain anti-clinorum	11	2.74	2.68 - 2.82	"	"
Precambrian gneiss in Chester Dome	7	2.69	2.66 - 2.73	"	"

Table 2-5. Porosity of crystalline rocks.

Lithology	Porosity (fractional)	Reference	Comments
Granite	0.003-0.011	Brace 1965	These porosities were obtained by using the expression $(\rho_s-\rho_b)/\rho_s$, and therefore may not represent effective porosity.
Quartzite	0.006	"	"
Granite	0.00013	Lundstrom and Stille 1978	This porosity was obtained from an in situ tracer test of a well in a fractured granite.

Table 2-6. Permeability of crystalline rocks.

Lithology	Confining Pressure (bars)	Permeability (m^2)	Reference	Comments
Westerly Granite	50	3.5×10^{-19} ($\pm 4.0 \times 10^{-20}$)	Brace et al. 1978	Experiments performed on core samples.
	100	2.3×10^{-19} ($\pm 2.5 \times 10^{-20}$)	"	"
	250	1.2×10^{-19} ($\pm 1.2 \times 10^{-20}$)	"	"
	500	6.3×10^{-20} ($\pm 7.0 \times 10^{-21}$)	"	"
	1000	3.5×10^{-20} ($\pm 4.0 \times 10^{-21}$)	"	"
	2000	1.6×10^{-20} ($\pm 3.0 \times 10^{-21}$)	"	"
	4000	4.2×10^{-21} ($\pm 8.0 \times 10^{-22}$)	"	"
	60	1.18×10^{-15}	Pratt et al. 1977	Measured along a joint in an in-place block of granite.
				NOTE: Lundstrom and Stille (1978) found a hydraulic conductivity of 0.4×10^{-10} m/s from in situ tests in granite. This value was found to be independent of pressure gradient but the hydraulic conductivity was reduced by 50% with a bedrock temperature increase from 10° to 35°C.

Rocks of Paleozoic Age

A relatively thin layer of Mississippian rocks overlies the Precambrian units in parts of the study area. The basal Mississippian unit is the Caloso Formation which consists of a sequence of basal sandstones, arkoses, and shales followed by a series of gray-cherty, sandy or pebbly micritic limestones. The Caloso is uncomformably overlain by the Mississippian age Kelly Limestone which is a gray, medium-to-coarse-grained, thick-bedded crinoidal biosparite (Armstrong 1962; Chapin et al. 1978). The Kelly Limestone is well jointed and brittle and may have good fracture permeability at fairly shallow depths. Ores deposited in the Kelly mining district by hydrothermal fluids circulation also suggest that the Kelly Limestone is relatively permeable (Chapin et al. 1978).

The Mississippian rocks in the study area are unconformably overlain by rocks of Pennsylvanian age: the Sandia Formation and Madera Limestone. The oldest of the Pennsylvanian rock units is the Sandia Formation. The Sandia Formation is a pod-shaped body which reaches a maximum thickness of 211 m (692 ft) along a north-south line through Socorro. This formation contains a varying suite of lithologies with sandstones predominating in the lower one-third of the unit and limestones and shales being the principal lithologies in the upper two-thirds. Overall, coarse-grained terrigenous clastics, principally sandstones, make up approximately 18 percent of the Sandia Formation. The grains of these deposits are generally poorly sorted and well cemented with silica and calcite, resulting in a very low intergranular porosity. Terrigenous mudrocks, mostly clay shales, make up approximately 70 percent of the Sandia Formation. Porosity in these rocks is low and occurs as microscopic fractures, vugs, and channels. The remainder of the Sandia Formation consists of carbonate rocks, principally carbonate

mudstones. In these units, intergranular porosity is low and secondary porosity also exists in channels and fractures (Siemers 1978).

The Sandia Formation grades upward into the Madera Limestone. In the study area, the Madera Limestone ranges in thickness from 152 to 457 m (499 to 1499 ft) (Chapin et al. 1978). Carbonate rocks, principally mudstones and wackestones, make up approximately 69 percent of the Madera Limestone. Terrigenous mudrocks, mainly mud shales, form approximately 27 percent of the Madera with the remainder composed of well-cemented granular terrigenous clastics (Seimers 1978). Primary porosity in all of the various lithologic units of the Madera is considered to be quite low; however, secondary porosity may be significant. Reportedly, a municipal well for the town of Magdalena produces 6.3×10^{-3} m^3/sec (100 gpm) from fractured Paleozoic limestones (Chapin et al. 1978).

The rocks of Paleozoic age which might be involved in the Socorro Peak geothermal system form a rather diverse suite of sedimentary lithologies. Physical parameters for similar lithologies are presented in Tables 2-7 through 2-10.

Values for specific storage of rocks similar to the Paleozoics in the Socorro Peak geothermal area could be quite variable, based on reported values. As an example, Mercer et al. (1975) used a specific storage of 1×10^{-3} m^{-1} for a suite of similar rocks in their modeling studies of the Wairakei geothermal system in New Zealand. Winograd and Thordarson (1975) estimate the specific storage of similar rocks to be on the order of 3×10^{-5} to 3×10^{-6} m^{-1}.

Oligocene to Early Miocene Rocks

Rocks of Oligocene age are separated from Pennsylvanian rocks in the Socorro Peak area by an erosional unconformity. The rocks of Oligocene and

Table 2-7. Permeability of sedimentary rocks.

Location	Lithology	Description	Depth of Sample (m)	Confining Pressure (kbar)	Pore Pressure (kbar)	Permeability (m^2) Temp. = 21°C	Permeability (m^2) Temp. = 104°C	Reference	Comments
Geysers, Calif.	Franciscan Greywacke	Intact rock	1190	0.34	0.034	1.97×10^{-20}	-	Pratt et al. 1977	Values obtained in the laboratory under in situ stress conditions from experiments on rocks from geothermal reservoirs. Note the effect of fractures on permeabilities.
		Open joint	1190	0.34	0.034	3194×10^{-17}	-		
Raft River, Idaho RRGE-3	Calcareous sandstone	Healed fracture	1520	0.34	0.149	2.96×10^{-17}	5.92×10^{-18}	"	
	Silty shale	Healed fracture (intact)	1522	0.34	0.149	9.87×10^{-19}	9.87×10^{-19}	"	
	Siltstone	Healed fracture	1608	0.34	0.172	2.96×10^{-17}	1.97×10^{-17}	"	
	Siltstone	Fracture filled with silt	1609	0.34	0.172	1.18×10^{-16}	3.95×10^{-17}	"	
						(data below presented without reference to temperature)			
	Limestone	----------	----	----	-----	4.72×10^{-13}	9.87×10^{-17}	Archie 1952	Laboratory samples.
	Sandstone	----------	----	----	-----	7.90×10^{-13}	4.64×10^{-16}	Muskat 1937	Laboratory samples.
----------	Very fine-grained clayey shale	----------	----	----	-----	1.00×10^{-21}	1.00×10^{-25}	Young, Low and McLatchie 1964	Values from laboratory experiments on core samples.
	Fine-grained silty sandstones and siltstones	----------	----	0.101	-----	4.80×10^{-22}	----------	"	Parallel to bedding
			----	0.131	-----	7.90×10^{-19}	----------	"	"
----------	Shale	----------	----	----	-----	4.00×10^{-18} (.02 N NaCl sol.)	----------	Gonduin and Scala 1958	Values from laboratory experiments on shale disks cut from cores perpendicular to bedding.
----------	Alluvial fan, fluvial, fanglomerate, lakebed and mud-flow deposits, unconsolidated to poorly consolidated	----------	----	----	-----	2.71×10^{-13}	3.79×10^{-12}	Winograd and Thordarson 1975	Values from laboratory tests on cores and pumping tests.

Table 2-8. Thermal conductivity of sedimentary rocks.

Lithology	Temperature (°C)	Depth of Sample (m)	Thermal Conductivity (mcal/cm-sec-°C)	Reference	Comments
Limestone	0		5.4 - 8.2	Clark 1966	
	100		4.9 - 7.0	"	
	200		4.8 - 6.5	"	
Shale	20		3.26	"	
	35	318 - 1685	3.55	"	
	35	1685 - 2796	4.20	"	
	35	-	5.70	"	
Sandstone	20		6.62 - 6.78	"	
	35	-	4.7	"	
	30	-	9.67 - 17.7	Woodside and Messmer 1961	Laboratory experiments on water saturated core samples.
Siltstone, minor limestone and shale	25	30 - 739	7.13 ± 0.18	Sass et al. 1971	Laboratory experiments on water saturated drill cuttings.
Dense blackshale, some sandstone and siltstone		739 - 1029	7.13 ± 0.22	"	
Quartzite sandstone, minor shale		1029 - 1128	10.67 ± 0.56	"	
Dolomite limestone	25	1509 - 2118	12.42 ± 0.51	"	
Argillaceous limestone, pyritic in parts	25	2118 - 2301	8.19 ± 0.75	"	
Quartzite sandstone	25	2301 - 2766	10.87 ± 0.78	"	

Table 2-9. Specific heat of sedimentary rocks.

Lithology	Temperature (°C)	Specific Heat (cal/g-°C)	Reference	Comments
Limestone	50	0.16 - 0.24	Goranson 1942	Computed from constituent mineral percentages
	65	0.20	"	
Shale	65	0.18	"	"
Sandstone	50	0.17 - 0.19	"	"
	59	0.22	"	"
	65	0.19	"	"

Table 2-10. Porosity (fractional) and saturated-bulk density of sedimentary rocks.

Lithology	Depth of Sample (ft)	Number of Samples	Porosity Range	Porosity Mean	Saturated Bulk Density (average, g/cm^3)	Reference	Comments
Cambrian Mount Simon sandstone	13,005 - 13,605	9	0.002 - 0.025	0.007	2.70	Daly et al. 1966	NOTE: The values listed are only representative values. For a more complete listing, see Daly et al. 1966.
Mississippian Berea sandstone	0 - 2,160	18	0.047 - 0.195	0.141	2.39	"	"
Cretaceous sandstones Wyoming	0 - 3,187	33	0.083 - 0.270	0.197	2.32	"	"
Carboniferous limestones Great Britain	Outcrop	24	0.022 - 0.149	0.057	2.56	"	"
Cretaceous Rose Limestone Texas	20.5 - 30.5	10	0.160 - 0.188	0.168	2.37	"	"
Oligocene and Miocene shale Venezuela	600	6	0.313 - 0.358	0.335	2.17	"	"
	3,500	9	0.178 - 0.256	0.211	2.35	"	"
	6,100	3	0.091 - 0.106	0.096	2.52	"	"
Limestone			0.066 - 0.557	0.300		Morris and Johnson 1967	
Mudrocks			0.014 - 0.452	0.350		"	
Siltstone				0.430		"	
Claystone				0.060		"	
Shale							
Sandstone			0.137 - 0.493	0.330		"	

early Miocene age include the Spears Formation, Hells Mesa Tuff, A-L Peak Tuff, a unit of Sixmile Canyon, tuff of the Lemitar Mountains, a unit of Luis Lopez, tuff of South Canyon, and the lavas of Water Canyon Mesa. These units form a complex suite of lithologies which are mainly welded tuffs with some andesitic to rhyolitic flows, breccias, and other minor volcaniclastics (Chapin et al. 1978). Because of erosion and the nature of their deposition these units have thicknesses which vary widely from place to place. In outcrops, many of the tuffs have been observed to be densely welded and brittle with well developed jointing and presumably good fracture permeability. Geochemical studies have shown that in many cases these tuffs display alteration and probably served as an important reservoir rock in an ancient geothermal system (Chapin et al. 1978).

Fortunately, similar lithologies are common in other geothermal systems and there has been a substantial amount of data published for these types of volcanic rock. Table 2-11 gives values for permeabilities of similar volcanic rocks. As noted earlier, the physical parameters may vary with depth of burial. Figure 2-9 shows a plot of permeability as a function of hydrostatic stress for fused tuff. This plot implies that the permeability-confining pressure relationship is hysteretic. Figure 2-9 also suggests that the effects of decreasing confining pressure are small compared to the effects of increasing pressure. Therefore, it is likely that the values of permeability determined from cores subject only to atmospheric confining pressure may actually be fairly representative of permeabilities at the depth sampled.

Table 2-12 gives values for thermal conductivities of various volcanic rocks similar to those in the Socorro Peak geothermal system. Note that one value is actually from rocks in the Socorro Peak geothermal system. Figure 2-10 (Keller 1960) shows an empirical correlation between values of thermal

Table 2-11. Permeability of volcanic rocks.

Lithology	Permeability (m^2)	Reference	Comments
Pumice breccias and vitric tuffs	1.00×10^{-13} - 1.00×10^{-14} 3.00×10^{-13} - 3.00×10^{-14}	Mercer et al. 1975 Mercer and Faust 1979	Values used for Wairakei Formation in geothermal modeling at Wairakei Geothermal system, New Zealand.
Welded tuff, fracture	2.96×10^{-11} - 4.94×10^{-12}	Sorey et al. 1978	Value determined by calibration of geothermal system model. It was noted that these values represent an integration of the effects of fracture permeability over the volume of the reservoir rock.
Ash	3.20×10^{-16} - 7.10×10^{-19}	"	Values from experiments performed on core samples.
Rhyolite flow	8.30×10^{-13} - 4.50×10^{-18}	"	
Rhyolite tuff	1.80×10^{-17} - 1.40×10^{-14}	"	
Basalt flow	5.50×10^{-17}	"	
Andesite flow	7.20×10^{-19}	"	

	Range	Average		
Bedded tuffs	1.68×10^{-14} - 7.5×10^{-19}	3.95×10^{-17}	Keller 1960	Values from experiments on core samples.
Bedded tuffs, pumaceous	6.02×10^{-14} - 3.65×10^{-15}	1.14×10^{-14}	"	
Friable tuffs	2.66×10^{-14} - 8.29×10^{-17}	1.38×10^{-15}	"	
Welded tuffs	5.72×10^{-14} - 8.88×10^{-19}	3.26×10^{-16}	"	
Unwelded ash-flow tuff	1.08×10^{-13}		Winograd and Thordarson 1975	Values from laboratory tests on cores and pumping tests.
Ash-fall and ash-flow tuffs non-welded to densely welded with local rhyolite flows and tuffaceous sandstones and siltstones.	3.25×10^{-16} - 3.25×10^{-18}		"	

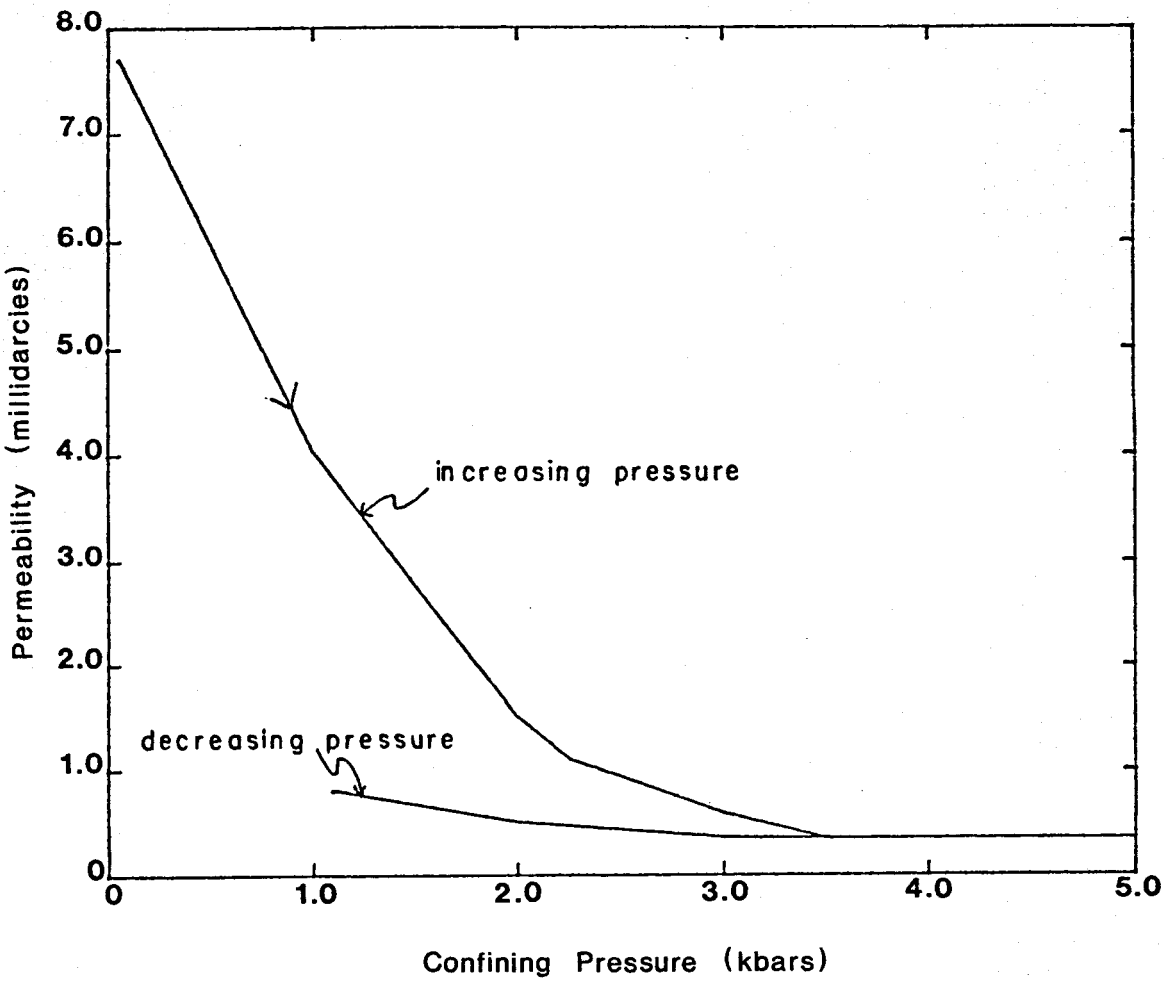

Figure 2-9. Plot of permeability as a function of hydrostatic stress for fused tuff (Pratt et al. 1977).

Table 2-12. Thermal conductivity of volcanic rocks.

Lithology	Thermal Conductivity (mcal/cm·sec·°C)	Reference	Comments
Volcanic breccia	4.0	Sanford 1977b	Value determined in the laboratory from samples of a volcanic breccia which outcrops in the Socorro KGRA.
Rhyolite flow	2.3	Sorey et al. 1978	Values determined from core samples.
Ash	2.1	"	"
Pumaceous tuff	2.2	"	"
Tuff	2.5	"	"
Rhyolite tuff	2.0 - 2.3	"	"
Basalt flow	3.6	"	"

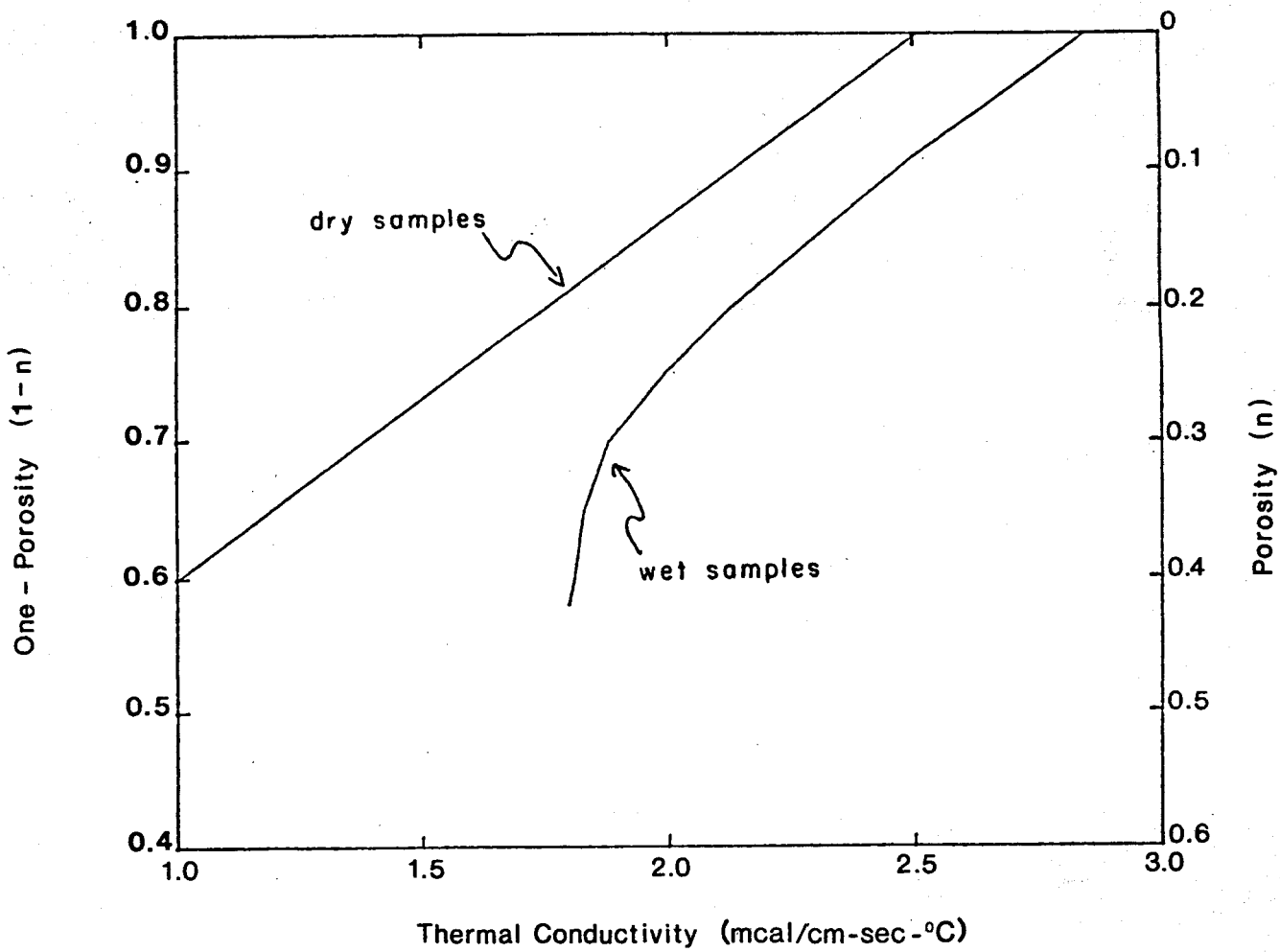

Figure 2-10. Empirical correlation between average values of thermal conductivity and porosity for samples of tuff (Keller 1960).

conductivity and porosity for tuffs from the Oak Spring Formation of Tertiary age at the Nevada Test Site. These tuffs were described as rhyolitic to quartz latitic in composition, and they include bedded tuffs, friable tuffs, and welded tuffs.

Tables 2-13 and 2-14 give values for porosity and density, respectively, for volcanic rocks. A value of 0.22 cal/g-°C for specific heat was found for the Waiora Formation (pumice breccias and vitric tuffs) by model calibration by Mercer et al. (1975). Approximate values for specific storage for volcanic rocks may be computed from the relation

$$S_s = \rho g(\alpha + n\beta).$$

For $\rho \cong 1000$ kg/m^3, $g = 9.8$ m/s^2, $\alpha = 2.9 \times 10^{-10}$ ms^2/kg (Mercer et al. 1975) to 5.0×10^{-10} ms^2/kg (Mercer and Faust 1979), $n = 0.12$ to 0.35 (Blankennagel and Weir 1973) or 0.30 to 0.47 (Sorey et al. 1978), and $\beta = 4.4 \times 10^{-10}$ ms^2/kg, the specific storage can be expected to range from 3.36×10^{-6} m^{-1} to about 6.95×10^{-6} m^{-1}.

Santa Fe Group

The uppermost rocks which form a significant part of the Socorro Peak geothermal system are probably rocks of the Santa Fe Group of Miocene to Pliocene age. These include the Popotosa Formation, the rhyolite of Socorro Peak, and the Sierra Ladrones Formation.

The thickest and most widespread facies of the lower Popotosa Formation consists of extremely well-indurated, dark reddish-brown, heterolithic mudflow deposits and conglomerates (Chamberlin 1980). This facies is distinguished by its dark reddish-brown color and extreme degree of induration by cryptocrystalline-silica cement (Bruning 1973). Bruning (1973) suggested that the anomalous dark reddish-brown color and high degree of induration of the

Table 2-13. Porosity (fractional) of volcanic rocks.

Lithology	Number of Cores	Range of Total Porosity	Average Total Porosity	Range in Number of Fractures Per Foot	Average of Number of Fractures Per Foot	Reference	Comments
Ash-flow tuff, non-welded to densely welded; mainly devitrified but glassy at base and top. Zeolitized tuff at base in subsurface	4	0.072 - 0.172	0.140	0.5 - 2.2	1.40	Blankennagel and Weir 1973	Values from laboratory experiments on core samples obtained at the Nevada Test Site.
Ash-flow tuff, densely welded and bedded ash-flow tuffs	9	0.128 - 0.362	0.220	0.7 - 2.5	1.40	"	"
Rhyolite lavas and partially welded ash-flow tuffs	4	0.137 - 0.311	0.229	0 - 0.1	<0.10	"	"
Rhyolite lavas and welded ash-flow and ash-fall tuffs	14	0.129 - 0.335	0.214	0 ->4.0	>0.70	"	"
Ash-flow tuff, densely welded, devitrified	14	0.042 - 0.240	0.121	0 - 3.2	0.90	"	"
Ash-flow tuff, non-welded to densely welded, devitrified	5	0.081 - 0.384	0.196	0 - 7.5	1.80	"	"
Ash-fall tuff and non-welded to partially welded ash-flow tuff	13	0.280 - 0.449	0.355	0 - 0.3	0.07	"	"
Rhyolite lavas and bedded ash-fall tuffs and non-welded ash-fall and ash-flow tuffs	84	0.123 - 0.439	0.262	0 - 1.4	0.18	"	"
Rhyolite lava and non-welded ash-fall and ash-flow tuffs	3	0.296 - 0.503	0.377	0 - 0.1	<0.10	"	"
Non-welded ash-fall and ash-flow tuff	12	0.194 - 0.386	0.283	0 - 0.3	0.06	"	"

Table 2-13. (continued).

Lithology	Number of Cores	Range of Total Porosity	Average Total Porosity	Range in Number of Fractures Per Foot	Average of Number of Fractures Per Foot	Reference	Comments
Pumaceous and vitric tuffs	0.2					Mercer et al. 1975	Values used for Waiora Formation in modeling the Wairakei geothermal system, New Zealand.
"	0.25					Mercer and Faust 1979	"
Bedded tuffs			0.388 ± 0.070			Keller 1960	Values from laboratory experiments on core samples from the Oak Spring Formation, Nevada.
Bedded tuffs (pumaceous)			0.402 ± 0.126			"	"
Friable tuffs			0.355 ± 0.138			"	"
Welded tuffs			0.141 ± 0.089			"	"
Tuffs and flows		0.030 - 0.480				Winograd and Thordarson 1975	Values obtained from laboratory experiments on core samples.
Ash		0.565 - 0.661				Sorey et al. 1975	"
Rhyolite flow		0.071 - 0.310				"	"
Pumaceous tuff		0.295 - 0.468				"	"
Rhyolite tuff		0.295 - 0.468				"	"
Basalt flow		0.139				"	"
Andesite flow		0.102				"	"

Table 2-14. Density of volcanic rocks.

Lithology	Grain or Powder Density (g/cm^3)	Reference	Comments
Bedded tuffs	2.44 ± 0.11 (one standard deviation)	Keller 1960	Laboratory experiments on core samples.
Bedded tuffs (pumaceous)	2.28 ± 0.12	"	"
Friable tuffs	2.33 ± 0.24	"	"
Welded tuffs	2.55 ± 0.09	"	"
Ash	2.36 - 2.69	Sorey et al. 1978	Laboratory experiments on core samples.
Pumaceous tuff	2.32	"	"
Rhyolite tuff	2.28 - 2.35	"	"
Rhyolite flow	2.52	"	"
Andesite flow	2.66	"	"
Basalt flow	2.87	"	"

lower Popotosa mudflow deposits and conglomerates were formed in situ by groundwater alteration. It has been suggested by Chapin et al. (1978) that the anomalous coloration and induration were acquired during potassium metasomatism related to an ancient geothermal system of late Miocene age. Field observations by Chamberlin (1980) led him to propose a syngeneic origin for the red color and silica cement and to envision the deposition of the mudflows and conglomerates in a hot spring environment which could account for both abundant ferric-hydroxide and silica in solution. Chamberlin (1980) noted that the dark red color and silica cement are limited in space and time to this one particular stratigraphic unit. The remainder of the lower Popotosa consists primarily of moderately-indurated muddy conglomerates and fine-grained deposits (Chamberlin 1980).

The upper Popotosa is comprised mostly of moderately-to-poorly indurated, fine-grained playa deposits with some intertonguing fanglomerates (Chamberlin 1980).

The rhyolite of Socorro Peak (Chapin et al. 1978) consists of silicic domes, flows, and tuffs which are, in places, interbedded with the upper Popotosa Formation. This unit is of variable thickness and probably has physical properties similar to those described in Tables 2-11 through 2-14.

The Sierra Ladrones Formation of Machette (1977) consists of piedmont-slope, river-channel, and flood-plain deposits with local intercalated basalt flows. The sediments form a suite of lithologies which include fanglomerates, well-sorted medium-grained sandstones, and mudstones. These sediments are, in general, less well-indurated than those of the Popotosa Formation and are considered to have more favorable fluid transmitting properties.

The physical properties of rocks similar to those of the Santa Fe Group are found under various lithologies as listed in Tables 2-7 through 2-14. It would appear that the Popotosa Formation would have little primary permeability; however, fracture permeability may be quite good as evidenced by the fact that Socorro Spring, Sedillo Spring, and an unnamed cold spring northeast of Strawberry Peak issue from the lower Popotosa Formation (Chapin et al. 1978).

Groundwater Recharge

Recharge to a groundwater system is one of the most difficult parameters to obtain in most hydrologic systems, particularly in semiarid basins. It is also one of the most important parameters required for model development. In this area of interest, there are essentially two types of recharge: (1) areal recharge and (2) recharge from infiltration in drainage channels. Areal recharge is that recharge which occurs over large areas and involves infiltration of precipitation directly through the soil and rock to the main body of the aquifer. Seepage from ephemeral streams may occur following flash floods in a usually dry arroyo. Recharge occurs along mountain fronts where water in mountain streams seeps into permeable sediments near the apex of alluvial fans.

The physiography in the vicinity of the Socorro Peak KGRA is quite variable and includes steep-sided mountains at great relief (Magdalena and Socorro-Lemitar mountains) and broad flat areas of very low relief (La Jencia Basin). The Magdalena Mountains reach elevations of over 3200 m (10,500 ft) in places and the La Jencia Basin has an elevation of the order of 1830 m (6000 ft). The lowest part of the study area has predominantly desert scrub such as creosote bush and grasses. There are some coniferous forests on the

upper elevations of the Magdalena Mountains and small areas of juniper, scrub oak, and mesquite growth elsewhere, mostly on the lower slopes of the Magdalenas and near arroyos.

Appendix A contains a map of water-table contours in the vicinity of the Socorro Peak KGRA. These contours show that the general direction of groundwater flow is east from the Magdalena Mountains area through the southern end of the La Jencia Basin and then through the Socorro Mountains, with some discharge occurring at springs along the eastern mountain front. The water-level contour map in Appendix A suggests that recharge occurs beneath Socorro Peak. However, the elevation of a single spring is the principal basis for drawing the contours as indicated in this area. Additional water-level information in many areas would be useful in defining the direction and rate of groundwater flow. Such data should be collected to determine hydraulic gradients within aquifers and across aquitards.

The precipitation which could contribute recharge to hydrogeologic units in the geothermal system varies considerably in time and space. Magdalena, located to the west of the KGRA at an elevation of 1993 m (6540 ft), has a mean annual precipitation of 29.82 cm (11.74 in) from 53 years of record. The mean annual temperature is reported to be 11.1°C (52.0°F) from 36 years of record. The potential evapotranspiration for Magdalena is calculated to be 93.5 cm (36.84 in) by the Blaney-Criddle method using a monthly crop coefficient representative of alfalfa (Gabin and Lesperance 1977). On the average, 57 percent of the precipitation falls in the summer months (i.e., July, August, and September) when the potential for evaporation is quite high.

The mean annual precipitation at Socorro (elevation 1398 m or 4585 ft) is 23.75 cm (9.35 in) based on 76 years of record. The mean annual temperature is reported to be 13.8°C (56.8°F) and the potential evapotranspiration is

calculated to be 117.22 cm (46.15 in) annually (Gabin and Lesperance 1977). On the average, 48 percent of the annual precipitation falls in the summer months.

Romero and Wilkening (unpublished manuscript) report that an average of 44.98 cm (17.71 in) of precipitation was received annually at the Langmuir Laboratory in the Magdalena Mountains at an elevation of 3240 m (10,630 ft) over the period 1966 through 1975, with 67 percent of that precipitation falling during the summer months.

Kelly Ranch, located on the margin of the La Jencia Basin at an elevation of 2042 m (6700 ft), receives a mean annual precipitation of 34.54 cm (13.60 in) from 28 years of record, with 59 percent of that falling in the summer months (Gabin and Lesperance 1977).

A class-A evaporation pan is maintained at the Bosque del Apache National Wildlife Refuge, located on the Rio Grande about 32 km (20 mi) south of Socorro at an elevation of 1377 m (4520 ft). The mean annual pan evaporation (8 years of record) is reported to be 247.57 cm (97.47 in) and the potential evapotranspiration is calculated to be 117.98 cm (46.45 in) (Gabin and Lesperance 1977). The Bosque del Apache National Wildlife Refuge receives an average of 22.45 cm (8.84 in) of precipitation annually based on 71 years of record.

These representative figures indicate that for the semiarid area adjacent to the Socorro Peak KGRA the average annual precipitation is much less than the average annual potential evapotranspiration. The figures related for potential evapotranspiration were determined on the basis of a ground cover consisting of alfalfa. The actual evapotranspiration would be dependent on the vegetation type and density and the associated soil type; however, it may be surmised that recharge to the aquifer system at the Socorro Peak KGRA is

relatively small and recharge from precipitation falling on the soil and percolating down through the soil horizon to the aquifer is probably not very significant. In fact, as stated by Wallace and Renard (1967), "Transmission losses from flow events, . . . , are a primary source of groundwater recharge in the southwestern United States. Direct recharge through the soil profile is almost nonexistent because of the high-potential evaporation and low precipitation."

A study of the recharge characteristics of the ephemeral stream systems in the Socorro Peak KGRA could contribute significantly to a computer simulation as well as to the general body of literature dealing with that subject. There has been some research dealing with the topics of transmission losses and recharge from ephemeral streams in arid or semiarid areas, for example, Wallace and Renard (1967) and Gelhar et al. (1979). There is no information on recharge along the Magdalena Mountain front, possibly the principal source of recharge to the geothermal reservoir.

Besbes et al. (1978) outline four techniques for estimating recharge from ephemeral streams: (1) estimation of recharge by considering flow in the unsaturated zone, which requires measurement of average stream width, stream-length contributing recharge, infiltration rate, and flow duration; (2) estimation of recharge by observation of water-table recovery in piezometers in the vicinity of the stream, which requires determination of the specific yield of the aquifer materials; (3) estimation of recharge by model calibration; and (4) estimation of recharge by assumption of a linear-reservoir model, which involves deconvolution of the fluctuations of the piezometers in the vicinity of the ephemeral streams.

Gelhar et al. (1979) used a stochastic model of infiltration from a perched ephemeral stream to a phreatic aquifer which was developed by using

spectral representation theory to solve the flow equation involved. The theory was applied by Gelhar et al. (1979) to a semiarid watershed area near Roswell, New Mexico. This method was also used to evaluate aquifer parameters in the vicinity of the ephemeral stream.

Although estimation of recharge by model calibration is probably the least costly method encountered, it requires knowledge of the spatial distribution of aquifer parameters and accurate water-level data throughout the basin. In the Socorro Peak KGRA, other aquifer parameters and water-level data are generally poorly known; therefore, estimation of recharge by model calibration could be subject to large errors.

Groundwater Discharge

Groundwater discharge from the Socorro Peak geothermal system occurs in the form of evapotranspiration, well pumpage (for domestic, stock, and other uses), spring flow, and underflow into the Rio Grande Valley. Evapotranspiration from the water table is negligible because the water table is generally very deep. In the La Jencia Basin and in the foothills of the Magdalena and Socorro mountains, nearly all of the well pumpage is from small domestic and stock wells. The actual amounts of water pumped from these wells is not known but is probably small.

There are a number of perennial springs in the geothermal system. These springs are located principally along the east flank of the Magdalena Mountains, in the Nogal Canyon drainage north of Socorro Peak, and south of Blue Canyon along the eastern front of the Socorro Mountains. Socorro and Sedillo springs, located along the Socorro Mountain front south of Blue Canyon, are the source of thermal waters (temperatures greater than 32°C or 90°F) and may well have formed an important water resource since prehistoric time. These springs presently supply water for municipal use to Socorro.

Probably the most significant component of groundwater discharge is underflow into the Rio Grande Valley (see Appendix A). Groundwater enters the Rio Grande Valley from the west where it is either discharged by municipal or irrigation wells or flows southward along with groundwater in the alluvium or valley-fill deposits of the Rio Grande Valley. Distinct pathways of water movement through the Socorro and Lemitar mountains have not been clearly identified.

There have been a number of general studies of the wells and springs in the vicinity of the study area including those by Waldron (1956); Bushman (1963); Hall (1963); Clark and Summers (1971); and Summers (1976). These studies provide a relatively good data base for studying discharge in the area of the Socorro Peak KGRA.

The groundwater discharge in the area (excluding underflow into the Rio Grande Valley) may be divided into thermal and nonthermal flow components. The area in which thermal discharge occurs is quite limited. According to Summers (1976), thermal waters issue from three springs and one well: Cook, Socorro, and Sedillo (or Evergreen as it is sometimes referred to) springs, and Blue Canyon Well (3S.1W.16.323). Socorro, Sedillo, and Cook springs are infiltration galleries which have been driven horizontally into the east face of Socorro Mountain to intercept the flow of natural springs. Summers (1976) also notes that water having a temperature of 42.2°C (108°F) was found in a core hole deep in a mine shaft north of Blue Canyon. An attempt was made by the author to investigate this core hole in May 1980, at which time the hole was found to be plugged at a depth of 1.2 m (4 ft).

It is not certain whether Cook Gallery is actually a source of thermal discharge. The entrance to the gallery is blocked so that water-temperature measurements must be made in a pond at the mouth of the tunnel rather than at

the discharge point. Clark and Summers (1971) give a temperature for Cook Gallery of 18.9°C (66°F). Summers (1976) gives a temperature for the Cook Gallery water of 13.3°C (56°F). It is probable that this temperature is lower than the temperature of the discharging water. However, based on available data, the water temperature at Cook Spring is less than the 32°C (90°F) limit for thermal water classification. Summers (1976) notes that temperatures in a tunnel about 122 m (400 ft) above Cook Gallery are above normal.

There have been a number of studies which have dealt specifically with the thermal waters at the Socorro Peak KGRA: Holmes (1963); Hall (1963); Summers (1976); and Gross and Wilcox (1980). Spring discharge in the Socorro Peak area has been measured periodically for nearly 80 years. The first discharge estimate was made in 1901 by F. A. Jones (1904), then president of the New Mexico School of Mines. Jones (1904) noted that the thermal waters "came from a fractured zone or fault, . . . , oozing and bubbling out at several places." Jones (1904) measured a volume of flow over a 24-hour period of 2650 m^3 (700,000 gallons), which is equivalent to 3.07 x $10^{-2} m^3/s$ (486 gpm). Jones (1904) also commented that an earthquake in the fall of 1898 had produced a visible increase in the volume of water discharged.

Waldron (1956) estimated the flow of Socorro Gallery at 5.68 x $10^{-2} m^3/s$ (900 gpm) and estimated the flow of Cook Gallery to be about 6.3 x $10^{-4} m^3/s$ (10 gpm). Summers (1976) relates the findings of Francis X. Bushman, who calculated the following discharges (in gpm) to the city of Socorro water supply:

Date	Socorro Gallery (3S.1W.22)	Sedillo Gallery (3S.1W.22)	Cook Gallery (3S.1W.15)
1955	305	155	-
1956	310	166	-
1957	313	172	5-10

It is interesting to note that the sum of the flows from Socorro and Sedillo galleries for any one year are quite close to the figure given by Jones (1904) for the total spring flow. Discharge rates (in gpm) measured by several observers are reported by Summers (1976):

Date	Socorro Gallery	Sedillo Gallery	Cook Gallery	Observer
1-24-57	353	---	---	U.S. Geological Survey
3-20-58	220	240	10	N.M.I.M.T.
4-15-64	291	---	---	U. S. Geological Survey, mean section calculation of a velocity-meter survey
5-25-64	277	---	---	F. R. Hall, volume-time method
10-23-65	292	---	---	K. Summers, modified Parshall flume

More recent measurements (in gpm) by Gross and Wilcox (1980) were obtained from the City of Socorro gauges:

Year	Month	Socorro Spring	Sedillo Spring
1977	July	274.5	107.8
	August	272.8	-
	September	282.7	94.6
	October	276.0	98.9
	November	265.2	97.4
1978	February	299.6	109.4

Summers (1976) installed a continuous water-level recorder in Socorro Gallery in 1962 and noted a nearly constant flow rate over a 48-month period. Summers also found that some segments of Socorro Gallery produce more water than others and different fractures in the Gallery produce waters having slightly different temperatures ranging from 32.4°C to 34.2°C (90.4°F to 93.6°F) (Summers 1976, Figure 27). This observation suggests that fracture-controlled pathways of thermal water circulation are quite complex.

The Blue Canyon Well, drilled in 1956, is located in Blue Canyon about 0.2 km (0.5 mi) west of the east face of the Socorro Mountains. Summers (1976) noted that the static water level in this well was about 1524 m (5000 ft) of elevation. Francis X. Bushman conducted a pumping test of the Blue

Canyon well in 1960 and determined the maximum sustained yield to be 1.20 x 10^{-3} m^3/s (19 gpm) (Summers 1976).

Thermal Characteristics

There have been a number of geophysical investigations which have addressed the problem of heat flows and thermal gradients along the Rio Grande Rift. Most of these efforts have been in the vicinity of the Socorro Peak KGRA, including investigations by Reiter et al. (1975); Sanford (1977b); Reiter and Smith (1977); Reiter, Shearer, and Edwards (1978); and Reiter, Mansure, and Shearer (1979).

These geophysical data suggest the existence of a zone of anomalous heat-flow values generally exceeding 2.5 HFU (1 HFU = 1 x 10^{-6} cal/cm^2 - sec) coinciding with the western margin of the Rio Grande Rift (Reiter et al. 1975). This zone contrasts with lower heat flows of 1.5 to 2.0 HFU in the eastern Colorado Plateau. Heat flows of 2.0 to more than 2.5 are common in the Basin and Range Province of southwestern New Mexico (see Figure 2-11).

Sanford (1977b) and Reiter and Smith (1977) give data relating to subsurface temperature in and near the Socorro Peak KGRA. These data, shown in Table 2-15, indicate that the distribution of heat flow in the KGRA is quite heterogeneous. Temperature gradients greater than 150°C/km appear to be confined to the eastern part of the Socorro Mountain block (Reiter and Smith 1977), where heat flows of 9.6 to 11.7 HFU have been observed (Sanford 1977b; Reiter and Smith 1977).

Swanberg (1979) uses an empirically-derived linear relationship between silica geotemperatures and heat flow to plot a heat-flow map of the Rio Grande Rift. Swanberg (1979) uses an equation of the form

$$T_{SiO_2} = mg + b,$$

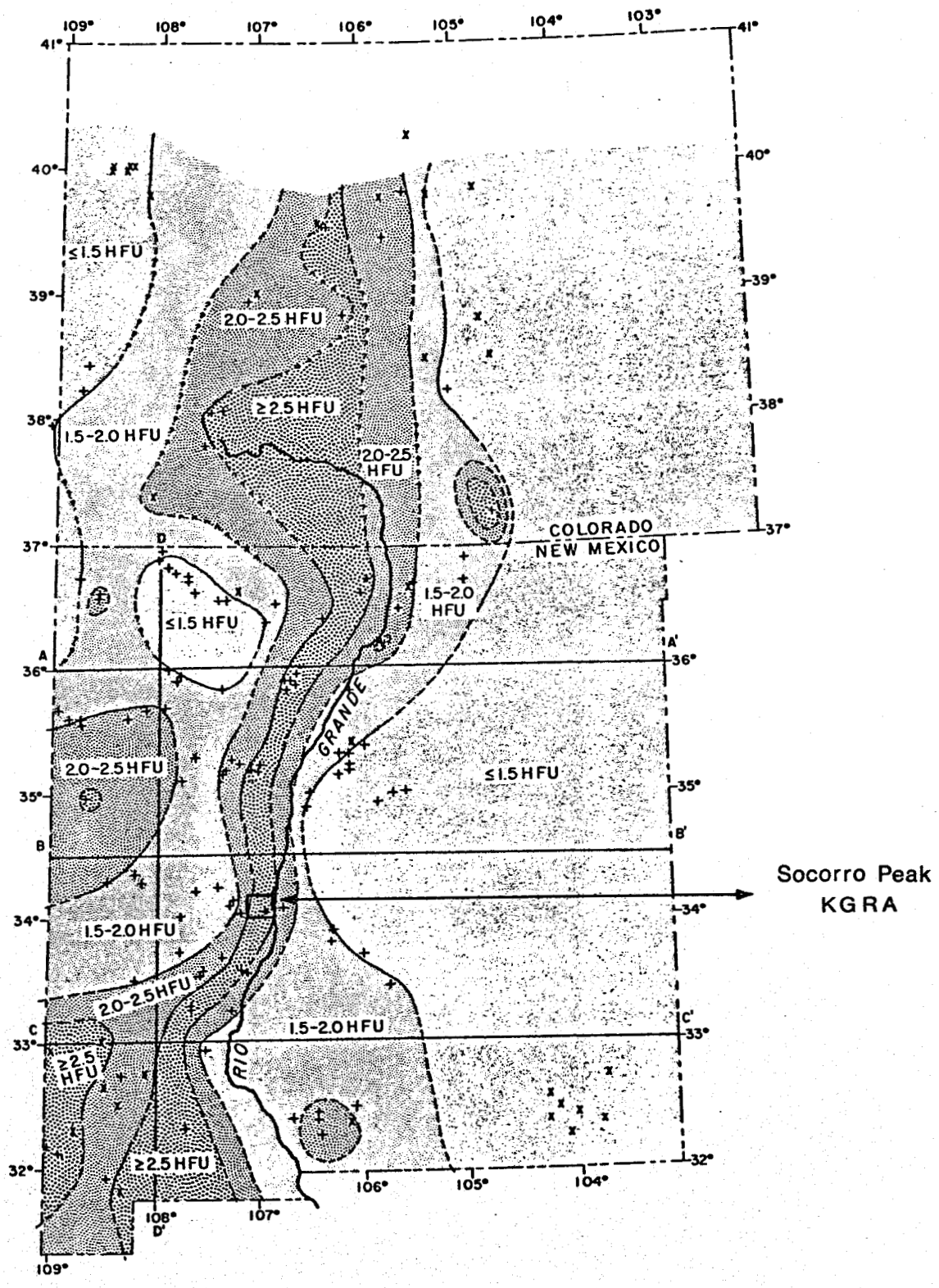

Figure 2-11. Terrestrial heat-flow contour map of New Mexico and southern Colorado. Contour interval, 0.5 HFU (Reiter et al. 1975).

Table 2-15. Drill-hole thermal data.

Borehole No. (this report)	Borehole No. (original reference)	Land Surface Elevation (m above sea level)	Depth to Water (m below surface)	Depth Interval (m below surface)	Temperature Gradient (°C/km)	Heat Flow (HFU)	Reference
1	1	1457	43	15.2 - 76.2	54.7		Sanford 1977b
2	2	1451	58	21.3 - 57.9	33.8		"
3	3	1488	not encountered	21.3 - 71.3	40.6		Reiter and Smith 1977
				10.0 - 20.0	119.0 ± 20.0		
				35.0 - 70.0	35.5 ± 0.2		"
4	4	1622	"	12.2 - 39.6	161.9	6.5	Sanford 1977b
5	5	1616	"	12.2 - 30.5	168.2	6.7	"
6	6	1642	"	15.2 - 33.5	183.7		"
				33.5 - 64.0	149.5		"
7	7	1510	18.3	18.3 - 42.7	159.1	9.6	"
				42.7 - 67.1	83.6		"
8	8	1511	21.1	12.2 - 21.3	242.6	9.7	"
9	9	1555[1]	not encountered	6.1 - 30.5	155.9		"
				30.5 - 54.4	129.4		"
				54.9 - 67.1	286.9		"
				11.0 - 51.0	159.0 ± 2.0	11.7 ± 1.2	Reiter and Smith 1977

[1] Drillhole was collared in a mine approximately 125 m below ground surface.

Table 2-15. (continued).

Borehole No. (this report)	Borehole No. (original reference)	Land Surface Elevation (m above sea level)	Depth to Water (m below surface)	Depth Interval (m below surface)	Temperature Gradient (°C/km)	Heat Flow (HFU)	Reference
10	2	1512	not reported	10 - 20	245.0 ± 24.0		Reiter and Smith 1977
11	4	1509	"	10 - 20	98.2 ± 12.2		"
				25 - 35	39.2 ± 0.7		"
				40 - 60	19.3 ± 0.4		"
				70 -100	24.3 ± 0.7		"
12	5	1536	"	10 - 20	83.7 ± 14.3		"
				25 - 60	45.6 ± 2.4		"
				90 -110	50.1 ± 6.6		"
13	6	1417	"	10 - 20	96.2 ± 6.7		"
14	7	1451	"	10 - 20	93.9 ± 13.4		"
15	8	1417	"	10 - 20	96.9 ± 1.9		"
				20 - 25	44.4		"
16	9	1695	"	10 - 20	97.9 ± 28.6		"
				15 - 25	47.8 ± 3.5		"
				25 - 35	28.0 ± 2.4		"
17	10	1786	"	10 - 20	107.0 ± 10.0		"
				20 - 30	73.0		"
18	11	1786	not reported	30 - 40	44.2		"
				40 - 50	20.7		"
				50 - 80	10.2 ± 0.4		"
19	North Baldy (NM)	2590	"	90 - 170	24.70 ± 1.10		Reiter et al. 1975
				150 - 210	33.86 ± 0.94	2.48 best	
				230 - 280	44.69 ± 2.09	estimate	"

where T_{SiO_2} is the silica geotemperature in degrees Celsius, g is the heat flow in mWm^{-2}, m is $0.67°C\text{-}m^2mW^{-1}$, and b is 13.2°C (55.7°F). Applying this formula to a silica geotemperature of 77°C (171°F) determined by Trainer (1975) for the Blue Canyon Well, the heat flow would be 2.27 HFU.

Vertical temperature gradients have been observed to decrease significantly in the valley fill to the east of the mountain front. It has been suggested by Bushman (1963) that the decrease in thermal gradients may be due to mixing with groundwater flowing southward in the Rio Grande Valley. Although the extent of elevated geothermal gradients to the south and west of Socorro Peak appear somewhat ambiguous, data suggest a decrease in geothermal gradients in those directions according to Reiter and Smith (1977).

Several authors have discussed the potential for fluid movement to affect the observed temperatures and heat fluxes within the Socorro Mountain block (Holmes 1963; Hall 1963; Summers 1976; Reiter and Smith 1977; Sanford 1977b; Chapin et al. 1978). The movement of fluids may also be controlled to a large extent by fractures, as noted earlier. According to Chapin et al. (1978), the flow of thermal waters to Socorro and Sedillo springs appears to be controlled by the intersection of ring fractures associated with the Socorro Cauldron and the rift fault zone bounding Socorro Peak along its eastern front. Chapin et al. (1978) also note the possibility that thermal waters are leaking upward along the range-bounding fault from a deep reservoir which is heated by a shallow magma body. The geology of these thermal springs is still not clearly understood.

Thermal waters are observed in a very limited area along the eastern part of the Socorro Mountains. These thermal waters are expected to comprise only a fraction of the total heated groundwater as most of the geothermal water may flow undetected into the Rio Grande valley fill.

Water temperatures from a large number of wells and springs in the vicinity of the Socorro Peak KGRA are given in Clark and Summers (1971). This report contains a compendium of data from a number of sources collected over a period of at least 15 years. It may be useful to collect similiar data within a small span of time using the same instruments in order to minimize measurement error. Temperature data have been collected specifically on wells and springs considered to be of geothermal significance. Most of this information is summarized by Summers (1976). Table 2-16 is a summary of water-temperature data which have been collected from 1852 through 1965. These data show only small fluctations of temperature over the 114-year period of measurement.

A continuous-temperature recorder was in operation at the bottom of the shaft at the Socorro Gallery from September 1962 to January 1965 (Summers 1976). During that period of time there were practically no variations in temperature noted. All variations noted were within the instrumental error of the recorder. The average temperature measured was 32.99°C (91.3°F) and, except for three low temperatures, all of the measurements fell within the range of 32.7°C to 33.1°C (90.9°F to 91.6°F). Both the recorded temperatures and discharges of Socorro Gallery remained remarkably constant over a fairly long period of record. These data could indicate that seasonal pulses of cooler shallow components of recharge do not mix with deeply circulating thermal waters. If a cool shallow component does exist, then the temperature and recharge are relatively uniform.

Summers (1976) interprets the uniform temperature and discharge at Socorro Spring to indicate that either: (1) no large recharge events occurred during the recording period, (2) the effects of these recharge events were damped out by long travel times, or (3) the quantity of recharge water was so

Table 2-16. Water temperatures (^{o}F) in the Socorro thermal area.

Date	Socorro Spring or Gallery (3S.1W.22.113)	Sedillo Spring or Gallery (3S.1W.22.131)	Cook Spring or Gallery (3S.1W.15.313)	Blue Canyon Well (35.1W.16.323)	Observer
1852	92.0	----	----	-----	Hammond (1966)
1890	90.0	----	----	-----	Surveyor's notes in N.M.B.M.M.R. files
1901	93.0	----	----	-----	Jones (1904)
1952	91.0	----	----	-----	Waldron (1956)
7-24-56	----	----	----	90-92	Bushman, notes in N.M.B.M.M.R. files
8-23-56	----	----	----	91.7	Bottom-hole temperature
3-20-57	88.8	90.0	66.0	-----	Hall
12-12-61	91.4	88.0	----	88.0	Hall (Blue Canyon Well measured at end of discharge pipe)
1-22-61	----	90.0	56.0	90.0	"
4-10-61	91.6	----	----	90.0	U.S. Geological Survey
10- 1-65	----	92.3	----	-----	Summers (at manhole above settling basin)
10-22-65	91.4	----	----	-----	Summers
10-25-65	----	----	----	91.5	Summers
4-10-65	91.6	----	----	90.0	U.S.Geological Survey
10- 1-65	----	92.3	----	-----	Summers (at manhole above settling basin)
10-22-65	91.4	----	----	-----	Summers
10-25-65	----	----	----	91.5	Summers

small that its effects were masked by more deeply circulating groundwater. Summers (1976) also recorded water temperatures from various fractures along the length of Socorro Gallery. These measurements show (Summers 1976, Figure 27) that water discharging from different fracture traces displays slight temperature differences ranging from 32.4°C to 34.2°C (90.4°F to 93.6°F). This result may indicate that individual fractures convey thermal water to the spring from different depths.

Because of the difficulty of access to Sedillo Gallery, temperature measurements have been made at the outlet of the discharge pipeline several hundred feet from the tunnel mouth or at a manhole at the lower end of the gallery. The temperature at the manhole on October 1, 1965, was 33.5°C (92.3°F) so that the water temperature at the point of discharge may well be higher.

Blue Canyon Well was tested by Francis X. Bushman who recorded the following temperature-depth relation on August 23, 1956 (Summers 1976):

Depth (ft)	Temperature (°F)	Remarks
217.5	89.8	water level = 216.8 ft casing perforated 217.5 to 250 ft
220	89.9	
223.5	89.95	
223.5	90.1	
223.5	90.15	
238.5	90.2	
243.5	90.3	
248.5	90.25	
253.5	90.4	
255	90.45	
258.5	90.5	bottom of casing
259.5	91.2	
260.5	91.6	
261.5	91.7	
262.5	91.8	
263.5	91.7	
264.5	---	bottom of hole

The following temperature-discharge relationship was recorded during a pumping test conducted July 23-24, 1956, by Bushman (Summers 1976):

Time (minutes after initiation of pumping)	Discharge (gpm)	Temperature (°F)
3	46	91
7	46.5	90
66	49.5	90.2
152	40.3	92
156	39.8	91.8
243	38.7	91.8
280	38	91.8
343	30.5	91.8
273	30.0	91.8
463	29.2	91.8
523	28.8	91.8
583	28.2	91.8
978	18.7	90.8
1128	18.4	90.6
1240	18.6	90.4
1333	18.7	90.3
1457	18.8	90.3

A vertical two-inch corehole drilled into Precambrian rock in Woods Tunnel, a nearly horizontal mining adit driven into the eastern face of Socorro Peak, encountered hot water. The collar elevation of this drill hole is about 1565 m (5135 ft) and its total depth is 79 m (260 ft) (Summers 1976). The water level was about 49 m (160 ft) below collar elevation or 1515 m (4975 ft) according to Summers (1976). The following temperature-depth relationship was found (Summers 1976):

	Temperature (°F)	
Depth (ft)	June 24, 1966	July 8, 1966
33	93.2	--
66	95.9	--
99	98.8	--
132	101.8	--
153	--	101.2
166	105.5	105.5
187	107.4	--
230	108.8	108.9

Overall, these temperatures are somewhat higher than those discharging from any of the thermal springs. Elevated water temperatures in some of the

deep wells support the argument that the geothermal reservoir is not limited to the areas near the springs, and that an appreciable amount of geothermal water discharges in the subsurface to cooler water in the Rio Grande valley fill.

Chemistry of Groundwater in the Socorro Peak Area

The chemistry of the groundwater in the Socorro Peak area has been studied by several researchers. Chemical analyses of groundwater samples are published in Waldron (1956); Hall (1963); Clark and Summers (1971); Summers et al. (1972); Summers (1976); and Gross and Wilcox (1980). Bushman (1963) discussed the quality of groundwater in the Rio Grande Valley near Socorro. Tritium concentrations in the groundwater have been analyzed and discussed by von Buttlar and Wendt (1958); von Buttlar (1959); Holmes (1963); and Gross and Wilcox (1980).

Primary Constituents

It is likely that one of the most important areas of recharge to the groundwater system in the Socorro Peak area is the mountain front along the eastern margin at the Magdalena Mountains. A study by Summers et al. (1972) indicates that groundwater in the Magdalena Mountains is generally of the calcium-bicarbonate ($Ca\text{-}HCO_3$) type. In this area, the total-dissolved solids concentration is less than 500 parts per million (ppm). In those samples with less than 150 ppm total dissolved solids, silica represents as much as 30 percent of the total.

Groundwater throughout the La Jencia Basin is also generally of the $Ca\text{-}HCO_3$ type (Gross and Wilcox 1980). Locally, some groundwater samples show relatively high concentrations of sulfate which are probably the result of contact with the upper gypsiferous member of the Popotosa Formation

or other gypsum-bearing sediments. On the other hand, water from Socorro, Sedillo and Cook springs, as well as water discharged from Blue Canyon Well, is of the sodium-bicarbonate ($Na-HCO_3$) type. Gross and Wilcox (1980) note that water from two wells in Socorro Canyon is of the Na, $Ca-SO_4$ and $Na-HCO_3$ types. Waldron (1956) attributed the chemical change to ion-exchange mechanisms, whereby water flowing east from the southern end of the La Jencia Basin exchanges Ca for Na along its flow path through the rhyolitic tuffs underlying the Popotosa Formation. Such an exchange might be facilitated if elevated temperatures were encountered at depth. Figure 2-12 shows a diagram of the chemistry of the groundwater in the area as well as a line indicating roughly where the ion exchange is taking place.

In a study of the mixing of thermal and nonthermal waters along the margin of the Rio Grande Rift, Trainer (1975) examined a sample of water from Blue Canyon Well and calculated a relatively low antecedent reservoir temperature of 77°C (171°F) by the SiO_2 geothermometer and 55°C (131°F) by the Ca-Na-K geothermometer. On the basis of proportions of principal ions relative to those from other Rio Grande Rift hotspots, Trainer (1975) concluded that the Blue Canyon Well water was a mixture of thermal and nonthermal water.

As shown in Figure 2-12, the concentration of total dissolved solids (TDS) of Socorro, Sedillo and Cook springs and Blue Canyon Well is relatively low, approximately 250 ppm TDS or about 350 to 400 micromhos per centimeter (μmhos/cm) electrical conductivity. Figure 2-12 also shows that the shallow water in wells in the southern end of the La Jencia Basin (Snake Ranch Flats) has total-dissolved solids concentrations which are quite similar to that of the groundwater discharging from the eastern side of the Socorro Mountains.

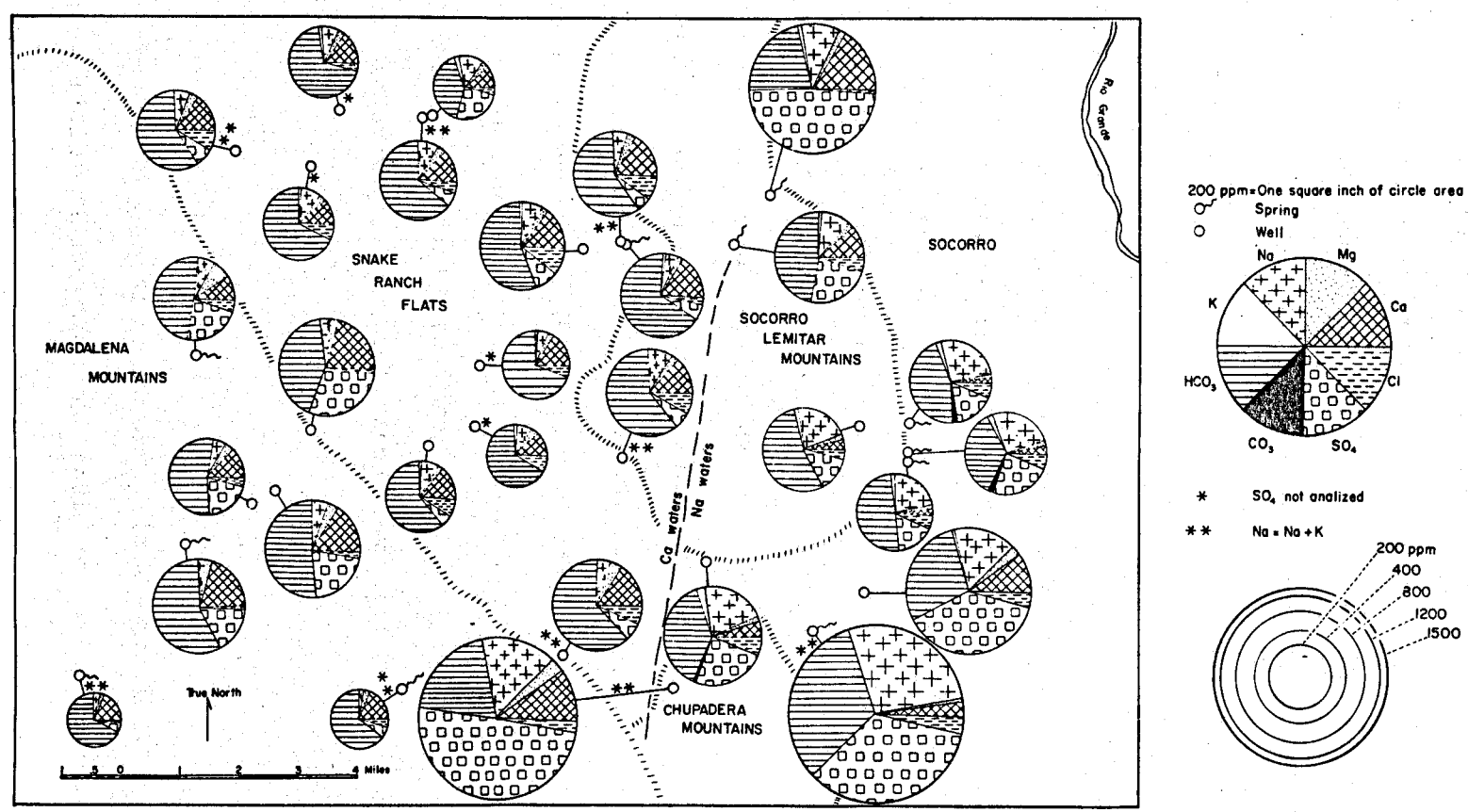

Figure 2-12. Distribution map of water quality and total dissolved solids (Gross and Wilcox 1980).

The electrical conductivities of water from Upper Nogal Canyon Spring and Lower Nogal Spring in Nogal Canyon north of Socorro Peak are somewhat higher, on the order of 480 μmhos/cm and 750 μmhos/cm, respectively. Groundwater from the Socorro Canyon area and south toward the Chupadera Mountains is generally high in total dissolved solids (see Figure 2-12).

Oxygen Isotopes

Gross and Wilcox (1980) present oxygen-18 and deuterium analyses of ten samples of thermal spring and well water, five samples of non-thermal springs and wells, and two Socorro precipitation samples. When plotted on a standard δD vs. $\delta^{18}O$ graph (see Figure 2-13), all of the samples plot near and slightly to the left of the meteoric line of Craig (1961). Thermal water usually plots to the right of the meteoric line. Gross and Wilcox (1980) conclude that water sampled from thermal wells and springs is of meteoric origin. Furthermore, they indicate that there is no evidence to suggest mixing between the sampled groundwater and deep thermal water. These findings seem to contradict those of Chapin et al. (1978), who suggest that the thermal waters at the springs are derived from upward leakage along a fault from a deep reservoir heated by a shallow magma body. Gross and Wilcox (1980) do not discuss the source of heat to account for the temperatures at the thermal springs and wells.

Tritium

As the result of large-scale atmospheric testing of thermonuclear devices during the period 1954 to 1963, environmental tritium concentrations significantly increased. It is possible to study residence times of groundwater by correlating peaks of tritium activity in spring waters with

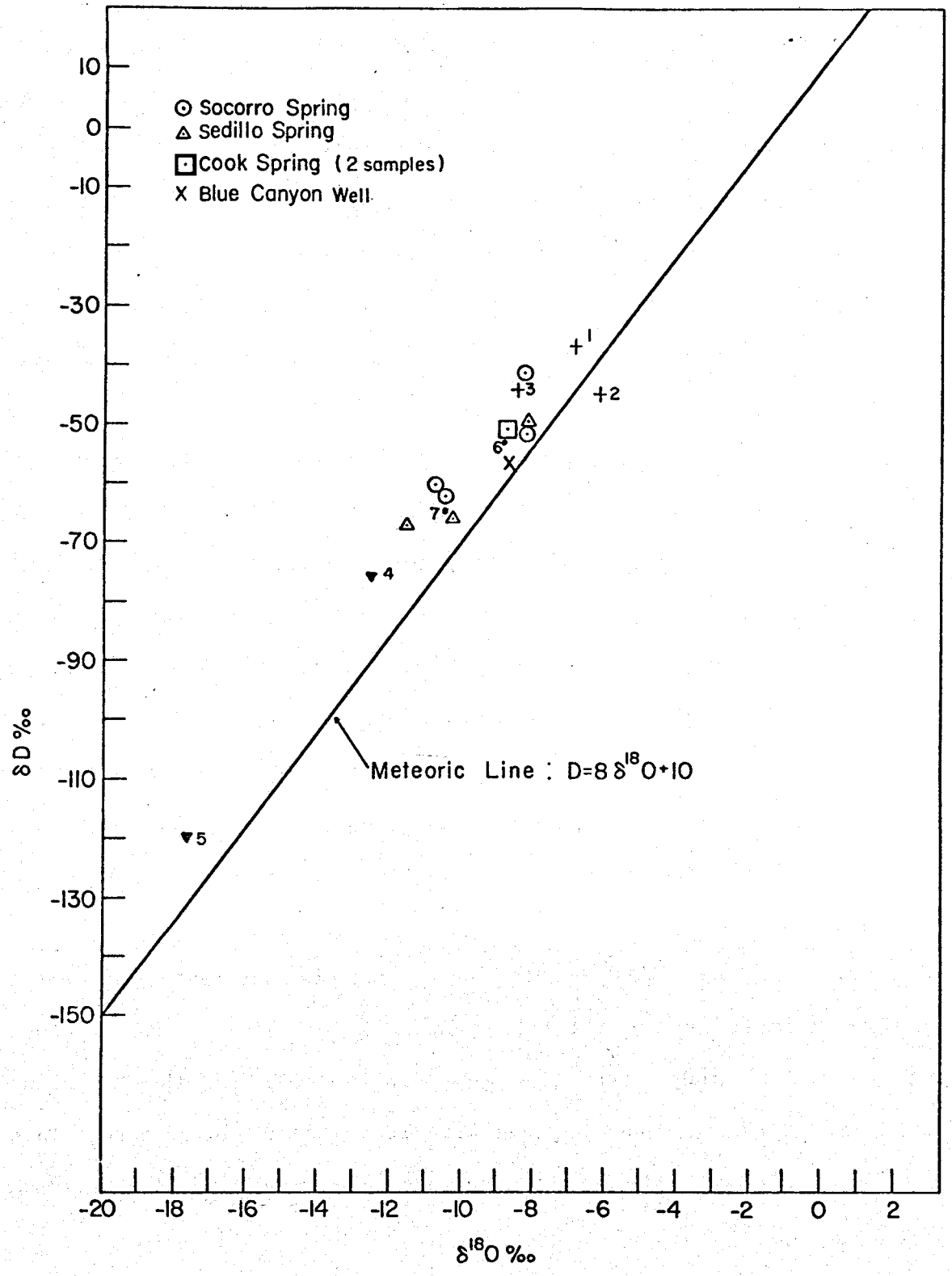

Figure 2-13. Deuterium and oxygen-18 in thermal and nonthermal waters (Gross and Wilcox 1980) (Numbers refer to nonthermal sampling points).

peaks of tritium activity in precipitation events. Residence times, calculated in this way, are often subject to multiple interpretations because of a number of complications, which include the mixing of waters of different ages and the complex relationship between precipitation and recharge events in a semiarid environment. As pointed out by Gross and Wilcox (1980), small precipitation events of high-tritium activity may contribute less tritium to recharge than a large precipitation event of low- or intermediate-tritium activity.

In applying this method of residence-time calculation, von Buttlar (1959) concluded, on the basis of sparse data, that the residence time of the thermal spring water was longer than four years. On the basis of additional data, Holmes (1963) concluded that an August 1958 tritium peak in water from Socorro Spring corresponded to increased tritium levels in precipitation falling in early 1954. From this evidence, an average residence time of about four years seems reasonable. Gross and Wilcox (1980) concur with the correlation of the Socorro Spring tritium peak by Holmes (1963), but note that Holmes did not take into account possible effects of the mixing of waters with different residence times.

Gross and Wilcox (1980) note some rather interesting general relationships between average tritium unit (TU) values* for various groundwaters in the study area (see Figure 2-14). Within the Magdalena Mountains, the groundwater appears young with TU values of 40 or more. This water is discharged from high-elevation springs and wells in shallow alluvium soon after entering the ground.

*Tritium activity is expressed in tritium units (TU), where one tritium unit equals one tritium atom per 10^{18} hydrogen atoms.

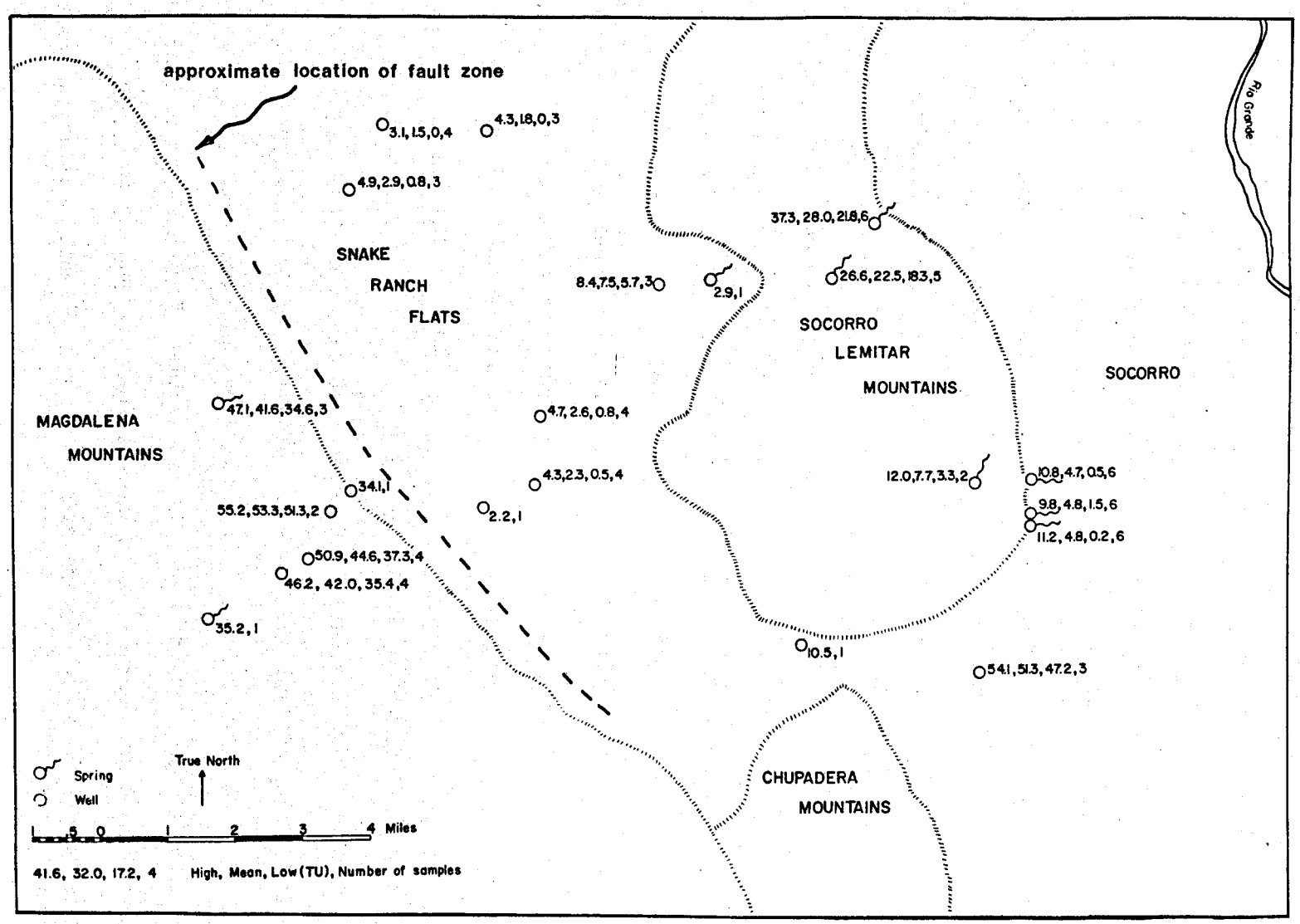

Figure 2-14. Distribution of tritium activity in groundwater and springs (modified from Gross and Wilcox 1980).

The TU values of groundwater from wells in the southern La Jencia Basin are quite low, generally averaging less than three, which indicates that this water is old relative to that in the Magdalena Mountains. All TU values to the west of a fault zone bounding the eastern margin of the Magdalena Mountains are high and the TU values just east of the fault zone are quite low (see Figure 2-14). This northwest-southeast trending fault zone is comprised of normal faults downthrown to the east such that Oligocene volcanics of the Magdalena Mountains contact younger alluvial deposits to the east (Osburn 1977). One interpretation of these data is that mountain-front recharge occurs along this fault zone and most of the young water flows down the fault zone and into the lower Santa Fe Group or older rocks. Thus, only a very small amount of shallow recharge would reach the shallow aquifer in the southern La Jencia Basin to the east of this fault zone. This interpretation follows that of Gross and Wilcox (1980), who postulate the existence of a shallow-groundwater system in the upper Santa Fe Group in the southern La Jencia Basin separated from a deeper flow system in the Lower Popotosa of the Santa Fe Group by a low permeable layer, presumably the Upper Popotosa. This deep-flow system may actually receive most of the mountain front recharge of young water and discharge at the springs.

The waters discharging from Socorro, Sedillo, and Cook springs all have TU values which average 4.7 to 4.8. Blue Canyon Well has TU values which average a little higher, i.e., 7.7, based on only two samples. These values are all slightly greater than the TU values from fairly shallow wells up-gradient in the southern La Jencia Basin. It should be noted that the tritium samples from Cook Spring are taken from a small pool at the mouth of the gallery and may have slightly higher TU values than the TU values at the actual discharge point of the gallery.

Waters which discharge from the the Upper and Lower Nogal Canyon springs to the north have TU values of 22.5 and 28.0, respectively, which indicates that recent recharge is an important component of their flow. Water-chemical data clearly distinguish the origin of springs in Nogal Canyon from the thermal springs.

Discussion and Interpretation of Hydrogeothermal System

In formulating a computer model of the geothermal system, it is important to have a reasonably good understanding of hydrogeologic controls on geothermal reservoir behavior. Available evidence indicates that the flow system is quite complex and not well understood at present. The following material summarizes lines of evidence which lead to interpretation about the geothermal system that may aid in developing a preliminary conceptual model for computer simulation:

1. Groundwater elevations in relatively shallow wells indicate that the general direction of groundwater flow is west to east from the Magdalena Mountain block across the southern La Jencia Basin through the Socorro Mountain block and into the Rio Grande Valley. A complex series of geologic events have produced different fault sets which may significantly influence the groundwater flow system. Range-bounding faults along the eastern margin of the Magdalena Mountains may be avenues of recharge to a deep-flow system. Faults associated with the transverse shear zone and ring fractures along the eastern margin of the Socorro Mountains may control groundwater discharge, particularly that of the thermal springs. The effects of fractures and faults or other structural controls on groundwater movement is speculative at the present time.

2. A large, sill-like magma body at mid-crustal depths has apparently injected small dike-like magma bodies upward near the southern end of the Socorro Mountains. These small magma bodies may have intruded to within 3 to 5 km (1.9 to 3.1 mi) of the surface. One result of this intrusion is probably the anomalously high heat flows and thermal gradients observed along the eastern part of the Socorro Mountain block. Thermal gradients away from this area do not appear anomalous.

3. Known areas where discharge of thermal waters occurs is limited to the southeast part of the Socorro Mountains (i.e., principally Sedillo Spring, Socorro Spring, and Blue Canyon Well). The temperature of these waters averages about 90°F (approximately 32°C). These temperatures indicate geothermal potential only in light of evidence for a shallow-magma heat source and high heat-flow measurements.

4. Correlation of tritium peaks of discharge water at Socorro Spring with precipitation indicates that at least some component of the discharge has a residence time in the reservoir of about four years.

5. The thermal water discharge has slightly higher TU values that the shallow groundwater up-gradient in the southern La Jencia Basin and significantly lower TU values than the groundwater in the Magdalena Mountain recharge area.

6. Groundwater discharged to the east of a north-south trending line in the Socorro and northern Chupadera Mountains is of the Na-HCO_3 type. This condition is generally considered indicative of cation exchange by circulation through the volcanic rock complex, although it has not been shown that cation exchange cannot occur in fine-grained facies of the Santa Fe Group.

7. The thermal discharge waters have relatively low concentrations of total dissolved solids, as do all of the waters up-gradient and west of the thermal discharge area. Much higher dissolved solids concentrations would be expected if the discharge was associated with deep-reservoir circulation.

8. All of the thermal springs and well waters tested, and all the tested nonthermal springs and well waters, plot close to, or slightly to the left of, the meteoric line on a graph of δD vs. $\delta^{18}O$. This result has been interpreted as indicating that the thermal waters are of meteoric origin and have not been heated by circulation through a deep geothermal reservoir.

There are very few hydrogeologic data available at this time from depths greater than a few hundred feet in the Socorro Peak KGRA. Water levels and most temperature and chemical data reflect very shallow groundwater conditions. Information from a larger number of wells is necessary to understand the fluid circulation within the geothermal system.

Based on the available data summarized above, Gross and Wilcox (1980) conceptualize the flow system as follows:

> "The tritium activity of the spring water is the label of local recharge, that is, precipitation that falls on the Socorro Mountain complex, and/or surface runoff following large thunderstorms, crosses the Snake Ranch Flats and is absorbed by the highly fractured and permeable volcanics forming the eastern edge of the flats. That is to say, the major portion of spring flow represents water that was recharged at the eastern edge of the Magdalena Mountains and took the long path, beneath the mudstone complex in the Snake Ranch Flats [(i.e., the deep-flow system across the southern La Jencia Basin)], but a minor component of the spring flow represents local recharge around the western flank and southern end of the Socorro Mountains. This conclusion does not seem unreasonable considering the size of the possible recharge area around the Socorro Mountains. The shallow recharge contribution is roughly estimated at 10 to 20 percent of the total spring flow, but is expected to vary from year to year with local climatic conditions."

In this scenario, the correlation of tritium peaks indicates that the local recharge component had a residence time of about four years. Mixing of the young local recharge component with the older deep-flow water could result in the average TU values found at the thermal discharge area being slightly higher than those of the southern La Jencia Basin. According to Gross and Wilcox (1980), the regional component which had the longer, deeper flow path had a residence time which is probably much longer than the half-life of tritium (i.e., 12.3 years). Deep and shallow components of the regional flow field within the Santa Fe Group would not contact very deep, hot regions of the reservoir. Presumably cation exchange occurs in the volcanic complex near the points of spring discharge. The excellent water quality of the thermal springs could be accounted for if salts in the Santa Fe Group were flushed through the system during pluvial periods, or if circulation occurs via fractures with limited contact area for chemical interaction.

Another interpretation of this evidence is that the primary component of flow to the thermal discharge area could be derived from local recharge, that is, precipitation falling along the western side of the Socorro Mountains as well as infiltration from surface runoff along the eastern margin of the southern La Jencia Basin. This interpretation could conceivably fit most of the data that have been presented. Heat would be transmitted to the water along its flow path through the Socorro Mountain block where high heat flow occurs. Cation exchange could occur as the groundwater contacts the volcanics in the Socorro Mountain block. In order to account for the observed tritium activity, the computed residence time of four years would be much too short.

In order to test whether this interpretation is reasonable, some rough calculations were performed to determine whether local recharge is sufficient to account for all of the spring flow. Using a planimeter and flow lines

superimposed on the water-level contour map (see Appendix A), recharge could occur over a maximum of 21.7 square kilometers (8.4 square miles) to provide local recharge to the springs. From data presented in Gross and Wilcox (1980), the average flow from Socorro Spring was calculated to be 1.76×10^{-2} m^3/sec (278.5 gpm) and the average flow of Sedillo Spring was 6.41×10^{-3} m^3/sec (101.6 gpm), which gives a mean yearly flow of roughly 756,440 m^3/year (613 acre-feet/year). Kelly Ranch, which is located in the La Jencia Basin at an elevation of 2042 m (6700 ft) receives a mean annual precipitation of 34.54 cm (13.60 in) (Gabin and Lesperance 1977). This figure was thought to be reasonably representative of the precipitation which would occur in the postulated recharge area. Based on this value, the precipitation falling on the supposed recharge area would be on the order of 7.5×10^6 m^3/year (6100-acre feet/year). It would be necessary for 10 percent of this amount to be reaching the groundwater system as recharge. This estimate appears to be high considering the semiarid conditions present in the proposed recharge area.

In a water-balance study in a similar semiarid watershed in southeastern Arizona, Renard (1970) found that the maximum groundwater recharge was about four percent of the mean annual precipitation. It appears, however, that tritium data do not support this second interpretation. That is, if the estimate by Holmes (1963) of a four-year residence time based on correlation of tritium peaks is correct, and if local recharge represents the major component of flow to the thermal discharge area, then the average TU values of the thermal springs are much too low.

Consequently, interpretations of the hydrogeothermal flow system are inconclusive. It is likely that the thermal discharge represents a mixing of several flow components. However, no model yet proposed satisfies every

detail of the evidence available. A computer simulation may assist in formulating a more consistent interpretation of circulation within the geothermal reservoir, although in the absence of subsurface data pertaining to hydraulic properties such a model could not be verified.

Summary of Model Parameters

In designing a two-dimensional groundwater flow model of the Socorro Peak KGRA, it is necessary to construct a schematic cross section such as that shown in Figure 2-15. The cross section shown in Figure 2-15 is a generalized, simplified diagram which is based on data presented in Chamberlin (1980); Sanford (1968); and Osburn (1977). Because the thicknesses of the geological units are to a large degree unknown in the subsurface, the diagram is not drawn to scale. It should be recognized that Figure 2-15 represents a typical, but hypothetical, cross section through the study area. In reality, a cross section would differ considerably in detail from place to place within the study area. Therefore, it may be desirable to consider a three-dimensional model should sufficient data become available.

Figure 2-15 refers to the different layers as they might be utilized in constructing a computer model. Each layer consists of units having similar hydrologic properties and may contain more than one geological formation. The values of the various physical parameters within one layer may vary and the reported range of values for a layer may overlap values for other layers. Because of the variation and overlap, a computer simulation at this time would require testing with a number of parameter combinations.

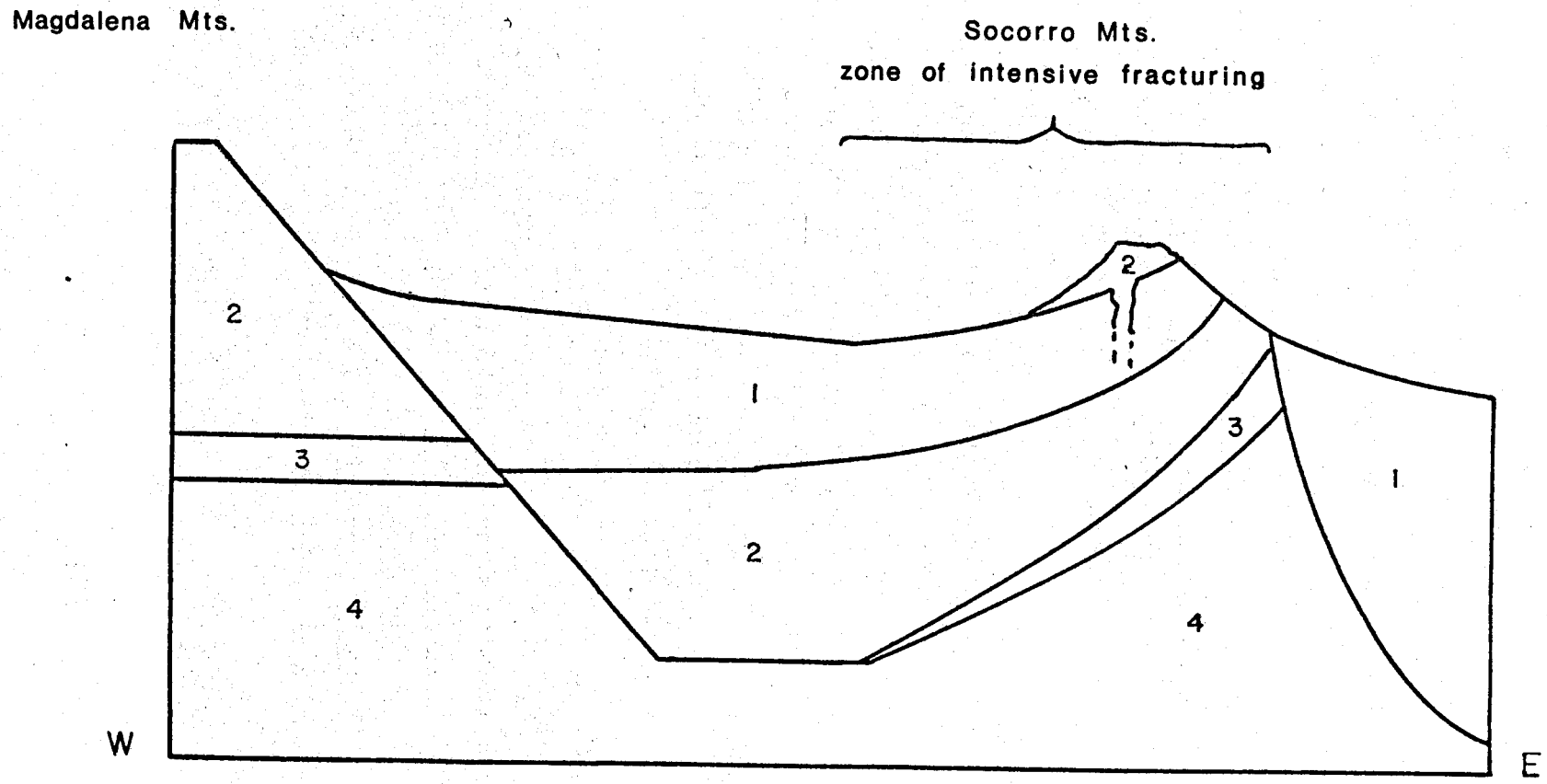

Figure 2-15. Simplified geological cross section for two-dimensional hydrogeothermal modeling. The numbers refer to layers for which parameters are described in the text.

Brief descriptions and ranges for the various parameter values for the layers may be summarized as follows:

Layer 1:

Description: Mostly terrigenous clastic sediments, locally poorly-consolidated alluvium and well-sorted, fine-to-medium-grained sandstones, but may be characterized overall as consisting of moderately-to-extremely well-indurated, fine-to-very-fine grained deposits.

Intrinsic permeability: $7.90 \times 10^{-13} - 1.0 \times 10^{-25}$ m^2

Specific storage: $1 \times 10^{-3} - 3 \times 10^{-6}$ m^{-1}

Thermal conductivity: 3.26 - 7.13 mcal/cm-sec-°C

Specific heat: 0.17 - 0.19 cal/g-°C

Layer 2:

Description: Mostly pyroclastic deposits, locally includes lava flows, domes, and volcanic breccias but may be characterized overall as consisting of welded-to-non-welded, jointed-to-unjointed, ash-fall and ash-flow tuffs.

Intrinsic permeability: $2.96 \times 10^{-11} - 7.1 \times 10^{-19}$ m^2

Specific storage: $3.36 \times 10^{-6} - 6.95 \times 10^{-6}$ m^{-1}

Thermal conductivity: 2.1 - 4.0 mcal/cm-sec-°C

Specific heat: 0.22 cal/g-°C

Layer 3:

Description: Moderate-to-well-indurated, probably fractured limestones, shales, and quartzitic sandstones.

Intrinsic permeability: $7.90 \times 10^{-13} - 1 \times 10^{-25}$ m^2

Specific storage: $1 \times 10^{-3} - 3 \times 10^{-6}$ m^{-1}

Thermal conductivity: 3.26-12.42 mcal/cm-sec-°C

Specific heat: 0.16-0.24 cal/g-°C

Layer 4:

Description: Crystalline metasedimentary and metavolcanic rocks with granitic, gabbroic, and diabase intrusions.
Intrinsic permeability: $3.5 \times 10^{-19} - 4.2 \times 10^{-21}$ m^2
Specific storage: $1.58 \times 10^{-6} - 1.73 \times 10^{-7}$ m^{-1}
Thermal conductivity: 4.82 - 13.6 mcal/cm-sec-°C
Specific heat: 0.155 - 0.318 cal/g-°C

As noted earlier, these values would have to be adjusted during the simulation to allow for the effects of fracturing and confining pressure, for example.

This simplified conceptual model does not account for differentiation of shallow and deep-flow paths as proposed within Layer 1 (Santa Fe Group) by Gross and Wilcox (1980). If additional hydrologic parameters become available from field tests, the model should be revised accordingly.

Recommendations

Collection of additional field data is considered a prerequisite to understanding the origin and potential for development of geothermal resources in the Socorro Peak KGRA. The data should include:

(1) deep drilling and testing for hydrogeologic parameters;

(2) water-level and temperature measurements in observation wells and in test wells constructed at various depths and locations in the KGRA; and

(3) water-quality analysis including oxygen-isotope and tritium analyses from various hydrologic units encountered during drilling of test holes and observation wells.

If sufficient data of this nature are collected, a geothermal-computer simulation would provide a useful tool for modeling fluid circulation within

and between the different lithologic units. In addition, detailed hydrologic budgets in the mountain areas and in the principal watersheds in the La Jencia Basin may provide useful estimates of groundwater recharge. Such studies may also help quantify the component of relatively young groundwater which some workers suggest appears in the geothermal springs.

Much information regarding the deeper subsurface has been obtained by private exploration companies and is not available to the public. Most of the holes are plugged after testing and are not accessible. Exploration crews drilled a number of deep holes in the Socorro Peak KGRA during 1980. A format should be established whereby this information pertaining to the hydrogeology of the area is available to the public so that research efforts to understand the physical processes governing the geothermal reservoir may be more productive. Our present knowledge of the system has not even progressed to the point where the impacts of exploration and development on the water supply of Socorro can be assessed adequately.

Acknowledgements

The authors would like to express their gratitude to the New Mexico Bureau of Mines and Mineral Resources for their cooperation on this project. We are specifically indebted to Dr. William J. Stone for providing valuable data for the water-level contour map and to Dr. Charles E. Chapin for many informative discussions pertaining to geologic structural features. Investigations by and discussions with Dr. Gerardo W. Gross of the New Mexico Institute of Mining and Technology Geoscience Department provided much of the background for interpreting the hydrologic framework. We would also like to acknowledge Dr. Lynn Gelhar for reviewing the report and for his many constructive comments.

References

Archie, G. E., 1952, Classification of carbonate-reservoir rocks and petrophysical considerations: American Association of Petroleum Geologists, Bulletin 36, p. 278-298.

Armstrong, A. K., 1962, Stratigraphy and paleontology of the Mississippian System in southwest New Mexico and adjacent southeastern Arizona: New Mexico Bureau of Mines and Mineral Resources, Memorial 8, 95 pp.

Bean, R. J., 1953, Relation of gravity anomalies to the geology of central Vermont and New Hampshire: Geological Society of America, Bulletin 64, p. 509-538.

Besbes, M., Delhomme, J. P., and DeMarsily, G., 1978, Estimating recharge from ephemeral streams in arid regions; a case study at Kairown, Tunisia: Water Resources Research, v. 14, p. 281-290.

Birch, F., 1942, Density at high pressure, compressibility, in Birch, F. Schairer, J. F., and Spicer, H. C., eds., Handbook of Physical Constants: Geological Society of America, Special Paper 36.

Birch, F. and Clark, H., 1940, The thermal conductivity of rocks and its dependence upon temperature and composition: American Journal of Science, v. 238, p. 529-558.

Blankennagel, R. K. and Weir, J. E., Jr., 1973, Geohydrology of the eastern part of Pahute Mesa, Nevada Test Site, Nye County, Nevada: U.S. Geological Survey, Professional Paper 712-B, 35 pp.

Brace, W. F., 1965, Some new measurements of linear compressibility of rocks: Journal of Geophysical Research, v. 70, p. 391-398.

Brace, W. F., Walsh, J. B., and Frangos, W. T., 1968, Permeability of granite under high pressure: Journal of Geophysical Research, v. 73, p. 2225-2236.

Brown, L. D., Krumhansl, P. A., Chapin, C. E., Sanford, A. R., Cook, F. A., Kaufman, S., Oliver, J. E., and Schilt, F. S., 1979, COCORP seismic reflection studies of the Rio Grande rift, in Riecker, R. E., ed., Rio Grande Rift, Tectonics and magmatism: American Geophysical Union, Washington, D.C., p. 169-184.

Bruning, J. E., 1973, Origin of the Popotosa Formation, northcentral Socorro County, New Mexico: New Mexico Institute of Mining and Technology, Ph.D. dissertation, 131 pp.

Burton, C., 1971, Geology of the Socorro Peak area: New Mexico Institute of Mining and Technology, independent study, 40 pp.

Bushman, F. X., 1963, Groundwater in the Socorro Valley, in 14th Field Conference Guidebook: New Mexico Geological Society, p. 155-159.

Caravella, F. J., 1976, A study of Poisson's ratio in the upper crust of the Socorro, New Mexico area: New Mexico Institute of Mining and Technology, Geophysics Open-File Report 11, 80 pp.

Chamberlin, R. M., 1980, Cenozoic stratigraphy and structure of the Socorro Peak volcanic center, central New Mexico: New Mexico Bureau of Mines and Mineral Resources, Open-File Report 118, 495 pp.

Chapin, C., 1980, Personal communication, New Mexico Bureau of Mines and Mineral Resources, Socorro, New Mexico.

Chapin, C. E., Blakestad, R. B., Bruning, J. E., Brown, D. M., Chamberlin, R. M., Krewedl, D. A., Siemers, W. T., Simon, D. B., and Wilkinson, W. H., 1974, Exploration framework of the Magdalena area, Socorro County, New Mexico, (abs.), in 25th Field Conference Guidebook: New Mexico Geological Society, p. 380.

Chapin, C. E., Blakestad, R. B., and Siemers, W. T., 1975, Geology of the Magdalena area, field trips to central New Mexico, part 2: Paleontologists and Mineralogists Annual Meeting, Albuquerque, American Association of Petroleum and Geological Society, Proceedings, p. 43-49.

Chapin, C. E., Chamberlin, R. M., Osburn, G. R., White, D. L., and Sanford, A. R., 1978, Exploration framework of the Socorro geothermal area, New Mexico: New Mexico Geological Society, Special Publication No. 7, p. 114-129.

Chapin, C. E., and Seager, W. R., 1975, Evolution of the Rio Grande Rift in the Socorro and Las Cruces areas, in 26th Field Conference Guidebook: New Mexico Geological Society, p. 297-321.

Clark, S. P., Jr., 1966, Thermal conductivity, in Clark, S. P.,ed., Handbook of Physical Constants, Revised Edition: Geological Society of America, Memorial 97, p. 587.

Clark, N. J., and Summers, W. K., 1971, Records of wells and springs in the Socorro and Magdalena areas, Socorro County, New Mexico, 1968: New Mexico Bureau of Mines and Mineral Resources, Circular 115, 51 pp.

Combs, J., 1980, Heat flow in the Coso geothermal area, Inyo County, California: Journal of Geophysical Research, v. 85, p. 2411-2424.

Craig, H., 1961, Isotopic variations in meteoric waters: Science, v. 133, p. 1702-1703.

Daly, R. A., Manger, G. E., and Clark, S. P., Jr., 1966, Density of rocks, in Clark, S. P.,ed., Handbook of Physical Constants, Revised Edition: Geological Society of America, Memorial 97, p. 587.

Debrine, B., Spiegel, Z., and Williams, D., 1963, Cenozoic sedimentary rocks in Socorro valley, New Mexico, in 14th Field Conference Guidebook: New Mexico Geological Society, p. 123-131.

Fischer, J. A., 1977, The use of relative travel-time residuals of P phases from teleseismic events to study the crust in the Socorro, New Mexico area: New Mexico Institute of Mining and Technology, Geophysics Open-File Report 14, 65 pp.

Gabin, V. L., and Lesperance, L. E., 1977, New Mexico climatological data; precipitation, temperature, evaporation, and wind monthly and annual means: W. K. Summers and Associates, Socorro, New Mexico, 436 pp.

Gelhar, L. W., Gross, G. W., and Duffy, C. J., 1979, Stochastic methods of analysing groundwater recharge: Canberra Symposium on the Hydrology of Areas of Low Precipitation, December, 1979, Proceedings, p. 313-321.

Gonduin, M. and Scale, C., 1958, Streaming potential and the SP log: American Institute of Mining Engineers Petroleum, Transactions, v. 213, p. 170-178.

Goranson, R. W., 1942, Heat Capacity, heat of fusion, in Birch, F., Schairer, J. F., and Spicer, H. C., eds., Handbook of Physical Constants: Waverly Press, Baltimore, Special Paper 36.

Gross, G. W., and Wilcox, R., 1981, Groundwater circulation in the Socorro geothermal area, in Icerman, L., Starkey, A., and Trentman, N., eds., State-coupled low temperature geothermal resource assessment program, fiscal year 1980: New Mexico Energy Institute at New Mexico State University, p. 2-97 - 2-192.

Hall, F. R., 1963, Springs in the vicinity of Socorro, New Mexico, in 14th Field Conference Guidebook: New Mexico Geological Society, p. 160-179.

Hammond, J. F., 1966, A Surgeon's Report on Socorro, New Mexico, 1852: Stagecoach Press, Santa Fe, New Mexico, 47 pp.

Holmes, C. R., 1963, Tritium studies, Socorro Spring, in 14th Field Conference Guidebook: New Mexico Geological Society, p. 152-159.

Jones, F. A., 1904, New Mexico Mines and Minerals: Santa Fe Printing Co., Santa Fe, New Mexico, 349 pp.

Keller, G. V., 1960, Physical properties of tuffs of the Oak Springs Formation, Nevada, in Geological Survey Research, 1960: U.S. Geological Survey, Professional Paper 400-B, p. 396-400.

Lasky, S. G., 1932, The ore deposits of Socorro County, New Mexico: New Mexico Bureau of Mines and Mineral Resources, Bulletin 8, 139 pp.

Lowell, G. R., 1967, Geology of the Blue Canyon area, Socorro Mountains, New Mexico: New Mexico Institute of Mining and Technology, independent study, 22 pp.

Lundstrom, L., and Stille, H., 1978, Large-scale permeability test of the granite in the Strips Mine and thermal-conductivity test: Swedish-American Cooperative Program on Radioactive Waste Storage in Mined Caverns in Crystalline Rock, Technical Project Report 2, Lawrence Berkeley Laboratory Report LBL-7052, 33 pp.

Machette, M., 1977, Geologic map of San Acacia 7½-minute quadrangle, Socorro County, New Mexico: U.S. Geological Survey, Geology Quadrangle Map, GQ-1415.

Mercer, J. W., and Faust, C. R., 1979, Geothermal reservoir simulation 3, application of liquid-and-vapor-dominated hydrothermal modeling techniques to Wairekei, New Zealand: Water Resources, v. 15, p. 653-671.

Mercer, J. W., Pinder, G. F., and Donaldson, I. G., 1975, A galerkin-finite element analysis of the hydrothermal system at Wairekei, New Zealand: Journal of Geophysical Research, v. 80, p. 2608-2621.

Miesch, A. T., 1956, Geology of the Luis Lopez manganese district, Socorro County, New Mexico: New Mexico Bureau of Mines and Mineral Resources, Circular 38, 31 pp.

Morris, D. A., and Johnson, A. I., 1967, Summary of the hydrologic and physical properties of rock and soil materials, as analyzed by the hydrologic laboratory of the U.S. Geological Survey, 1948-1960: U.S. Geological Survey, Water-Supply Paper 1839-D, p. 42.

Muskat, M., 1946, The flow of homogeneous fluids through porous media, First edition: McGraw-Hill, Ann Arbor, Mich., 763 pp.

Osburn, G. R., 1977, Geology of the eastern Magdalena Mountains, Water Canyon to Pound Ranch, Socorro County, New Mexico: New Mexico Institute of Mining and Technology, M.S. thesis, 136 pp.

Pratt, H. R., Swolfs, H. S., Lingle, R., and Nielsen, R. R., 1977, In situ and laboratory measurements of velocity and permeability, in Heacock, J. G., ed., The earth's crust: American Geophysical Union, Washington, D.C., Geophysical Monograph, v. 20, p. 215-231.

Reilinger, R. E., Brown, L. D., and Oliver, J. E., 1979, Recent vertical crustal movements from leveling observations in the vicinity of the Rio Grande Rift, in Riecker, R. E., ed., Rio Grande Rift, Tectonics and magmatism: American Geophysical Union, Washington, DC., p. 223-236.

Reilinger, R. E. and Oliver, J. E., 1976, Modern uplift associated with a proposed magma body in the vicinity of Socorro, New Mexico: Geology, v. 4, p. 573-586.

Reiter, M., Edwards, C. L., Hartman, H., and Weidman, C., 1975, Terrestrial heat flow along the Rio Grande Rift, New Mexico and southern Colorado: Geological Society of America, Bulletin 86, p. 811-818.

Reiter, M., Mansure, A. J., and Shearer, C., 1979, Geothermal characteristics of the Rio Grande Rift within the southern Rocky Mountain complex, in Riecker, R. E., ed., Rio Grande Rift, Tectonics and magmatism, American Geophysical Union, Washington, DC., p. 253-268.

Reiter, M., Shearer, C., and Edwards, C. L., 1978, Geothermal anomalies along the Rio Grande Rift in New Mexico: Geology, v. 6, p. 85-88.

Reiter, M., and Smith, R., 1977, Subsurface temperature data in the Socorro Peak KGRA, New Mexico: Geothermal Energy Magazine, v. 5, p. 37-41.

Renard, K. G., 1970, The hydrology of semiarid rangeland watersheds: U.S.D.A. Agricultural Research Service, Report ARS41-162, 26 pp.

Rinehart, E. J., 1976, The use of microearthquakes to map an extensive magma body in the Socorro, New Mexico area: New Mexico Institute of Mining and Technology, Geophysics Open-File Report 10, 60 pp.

Rinehart, E. J., Sanford, A. R., and Ward, R. M., 1979, Geographic extent and shape of an extensive magma body at midcrustal depths in the Rio Grande Rift near Socorro, New Mexico, in Riecker, R. E., ed., Rio Grande Rift, Tectonics and magmatism: American Geophysical Union, Washington, DC., p. 237-252.

Romero, V. D., and Wilkening, M. H., 1977, Summer precipitation network, Socorro County, New Mexico - 1966-1975: New Mexico Institute of Mining and Technology, Physics Department, unpublished report, 5 pp.

Sanford, A. R., 1968, Gravity survey in central Socorro County, New Mexico: New Mexico Bureau of Mines and Mineral Resources, Circular 91, 14 pp.

Sanford, A. R., 1977a, Seismic investigation of a magma layer in the crust beneath the Rio Grande Rift near Socorro, New Mexico: New Mexico Institute of Mining and Technology, Geophysics Open-File Report 18, 21 pp.

Sanford, A. R., 1977b, Temperature gradient and heat-flow measurements in the Socorro, New Mexico area, 1965-1968: New Mexico Institute of Mining and Technology, Geophysics Open-File Report 15, 18 pp.

Sanford, A. R., 1978, Characteristics of Rio Grande Rift in vicinity of Socorro, New Mexico, from geophysical studies: New Mexico Bureau of Mines and Mineral Resources, Circular 163, p. 116-121.

Sanford, A. R., 1980, Personal communication, New Mexico Institute of Mining and Techonlogy, Socorro, New Mexico.

Sanford, A. R., Alptekin, O., and Toppozada, T. R., 1973, Use of reflection phase on microearthquake seismograms to map an unusual discontinuity beneath the Rio Grande Rift: Seismological Society of America, Bulletin 63, p. 2021-2034.

Sanford, A. R., and Long, L. T., 1965, Microearthquake crustal reflections, Socorro, New Mexico: Seismological Society of America, Bulletin 55, p. 579-586.

Sanford, A. R., Mott, R. P., Jr., Shuleski, P. J., Rinehart, E. J., Caravella, F. J., Ward, R. M., and Wallace, T. C., 1977, Geophysical evidence for a magma body in the crust in the vicinity of Socorro, N.M.: American Geophysical Union, Washington, D.C., Geophysical Monograph, v. 20, p. 385-403.

Sanford, A. R., Rinehart, E., Shuleski, P. J., and Johnston, J. A., 1977, Evidence from microearthquake studies for small magma bodies in the upper crust of the Rio Grande Rift near Socorro, New Mexico: New Mexico Institute of Mining and Technology, Geophysics Open-File Report 19, 13 pp.

Sass, J. H., Lachenbruch, A. H., and Munroe, R. J., 1971, Thermal conductivity of rocks from measurements on fragments and its application to heat-flow determinations: Journal of Geophysical Research, v. 76, p. 3391-3401.

Shuleski, P. J., 1976, Seismic fault motion and SV screening by shallow magma bodies in the vicinity of Socorro, New Mexico: New Mexico Institute of Mining and Technology, Geophysics Open-File Report 8, 94 pp.

Shuleski, P. J., Caravella, F. J., Rinehart, E. J., Sanford, A. R., Wallace, T. C., and Ward, R. M., 1977, Seismic studies of shallow magma bodies beneath the Rio Grande Rift in the vicinity of Socorro, New Mexico: New Mexico Institute of Mining and Technology, Geophysics Open-File Report 13, 8 pp.

Sibbitt, W. L., Dodson, J. G., and Tester, J. W., 1979, Thermal conductivity of crystalline rocks associated with energy extraction from hot-dry rock geothermal systems: Journal of Geophysical Research, v. 84, p. 1117-1124.

Siemers, W. T., 1978, Stratigraphy and petrology of the Pennsylvanian system of the Socorro region, west-central New Mexico: New Mexico Institute of Mining and Technology, Ph.D. dissertation, 259 pp.

Smith, C. T., 1963, Preliminary notes on the geology of part of the Socorro Mountains, Socorro County, New Mexico, in 14th Field Conference Guidebook: New Mexico Geological Society, p. 185-196.

Sorey, M. L., Lewis, R. E., Olmstead, F. H., 1978, The hydrothermal system of Long Valley caldera, California: U.S. Geological Survey, Professional Paper 1044-A, 60 pp.

Summers, W. K., 1976, Catalogue of thermal waters in New Mexico: New Mexico Bureau of Mines and Mineral Resources, Hydrologic Report 4, 80 pp.

Summers, W. K., Schwab, G. E., and Brandvold, L. A., 1972, Groundwater characteristics in a recharge area, Magdalena Mountains, Socorro County, New Mexico: New Mexico Bureau of Mines and Mineral Resources, Circular 124, 18 pp.

Swanberg, C. A., 1979, Chemistry of thermal and non-thermal groundwaters in the Rio Grande Rift and adjacent tectonic provinces, in Riecker, R. E., ed., Rio Grande Rift, Tectonics and magmatism: American Geophysical Union, Washington, DC., p. 279-288.

Trainer, F. W., 1975, Mixing of thermal and nonthermal waters in the margin of the Rio Grande Rift, Jemez Mountains, New Mexico, in 26th Field Conference Guidebook: New Mexico Geological Society, p. 213-218.

von Buttlar, H., 1959, Groundwater studies in New Mexico using tritium as a tracer, II: Journal Geophysical Research, v. 64, p. 1031-1038.

von Buttlar, H., and Wendt, I., 1958, Groundwater studies in New Mexico using tritium as a tracer: American Geophysical Union, Washington, D.C., Transactions, v. 39, p. 660-668.

Waldron, J. F., 1956, Reconnaissance geology and groundwater study of a part of Socorro County, New Mexico: Stanford University, Ph.D. dissertation, 255 pp.

Wallace, D. E., and Renard, K. G., 1967, Contribution to regional water table from transmission losses of ephemeral stream beds: American Society of Agricultural Engineers, Transactions, v. 10, p. 786-792.

Winogard, I. J., and Thordarson, W., 1975, Hydrogeologic and hydrochemical framework, south-central Great Basin, Nevada-California, with special reference to the Nevada Test Site: U.S. Geological Survey, Professional Paper 712-C, 126 pp.

Woodside, W., and Messmer, J. H., 1961, Thermal conductivity of porous media. II. consolidated rocks: Journal of Applied Physics, v. 32, p. 1699-1706.

Young, A., Low, P. F., and McLatchie, A. S., 1964, Permeability studies of argillaceous rocks: Journal of Geophysical Research, v. 69, p. 4237-4245.

Zisman, W. A., 1933, Compressibility and anisotropy of rocks at and near the earth's surface: National Academy of Science, Proceedings, v. 19, p. 666-679.

Appendix A

Water-level contour map

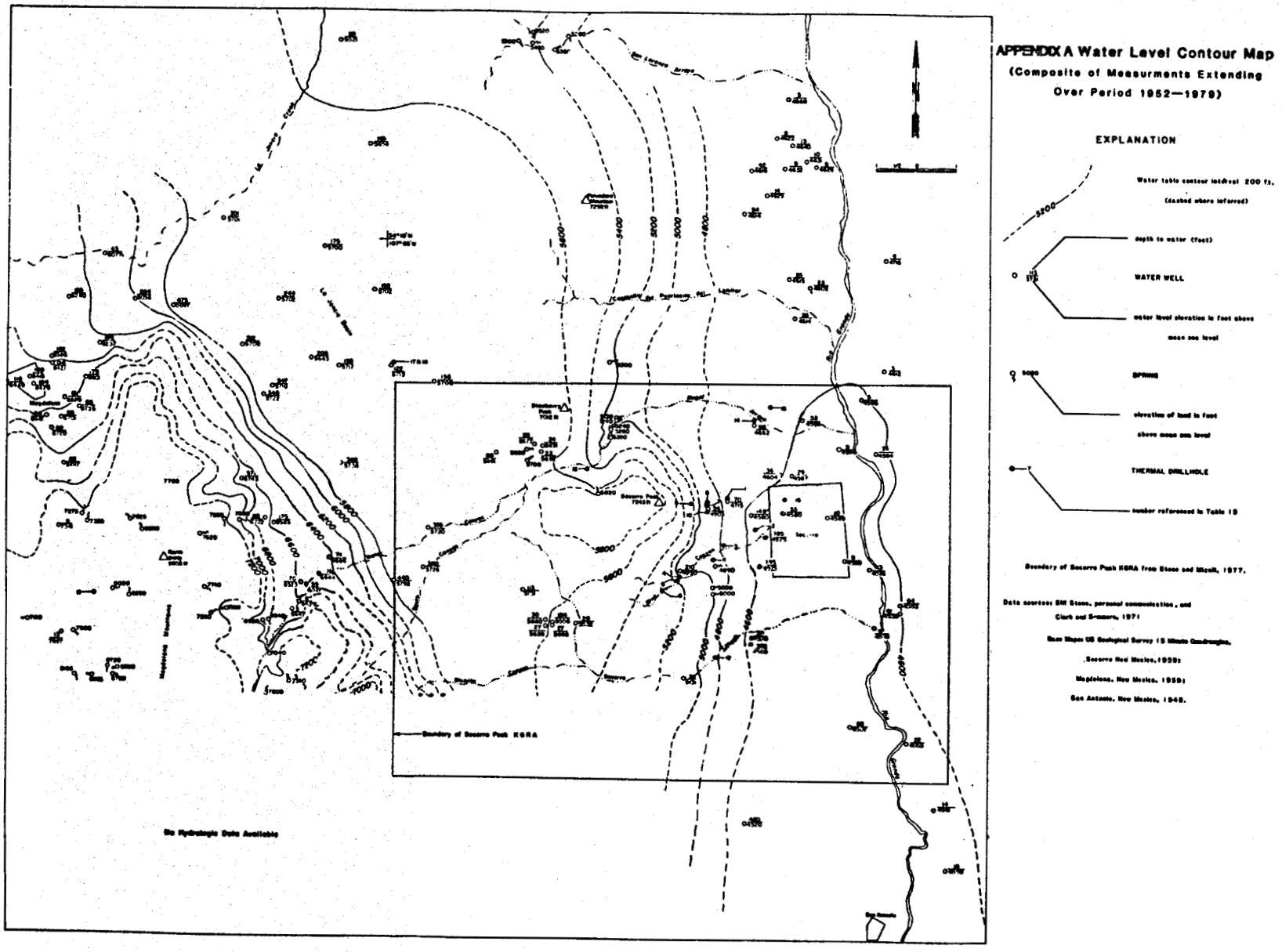

Figure 2A-1. Water-level contour map.

Part 3

Groundwater Circulation in the Socorro Geothermal Area*

Introduction

Socorro and Sedillo springs contribute a major portion of the water supply for Socorro, New Mexico. This report attempts to define more precisely the groundwater system contributing to these thermal springs with the aid of geological, hydrological and groundwater quality, tritium activity, and stable-isotope data. An important question is whether or not a hydraulic connection exists between the shallow groundwater system and the deep geothermal system. This study is partly an extension of the work of Holmes (1963), which attempted to determine groundwater-residence times and approximate groundwater velocities using tritium activity in spring water and precipitation.

Physiography

The study area, a rectangular section of 247-square miles in central New Mexico, (see Figure 2-16), lies in the eastern portion of the Basin and Range Province. The area is typical of Basin and Range topography. Two north-south trending fault-block mountain ranges are bounded by alluvial-fill basins. The western boundary of the area is made up by the Magdalena Mountains (see Figure 2-17). This westward-dipping fault-block range reaches a height of about

*The principal authors of Chapter 2, Part 3 are Dr. Gerardo W. Gross, Professor of Geophysics, and Ralph Wilcox, Graduate Research Assistant, Department of Geophysics, New Mexico Institute of Mining and Technology.

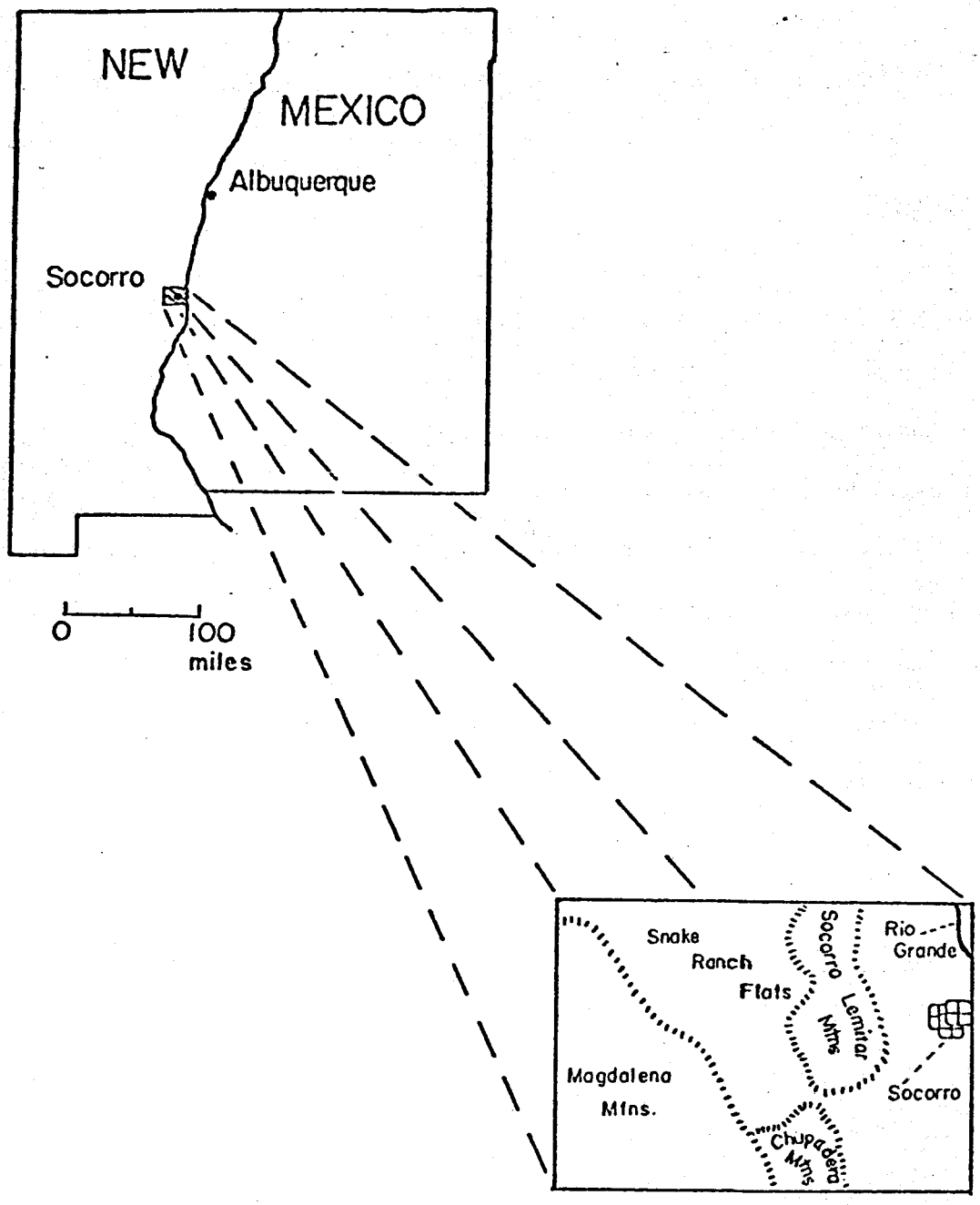

Figure 2-16. Location of the study area.

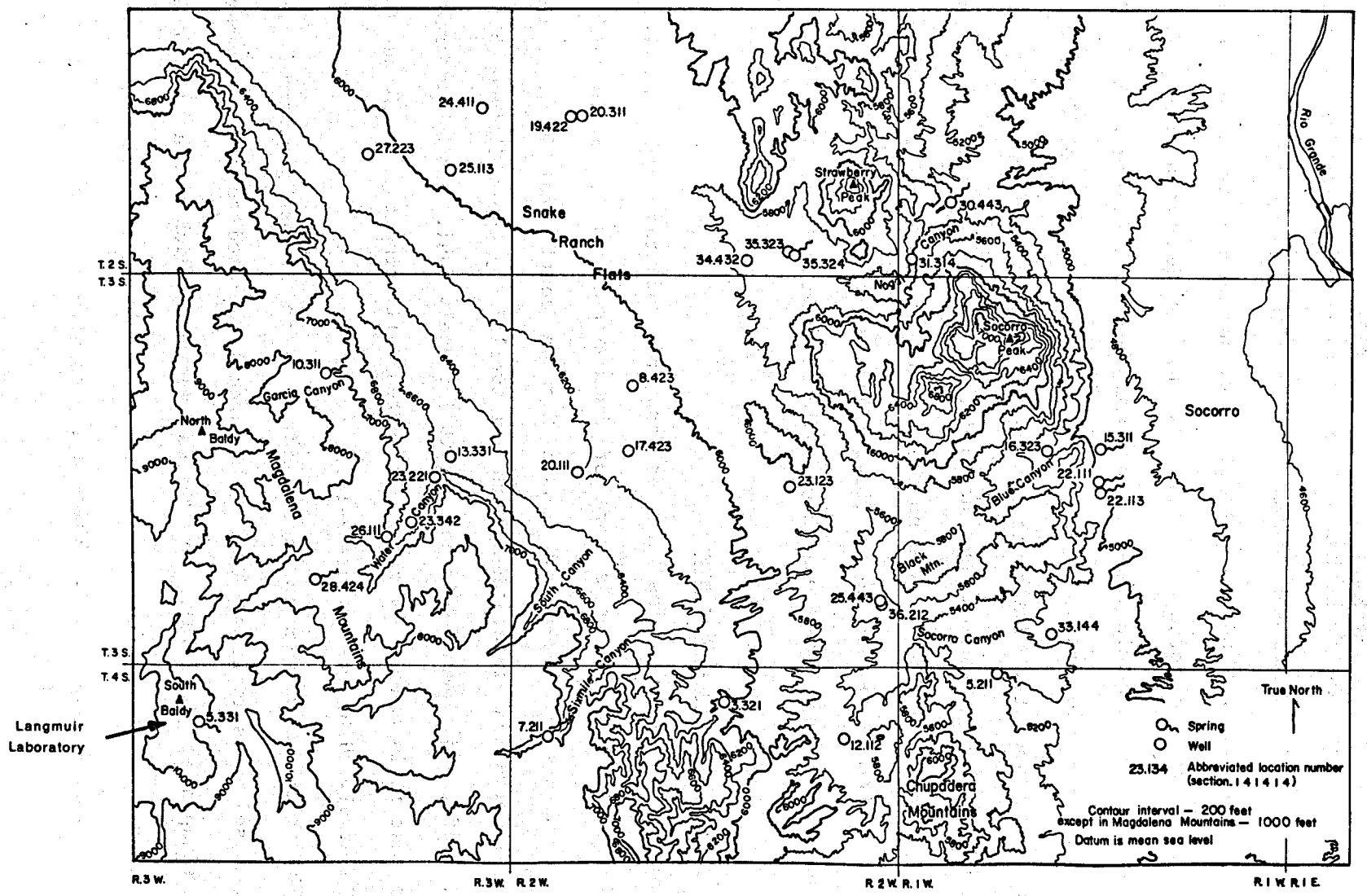

Figure 2-17. Physiography and sampling locations.

10,099 ft on South Baldy. East of this range lies the La Jencia Basin, which is a graben filled to an unknown depth with alluvial sediments. Physiographically, the Snake Ranch Flats is the southern extension of the La Jencia Basin. The flats are relatively featureless, except where dissected by major arroyos, with a gentle eastward slope, and an average elevation of 6000 ft. The flats are bordered on the east by the Socorro-Lemitar mountains. This horst-block mountain range is approximately 7200 ft high. East of this range lies the Rio Grande alluvial valley and the town of Socorro at an elevation of 4600 ft. The southern boundary of the study area is where the Snake Ranch Flats pinch out and the Magdalena and Chupadera mountains combine to form a group of hills. The northern boundary is determined on the flats where groundwater appears to be flowing northward (into the La Jencia Creek drainage basin) away from areas which could contribute to the thermal springs.

Setting of Thermal Springs

Socorro Mountain forms the eastern rim of the Snake Ranch Flats structural basin. It has a core of Precambrian and Paleozoic rocks but consists mainly of lower and middle Miocene continental basin sediments (Popotosa Formation) interbedded with and overlain by upper Miocene rhyolitic domes, tuffs, and flows. This complex is intensely faulted and fractured, and to the east it is bounded by the fault system delimiting the Rio Grande Graben (Chapin et al. 1978) (see Figure 2-18).

The volcanic complex is characterized by an intense geothermal anomaly which, based on seismic studies, is apparently related to magma chambers at depth (Chapin et al. 1978). The thermal springs, which are a main focus of this discussion, issue from a fracture system in this complex where it is upfaulted against basin fill. There are presently three springs, from north

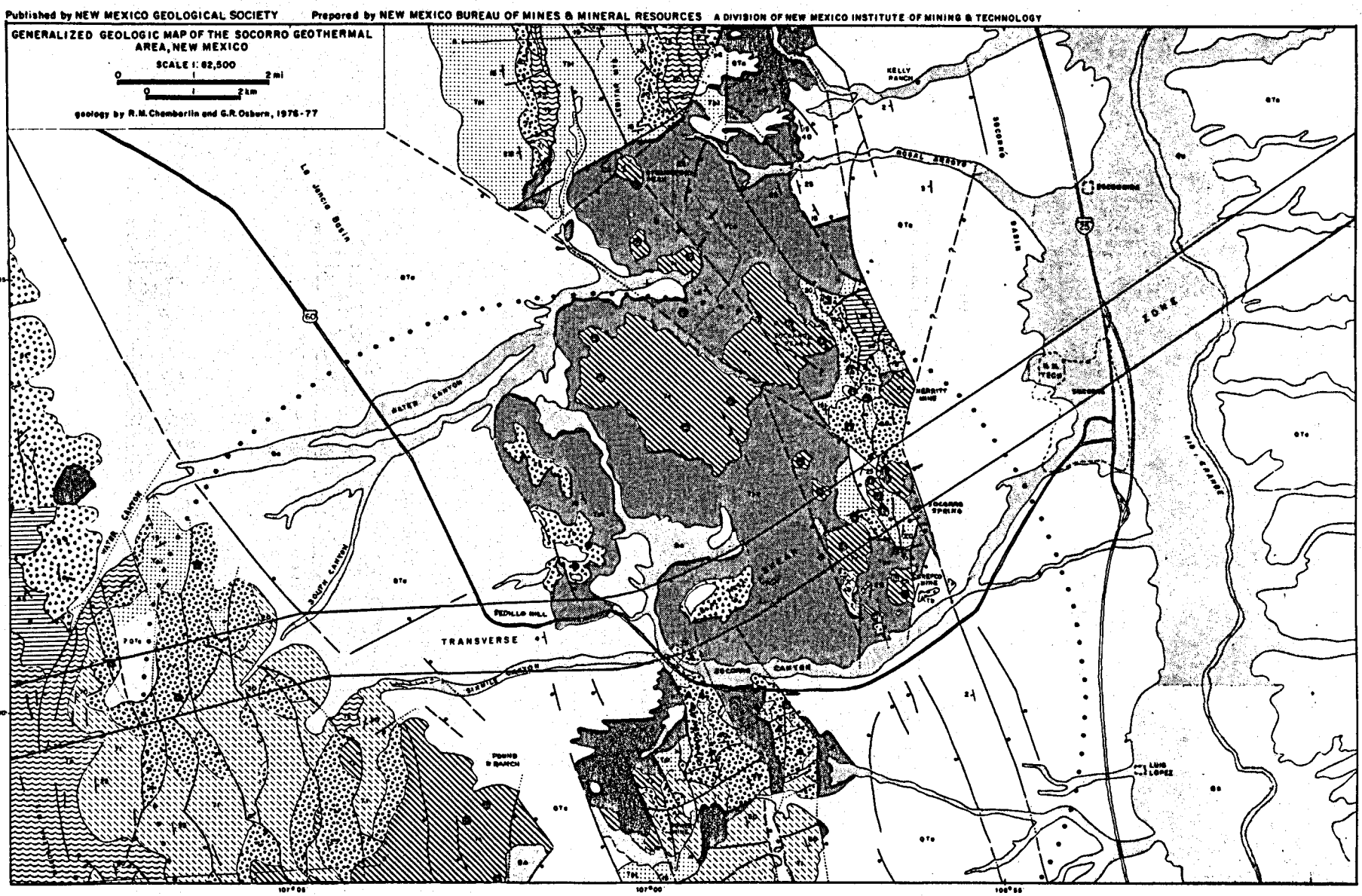

Figure 2-18. Generalized geologic map of the Socorro geothermal area, New Mexico.(Chapin et al. 1978). See following page for legend.

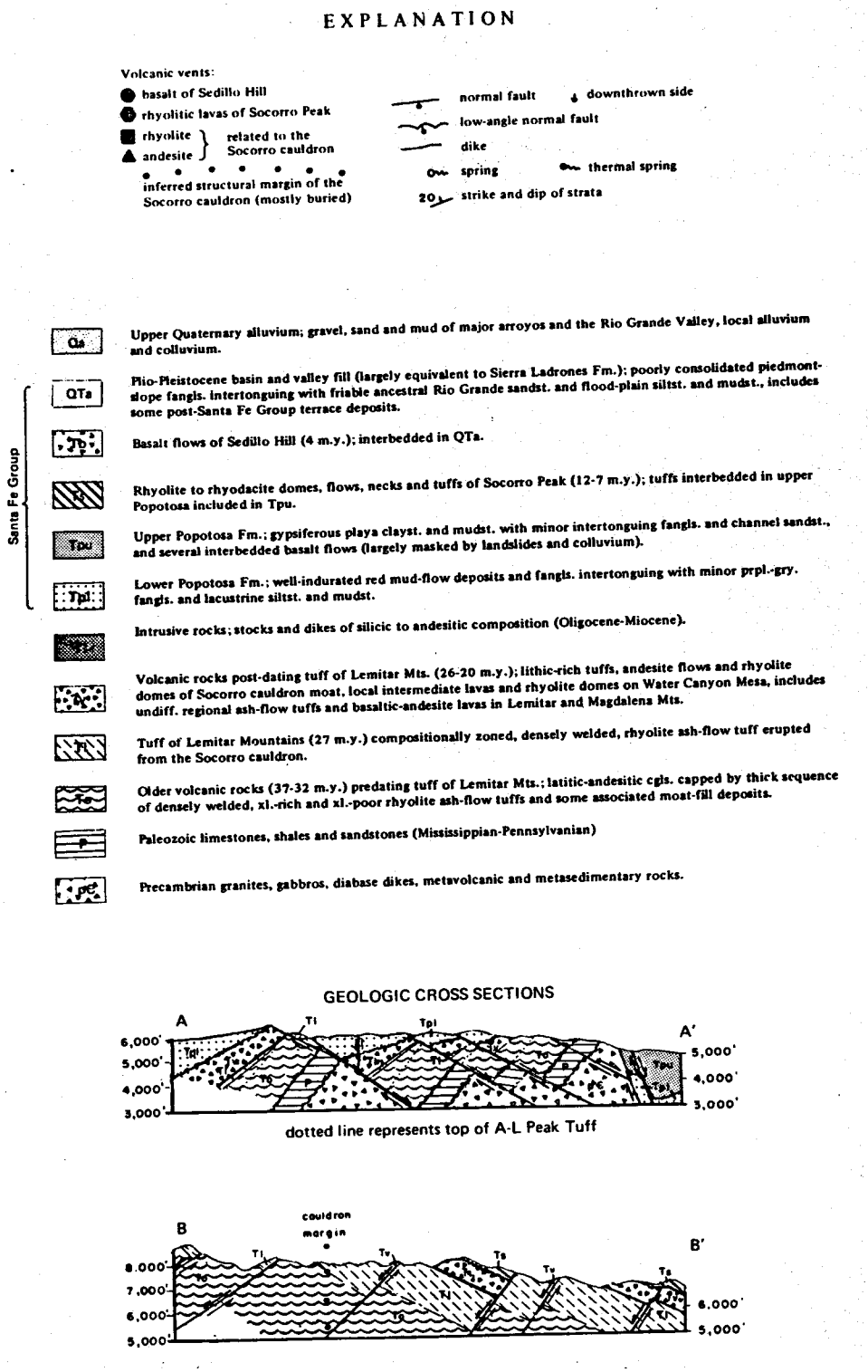

Figure 2-18. (continued).

to south: Cook (3.1.15.311), Socorro (22.111) and Sedillo (22.113). It is the latter two which supply water to the city of Socorro. Cook Spring is nearly dry. In addition, there is Blue Canyon Well (16.323), which also produces water of above-normal temperature and contains a dissolved solids content similar to that of the springs.

Surface Drainage

The Magdalena Mountains drain into the Snake Ranch Flats through several major canyons which dissect the range front. Nogal Canyon and Socorro Canyon provide through-drainage for the Snake Ranch Flats into the Rio Grande Valley. Without these two canyons which cut the Socorro-Lemitar and Chupadera mountains, the Snake Ranch Flats would be essentially a closed basin, which it probably was in the past. There are no perennial streams in the area, except the Rio Grande and sections of arroyo channels near springs.

Climate

The climate of the area ranges from semiarid in Socorro, 7.9 inches of precipitation per year, to alpine near the peaks of the Magdalena Mountains, 17.7 inches per annum (Romero and Wilkening 1977). Continuous weather records are available from Socorro (4600 ft) and Kelly Ranch (6700 ft) in the eastern part of the study area. During the summer, records are also taken at Langmuir Laboratory, an atmospheric research facility of New Mexico Institute of Mining and Technology, which is located at 10,631 ft near the summit of the Magdalena Mountains on the west side of the study area (Romero and Wilkening 1977).

Procedure

Sampling of Socorro and Sedillo springs, and analysis for tritium activity, was done irregularly from 1957 to 1964. Socorro precipitation samples have been analyzed until the present, except for the period September 1968 to June 1971. The correlation of peaks in these two data sets may indicate a groundwater residence time within the aquifer contributing flow to the thermal springs.

Sampling of the thermal springs was resumed in February 1977 and Cook Spring was included. Based on previous work of Waldron (1956) and Hall (1963), a series of springs and wells within the Socorro-Lemitar mountains, the Snake Ranch Flats, and the Magdalena Mountains were also chosen for the study. Samples for tritium analysis were then collected from the group of wells and springs at intervals of about two months. The coordinate system used for locating springs and wells is included in Appendix A. The springs and wells, their location, and their characteristics are tabulated in Appendix B. Where possible, water levels were measured to determine piezometric head distribution over the area. Where wells could not be measured, older data were used (Clark and Summers 1971).

Chemical analyses of groundwater were performed for major ions for each well or spring being sampled for the study. In addition, there were older chemical data obtained from other references (see Appendix C). The stable isotopes deuterium and oxygen-18 were measured in 17 samples.

Geologic information has been compiled from previous work and from ongoing studies of the New Mexico Bureau of Mines and Mineral Resources, notably the investigations by Chapin and his co-workers. Spring-flow rates have been furnished by the City of Socorro and SER, Inc., a local private consulting firm. Precipitation data were obtained from the U.S. Weather Bureau for the Socorro and Kelly Ranch stations (see Appendix D).

Previous Investigations

Waldron (1956) sampled and described the thermal springs. Hall (1963) gave a close account of spring water quality in the Socorro area and noted the change from predominantly calcium-bicarbonate water in the western part of the study region to sodium-bicarbonate east of the Socorro-Lemitar Range, which was attributed to cation exchange with the Socorro-Lemitar rhyolitic volcanics. Holmes (1963) used atmospheric tritium as a tracer in an attempt to determine the residence time of spring water underground. Summers (1976) described the thermal characteristics of the springs. Denny (1940, 1941) detailed the Tertiary and Quaternary geology of the area just north of the Lemitar Mountains. Machette (1978) mapped the San Acacia Quadrangle and redefined the Santa Fe Group (Miocene to Pleistocene) in this area. Bruning (1973) described the Popotosa Formation in detail. Osburn (1978) mapped the western part of the study area and Chamberlin (1978) mapped the eastern portion. Chapin et al. (1978) discussed the Socorro geothermal area in the context of regional tectonic history and showed that the Socorro geothermal area occupies the site of an Oligocene cauldron. This latter work is fundamental to an understanding of the study area because it creates the conceptual framework within which geologic, geothermal, and seismic phenomena relate to each other and to present-day groundwater circulation.

Hydrogeology

The study area is located within the Rio Grande Rift. The two fault-block mountain ranges, Magdalena and Socorro-Lemitar, consist of thick Tertiary volcanic piles with some interbedded basin-fill sediment, underlain by a thin sequence of Paleozoic sedimentary rocks and by a Precambrian basement of metasedimentary, metavolcanic, and plutonic rocks (Chapin et al.

1978) (see Figure 2-19). The Snake Ranch Flats is a graben-type feature which probably has the same sequence of rocks underlying a thick unit of Tertiary-Quaternary fill sediments. The area is characterized by dipping strata and an abundance of northwest-southeast trending normal faulting.

Through most of the Tertiary period, this area has been tectonically active with periods of intense volcanism. High degrees of fracture permeability have developed in most well-indurated rocks (Chapin et al. 1978). Stratigraphic throw as a result of faulting has created very jumbled lateral relationships between rock units. All of these factors have combined to produce a geologically-complicated groundwater system from which Socorro and Sedillo springs issue. Even though the system is geologically complex, the high degree of fracturing associated with the tectonism may have created relatively homogeneous intervals of permeability corresponding with depth of burial.

Popotosa Formation (Lower Santa Fe Group)

According to Chapin et al. (1978), the Socorro Cauldron was formed about 27 m.y. ago. Its formation was related to the tectonism that created the Rio Grande Graben. A potassium anomaly in volcanic rocks of the cauldron is believed to be related to the geothermal system of that time.

A broad sedimentary basin, the Popotosa Basin, spanned the Rio Grande Rift in the Socorro area 26 m.y. ago. The basin extended from the Gallinas Uplift in the west to the mesas east of the Rio Grande and from the Ladron Mountains in the north to the Magdalena and Chupadera mountains to the southwest and southeast. The lowest part of this basin is presently occupied by the Socorro-Lemitar mountains. From the surrounding mountain ranges, the basin was filled by up to 1500 feet of alluvial-fan and piedmont-slope

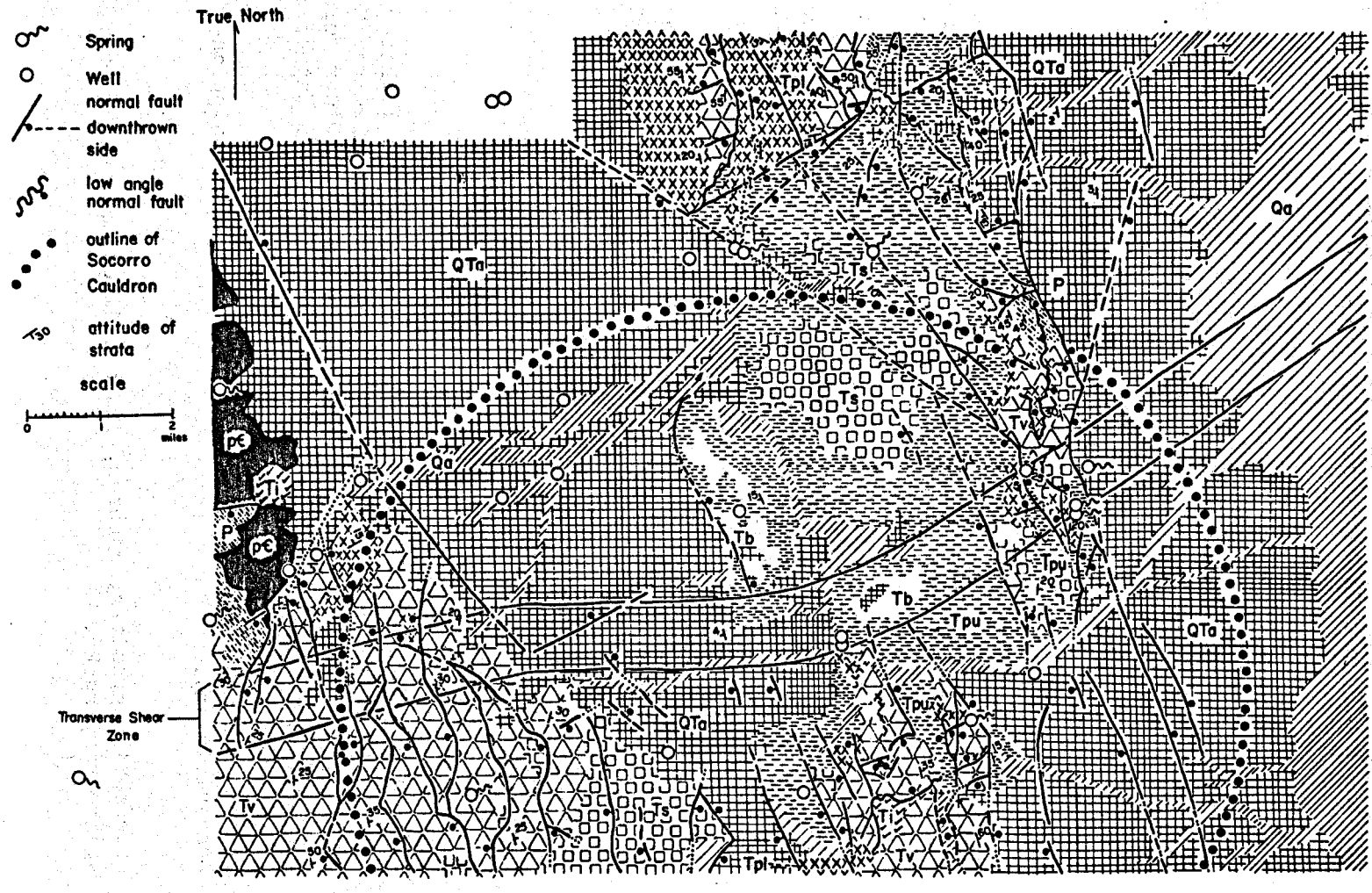

Figure 2-19. Geologic map (after Chapin et al. 1978). See following page for legend.

Upper Quaternary alluvium; gravel, sand and mud of major arroyos and of the Rio Grande Valley; local alluvium and colluvium.

Santa Fe Group

Sierra Ladrones Formation. Pliocene-Pleistocene basin and valley fill; poorly consolidated piedmont-slope fanglomerates intertonguing with ancestral Rio Grande sandstone and floodplain siltstone and mudstone.

Basalt flows of Sedillo Hill (4 m.y.); interbedded in QTa.

Rhyolite to rhyodacite domes, flows, necks, and tuffs of Socorro Peak (12 to 7 m.y.); tuffs interbedded in Upper Popotosa included in Tpu.

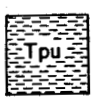

Upper Popotosa Formation. (upper Miocene); gypsiferous playa clays with minor intertonguing fanglomerates and channel sandstones; interbedded basalt flows.

Lower Popotosa Formation. (lower Miocene); indurated red mudflow deposits and fanglomerates intertonguing with minor purple-gray fanglomerates and lacustrine clays and silts.

Intrusive rocks; silicic to andesitic stocks and dikes (Oligocene-Miocene).

Unit of Luis Lopez. Volcanic rocks (26 to 20 m.y.); lithic-rich tuffs, andesite flows, and rhyolite domes. Tuff of Lemitar Mountains (27 m.y.); densely-welded rhyolite ash-flow tuffs. Older volcanic rocks (37 to 32 m.y.); lithic-andesitic conglomerates capped by densely-welded rhyolite ash-flow tuffs.

Paleozoic limestones, shales, and sandstones (Mississippian-Pennsylvanian).

Precambrian granites, gabbros, diabase dikes, metavolcanic and metasedimentary rocks.

Figure 2-19. (continued).

deposits (lower Popotosa) and these in turn were topped with playa lake deposits (800 to 2500 feet). Rhyolitic intrusions and vulcanism along the northern moat of the Socorro Cauldron (buried under the Popotosa Basin) occurred sometime between 12 and seven m.y. ago and spilled into and over the basin sediments.

According to Chapin and Seager (1975), the Magdalena Uplift was a faulted horst within the Popotosa Basin prior to 10 m.y. ago (see Figure 2-20). Its erosion contributed to the basin fill (Bruning 1973; Chapin and Seager 1975). In the Socorro Mountain area, fanglomerate and playa sediments of the Popotosa Formation are intruded with and overlain by volcanic domes and flows. One flow overlying the Popotosa Formation on Socorro Peak has been dated at 10.7 m.y. ago. There is no evidence of any Popotosa deposition younger than the Socorro Peak vulcanism. In the Socorro area, the Popotosa Formation consists of a lower member mostly of poorly-sorted, well-indurated fanglomerates, some playa sediments, and an upper member of mostly gypsiferous playa silts and clays.

Sierra Ladrones Formation (Upper Santa Fe Group)

Present-day structure and relief of the Socorro-Lemitar mountains was defined either contemporaneously with or shortly following the vulcanism in the area (i.e., seven to four m.y. ago). The Popotosa Formation was tilted and faulted during this activity. Creation of the Snake Ranch Flats as a structural basin was accomplished by renewed uplift of the Magdalena Mountain fault block. Downwarping of the basin and basin-fill processes have gone on more or less continuously since early Miocene time. Formation of an ancestral Rio Grande drainage system possibly occurred during the breakup of the Popotosa Basin. Broad, gently sloping piedmont planes descended toward the

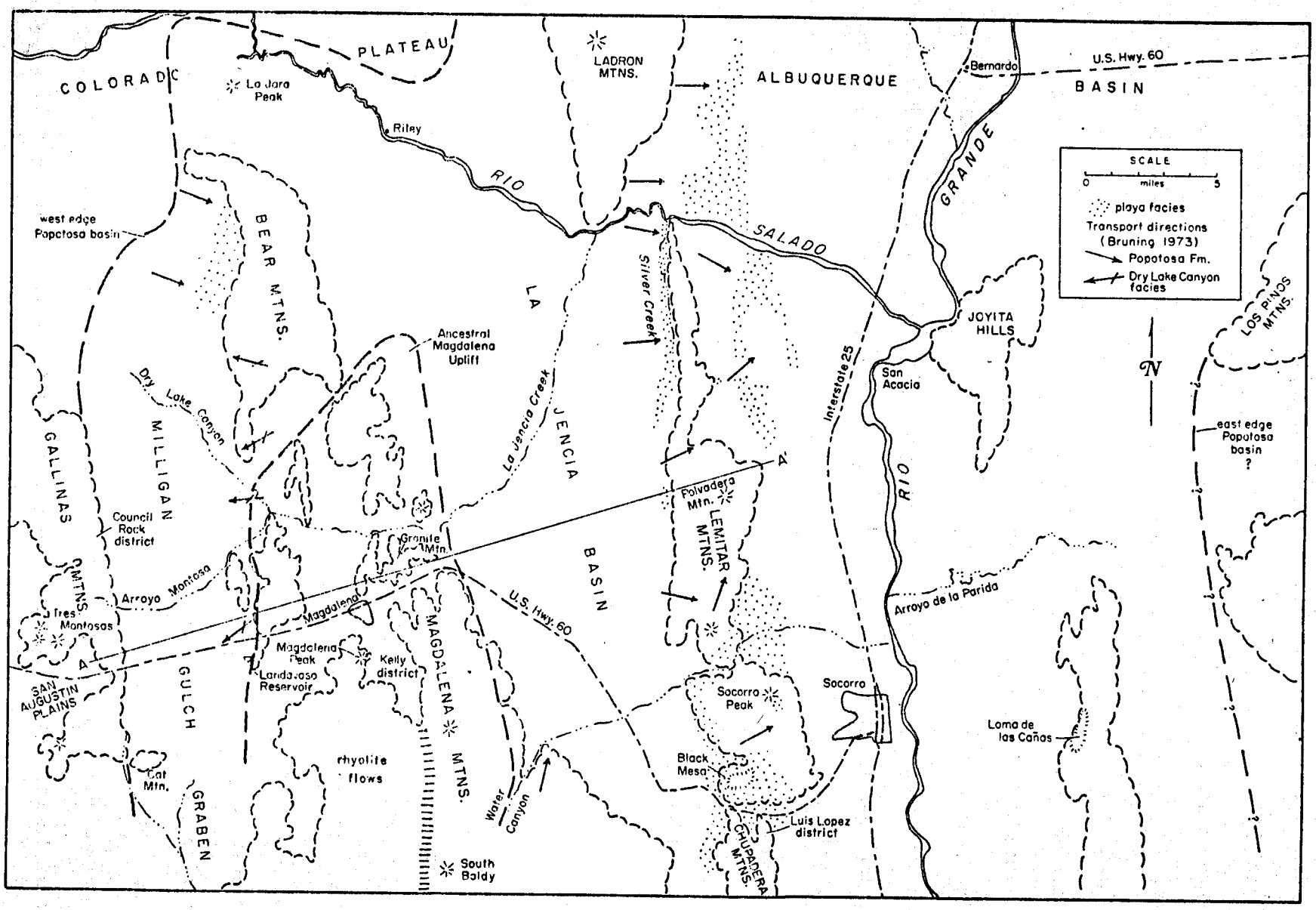

Figure 2-20. Sketch map of the Socorro area showing the Pliocene Popotosa Basin and its segmentation by modern intrabasin horsts (Chapin and Seager 1975).

river and were covered with granular piedmont-slope deposits, known as the Sierra Ladrones Formation.

The Sierra Ladrones Formation (Machette 1978) represents the Upper Santa Fe Group in the study area. It overlies the Popotosa Formation with an angular unconformity and consists of river channel and flood-plain deposits (mainly sand), of the ancestral Rio Grande, laterally intertongued with piedmont-slope fanglomerates and sands derived from the present highlands. Basalt flows (four m.y.) are intercalated in these sediments; deformation is very much less than in the Popotosa Formation. The Sierra Ladrones Formation is an important aquifer along the eastern flank of the Rio Grande Graben in the study area.

Quaternary Sediments

Quaternary sediments on the Snake Ranch Flats are very similar to the Upper Santa Fe Group. Waldron (1956) divided the Quaternary deposits of the Snake Ranch Flats into three groups: (1) the alluvial fans adjacent to the eastern flank of the Magdalena Mountains, and alluvium deposited in arroyos on the flats; (2) peripediment gravels on the flanks of the Socorro-Lemitar mountains and at the southern end of the flats; and (3) lake sediments in the interior of the flats.

On the east slope of the Magdalena Mountains, alluvial fans composed of pebbles and boulders of granite, gneiss, schist, limestone, and volcanics are set in an unconsolidated matrix of sands and silts. Waldron (1956) estimated that the thickness of the Quaternary alluvial cover varied from 100 to 400 feet over the basin. Since basin-fill processes have been going on more or less continuously since the creation of the basin, it would be virtually impossible to draw the line between Upper Santa Fe Group and Quaternary

alluvium. Peripediment gravels on the flanks of the Socorro-Lemitar mountains and at the southern end of the flats are composed of volcanic pebbles, cobbles, and boulders over and in an unconsolidated matrix of sand and silt. This gravel veneer is a deflation-lag deposit. The lake deposits are confined to a one square-mile patch in the lowest part of the basin and consist of red-brown silts and silty clays. There is no evidence that the lake was ever larger.

Possible Thickness of Santa Fe Group on the Snake Ranch Flats

There are no wells on the flats which penetrate the entire Santa Fe Group. The deepest well on the flats (20.111) is 540 feet (see Appendix B, Table 2B-1), and it does not completely penetrate the upper Santa Fe Group. Drillers' logs were located for wells 20.111, 27.223, and 20.311 (see Table 2B-1) on the Snake Ranch Flats.

Sanford (1968) ran a gravity survey over the Snake Ranch Flats and discovered that the residual Bouguer anomalies indicated a depression nearly as deep as the Rio Grande depression. This structure probably is the result of step faulting, and possibly tilting, over a broad zone from the mountain front to near the center of the depression (Sanford 1968). Step faulting has been detected as far as two miles basinward from the fault-line scarp of the Magdalena Mountains. A seismic-reflecting horizon has been dropped about 100 ft in this area (Waldron 1956). The results of recent step faulting may be seen on the alluvial fans in the northeastern part of the Magdalena Mountains. This faulting has cut the fans along a nearly north-south trend and created a terrace 20 ft high in places. There are some anomalously high water-table gradients (Waldron 1956), as evidenced by well levels, in the northern part of the Snake Ranch Flats. These are suspected to be the result of step faulting.

In order to determine the depth of the basin, Sanford (1968) first compiled a pre-Santa Fe Group geologic section for the basin (see Figure 2-21). The section was based primarily on lithologies and thicknesses of rocks exposed in the low hills east of the Rio Grande Valley. The total thickness of this section from Precambrian to the base of the Santa Fe was 8700 feet. This section was divided up into 1000-ft subsections, and percentages of sandstone, shale, limestone, and volcanics for each subsection were determined. These percentages were then multiplied by mean densities of each rock type and totaled to obtain the average density for each 1000-ft subsection.

Whether or not the basin actually contains the assumed rock section, could not be ascertained by Sanford (1968) with geological and geophysical data available at the time. However, detailed geological work of recent years supports the contention that the section is not all present in the Snake Ranch Flats. A broad uplift during Laramide times took place in what is now the southern part of La Jencia Basin covering the area west of the Rio Grande presently occupied by Socorro Mountain, Snake Ranch Flats, and the Magdalena Range. This uplift explains why the upper Permian and all of the Mesozoic are missing in the Socorro-Lemitar and in the southern Magdalena mountains (Smith 1963; Chamberlin, personal communication 1980). It is therefore likely that these strata are also missing in the basement of the Snake Ranch Flats Depression.

Sanford (1968) then constructed hypothetical geologic cross sections of the basin using the assumed geologic section (see Figures 2-22 through 2-24). The faulted basin was represented as having one normal fault at each margin to reduce the labor involved in computing gravity anomalies.

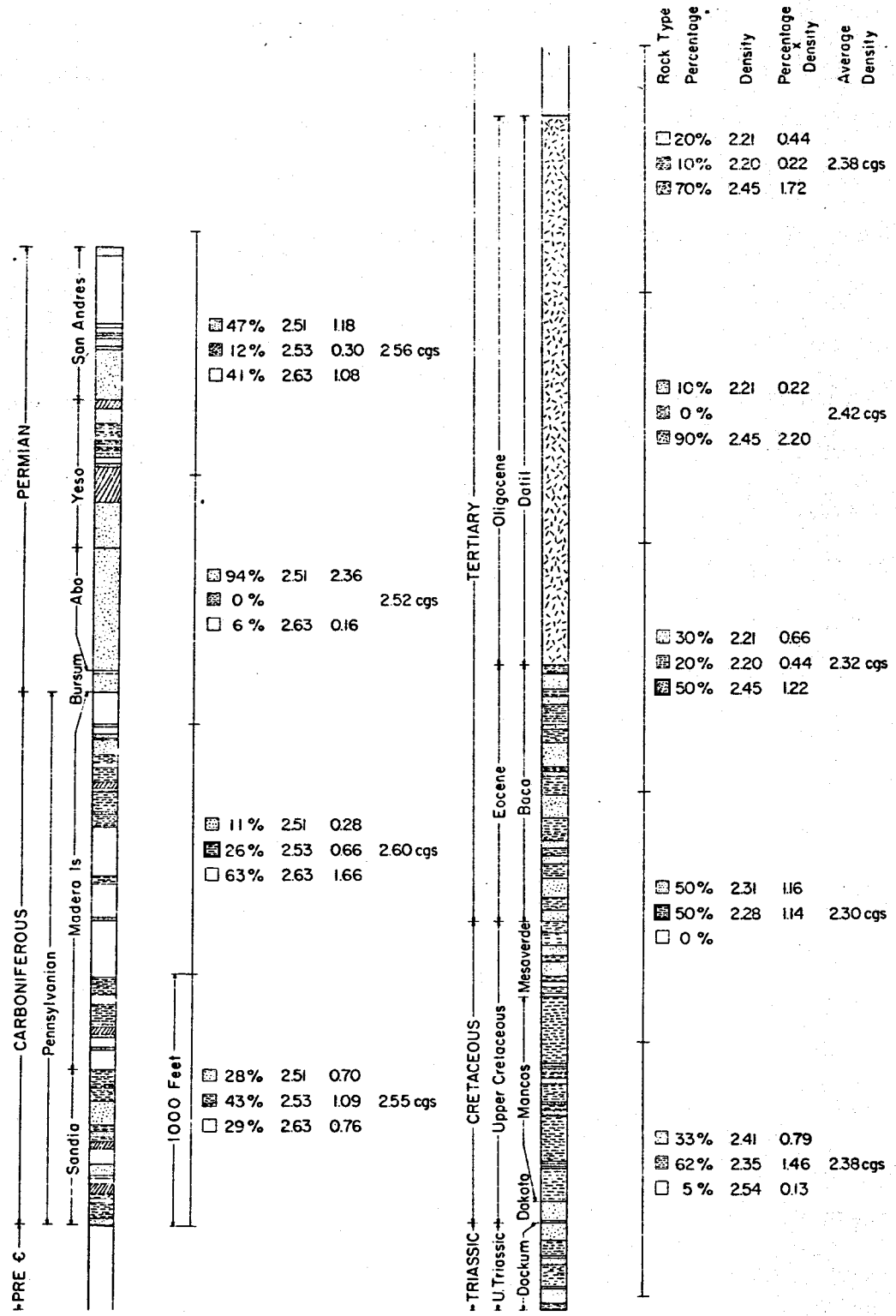

Figure 2-21. Geologic column used in gravity interpretations (Sanford 1968).

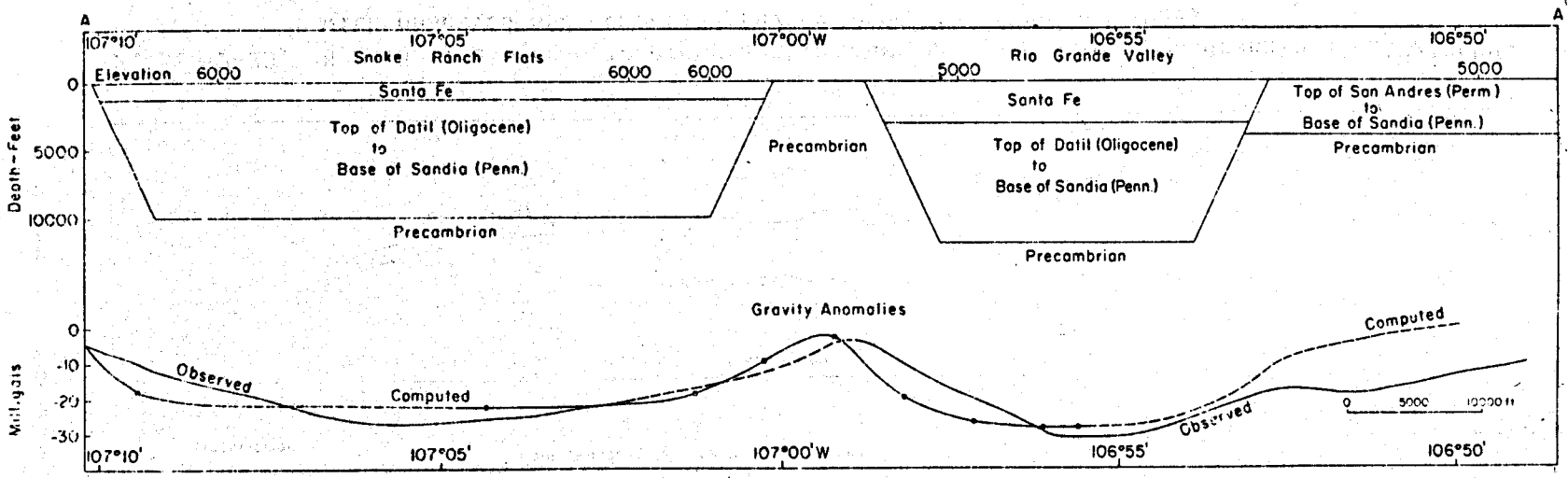

Figure 2-22. Hypothetical geologic section through the Magdalena Quadrangle at 34°7'30"N with observed and computed gravity anomalies (Sanford 1968).

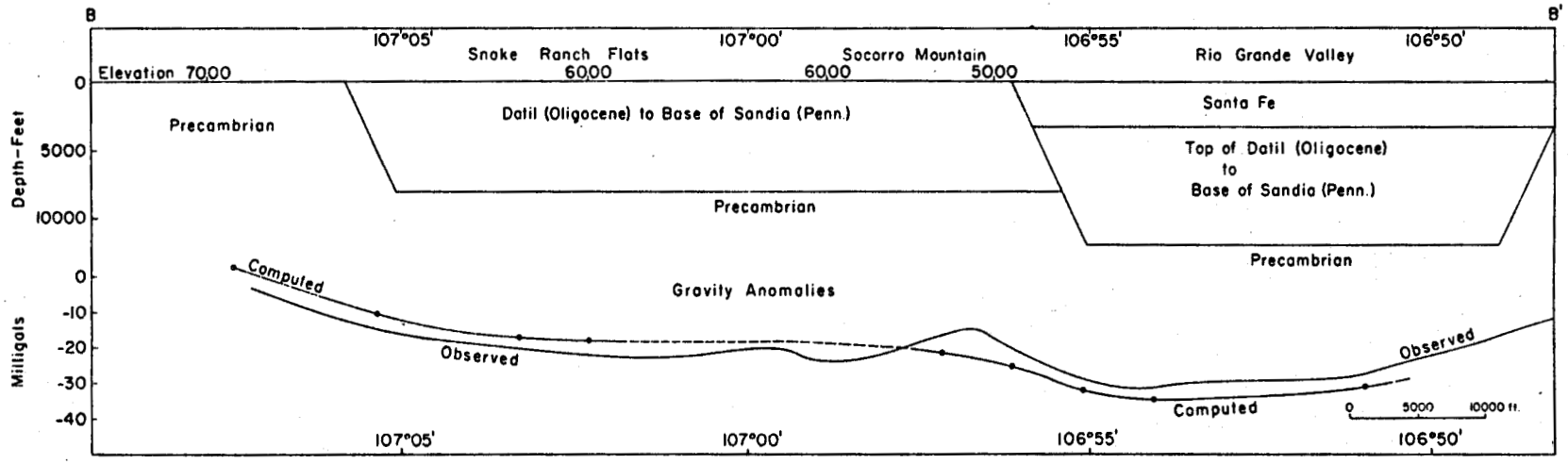

Figure 2-23. Hypothetical geologic cross section through the Socorro Quadrangle at 34°2'30"N with observed and computed gravity anomalies (Sanford 1968).

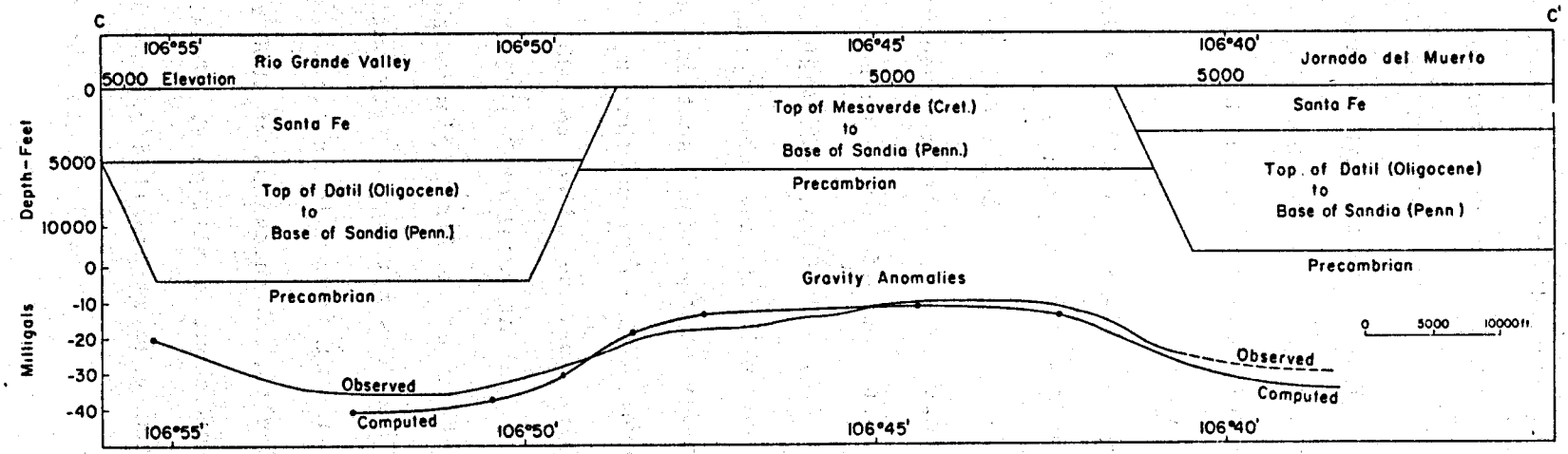

Figure 2-24. Hypothetical geologic section crossing the San Antonio and Carthage Quadrangles at about 33°53'N with observed and computed gravity anomalies (Sanford 1968).

To estimate the thickness of the Santa Fe Group under the Snake Ranch Flats, the model proposed by Sanford (1968) was used, but an altered geologic column was assumed. The assumption is that, the Abo Formation through Baca Formation (see Figure 2-21) are not present in the Snake Ranch Flats Depression. This is a section of 4280 ft with a mean density of 2.41 g/cc. Then, in order to arrive at the same computed anomaly, a thickness of Santa Fe Group must be added to the column on top of the Datil volcanics. The gravity defect of removed material is

$$\Delta g_R = 2\pi\ k\Delta\rho_R h_R = 2\pi\ k(2.67 - 2.41)\ h_R = 0.52\pi\ kh_R,$$

where k = the universal gravitational constant, $\Delta\rho_R$ = the difference between the density adopted for the plate correction and the mean density of the removed section, and h_R = the thickness of the removed section.

The gravity defect of added material with a mean density of 2.20 g/cc is

$$\Delta g_A = 2\pi k\Delta\rho_A h_A = 2\pi k(2.67 - 2.20)\ h_A = 0.94\pi k h_A,$$

where $\Delta\rho_A$ = the difference between the density adopted for the plate correction and the mean density of the added section, and h_A = the thickness of the added section. However, $\Delta g_R = \Delta g_A$ so that $h_A = (0.52/0.94)h_R = 0.553$ (4280) = 2367 ft. This value must be added to 1000 ft of Santa Fe Group already there to obtain an equivalent total of 3367 ft.

Sanford (1968) noted that at a first glance the comparison between observed and computed anomalies does not appear very satisfactory and ascribed most of the mismatch as resulting from using one fault at the basin margins instead of using multiple faults. A thickness of 1000 feet of Santa Fe Group will result in an anomaly of about 6 milligals. Thus, the first order fit between observed and computed gravity profiles can be improved by adding an additional few hundred feet of Santa Fe Group to the structural depression model.

Structural Controls of the Groundwater System

The generalized geologic map (see Figure 2-18) shows that all of the springs in and adjacent to the Socorro-Lemitar mountains are fault controlled. Impermeable aquitard rocks have been down faulted against permeable, aquifer rocks in each case. Socorro and Sedillo springs (22.111) and 22.113), respectively, issue from fractures in the lower member (?) of the Popotosa Formation where it is interbedded and/or in fault contact with rhyolitic ash-flow tuffs, and the downfaulted aquitard is the upper member (?) of the Popotosa Formation*. The upper member of the Popotosa Formation also appears to be the aquitard for Lower Nogal Canyon Spring (30.443), Upper Nogal Canyon Spring (31.314), and Snake Ranch Spring (35.324).

There are two major crustal lineaments which intersect in the Socorro area (Chapin et al. 1978) (see Figure 2-25), namely, the Morenci and the Capitan lineaments. These lineaments are deeply penetrating flaws in the lithosphere which influence the deformation of brittle near-surface rocks. One of these, the Morenci Lineament, has a near-surface expression as a transverse shear zone (see Figure 2-19) in the study area (Chapin et al. 1978). To the north of a line extending from Socorro to South Baldy in the Magdalena Mountains, strata are dipping to the west and are down faulted to the east. South of this line, strata dip to the east and are down faulted to the west. How this shear zone affects the groundwater system is not known. However, it seems reasonable to assume that along this shear zone a high degree of fracturing and brecciation has occurred which could have created a high-permeability zone that channels groundwater flow. Socorro and Sedillo springs issue along the transverse shear zone (see Figure 2-19). However, the

*There is some disagreement among investigators about the detailed stratigraphic correlation and structural relationships in the vicinity of the springs. For the purposes of this discussion, these relationships need not be decisive and are not being explored further.

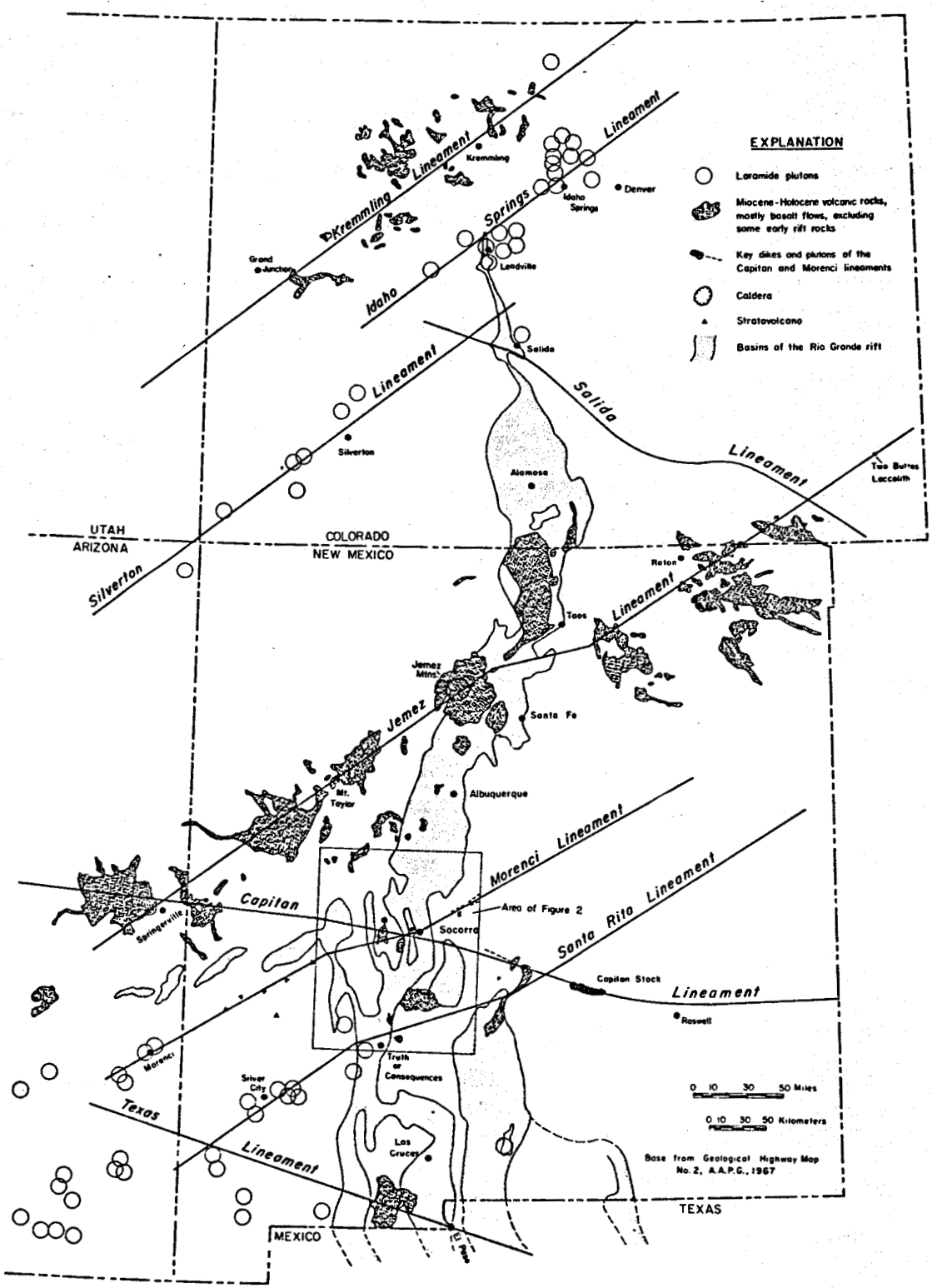

Figure 2-25. Generalized map of the Rio Grande Rift and major crustal lineaments (Chapin et al. 1978).

indicated shear zone location is only approximate (Chamberlin, personal communication 1980).

Another major geological structure which may affect the groundwater system in the study area is the Socorro Cauldron. This elliptical subsidence structure (see Figure 2-19) was formed by the collapse of the roof of a large magma body as the result of huge ash-flow eruptions. After collapse, the floor of the cauldron was probably domed upward by magma pressure to create a central resurgent dome separated from the cauldron walls by a topographic low called a moat. This moat was underlain by deeply penetrating ring fractures which allowed magma an easy path to the surface. The moat filled with lava flows and domes, tuffs, and sedimentary debris from the cauldron walls and resurgent dome. These moat deposits (unit of Luis Lopez of Chapin et al. 1978) are a permeable sequence of rocks which may be a significant part of the groundwater system today. The moat deposits are found throughout the Socorro Mountains in the study area and overlie the tuff of the Lemitar Mountains which is also very permeable (Chamberlin, personal communication 1980).

Characteristics of Thermal Springs

Both Socorro and Sedillo springs probably issue from the lower member of the Popotosa Formation. Socorro Spring issues from a series of joints (Summers 1976) in a gallery which has been dug to intercept spring flow. Sedillo Spring probably issues from the same joint set. The water issuing from these springs is of excellent quality and consistently ranges between 90°F and 92°F in temperature.

Spring flow has been monitored inconsistently since 1953 by the City of Socorro (see Figure 2-26). The values shown on this figure are questionable, however, because the City of Socorro gauges have always given values that

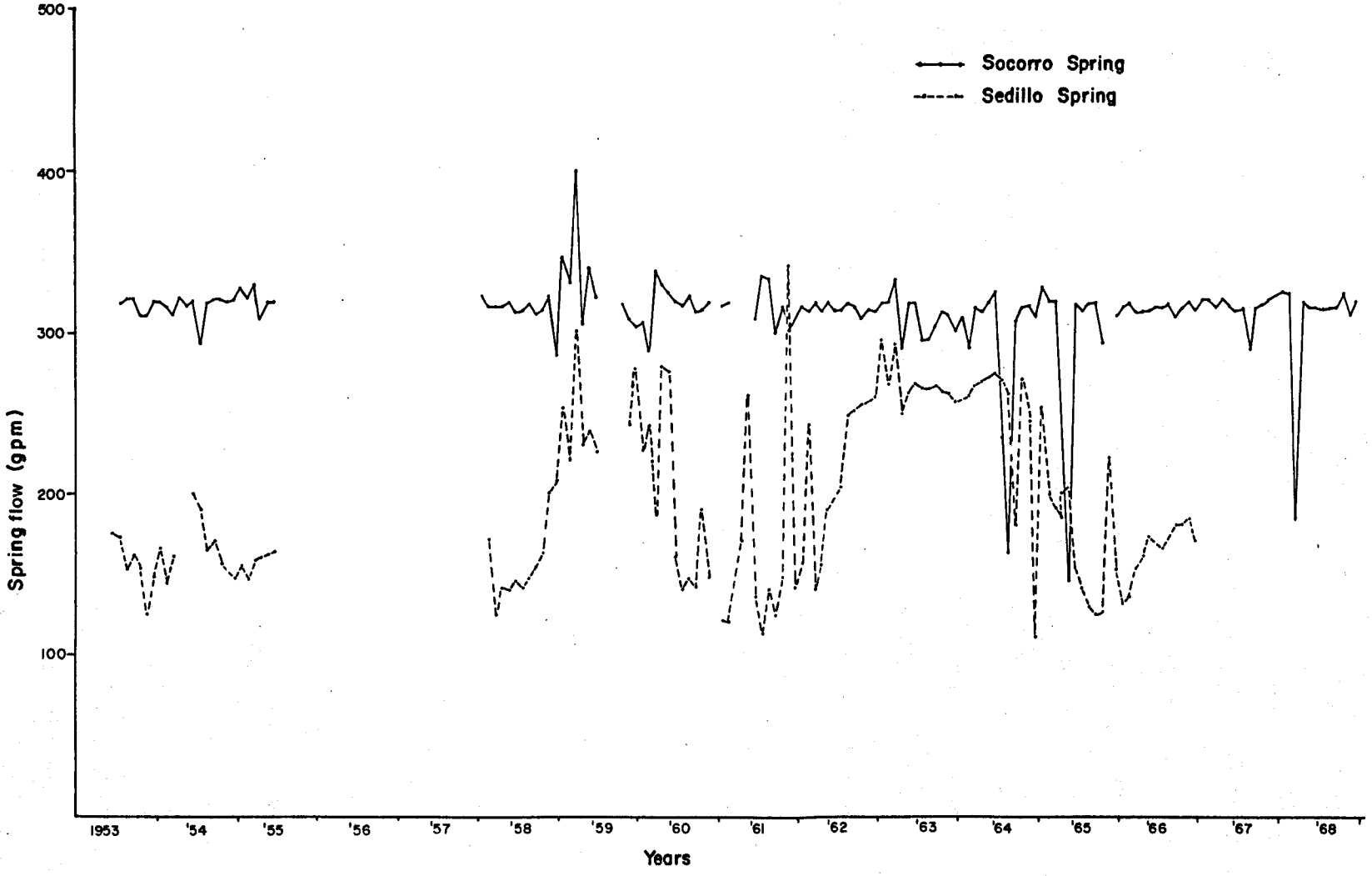

Figure 2-26. Socorro and Sedillo spring flow, 1953-1968.

conflict with those determined by some other means. Figure 2-26 shows that Socorro Spring usually issues about 315 gpm. When recent gauge readings were obtained and monthly average flow values calculated, the following results (in gpm) were obtained:

Year	Month	Socorro Spring	Sedillo Spring
1977	July	274.5	107.8
	August	272.8	---
	September	282.7	94.6
	October	276.0	98.9
	November	265.2	97.4
1978	February	299.6	109.4

These values are lower than those given in Figure 2-26, and it seems that they are more correct, at least for Socorro Spring, since the values are closer to values measured by Hall (1963) and Summers (1965).

The elevation of the water table in the study area is shown in Figure 2-27. The two elliptical contours going around Socorro Mountain have been drawn to indicate that here is some local recharge to the springs.

Groundwater Quality

Hall (1963) devised a method of chemical classification which is adopted here. A water-quality type is derived from dominant ions, in terms of percentages of equivalents per million (epm) as 100 percent cations and 100 percent anions. According to Hall (1963), criteria for both cations and anions are: (1) if one ion is greater than 50 percent, then it determines the water-quality type, and (2) if no ion is greater than 50 percent, then the ions greater than 25 percent are given in decreasing order from left to right. Figure 2-28 shows the range of water quality types for the study area. Figure 2-29 shows the range of water chemistry and total dissolved solids represented by pie diagrams. Chemical analyses data are presented in Appendix C.

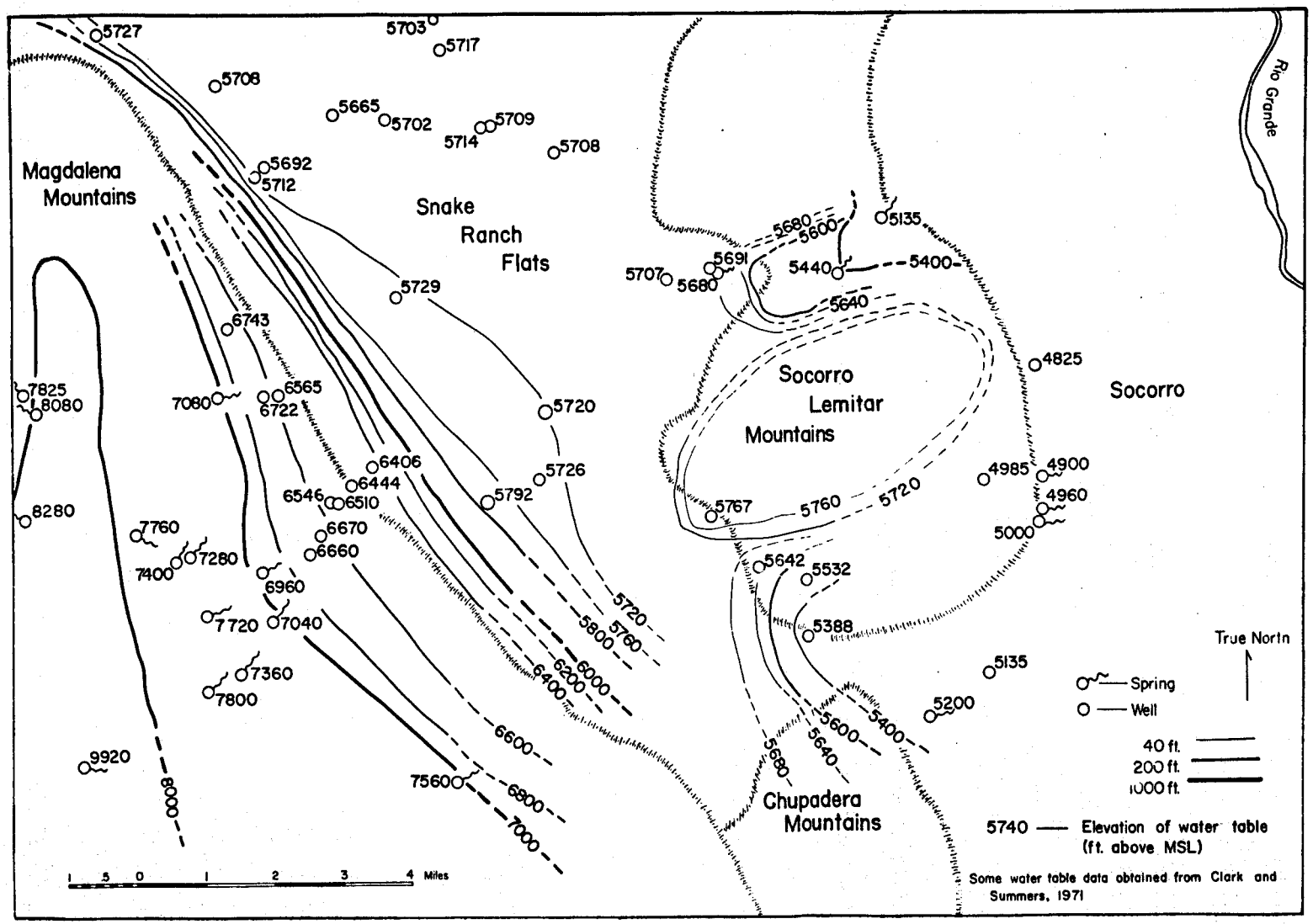

Figure 2-27. Water-table map.

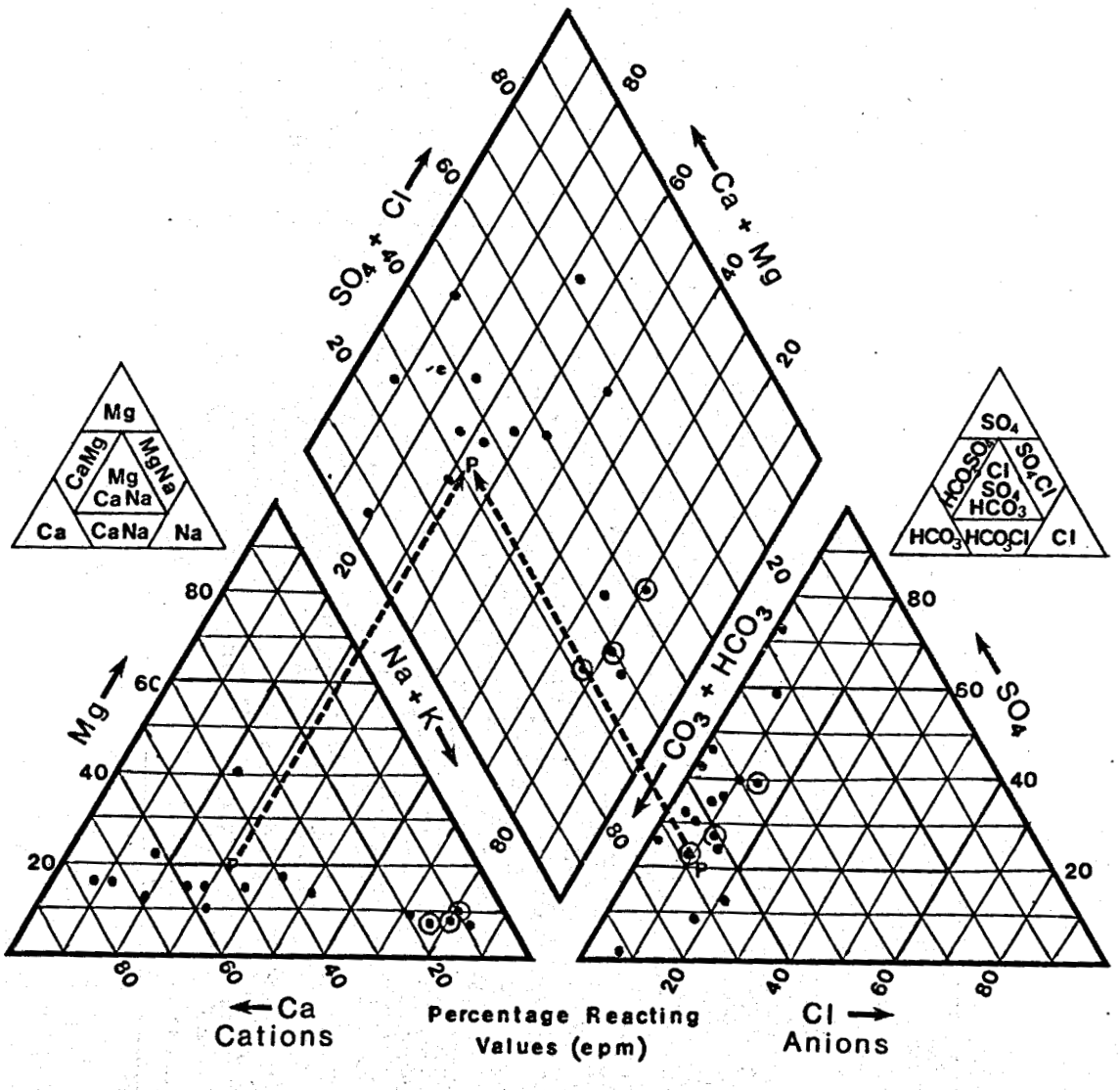

Figure 2-28. Water-quality diagram. The point P indicates the chemistry of average potable groundwater. Dashed lines show the method of plotting points in the diamond-shaped field. The solid black circles and the circumsribed black circles refer to nonthermal and thermal springs and wells, respectively (format after Davis and DeWiest [1967]). These data are tabulated in Appendix C.

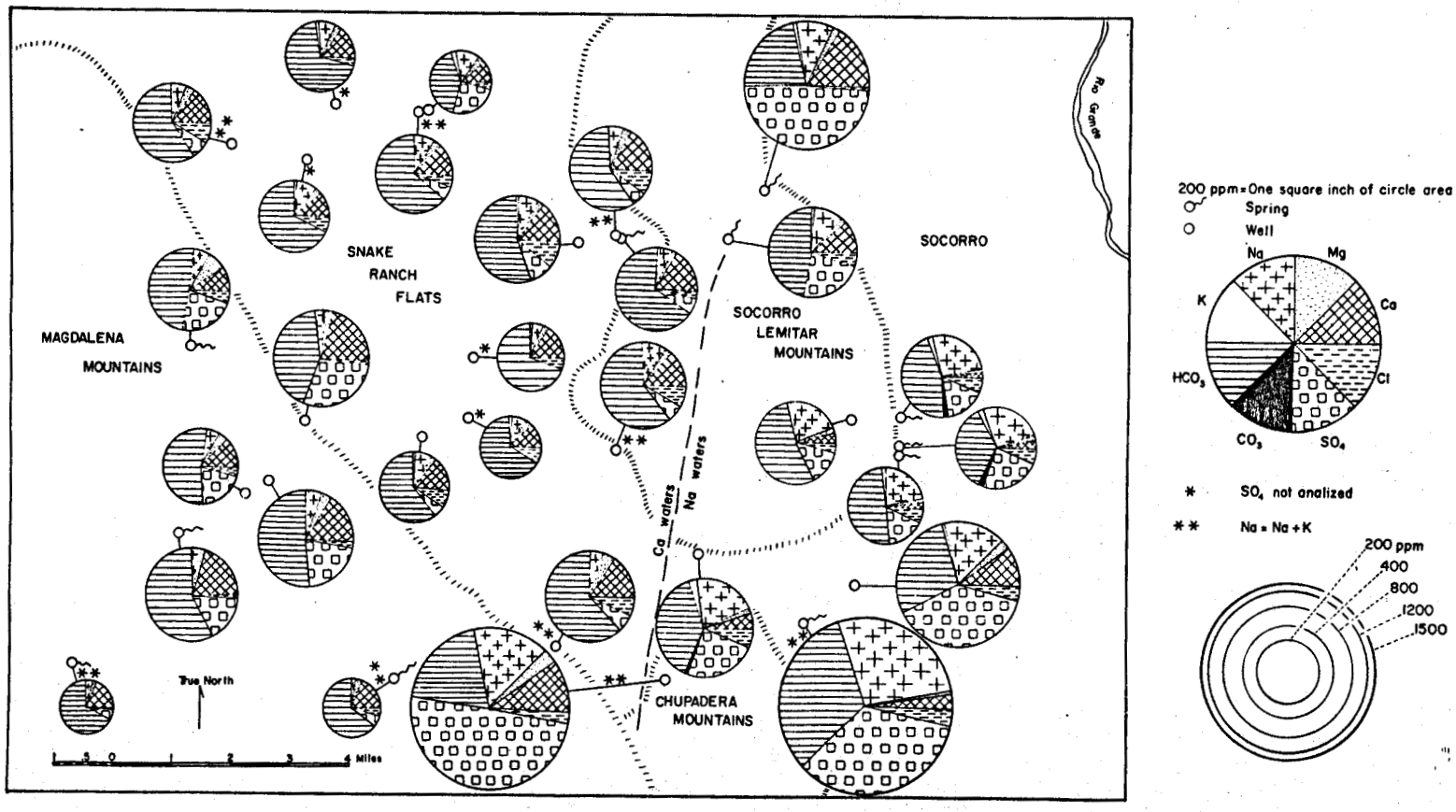

Figure 2-29. Distribution map of water quality and total dissolved solids.

Spring and well water from the Magdalena Mountains is all of the Ca-HCO_3 type, except for Garcia Canyon Spring (10.311) which is of the Mg, Ca-HCO_3 type. Hall (1963) noted that the thermal springs (22.111 and 22.113), along with Cook Spring (15.311) and thermal Blue Canyon Well (16.323), discharged Na-HCO_3-type water and that ion exchange, sodium for calcium, must be going on somewhere within the system between the Snake Ranch Flats and the location of these springs and wells. Two wells in Socorro Canyon (33.144 and 36.212) yield Na, Ca-SO_4, and Na-HCO_3-type waters, respectively.

Well (12.112) and spring (5.211) within the Chupadera Mountains issue Na, Ca-SO_4, and Na-HCO_3-type waters, respectively. Hall (1963) has also observed that Domingo Spring (3S.1W.6.331), which receives recharge from local precipitation only, discharges Na-HCO_3-type water. In this instance, the Na-HCO_3-type water is due to leaching of the rhyolitic material throughwhich the spring issues, rather than ion exchange. This spring was not sampled during this study and is not shown in the illustrations. A rough line has been drawn through the Socorro-Lemitar and the Chupadera mountains to indicate where the ion exchange is taking place (see Figure 2-27).

Springs and wells which have water high in sulfate, such as Lower Nogal Canyon Spring (30.443), Chupadera Spring (5.211), and Gianero Windmill (12.112), tap groundwater which has probably had prolonged contact with the upper gypsiferous member of the Popotosa Formation.

Environmental Tritium in Groundwater and Precipitation

The unstable hydrogen isotope tritum (H^3) is useful for understanding certain groundwater systems. Tritium is produced naturally in the earth's stratosphere when atmospheric nitrogen molecules are bombarded by cosmic rays. Tritium is readily incorporated into the vapor system of the atmosphere and

falls to earth in precipitation. Because tritium has a half life of 12.3 years, it is only suitable for dating water up to about 50 years old. Natural tritium levels in atmospheric moisture were of the order of 10 TU* prior to 1954. Beginning with that year, they were dramatically increased by atmospheric testing of thermonuclear devices, which ended in 1963 with the adoption of the Nuclear Test-Ban Treaty. Tritium activity in atmospheric moisture, peaked out in 1963 to 1964, and has been decreasing since. These developments are reflected in Figure 2-30, which shows tritium activity in precipitation at Socorro, New Mexico, as a function of time for the period 1957 (when tritium measurements started at NMIMT) to 1976.

The increased levels of environmental tritium activity are the basis for a method of tracing natural waters. By correlating tritium peaks in precipitation with tritium peaks in groundwater supplies, residence times and velocities of water migration have been determined (Holmes 1963; Rabinowitz et al. 1977).

Holmes (1963) examined three years (1957 to 1959) of tritium data for Socorro Spring and Socorro precipitation and concluded that an August 1958 peak in tritium activity in Socorro Spring water correlates with the mid-1954 tritium activity rise in precipitation, which was caused by the first, or Castle, series of atmospheric thermonuclear tests. Thus, the residence time of Socorro Spring water (i.e., the time elapsed between precipitation in the recharge area and its reappearance in the spring) is at most four years.

For this study, some of the tritium data Holmes (1963) used could not be located in the laboratory records. Other data not used by Holmes were located for the year 1957 (see Figure 2-30), and it appears that the 1957 line of tritium activity in spring water given by Holmes (1963), though based on only

*Tritium activity is expressed in tritium units (TU), where one tritium unit equals one tritium atom per 10^{18} hydrogen atoms.

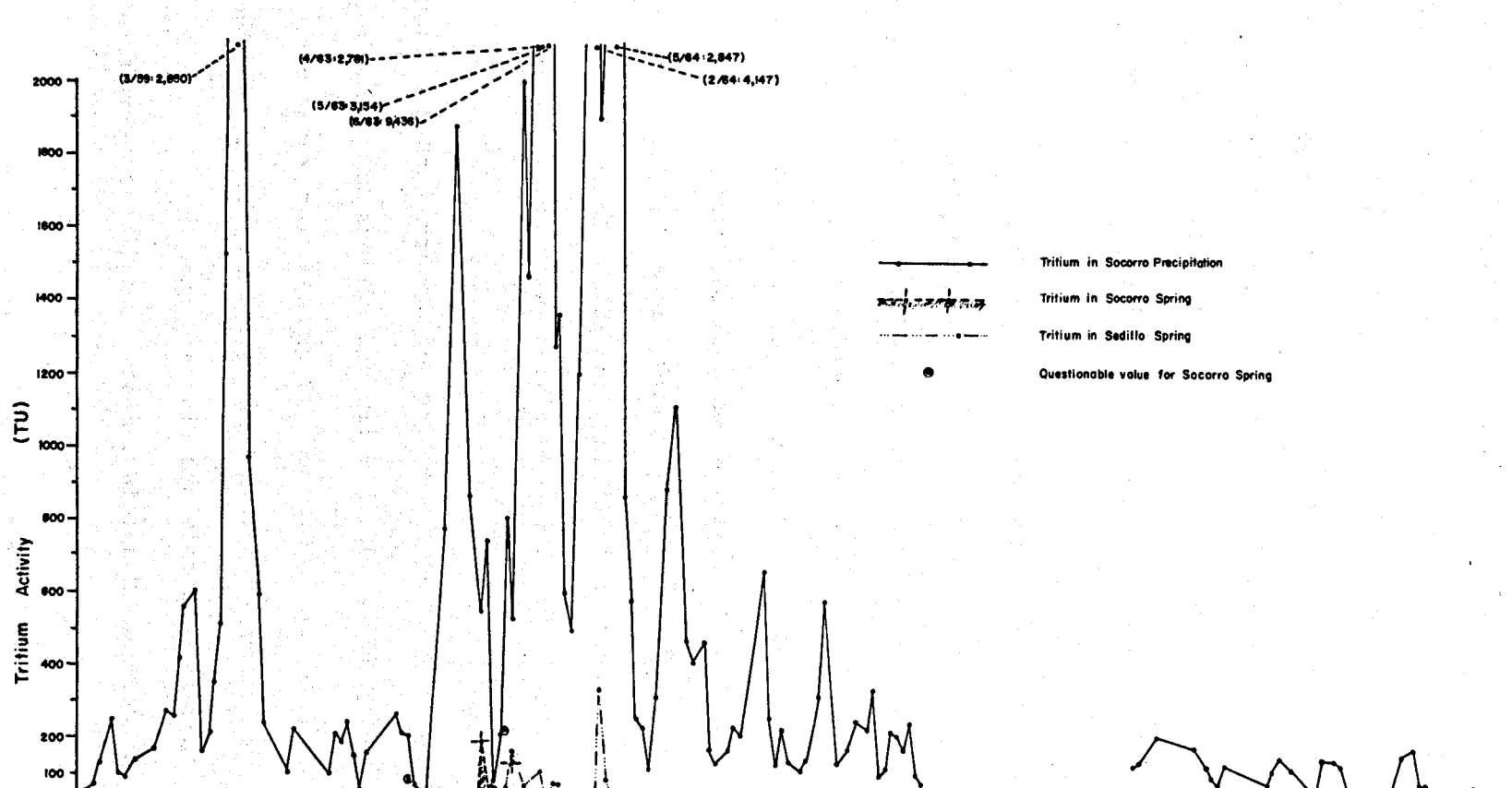

Figure 2-30. Tritium activity in Socorro precipitation, Socorro Spring, and Sedillo Spring.

two data points, was correct. Sampling of Socorro Spring stopped in early 1959 and was resumed for only two periods of about six months each in 1961 and 1962. There are some questionable data points within this group of samples.

Sedillo Spring was sampled regularly for three years (1962 to 1964). Socorro precipitation, on the other hand, has been sampled regularly, except for a three-year gap (mid-1968 to mid-1971), since 1957 (see Figure 2-30). Sedillo Spring is characterized by seasonal peaks of tritium activity. The highest peak was seen in June 1963 (9436 TU). The peak amplitude has been steadily declining since that time.

The three years of data for Sedillo Spring show very elevated levels compared to recent values (see Figure 2-30 and Appendix D) and even relative to the peak in Socorro Spring studied by Holmes (1963). The major peak in March 1964 (334 TU) should correspond to a tritium-activity peak in precipitation in early 1960 if the hypothesis by Holmes (1963) is correct. There was no significant precipitation peak observed in early 1960, but there was one in March 1959. This latter peak correlates better with the December 1962 activity peak in Sedillo Spring (165 TU). Similarly, the July 1962 peak in Socorro Spring (192 TU) correlates with the August 1958 peak in precipitation (608 TU).

For the present study, sampling of Socorro and Sedillo springs was resumed in February 1977. Other wells and springs have also been sampled in order to investigate the nature of the groundwater reservoir. Figure 2-31 shows the distribution of groundwater tritium activity in the study area determined on the basis of this sampling program.

Within the Magdalena Mountains, most of the water seems to be quite young with TU values greater than 40. This is not surprising if one considers that: (1) the springs issue from high mountain groundwater systems in limestone; (2)

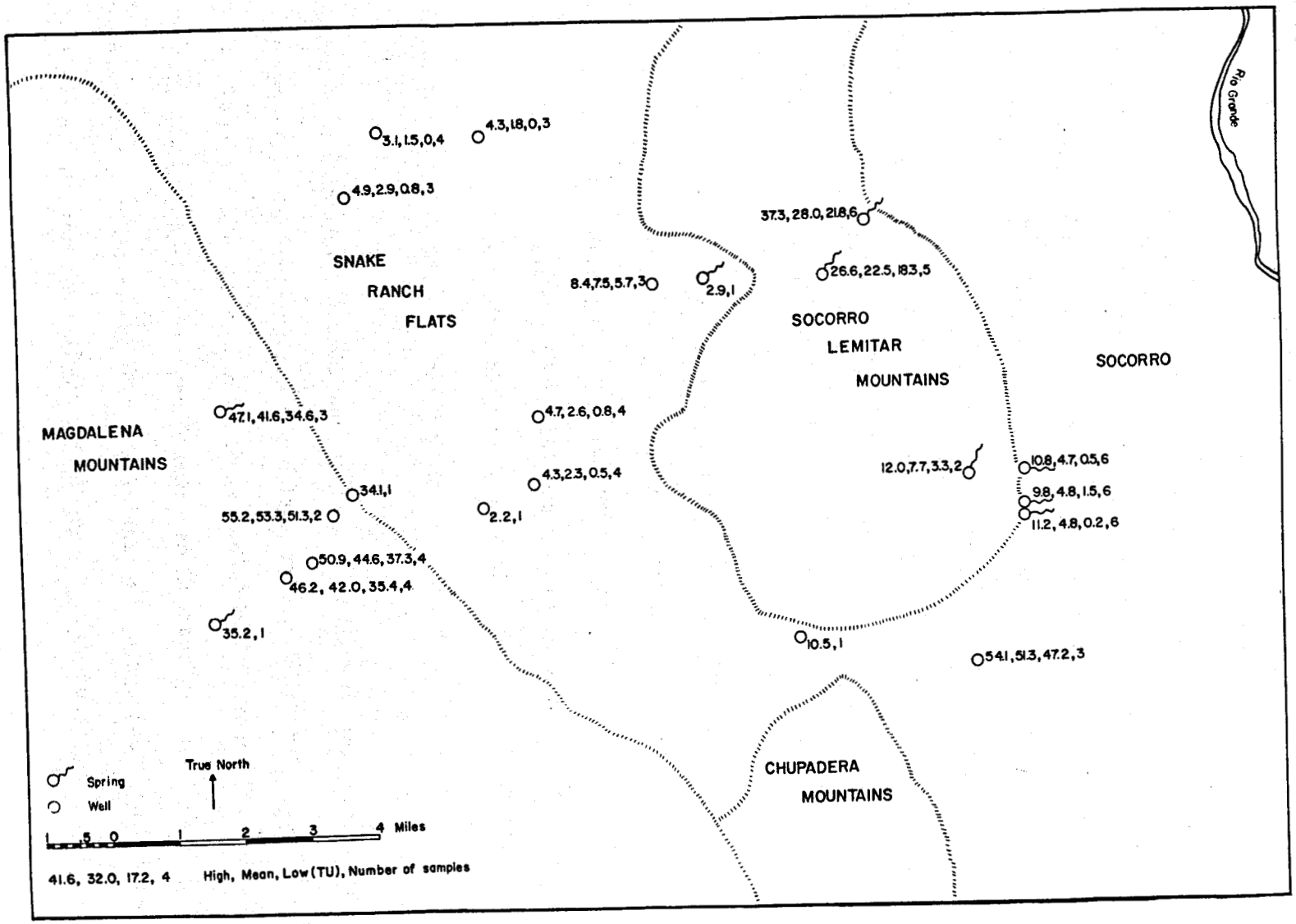

Figure 2-31. Distribution of tritium activity in groundwater and springs.

the wells are sunk into the alluvium covering of the canyon floor which is very permeable and shallow; and (3) the water table has a high gradient going down the canyons.

In the Snake Ranch Flats, however, the groundwater is old relative to that in the Magdalena Mountains; TU values are less than 3. This result seems to indicate that the groundwater reservoir in the flats is quite large, and the recharge from the Magdalena Mountains is strongly diluted within this reservoir, or that recharge from the Magdalena Mountains is smaller than originally thought. Verhagen et al. (1970) noted the same phenomenon in the alluvial Lobatse Basin in southern Africa. Vertical stratification of tritium activity in the aquifer was also noted. For example, tritium values decreased to near zero with depth.

The two springs within Nogal Canyon show an interesting relationship (see Figure 2-32). The tritium activity in these springs seems to vary somewhat in phase, with Lower Nogal Canyon Spring always being higher in tritium. These two springs are fault controlled, and the water issuing from these springs is partly from the Snake Ranch Flats as evidenced by the moderate tritium values (20 to 30 TU). The lower spring may receive a larger component of local recharge.

The values for the thermal springs and Blue Canyon Well are plotted in Figure 2-33. There is good correlation between tritium values in Sedillo and Cook springs. Socorro Spring and Blue Canyon Well also follow the same general trend, which indicates, especially when the similar water quality is considered, that Cook Spring is part of the same groundwater system as Socorro and Sedillo springs and Blue Canyon Well. Whether or not the water issuing from Cook Spring was ever heated and cooled along its route cannot be determined from the available data. These three springs have mean values of

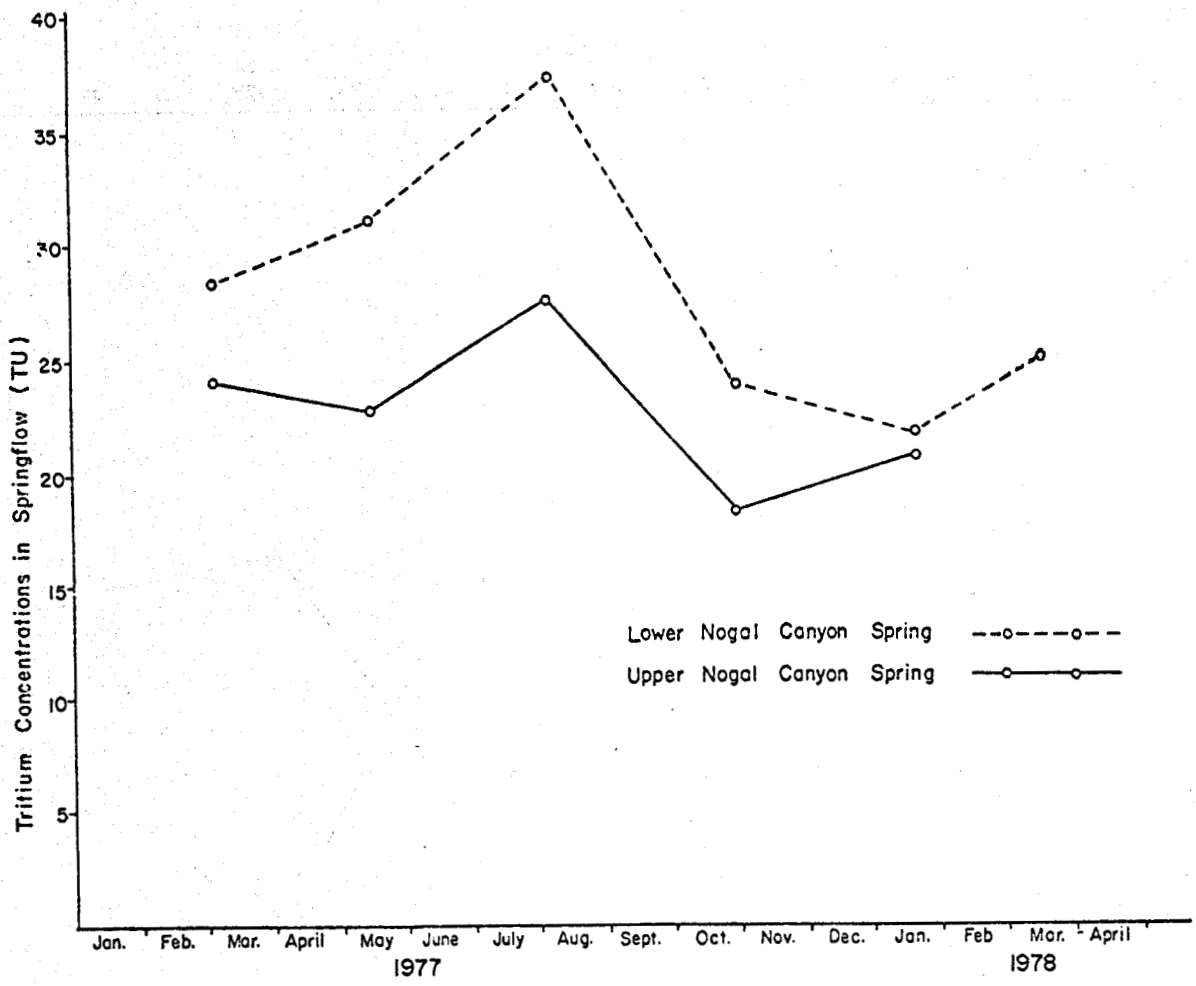

Figure 2-32. Tritium activity in Upper and Lower Nogal Canyon springs, 1977-1978. Typical error bar is ± 1 TU. For individual values, see listing in Appendix D.

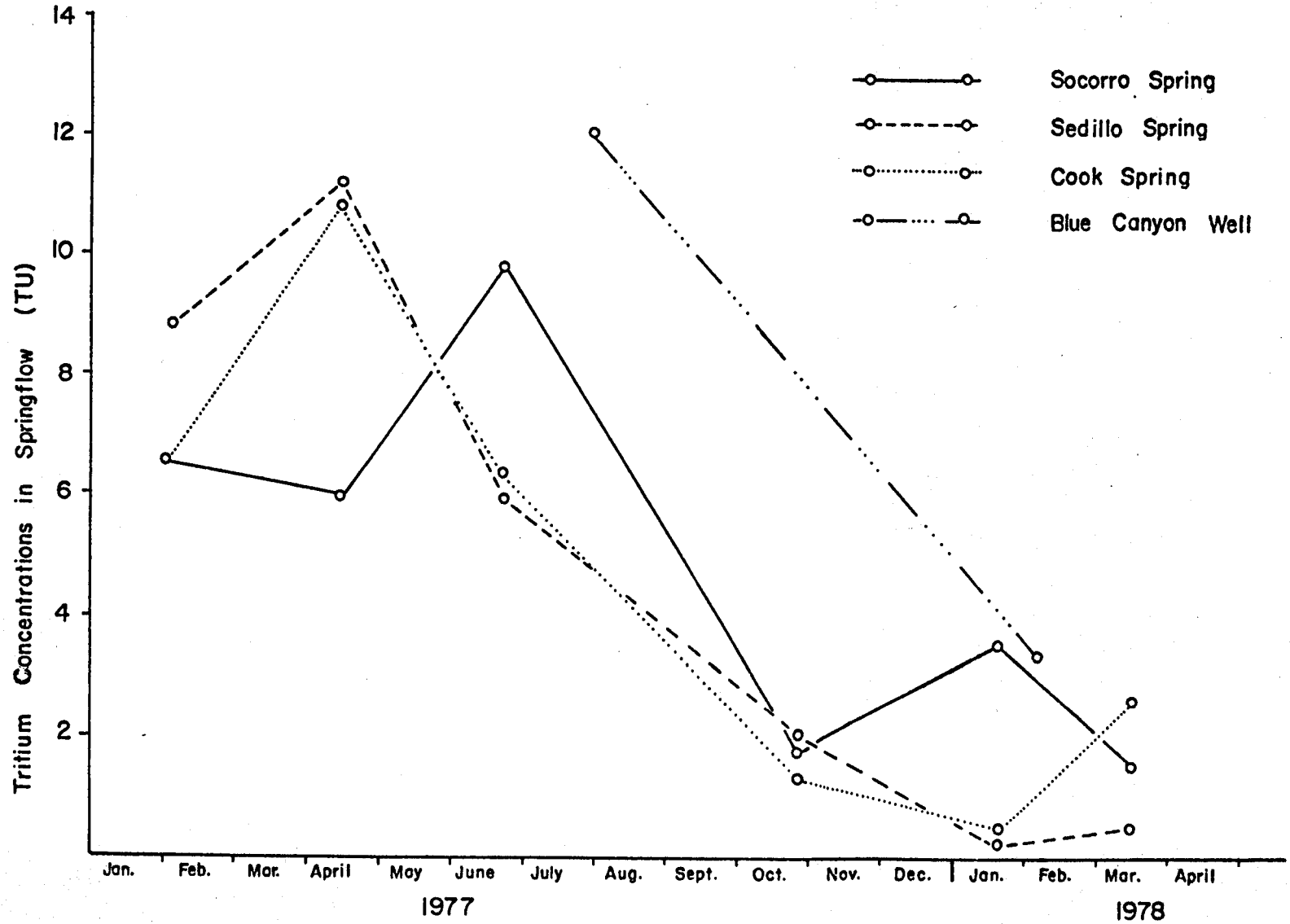

Figure 2-33. Tritium activity in thermal waters, 1977-1978. Typical error bar is ± 1 TU. For individual values, see listing in Appendix D.

about 4.8 TU, which is about 2.0 TU higher than the Snake Ranch Flats system. This fact suggests that there is a local component of recharge which is, at least in part, supplying tritium to the spring water.

Oxygen-18 and Deuterium

Ten samples of thermal spring and well water were analyzed for their oxygen-18 and deuterium content. The data are exhibited in Table 2-17 and Figure 2-34. Five samples from nonthermal springs and wells and two precipitation samples are given for comparison. Tritium activity for these 17 samples is also indicated in Table 2-17.

The data fall in two groupings. On the standard plot of δD vs. $\delta^{18}O$ (see Figure 2-34), both are close to and slightly to the left of the meteoric line of Craig (1961). Typical thermal waters tend to be displaced to the right of this line (Faure 1977, Figure 18.11). Isotopic exchange of groundwater with the reservoir rocks, which are generally low in hydrogen content, usually affects primarily the isotopic oxygen composition. On the basis of the limited evidence available here, no such interaction can be detected.

Discussion of Results

Hydrogeology

Preliminary drilling evidence (Chapin, personal communication 1980) indicates that, in the Snake Ranch Flats, the permeable gravel and sand deposits which top the basin fill are underlain at 1000 ft or deeper by a thick complex of impermeable playa mudstones. These, in turn, are underlain by permeable strata. These observations suggest that the hydrologic system consists of two independent aquifers, a shallow aquifer above the mudstones,

Table 2-17. Deuterium, oxygen-18, and tritium in thermal and nonthermal waters.

Location	Notation in Figure 2-34	Sample Number	Date	Oxygen-18 δO^{18} (‰)	Deuterium δD (‰)	Tritium (TU)
Socorro Spring	---	2320	4/14/77	-10.8	- 61.0	5.9
	---	2348	6/22/77	- 8.1	- 51.7*	9.8
	---	2423	1/19/78	-10.5	- 62.0	3.5
	---	2428	3/14/78	- 8.4	- 41.7*	1.5
Sedillo Spring	---	2429	3/14/78	- 8.1	- 49.8*	0.5
	---	2321	4/14/77	-10.2	- 66.0	11.2
	---	2422	1/19/78	-11.5	- 67.0	0.2
Cook Spring	---	2322	4/14/77	- 8.6	- 51.0*	10.8
	---	2424	1/19/78	- 8.6	- 50.5*	0.5
Blue Canyon Well	---	2425	2/06/78	- 8.6	- 56.7*	3.3
Upper Nogal Canyon Spring	(6)	2421	1/19/78	- 8.6	- 52.0	20.8
Lower Nogal Canyon Spring	(7)	2420	1/19/78	-10.3	- 65.0	21.8
Strozzi Windmill	(1)	2375	3/12/77	- 6.7	- 37.8	0.0
Armijo Windmill	(2)	2325	5/13/77	- 6.1	- 45.9	54.1
Kelly Ranch deep well	(3)	2381	9/19/77	- 8.2	- 44.4	0.0
Socorro Rain	(4)	2537	3/21-22/77	-12.2	- 76.0	44.5
Socorro Snow	(5)	----	1/19-20/77	-17.9	-120.0	**--

*Analysis by Dr. Gary Landis, Department of Geology, the University of New Mexico. All others by Geochron Laboratories, Cambridge, Massachusetts.

**Tritium activity was not measured separately from other precipitation for the month (Sample #2479, 40.6 TU).

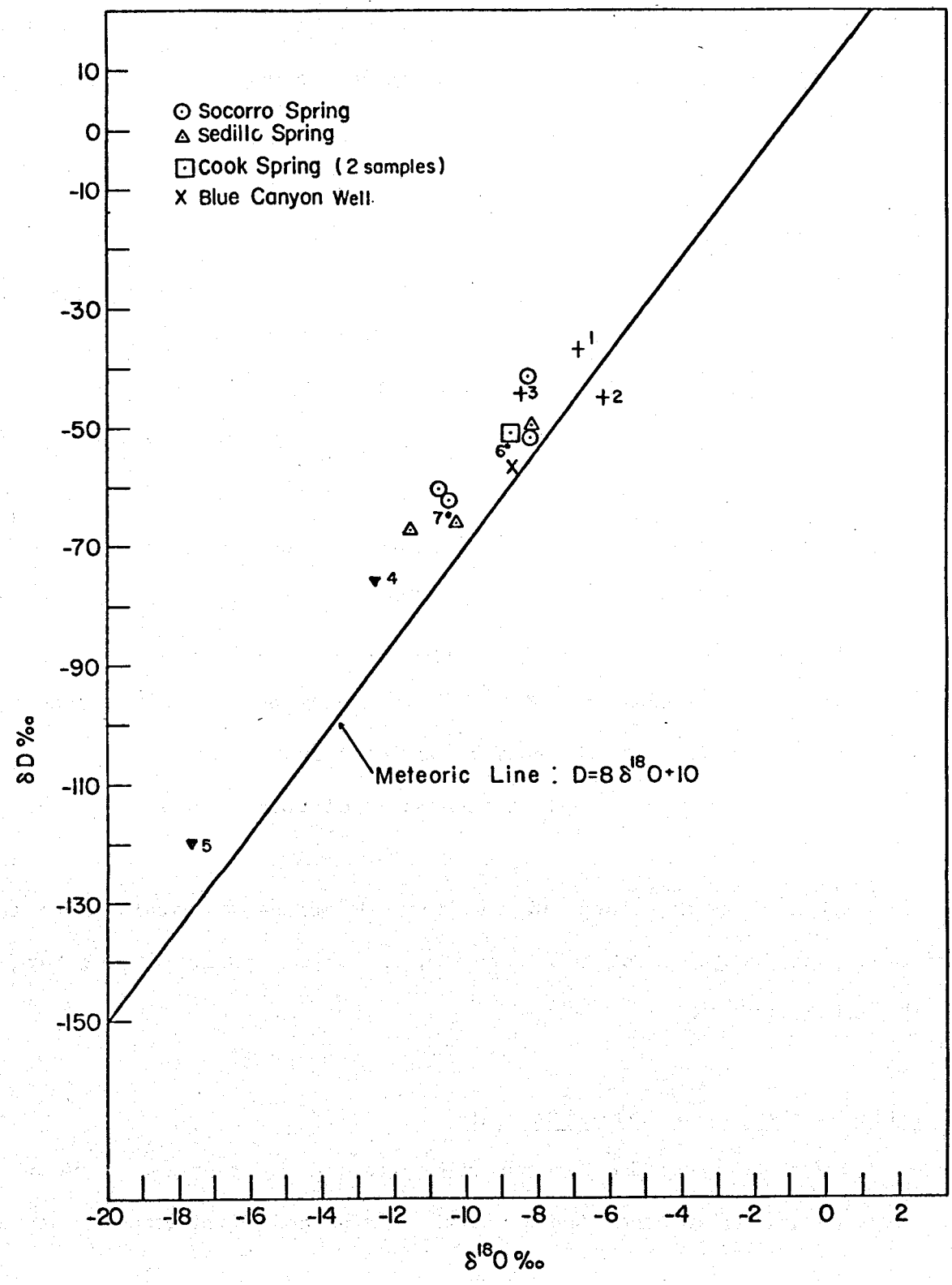

Figure 2-34. Deuterium and oxygen-18 in thermal and nonthermal waters. (Numbers refer to nonthermal sampling points specified in Table 2-17).

and a deeper aquifer below the mudstones. Within the Snake Ranch Flats, these two aquifers are not connected. Water from the Magdalena Mountains flows below the mudstones into the volcanic complex of Socorro Mountain where it feeds the springs.

Groundwater Quality

The $Na-HCO_3$ character of the thermal springs indicates that the groundwater interacts with the volcanic complex (Hall 1963), perhaps aided by above-normal temperatures. Chapin et al. (1978) found a strong potassium anomaly in the feldspars of the ash-flow tuff sheets of the Socorro Mountain volcanic complex. Plagioclase feldspars have been replaced by potassium feldspar. Such alteration is typical of geothermal aqueous systems and, in this case, it is attributed to the Oligocene geothermal system. The sodium removed from the plagioclases in this metasomatic reaction may have been transported away by groundwater. Mafic flows interbedded with the ash-flow tuffs are enriched in sodium. The sodium character of the present groundwater in the Socorro Mountain area may indicate that a similar process is now going on in connection with the present geothermal anomaly. On the other hand, deuterium and oxygen-18 values of the thermal springs indicate that the interaction with bedrock must have been minor. These springs do not have a truly thermal character.

Tritium Activity and Tritium Rainout

The tritium activity in Socorro precipitation is representative of a broad region including the Snake Ranch Flats and Magdalena Mountains (Rabinowitz et al. 1977). This assertion does not, however, apply to tritium rainout, the product of tritium activity and precipitation. Tritium rainout

rather than activity is the parameter determining the tritium activity of groundwater and springs.

Kelly Ranch is located at the western edge of the Snake Ranch Flats, and precipitation records there may be representative of recharge to the springs. Tritium rainout at Kelly Ranch is shown in Figure 2-35 and Appendix D. Tritium rainout computed on the basis of Socorro precipitation (see Figure 2-36 and Appendix D) show a similar pattern but, since Socorro precipitation is lower on the average, the peak amplitudes tend to be lower.

The Magdalena Mountains are believed to supply the major part of recharge to the aquifer that supplies the springs. Unfortunately, precipitation data for the Magdalena Mountains have only become available since about 1964 and then only for the summer season. These data are available from Langmuir Laboratory near the summit of South Baldy (see Figure 2-17). Because mean annual rainfall is much higher at Langmuir Laboratory (17.7 inches at 10,631 ft elevation) than at Socorro (7.9 inches, at 4600 ft elevation), tritium rainout must also be higher and may possibly show peaks that are not apparent at Kelly Ranch or Socorro. Tritium activity peaks in precipitation may not correspond to those in recharge because: (1) a small precipitation event of high activity may contribute less tritium to recharge than a large precipitation event of low or intermediate activity; and (2) recharge is not linear with precipitation (Gross et al. 1976; Rabinowitz et al. 1977).

Correlation of Tritium Activity in Springs with Precipitation

A direct correlation of tritium activity peaks in groundwater with those in precipitation is possible only in special cases. The correlation shown by Holmes (1963) for the Socorro peak may have been such a special case because the measurements occurred so early after the onset of the rise in atmospheric

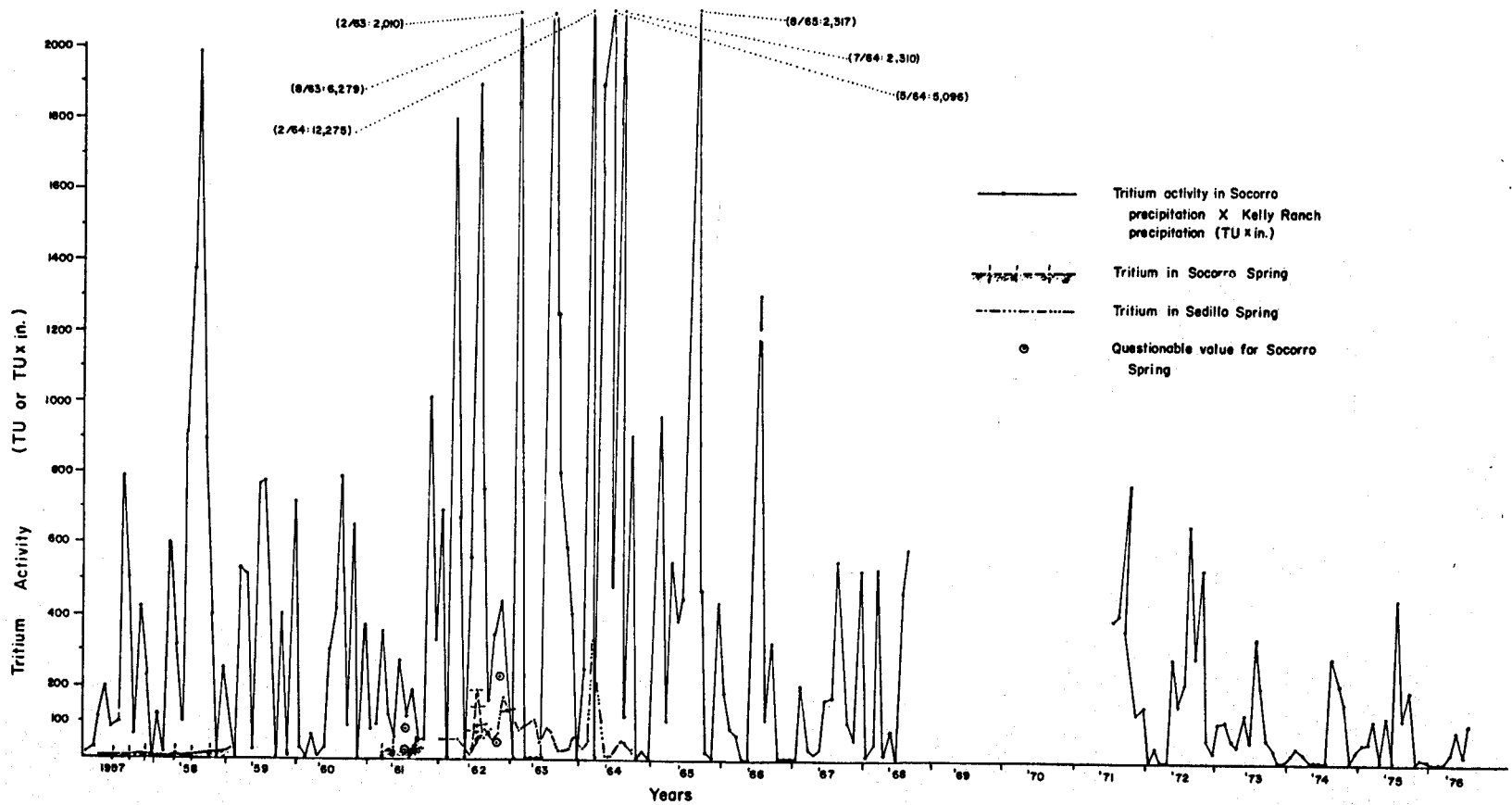

Figure 2-35. Tritium rainout computed from Kelly Ranch precipitation records and tritium activity in Socorro Spring, 1956-1976.

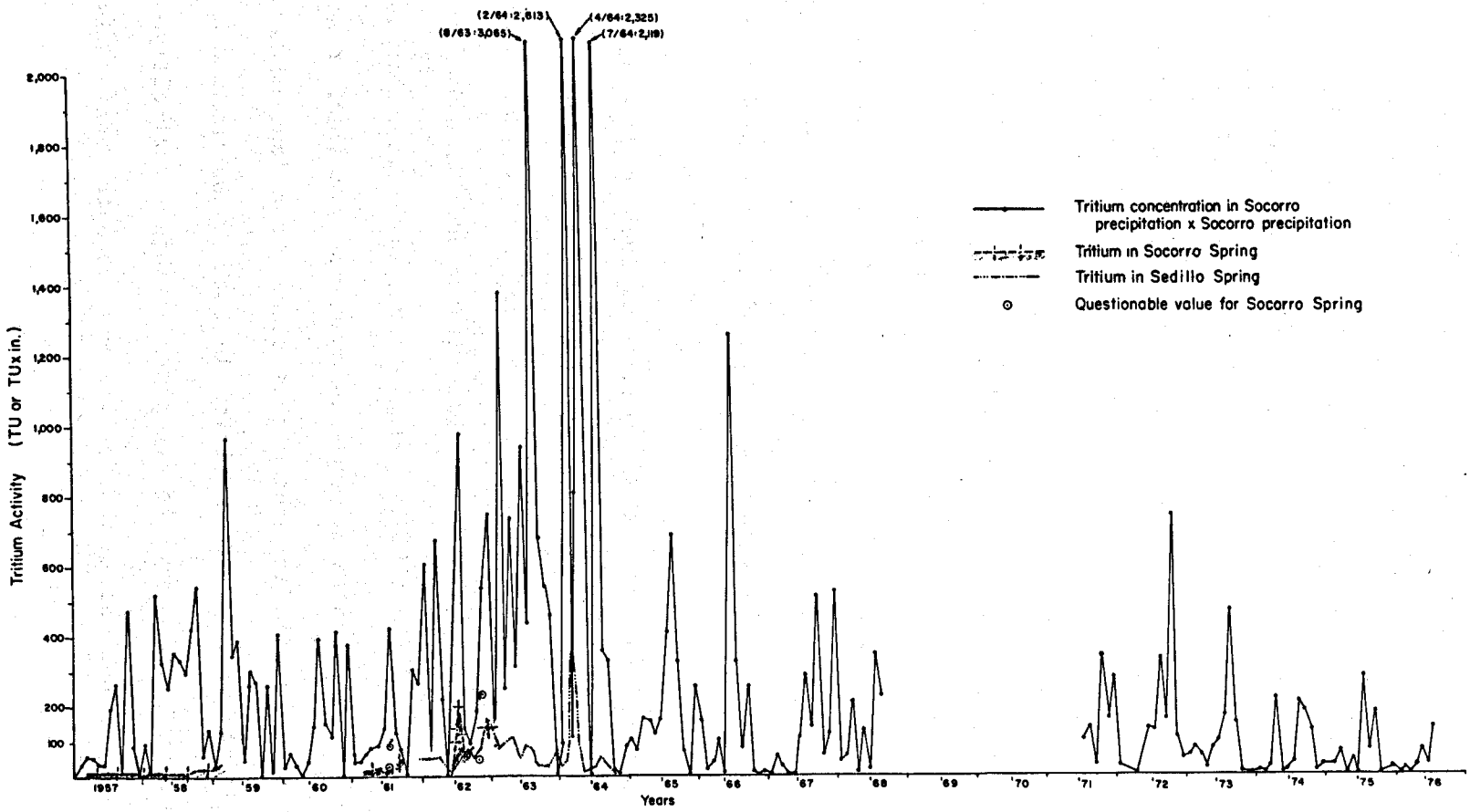

Figure 2-36. Tritium rainout computed from Socorro precipitation records and tritium activity in Socorro Spring, 1956-1976.

tritium activity. However, even in this case, the approach cannot yield quantitative information concerning the mixing (dispersion) of recharge contributions from different sources or following different flowpaths. In the case of the Socorro Spring system, there are three possible recharge contributions: (1) water from the Magdalena Mountains following a deep path of long travel time (i.e., beneath the mudstone complex in the Snake Ranch Flats); (2) water from the Magdalena Mountains following a shallow path of intermediate travel time (i.e., above the mudstone complex); and (3) direct recharge over the Socorro Mountain complex, a fast recharge component. In order to investigate recharge quantitatively further, it would be necessary to integrate all the tritium rainout contributions over the recharge area and then calculate the effective tritium recharge as a function of time (Rabinowitz et al. 1977). The effective tritium activity in recharge deduced from this curve could then be compared to and correlated with the spring measurements.

Data required for these computations include precipitation distribution over the recharge area for the appropriate time interval; recharge fraction; size, configuration, and storage coefficient of the aquifer, or, alternatively, a dispersion coefficient for the aquifer. Most of this information is not available and, in fact, one purpose of isotope studies is to obtain the parameters (such as recharge fraction, residence time, and aquifer size) needed for the computation. When long series of measurements are available for tritium activity in both groundwater and precipitation, a mean mixing ratio may be computed without explicitly including other parameters (Gross et al. 1980). An adequate series is available for precipitation, but measurements for the springs are inadequate in total time span, continuity, and frequency. The discussion of what these tritium

measurements mean in terms of the hydrologic characteristics of the aquifer system is therefore somewhat speculative.

Alternative Interpretation of Spring Recharge

The correlation proposed by Holmes (1963) for the 1958 tritium peak in spring water with the 1954 rise of tritium activity in atmosperic water sets a maximum time frame for the tritium activity in the spring (i.e., it cannot be older than four years), but the correlation does not account for the activity amplitude in relation to the amplitude of tritium activity in precipitation*. Two main factors determine the amplitude ratio: (1) mixing (dispersion) of the labeled water in the groundwater reservoir, assumed to be unlabeled initially and (2) radioactive decay. For a residence time of four years, radioactive decay alone would reduce tritium activity to about 80 percent of its initial value. Subsequent peaks (e.g., that of 1962) appear to conform moderately well to the four-year delay pattern.

The 1964 peak in Sedillo Spring activity poses some difficulty for correlation. The greatest problem is to account for the relative amplitudes. For the years in question, atmospheric activity shows very large fluctuations from month to month (see Figure 2-30), which are averaged out in spring flow to a certain extent. The reduction due to this averaging is likely to be larger than that due to radioactive decay. However, if all recharge occurs at the western edge of the Snake Ranch Flats and has a residence time of four years, then the spring water should after four years (that is, starting in 1958) begin to approach the mean tritium activity of precipitation. This is clearly not the case, and is evident especially from the most recent data because the seasonal fluctuations in tritium activity are becoming progressively smaller.

*No measurement of tritium activity in 1954 precipitation at Socorro is available.

For this reason, two alternative interpretations are offered. First, all recharge to the springs originates in the Magdalena Mountains or near the western edge of the Snake Ranch Flats and follows paths of different lengths and travel times across the Snake Ranch Flats and the Socorro Mountain complex. These streamlines converge in the discharge zone so that they appear mixed in the springs. The tritium activity of the spring water, therefore, represents the diluted activity of the shallowest (shortest) of these streamlines. The residence time of water along this shallow path is of the order of four years. Second, the tritium activity of the spring water is the label of local recharge, that is, precipitation that falls on the Socorro Mountain complex, and/or surface runoff following large thunderstorms, crosses the Snake Ranch Flats and is absorbed by the highly fractured and permeable volcanics forming the eastern edge of the flats. That is to say, the major portion of spring flow represents water that was recharged at the eastern edge of the Magdalena Mountains and took the long path, beneath the mudstone complex in the Snake Ranch Flats, but a minor component of the spring flow represents local recharge around the western flank and southern end of the Socorro Mountains. This conclusion does not seem unreasonable considering the size of the possible recharge area around the Socorro Mountains. The shallow recharge contribution is roughly estimated at 10 to 20 percent of the total spring flow, but is expected to vary from year to year with local climatic conditions.

Of the two alternative hypotheses, the second one is favored because the tritium activity of groundwater in Snake Ranch Flats is lower than the activity of spring flow (see Figure 2-31) and because the geologic structure of the sedimentary basin of the Snake Ranch Flats seems to indicate long residence times.

The combined geological, geochemical, and isotopic evidence indicates that a major component of spring recharge proceeds along a relatively deep path. Temperature and residence time along the path are such that: (1) cation exchange with bedrock takes place accounting for the $Na\text{-}HCO_3$ character of the water; (2) the residence time for this deep component appears to be much longer than the half-life of tritium (i.e., 12.3 years); and (3) oxygen-18 and deuterium exchange with bedrock are negligible.

Summary

Recharge to the thermal spring system of Socorro consists of two main components that follow different paths of different travel times. A regional component is fed by precipitation on the Magdalena Mountains which is transmitted to the fracture system of the springs through permeable strata of the Santa Fe Group (3000 to 4000 ft). The residence time of this component is probably longer than the 12.3-year half-life of tritium. A local recharge component is fed by precipitation that falls directly on the volcanic complex of the Socorro Mountains and/or is transmitted from the Magdalena Mountains as surface runoff across the Snake Ranch Flats Basin. The residence time of this water source is of the order of four years. These recharge components were differentiated on the basis of their tritium label, which yields a mixing ratio of the order of 9:1 for the regional versus the local component.

Cation exchange, sodium for calcium, takes place along a roughly north-south trending line in the Socorro and Chupadera mountains and is related to the geothermal anomaly of the Socorro Mountains. Deuterium and oxygen-18 determinations in samples of spring and well waters of the geothermal anomaly indicate that these waters are of meteoric origin and have not been mixed with deep thermal waters.

Recommendations for Future Work

1. Chemical equilibrium computations with the water quality data might make it possible to determine a temperature for the cationic exchange reaction and thus the depth of groundwater flow to the thermal springs.

2. The water-table map should be subjected to statistical computations (e.g., kriging) which allow the determination of the most likely contour patterns for a limited set of data points and the placement of confidence limits on alternative contour configurations. Additional water-table measurements in wells not studied for this report should be obtained if possible.

3. Tritium measurements should continue in order to detect systematic time variations in the tritium content of the springs and to relate these variations to recharge processes. An important related question is the role of the through-flowing arroyos for the recharge to the Socorro Spring aquifer and to the Rio Grande aquifer. This question has broader implications for an understanding of recharge processes in the Basin and Range environment.

4. Flow measurements at Socorro Spring have been reliable in the past and accurate monitoring of spring flow should be continued because of its importance to future investigations.

5. The fracture system from which Cook, Socorro, and Sedillo springs issue should be mapped and correlated between the springs. There is some evidence that the springs are closely coupled hydraulically. This possibility needs to be studied to gain a better understanding of the hydraulic system because of its importance with respect to the management of the spring waters.

6. Another topic for investigation is the relation between the aquifer that feeds the thermal springs and the aquifer or aquifers in the Rio Grande Graben.

7. Water chemistry of the Socorro thermal system should be compared with other thermal springs, especially those along the Rio Grande. In particular, the tritium, oxygen-18, and deuterium values should be investigated. These data could lead to broader conclusions concerning regional aquifer systems.

Acknowledgements

We are heavily indebted to Drs. Richard Chamberlin and Charles Chapin (New Mexico Bureau of Mines and Mineral Resources) for much insight into the geology of the area. Led by Prof. Clay Smith and Mr. Richard Griego, sanitarian for the City of Socorro, we were able to visit the springs which are accessible only with difficulty through underground workings. Lynn Brandvold, chemist for the New Mexico Bureau of Mines and Mineral Resources, did water quality analyses. Dave Goodrich, Paul Davis, Steve Mizell, Roger Ward, and John Beasley assisted with the collecting of water samples. The City of Socorro allowed sampling of Socorro and Sedillo springs. Our appreciation goes especially to Messrs. James Coles, Director of Utilities, and Richard Griego, Sanitarian, for their support. We also thank the ranchers who gave consent to sample their wells and who supplied well data, notably Joyce Gaines, J. B. Kelly, Allie Strozzi, Tom Kelly, Nathan Hall, and Zeke Armijo.

The manuscript was critically read by Drs. Chapin, Gelhar, and Sanford who suggested many improvements. The responsibility for any errors or omissions rests with the authors.

References

Billings, G. K., 1974, Socorro's water supply: SER, Inc., Socorro, New Mexico, unpublished report.

Bruning, J. E., 1973, Origin of the Popotosa Formation, northcentral Socorro County: New Mexico Institute of Mining and Technology, Ph.D. dissertation, 132 pp.

Chamberlin, R. M., 1978, Geologic maps and cross sections of the Lemitar, Socorro, and northern Chupadera Mountains: New Mexico Bureau of Mines and Mineral Resources, Open-file Report 88.

Chamberlin, R. M., 1980, Personal communiciation, New Mexico Bureau of Mines and Mineral Resources, Socorro, New Mexico.

Chapin, C. E., 1980, Personal communiciation, New Mexico Bureau of Mines and Mineral Resources, Socorro, New Mexico.

Chapin, C. E. and Seager W. R., 1975, Evolution framework of the Rio Grande Rift in the Socorro and Las Cruces area, in 26th Field Conference Guidebook: New Mexico Geological Society, p. 297-321.

Chapin, C. E., Chamberlin, R. M.,Osburn, G. R., White, D. W., and Sanford, A. R. 1978, Exploration framework of the Socorro geothermal area, in Field guide to selected cauldrons and mining districts of the Datil-Mogollon volcanic field, New Mexico: New Mexico Geological Society, Special Publication 7, p. 115-129.

Clark, N. J. and Summers, W. K. 1971, Records of wells and springs in the Socorro and Magdalena areas, Socorro County, New Mexico (1968): New Mexico Bureau of Mines and Mineral Resources, Circular 115, 51 pp.

Craig, H., 1961, "Isotopic variations in meteoric waters: Science, v. 133, p. 172-1703.

Denny, C. S., 1940, Tertiary geology of the San Acacia area, New Mexico: Journal of Geology, v. 49, p. 73-105.

Denny, C. S., 1941, Quaternary geology of the San Acacia area, New Mexico: Journal of Geology, v. 49, p. 225-260.

Faure, G., 1977, Principles of isotope geology: John Wiley, New York, 464 pp.

Gross, G. W., Hoy, R. N., and Duffy, C. J., 1976, Application of environmental tritium in the measurement of recharge and aquifer parameters in a semiarid limestone terrain: New Mexico Water Resources Research Institute, Report 080, 212 pp.

Gross, G. W., Davis, P., and Rehfeldt, K. R., 1980, Paul Spring: an investigation of recharge in the Roswell (New Mexico) artesian basin: New Mexico Water Research Institute, Report 113, 135 pp.

Hall, F. R., 1963, Springs in the vicinity of Socorro, New Mexico, in 14th Field Conference Guidebook: New Mexico Geological Society, p. 160-179.

Holmes, C. R., 1963, Tritium studies, Socorro Spring, in 14th Field Conference Guidebook: New Mexico Geological Society, p. 152-154.

Machette, M. N., 1978, Geologic map of the San Acacia Quadrangle, Socorro County, New Mexico: U. S. Geological Survey, Geological Quadrangle Map 1415.

Osburn, G. R., 1978, Geology of the eastern Magdalena Mountains, Water Canyon to Pound Ranch, Socorro County, New Mexico: New Mexico Institute of Mining and Technology, M.S. thesis, 136 pp.

Rabinowitz, D. D. and Gross, G. W., 1972, Environmental tritium as a hydrometeorologic tool in the Roswell Basin, New Mexico: New Mexico Water Resources Research Institute, Report 016, 168 pp.

Rabinwowitz, D. D., Gross, G. W., and Holmes, C. R., 1977, Environmental tritium as a hydrometeorologic tool in the Roswell Basin, New Mexico: Journal of Hydrology, v. 32, p. 3-46.

Romero, V. D., and Wilkening, M. H., 1977, Summer precipitation network Socorro County, New Mexico - 1966 to 1975: New Mexico Institute of Mining and Technology, Physics Department, unpublished report, 5 pp.

Sanford, A. R., 1968, Gravity survey in central Socorro County, New Mexico: New Mexico Bureau of Mines and Mineral Resources, Circular 91, 14 pp.

Scofield, C. S., 1938, Quality of groundwater in the Rio Grande Basin north of Fort Quitman, Texas: U. S. Geological Survey, Water Supply Paper 839, 296 pp.

Scott, R. C. and Barker, F. B., 1963, Data on uranium and radium in groundwater of the United States 1954 to 1957: U. S. Geological Survey, Professional Paper 42-C, 115 pp.

Smith C. T., 1963, Preliminary notes on the geology of part of the Socorro Mountains, Socorro County New Mexico, in 14th Field Conference Guidebook: New Mexico Geological Society, p. 185-196.

Summers, W. K., 1965, A preliminary report on New Mexico's geothermal energy resources: New Mexico Bureau of Mines and Mineral Resources, Circular 80, 41 pp.

Summers, W. K., 1976, Catalog of thermal waters in New Mexico: New Mexico Bureau of Mines and Mineral Resources, Hydrology Report 4, 80 pp.

Verhagen, B., Sellschop, J. P. F., and Jennings, C. M. H., 1970, Contribution of environmental tritium measurements to some geophysical problems in South Africa, in Isotope Hydrology 1970, International Atomic Energy Agency, Vienna, p. 289-312.

Waldron, J. F., 1956, Reconnaissance geology and ground water study of a part of Socorro County, New Mexico: Stanford University, M.S. thesis, 255 pp.

Appendix A

Coordinate System for Locating Springs and Wells

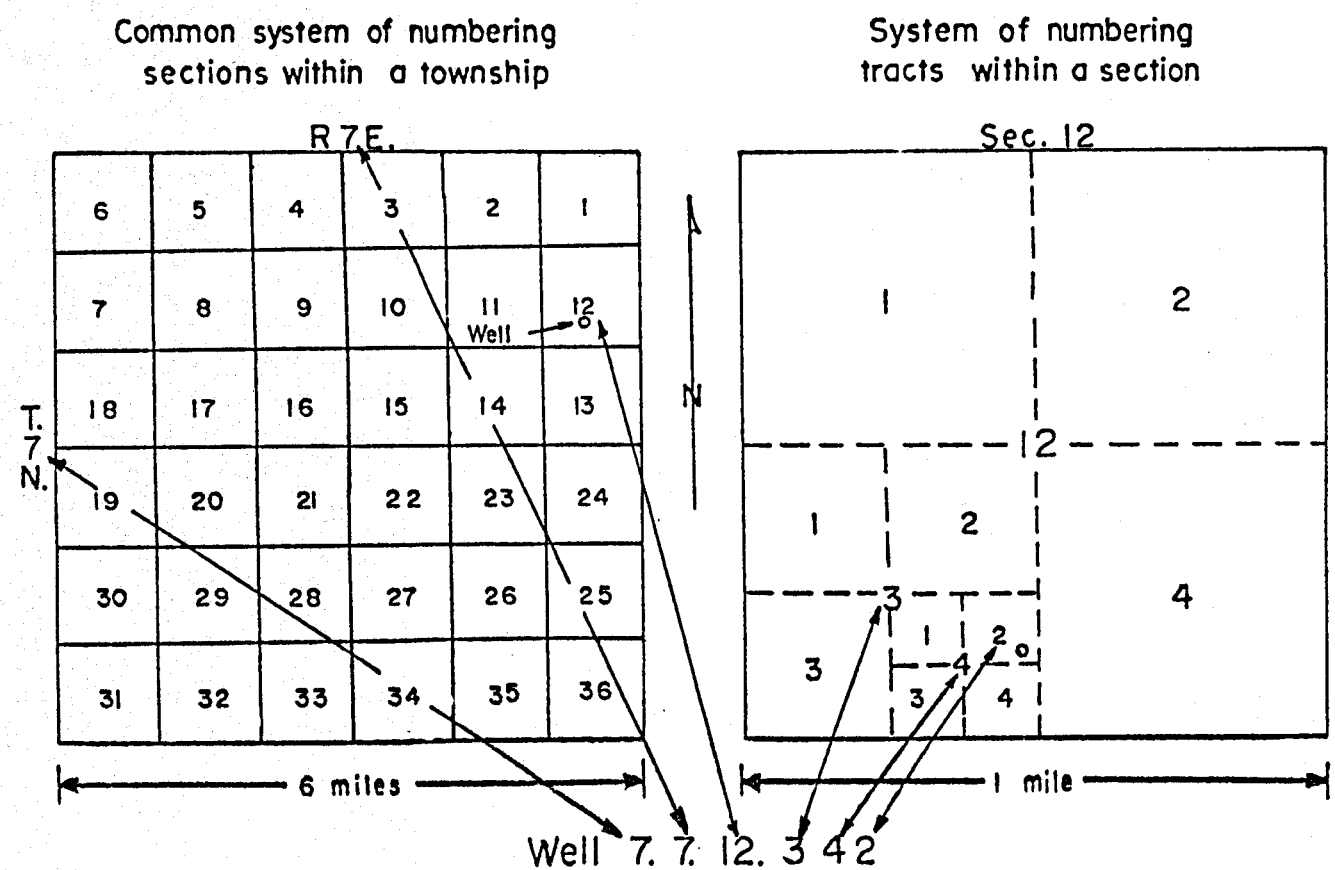

Figure 2A-2. Coordinate system for locating springs and wells. For readibility, the designations N and E (or W) are omitted throughout this chapter. Range and township are generally omitted in the text and figures.

Appendix B

Well and Spring Data

Table 2B-1. Well data.

Location Number	Name	Geologic Source	Altitude (ft)	Depth (ft)	Depth to Water (ft)	Date Measured	Use	Source
3.1.16.323	Blue Canyon Well	Lower member Popotosa Formation	5200	300	219	8-77	Domestic	This well yields warm water (91° F). See log for this well in Table 2B-3.
3.1.33.144	Armijo Windmill	Quaternary alluvium or Upper Santa Fe Group	5155	58	20	8-77	Stock watering	
2.2.20.311	B. Kelly Ranch (deep well)	Upper Santa Fe Group	5842	275	131	8-77	Stock watering	This well is equipped with an electric pump. See driller's log for this well (Table 2B-3).
2.2.18.422	B. Kelly Ranch	Upper Santa Fe Group	5835	160	---	----	Stock watering	This well seems to have caved in from 125 feet down.
2.2.34.432	Snake Ranch Windmill	Upper Santa Fe Group	5797	134	90	8-77	Stock watering	
2.2.35.323	Snake Ranch Windmill	Upper Santa Fe Group	5715	---	24	8-77	not used	
3.2.8.423	Water Canyon Lodge Well	Upper Santa Fe Group	5075	400	355	6-60	Domestic	Electrical pump (Clark and Summers 1971).

Table 2B-1. (continued).

Location Number	Name	Geologic Source	Altitude (ft)	Depth (ft)	Depth to Water (ft)	Date Measured	Use	Source
3.2.17.423	South Canyon Windmill	Upper Santa Fe Group	6106	400	380	6-60	Stock watering	(Clark and Summers 1971).
3.2.20.111	Upper South Canyon Windmill	Upper Santa Fe Group	6232	540	440	6-60	Stock watering	See driller's log for this well in Table 2B-3. (Clark and Summers 1971).
3.2.23.123	Sedillo Windmill	--------	5879	173	112	8-77	Stock watering	
3.2.25.443	Sedillo Windmill	--------	5520	180	122	8-77	Stock watering	
4.2.12.112	Gianero Windmill	--------	5955	115	---	----	Domestic	
4.2.12.112	Gianero Windmill	--------	5652	300	---	----	Stock watering	See driller's log for this well in Table 2B-3.
2.3.24.411	Allie Strozzi Well	Upper Santa Fe Group	5860	160	158	6-60	Domestic	(Clark and Summers 1971).
2.3.25.115	J. B. Kelly Windmill	Upper Santa Fe Group	5955	217	---	----	Stock watering	
2.3.27.223	Courtney Well	Upper Santa Fe Group	6040	415	348	8-67	Stock watering	See driller's log for this well in Table 2B-3. (Clark and Summers 1971).

Table 2B-1. (continued).

Location Number	Name	Geologic Source	Altitude (ft)	Depth (ft)	Depth to Water (ft)	Date Measured	Use	Source
3.3.23.221	Nathan Hall Windmill	Quaternary alluvium	6593	95	47	8-77	Stock watering	
3.3.13.331	Cibola National Forest Windmill	Quaternary alluvium	6593		76	8-77	Stock watering	
3.3.23.342	Tom Kelly Well	Quaternary alluvium	6677	65	17	7-67	Domestic	Electric pump (Clark and Summers 1971).
3.3.26.111	Water Canyon Campground Well	Quaternary	6800				Domestic	Hand pump.

Table 2B-2. Spring data.

Location Number	Name	Geologic Source	Yield Rate (gpm)	Date	Use	Altitude (ft)	Source
3.1.22.111	Socorro Spring	Lower member Popotosa Formation	310	----	Municipal	4960	This spring is fault controlled. It issues warm water (91° F) from an adit at the base of a shaft dug to intercept water. It issues through joints.
3.1.22.113	Sedillo Spring	Lower member Popotosa Formation	100-300	----	Municipal	5000	This spring is fault controlled. It issues warm water (91° F) from an adit at the base of a shaft dug to intercept water.
3.1.15.311	Cook Spring	Rhyolite of Socorro Peak	15	1974	Stock watering	4900	Adit dug several hundred feet to intercept water (Billings 1974).
2.1.30.443	Lower Nogal Canyon Spring	Quaternary alluvium or Socorro Peak volcanics	1	3-78	Stock watering	5135	This spring is fault controlled.
2.1.31.314	Upper Nogal Canyon Spring	Quaternary alluvium or older volcanic rocks	1	1-78	Stock watering	5200	This spring is fault controlled.
4.1.5.211	Chupadera Spring	Lower member Popotosa Formation	1	5-62	Stock watering	5200	This spring has dried up since 1962 (Hall 1963).
4.2.7.211	Box Spring	Older volcanic rocks	1	2-63	Stock watering	7560	This spring has dried up since 1963.
2.2.35.324	Snake Ranch	Upper Santa Fe Group	1- 2	11-77	Stock watering	5680	This spring is fault controlled.

Table 2B-2. (continued).

Location Number	Name	Geologic Source	Yield Rate (gpm)	Date	Use	Altitude (ft)	Source
3.3.10.311	Garcia Canyon Spring	Paleozoic limestone	2	7-62	Stock watering	7080	This spring is controlled by a limestone bed crossing an arroyo.
3.3.28.424	Copper Canyon Spring	Paleozoic limestone	1	10-77	Stock watering	7720	This spring issues from a black limestone.
4.3.5.311	Baldy Spring	---------	-	-----	Domestic and stock watering	9920	

Table 2B-3. Well logs.

Blue Canyon Well (16.323) from Clark (1971)

Section penetrated	Top	Bottom	Thickness (ft)
Gravel	0	25	25
Rhyolite tuff breccia, in part welded	25	295	270
Andesite	295	300TD	5

Upper South Canyon Windmill (20.111) from Waldron (1956)

Section penetrated	Top	Bottom	Thickness
Red clay, gravel	0	400	400
Sand (water)	400	550TD	150

Gianero Windmill (12.112) from Waldron (1956)

Section penetrated	Top	Bottom	Thickness
Fill, with black volcanic rock at base	0	96	96
Clay (water at top of clay)	96	250	154
"Shaley rock"	250	300	50
Clay	300TD	---	---

Courtney Well (27.223) from Waldron (1956)

Section penetrated	Top	Bottom	Thickness
Boulders	0	240	240
Course to medium sand	240	360	120
Fine sand	360	420TD	60

(First water at 385 feet, separated from second aquifer by thin black seam 2 feet thick)

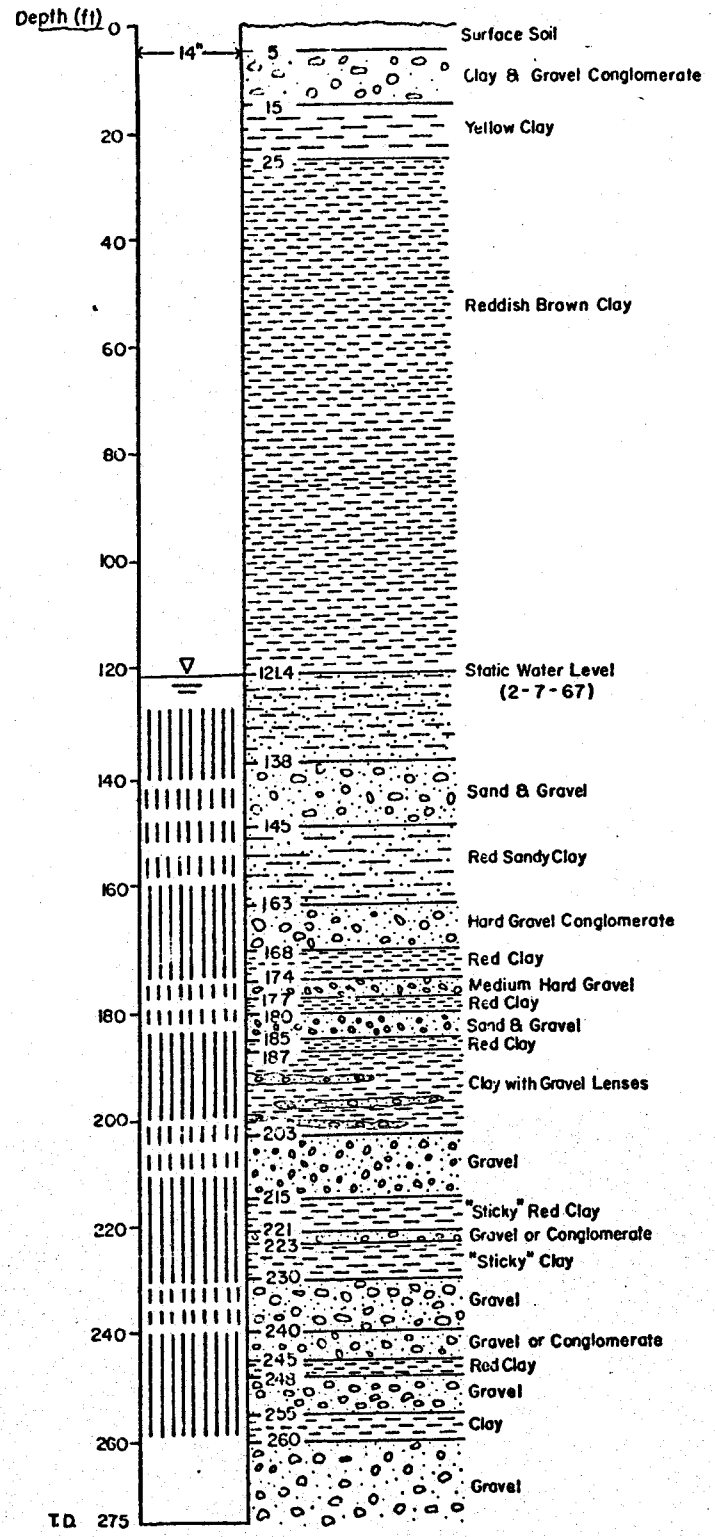

Figure 2B-1. Driller's log of J. B. Kelly Ranch deep well (2.2.20.311).

Appendix C

Water Quality Data

(All concentrations in ppm; hardness expressed as $CaCO_3$)

Table 2C-1. Water-quality analyses.

Location Number	Name	Source	Date Collected	Temp. (°F)	pH	SiO_2	Ca	Mg	Na	K	HCO_3	CO_3	SO_4	Cl	F	B	Fe	Hard-ness	Conductivity (µmhos/cm)	T.D.S.
3.1.22.1113	Socorro	(8)	1903	----	---	28	22	3.0	27	56.0	114	---	79	16	---	-----	-----	68	----	286
	Spring	(8)	5-24-31	----	---	33	42	27.0	12	C	85	22.0	102	38	---	-----	-----	215	----	318
		(3)	2-17-36	----	---	-----	19	4.0	55	5.0	168	---	30	14	---	-----	-----	63	340	210
		(3)	12- 4-36	----	---	-----	18	5.0	53	C	156	---	30	13	1.00	-----	-----	64	347	---
		(8)	2-10-48	----	---	28	20	4.7	54	C	165	---	31	13	---	-----	-----	70	352	233
		(2)	1952	91	8.2	-----	19	5.0	53	C	163	---	30	13	---	-----	-----	68	----	---
		(4)	1-24-57	90	7.8	27	18	3.9	52	2.8	154	0	28	15	0.60	-----	-----	61	348	224
		(5)	3-20-58	90	8.4	39	---	---	55	3.0	160	5.0	33	16	0.70	0.06	-----	74	362	231
		(1)	12-12-61	91.4	8.1	-----	18	5.0	50	C	163	0	28	8	---	-----	-----	64	370	---
		(9)	2- 5-63	91	7.8	-----	13	5.0	52	C	156	0	20	12	---	-----	-----	52	356	---
		(8)	1-10-64	----	7.8	31	18	4.6	52	3.0	164	0	31	13	0.60	0.09	0.12	64	352	36
		(5)	4-10-65	91.6	7.8	18	4.4	---	--	---	155	---	---	--	---	-----	-----	63	346	---
		(8)	10-23-65	91.4	9.4	18	18	4.0	53	3.0	133	1.0	0	16	0.55	0.07	0.13	---	-----	232
		(7)	2- 4-77	90	---	-----	10.6	3.6	79	4.0	109	5.0	75	20	---	-----	-----	---	370	---
		(6)	7- -77	----	7.81	25	18	4.2	50	3.4	150	---	23	12	---	0.80	-----	---	342	---
3.1.22.1131	Sedillo	(5)	3-20-58	----	8.2	27	---	---	54	2.9	159	0	33	14	0.80	0.05	-----	63	---	211
	Spring	(1)	12-12-61	88	8.4	-----	18	5.0	50	C	154	5.0	24	10	---	-----	-----	64	370	---
		(8)	1-22-64	90	7.9	31	20	3.2	54	3.0	164	0	31	12	0.60	0.08	0.07	63	352	237
		(8)	10-23-65	----	8.6	17	18	4.0	55	3.1	109	8.0	0	--	-----	0.10	1.04	60	336	249
		(7)	2- 4-77	----	8.4	-----	8.3	3.8	59	3.9	137	1.2	48	16	-----	-----	-----	---	360	---
		(6)	7- -77	91.4	7.9	25	17	4.4	51	3.3	151	---	22	15	-----	0.12	-----	---	340	---
3.1.15.3114	Cook	(5)	3-20-58	----	8.1	28.0	---	---	66	3.0	175	---	44	14	1.00	0.08	-----	62	393	243
	Spring	(1)	3-23-62	----	8.8	-----	17	5.0	63	C	163	5.0	40	12	-----	-----	-----	62	412	---
		(8)	9-24-64	----	8.4	26.0	13	4.0	68	3.4	158	3.0	42	14	0.80	0.13	0.58	49	391	250

Table 2C-1. (continued).

Location Number	Name	Source	Date Collected	Temp. (°F)	pH	SiO_2	Ca	Mg	Na	K	HCO_3	CO_3	SO_4	Cl	F	B	Fe	Hard-ness	Conductivity (μmhos/cm)	T.D.S.
3.1.151.3114	Cook Spring	(8)	5-20-74	----	7.80	----	17.0	6.7	67	2.0	198	---	41	21	0.8	-----	<0.25	72	466	264
		(7)	2- 4-77	----	8.80	----	6.7	3.6	82	3.9	142	5.0	53	20	---	-----	-----	---	420	---
		(6)	7- -77	75.0	7.69	22.5	18.0	4.2	65	3.4	168	---	32	17	---	0.13	-----	---	296	---
3.1.16.323	Blue Canyon Well	(5)	7-24-56	40.4	----	26.0	----	---	--	---	145	8.0	37	14	0.6	0.08	-----	78	380	---
		(1)	12-20-61	88.0	----	18.0	18.0	5.0	--	---	166	0	32	17	---	-----	-----	68	390	---
		(5)	4-10-65	89.0	7.60	27.0	20.0	4.6	56	3.0	163	0	36	14	---	-----	-----	69	375	---
		(7)	8- 1-77	----	8.40	----	13.4	3.5	70	4.0	167	0	44	12	---	-----	-----	---	410	---
2.2.31.314	Upper Nogal Canyon Spring	(1)	5- 3-62	61.0	7.90	----	62.0	9.0	32	---	239	0	40	16	---	-----	-----	192	505	---
		(7)	3- 4-77	----	7.80	----	45.0	8.3	38	3.0	178	0	85	16	---	-----	-----	---	460	---
2.2.30.443	Lower Nogal Canyon Spring	(1)	5- 3-62	66.0	7.00	----	89.0	11.0	62	---	268	0	136	20	---	-----	-----	256	727	---
		(7)	3- 4-77	----	8.00	----	20.0	12.1	73	4.9	162	0	352	4	---	-----	-----	---	770	---
3.1.33.144	Armijo Windmill	(7)	5-13-77	----	8.00	----	72.0	17.5	110	4.3	195	0	271	28	---	-----	-----	---	1000	---
3.2.36.212	Armijo Windmill	(7)	5-13-77	----	8.40	----	22.0	6.2	90	10.5	165	2.5	103	28	---	-----	-----	---	620	---
4.1.5.211	Chupadera Spring	(1)	5-17-62	63.0	8.30	----	39.0	3.0	372	---	444	0	476	43	---	-----	-----	110	1872	---
4.2.7.211	Box Spring	(1)	2- 8-63	46.0	7.80	----	30.0	5.0	3	---	102	0	10	6	---	-----	-----	95	219	---
4.3.5.331	Mt. Baldy Spring	(1)	6-11-62	----	7.80	----	25.0	3.0	5	---	90	0	8	2	---	-----	-----	74	159	---
4.2.12.112	Gianero Windmill	(2)	1952	68.0	7.60	----	23.0	35.0	185	---	230	---	608	24	---	-----	-----	---	-----	792
4.2.3.321	Gianero Windmill	(2)	1952	72.0	7.50	----	58.0	16.0	17	---	230	---	24	24	---	-----	-----	---	-----	316

Table 2C-1. (continued).

Location Number	Name	Source	Date Collected	Temp. (°F)	pH	SiO_2	Ca	Mg	Na	K	HCO_3	CO_3	SO_4	Cl	F	B	Fe	Hard-ness	Conductivity (μmhos/cm)	T.D.S.
3.2.25,443	Sedillo Windmill	(2)	1952	---	---	----	29	8.0	----	---	----	---	108	22	---	----	----	---	----	---
3.2.23.123	Sedillo Windmill	(2)	1952	64	7.7	----	47	8.0	34.0	---	205	---	20	26	---	----	----	---	----	280
3.3.28.424	Copper Canyon Spring	(7)	10-29-77	---	7.9	----	79	11.0	9.7	1.2	228	0	65	4	---	----	----	---	400	---
3.3.26.111	North Fork, Water Canyon	(1)	5-10-62	64	8.5	----	62	12.0	19.0	---	229	5	34	10	---	----	----	206	440	---
3.3.27.211	North Fork, Water Canyon	(1)	2- 8-63	48	8.2	----	16	16.0	5.0	---	355	0	44	0	---	----	----	326	632	---
3.3.26.113	Water Canyon	(1)	5-10-62	73	8.7	----	54	9.0	15.0	---	188	10	20	8	---	----	----	170	358	---
3.3.34.332	Water Canyon	(1)	2- 8-63	45	7.8	----	65	10.0	10.0	---	237	0	10	15	---	----	----	202	430	---
3.3.26.111	Water Canyon Campground Well	(7)	3- 4-77	---	8.1	----	33	17.0	15.3	1.2	142	0	53	8	---	----	----	---	300	---
3.3.23.342	Tom Kelly Well	(7)	3- 4-77	---	7.9	----	68	14.9	18.8	1.6	213	0	87	10	---	----	----	---	520	---
3.3.13.331	Cibola National Forest Well	(7)	10-29-77	---	7.8	----	91	12.2	14.1	1.3	178	0	125	4	---	----	----	---	450	---
3.2.20.1111	Strozzi Windmill	(7)	5-13-77	---	7.7	----	35	5.2	19.1	2.4	137	0	12	18	---	----	----	---	310	---
3.2.14.423	Strozzi Windmill	(7)	5-13-77	---	8.0	----	25	6.2	17.3	2.2	122	0	---	14	---	----	----	---	260	---
3.3.10.311	Garcia Canyon Spring	(1)	7-26-62	63	7.8	----	106	23.0	9.0	---	388	0	48	8	---	----	----	358	705	---
		(7)	5-16-77	---	8.0	----	31	20.2	21.2	1.4	152	0	70	12	---	----	----	---	420	---

Table 2C-1. (continued).

Location Number	Name		Date Collected	Temp. (°F)	pH	SiO_2	Ca	Mg	Na	K	HCO_3	CO_3	SO_4	Cl	F	B	Fe	Hard-ness	Conductivity (μmhos/cm)	T.D.S.
3.2.8.423	Water Canyon	(2)	1952	64	7.7	----	61	8	40	---	278	---	24	14	---	---	----	186	-----	234
	Lodge Well	(1)	3-4-77	---	7.9	----	35	6.4	12.0	1.7	152	0	---	12	---	---	----	---	300	---
2.2.35.324	Snake Ranch	(5)	6-25-60	---	7.4	31	---	---	23	---	201	0	12	15	0.4	---	----	150	353	---
	Spring	(1)	5-10-62	61	8.2	----	---	---	26	---	237	0	20	12	---	---	----	176	414	---
		(7)	11-29-77	---	7.9	----	55	5.6	16	1.5	218	0	20	10	---	---	----	---	370	---
2.2.35.323	Snake Ranch Windmill	(2)	1952	60	7.9	----	59	9	20	---	200	---	16	34	---	---	----	186	-----	270
2.2.34.432	Snake Ranch	(2)	1952	66	7.8	----	68	10	19	---	244	---	16	26	---	---	----	210	-----	290
	Windmill	(7)	5-16-77	---	7.9	----	54	8.3	26	2.0	195	0	30	36	---	---	----	---	430	---
2.2.19.422	B. Kelly Ranch Well	(2)	1952	64	7.8	----	38	9	24	---	181	---	16	14	---	---	----	132	-----	188
2.2.20.311	B. Kelly Ranch Well	(7)	5-16-77	---	8.0	----	21	5.5	23.6	3.0	74	0	45	8	---	---	----	---	260	---
2.3.24.411	Allie Strozzi	(2)	1952	---	8.3	----	35	9	35	---	190	---	20	14	---	---	----	126	-----	196
	Well	(7)	5-12-77	---	7.9	----	34	6.4	17.9	1.9	157	0	---	8	---	---	----	---	300	---
2.3.25.133	J. B. Kelly	(2)	1952	68	7.7	----	34	11	25	---	171	---	20	16	---	---	----	128	-----	188
	Windmill	(7)	5-12-77	---	8.0	----	26.1	6.5	22.8	1.5	157	0	---	16	---	---	----	---	290	---
2.3.27.223	Courtney Well	(2)	1952	73	7.8	----	44	10	18	---	166	---	22	22	---	---	----	150	-----	206

Sources: (1) Hall (1963); (2) Waldron (1956); (3) Scofield (1939); (4) Scott and Barker (1963); (5) USGS unpublished data; (6) City of Socorro, Water Department; (7) New Mexico Bureau of Mines and Mineral Resources; (8) Billings (1974); and (9) Summers (1965).

Note: The letter C indicates that Na and K values were calculated.

Appendix D

Tritium and Precipitation Data

and

Spring and Well Tritium Data

Most precipitation data are from the U.S. Weather Bureau* monthly reports for the Socorro and Kelly Ranch stations. In some instances, the Socorro precipitation data had not been recorded, although tritium activity was measured in Socorro precipitation. In these cases, precipitation amounts from other stations were used, namely, Albuquerque, Mount Withington, Snake Ranch Flats, and Langmuir Laboratory. The last three locations are atmospheric physics research stations operated in the study area by New Mexico Institute of Mining and Technology Physics Department which has the files. The Albuquerque data are from the U.S. Weather Bureau.

Tritium activities were measured at the New Mexico Institute of Mining and Technology. Listings of tritium in precipitation were given by Rabinowitz and Gross (1972) and by Gross et al. (1976). These data were carefully checked against the original tritium laboratory records and some were recomputed. However, the original records for sample numbers approximately between 1113 and 1233 could not be located. Tritium data for 1977 and 1978 are new determinations.

Monthly average tritium activity in precipitation was computed as follows. If only one event was measured for tritium in a given month then that value was used as the monthly value. When more than one event was measured during a given month, then a weighted average value was used for that month, viz.

*Climatological Data - New Mexico: National Oceanic and Atmospheric Administration. Environmental Data Service. National Climatic Center. Asheville, NC 28801.

$$T_m = \frac{\sum_{i}^{n} T_i P_i}{\sum_{i}^{n} P_i},$$

where T_m = monthly weighted average tritium activity (TU) in precipitation, n = number of events analyzed for tritium during a month, T_i = tritium activity (TU) for the i^{th} event, and P_i = precipitation amount (inches) for the i^{th} event. For months when no tritium in precipitation was measured, tritium activities were determined by linear interpolation from the preceding and following monthly values (see Table 2C-1).

Tritium activities of springs and wells in the Socorro area prior to 1977 have never before been compiled systematically, nor have they been carefully checked against the original laboratory records (see Table 2D-2).

Table 2D-1. Tritium and precipitation data.

Date	TU in Socorro Precipitation	Socorro Precipitation (inches)	Kelly Ranch Precipitation (inches)	TU times Socorro ppt	TU times Socorro ppt	Sample #
1957						
1	42 ± 4.0	0.21	0.34	9	14	74
2	58 ± 1.7	0.60	0.40	35	23	89
3	74 ± .7	0.80	1.58	59	117	99
4	133 ± 8.0	0.40	1.48	53	197	113
5	194*	0.20	0.44	39	85	
6	254 ± 14.0	0.15	0.38	38	97	137,139
7	103 ± 1.7	1.92	7.70	198	793	141,142, 147,192
8	96 ± 1.2	2.73	5.30	262	509	153,157, 175,194
9	119*	0.12	0.57	14	68	
10	141 ± 4.2	3.34	3.00	471	423	167,168, 171,173
11	152*	0.57	1.52	87	231	
12	163*	0.06	0.00	10	0	
1958						
1	173 ± 4.0	0.55	0.70	95	121	196
2	224*	0.05	0.09	11	20	
3	275 ± 7.8	1.89	2.21	520	608	209,213, 216,223

Table 2D-1. (continued).

Date	Socorro ppt	TU in Socorro Precipitation	Socorro Precipitation (inches)	Kelly Ranch Precipitation (inches)	TU times Socorro ppt	TU times Kelly Ranch ppt	Sample #
4	26	261 ± 41.3	1.25	1.25	326	326	225,226
5	52	420 ± 11.5	0.60	0.25	252	105	229,230, 236,238
6	53	561 ± 21.6	0.63	1.64	353	920	243,260 (?)
7	53	585*	0.57	2.34	333	1369	261 (?)
8	98	608 ± 57.3	0.49	3.27	298	1988	262 (?), 263 (?), 278,280, 281,283
9	22	165 ± 14.67	2.56	5.42	422	894	270-272, 284,287, 301
10	41	218 ± 11.0	2.48	1.84	541	401	291,291B, 299
11	57	354 ± 35.0	0.16	0.00	57	0	305 (?)
12	37	514 ± 51.0	0.27	0.50	137	257	308 (?)
1959							
1	31	1526	0.02(1)	0.10	31	153	383
2	131	2188*	0.06	0.00	131	0	
3	969	2850	0.34(1)	0.19	969	542	384
4	340	971 ± 2.0	0.35	0.53	340	515	409,410
5	391	781*	0.50	0.03	391	23	

Table 2D-1. (continued).

Date	TU in Socorro Precipitation	Socorro Precipitation (inches)	Kelly Ranch Precipitation (inches)	TU times Socorro ppt	TU times Kelly Ranch ppt	Sample #
6	591 ± 2.0	0.08	1.31	47	774	416
7	242 ± 3.0	1.26(2)	3.22	305	779	404
8	209*	1.30	2.95	272	617	
9	176*	0.00	0.00	0	0	
10	143*	1.87	2.79	267	399	
11	109 ± 4.0	0.11(2)	0.09	12	10	405
12	233 ± 4.0	1.75	3.09	408	720	403
1960						
1	212*	0.11	0.14	23	30	
2	191*	0.36	0.00	69	0	
3	170*	0.19	0.40	32	68	
4	149*	0.00	0.00	0	0	
5	128*	0.33	0.20	42	26	
6	108 ± 2.0	1.35(2)	2.86	146	309	408
7	220 ± 4.0	1.80	1.93	396	425	422
8	193 ± 2.7	0.78	4.10	151	791	412,413, 426
9	247 ± 5.5	0.46	0.40	114	99	429,433
10	155 ± 5.8	2.66	4.24	412	657	431,433, 434,436
11	64 ± 4.0	0.01(2)	0.00	1	0	438

Table 2D-1. (continued).

Date	TU in Socorro Precipitation	Socorro Precipitation (inches)	Kelly Ranch Precipitation (inches)	TU times Socorro ppt	TU times Kelly Ranch ppt	Sample #
12	162 ± 2.0	2.34	2.30	379	373	439
1961						
1	184*	0.22	0.44	40	81	
2	206*	0.20	0.48	41	99	
3	228*	0.29	1.55	66	353	
4	250*	0.33	0.51	83	128	
5	271 ± 27.0	0.32	0.19	87	51	457
6	219 ± 8.0	0.63	1.26	138	276	456,530, 531
7	211 ± 9.3	2.01	0.57	424	120	514,532, 540,571, 581,663
8	75 ± 14.0	1.68	2.55	126	191	515,646
9	61 ± 9.0	1.24	0.87	76	53	544
10	60 ± 32.3	0.08	0.90	5	54	469,605, 647,759-I
11	361 ± 8.3	0.85	2.82	307	1018	587,603, 616,643
12	569*	0.45	0.59	256	336	
1962						
1	777 ± 14.0	0.78	0.90	606	699	478,618, 793-I

Table 2D-1. (continued).

Date	TU in Socorro Precipitation	Socorro Precipitation (inches)	Kelly Ranch Precipitation (inches)	TU times Socorro ppt	TU times Kelly Ranch ppt	Sample #
2	1326*	0.04	0.00	53	0	
3	1874 ± 2.0	0.36	0.96	675	1795	488
4	1373*	0.16	0.49	220	673	
5	872 ± 3.0	0.00(1)	0.00	0	0	584
6	714*± 1.0	0.46	0.79	328	564	505
7	555 ± 2.0	1.76	3.41	977	1893	506,508-511
8	743 ± 3.0	0.19	1.02	141	758	564,574,591
9	82 ± 7.7	1.10	2.06	90	169	543,568,570
10	213 ± 10.2	0.87	1.65	185	351	539,541,572,606,638
11	805 ± 18.5	0.67	0.55	539	443	635,640
12	536 ± 3.5	1.40	9.48	750	257	567,634
1963						
1	1259*	0.07	0.00	89	0	
2	2001 ± 4.6	0.69	1.10	1381	2201	592,593,597,599,633
3	1464 ± 20.0	0.17	0.00	249	0	644
4	2781 ± 3.0	0.26	0.00	723	0	632

Table 2D-1. (continued).

Date	TU in Socorro Precipitation	Socorro Precipitation (inches)	Kelly Ranch Precipitation (inches)	TU times Socorro ppt	TU times Kelly Ranch ppt	Sample #
5	3154 ± 16.0	0.10	0.00	315	0	1107
6	9436 ± 24.0	0.10(2)	0.00	940	0	651,1106
7	1274 ± 29.4	0.34	2.62	433	3338	661, 664, 667, 940-I 941-X
8	1362 ± 10.3	2.25	4.61	3065	6279	682, 712, 722, 730, 956
9	602 ± 4.0	1.13	1.34	680	807	957-I
10	504 ± 2.0	1.07	1.18	539	595	957-I, 958 959
11	1200 ± 19.6	0.38	0.34	455	408	901-I, 901-A, 943-I
12	2182*	0.00	0.00	0	0	
1964						
1	3164*	0.03	0.08	95	253	
2	4147 ± 14.0	0.63	2.96	2613	12,275	738
3	1897 ±418.0	0.06	0.00	114	0	903-U
4	2372*	0.98	0.80	2325	1898	1108 (?)
5	2847 ± 62.0	0.35	1.79	996	5096	1109
6	1856*	0.00	0.29	0	483	

Table 2D-1. (continued).

Date	TU in Socorro Precipitation	Socorro Precipitation (inches)	Kelly Ranch Precipitation (inches)	TU times Socorro ppt	TU times Kelly Ranch ppt	Sample #
7	865	2.45	2.67	2119	2310	
8	580	0.61	0.21	354	122	
9	258	1.28	2.75	330	908	
10	233	0.07	0.00	16	0	
11	120 ± 40.0	0.05	0.19	5	23	898-I
12	314 ± 14.0	0.27	0.00	85	0	906-I
1965						
1	600*	0.17	0.00	102	0	
2	885 ± 99.0	0.08	1.09	71	965	937-I
3	1116 ± 84.0	0.15	0.10	167	112	938-I
4	794*	0.20	0.71	159	564	
5	471	0.25	0.83	118	391	
6	410 ± 1	0.40	1.10	164	451	970
7	439*	0.93	2.31	409	1014	
8	468 ± 2.0	1.47	4.95	688	2317	980-A
9	178 ± 1.0	1.81	2.67	322	475	993
10	134 ± 1.0	0.50	0.18	67	24	1006
11	155*	0.02	0.00	3	0	
12	175 ± 4.5	1.44	2.52	252	441	1003,1046

Table 2D-1. (continued).

Date	TU in Socorro Precipitation	Socorro Precipitation (inches)	Kelly Ranch Precipitation (inches)	TU times Socorro ppt	TU times Kelly Ranch ppt	Sample #
1966						
1	234 ± 3.0	0.67	0.82	157	192	1045
2	217 ± 12.0	0.06	0.41	13	89	1044
3	329	0.10	0.20	33	66	
4	440*	0.24	0.00	106	0	
5	552*	0.01	0.00	6	0	
6	663 ± 18.0	1.90	1.13	1260	749	1078
7	262 ± 7.7	1.23(3)	4.99	322	1307	1083,1084 1186
8	132 ± 6.0	0.60(4)	0.84	79	111	1187,1190
9	230 ± 8.0	1.09	1.44	251	331	1191
10	140 ± 7.0	0.05	0.00	7	0	1113
11	129*	0.00	0.00	0	0	
12	117 ± 5.0	0.06(4)	0.00	7	0	1114
1967						
1	147 ± 14.0	0.00	0.00	0	0	1119
2	233*	0.24	0.90	56	210	
3	319 ± 9.5	0.07	0.09	22	29	1130,1155
4	583 ± 10.0	0.00	0.03	0	17	1153
5	358*	0.00	0.09	0	32	

Table 2D-1. (continued).

Date	TU in Socorro Precipitation	Socorro Precipitation (inches)	Kelly Ranch Precipitation (inches)	TU times Socorro ppt	TU times Kelly Ranch ppt	Sample #
6	133 ± 7.5	0.81	1.30	108	173	1151,1154
7	157*	1.81	1.12	284	176	
8	180 ± 6.0	0.76	3.66	137	559	1218
9	253 ± 6.0	2.01	2.39	509	605	1217
10	243*	0.23	0.45	56	109	1215,1216
11	232 ± 10.0	0.51	0.26	118	60	1188,1189
12	340 ± 29.5	1.54	1.56	524	530	1192,1193
1968						
1	100 ± 5.0	0.40	0.16	40	16	1212,1233
2	127 ± 8.0	0.48	0.37	51	47	1226
3	226 ± 8.0	0.91	2.38	206	538	1213,1227
4	214 ± 6.0	0.03	0.08	6	17	1214
5	174 ± 6.0	0.71	0.49	124	85	1207
6	244 ± 7.0	0.05	0.00	12	0	1208
7	103 ± 6.5	3.32	4.60	342	474	1200,1205 1206,1232
8	80 ± 5.0	2.81	7.47	226	598	1210,1211
9	--- ---	----	----	---	---	---- ----
10	--- ---	----	----	---	---	---- ----
11	--- ---	----	----	---	---	---- ----

Table 2D-1. (continued)

Date	TU in Socorro Precipitation	Socorro Precipitation (inches)	Kelly Ranch Precipitation (inches)	TU times Socorro ppt	TU times Kelly Ranch ppt	Sample #
12	--- ---	----	----	---	---	---- ----
1-1969 through 6-1971	--- ---	----	----	---	---	---- ----
1971						
7	138	0.72	1.97	99	399	1374
8	144	0.91	2.86	131	412	1375
9	168*	1.39	2.89	25	270	
10	192*	1.43	2.17	336	774	
11	216	0.72	0.65	156	140	1429
12	211*	1.21	0.78	274	152	
1972						
1	206*	0.12	0.00	25	0	
2	202*	0.07	0.20	14	40	
3	197*	0.02	0.00	4	0	
4	192*	0.00	0.00	0	0	
5	187 ± 1.9	0.38	1.55	71	290	1428,1454C
6	161*	0.81	0.95	130	153	
7	135 ± 1.7	0.93	1.65	126	223	1433,1455C
8	103 ± 1.5	3.20	6.45	330	664	1435,1437 1440,1456C
9	81 ± 1.8	1.94	3.60	157	292	1441,1457C

Table 2D-1. (continued).

Date	TU in Socorro Precipitation	Socorro Precipitation (inches)	Kelly Ranch Precipitation (inches)	TU times Socorro ppt	TU times Kelly Ranch ppt	Sample #
10	138 ± 1.4	5.37	3194	741	544	1458C
11	131*	0.80	0.52	105	68	
12	124*	0.33	0.19	41	24	
1973						
1	117*	0.46	0.98	54	115	
2	109*	0.71	1.12	77	122	
3	102*	0.53	0.61	54	62	
4	95*	0.16	0.50	15	48	
5	88 ± 0.3	0.87	1.50	77	132	1493
6	124 ± 0.4	0.77	0.47	95	58	1494,1526
7	161 ± 0.4	1.03	2.18	166	351	1495,1497C
8	144*	3.24	1.49	467	215	
9	127 ± 1.6	1.12	0.54	142	69	1525
10	110*	0.04	0.30	4	33	
11	93*	0.00	0.00	0	0	
12	76*	0.00	0.00	0	0	
1974						
1	59 ± 1.7	0.10	0.41	6	24	1852,1853
2	158 ± 2.1	0.03	0.30	5	47	1854
3	157*	0.14	0.18	22	28	

Table 2D-1. (continued).

Date	TU in Socorro Precipitation	Socorro Precipitation (inches)	Kelly Ranch Precipitation (inches)	TU times Socorro ppt	TU times Kelly Ranch ppt	Sample #
4	155 ± 2.4	1.38	0.06	214	9	1855
5	140 ± 2.7	0.01	0.06	1	8	1856,1857
6	88*	0.11	0.04	10	6	
7	36 ± 0.9	0.85	1.69	31	1	1730,1850, 1851
8	81 ± 0.5	2.52	3.60	204	292	1731 (CR8)
9	65 ± 0.5	2.67	3.39	174	220	1732,1733
10	39 ± 0.6	3.32	4.37	129	170	1734
11	45 ± 0.7	0.05	0.07	2	3	1738
12	50 ± 0.5	0.48	0.63	24	32	1739,1740
1975						
1	50 ± 0.5	0.46	1.05	23	53	1741
2	109*	o.23	0.54	25	59	
3	168 ± 3.0	0.40	0.73	67	123	1860
4	179*	0.00	0.05	0	9	
5	189 ± 2.0	0.23	0.69	43	130	1858,1859
6	93 ± 2.5	0.00	0.09	0	8	1861
7	90 ± 2.4	3.07	5.09	276	458	1862,1864, 1940
8	46 ± 2.1	1.47	2.63	276	121	1863,1939 1942,1943

Table 2D-1. (continued).

Date	TU in Socorro Precipitation	Socorro Precipitation (inches)	Kelly Ranch Precipitation (inches)	TU times Socorro ppt	TU times Kelly Ranch ppt	Sample #
9	43 ± 1.4	4.12	4.68	177	201	1941,1944-1947,2176
10	33*	0.01	0.21	0	7	
11	23 ± 1.1	0.25	0.65	6	15	2177
12	67 ± 1.7	0.24	0.15	16	10	2178
1976						
1	45 ± 1.7	0.00	0.00	0	0	2184
2	34 ± 1.1	0.48	0.00	14	0	2179
3	84 ± 2.0	0.00	0.00	0	0	2182
4	30 ± 1.5	0.60	1.05	18	32	2180
5	74 ± 1.3	0.94	1.27	70	94	2183
6	55*	0.48	0.43	26	24	
7	36 ± 1.3	3.61	3.12	120	112	2181

*These values are interpolated data.
Numerical superscripts refer to the following sources: (1) Albuquerque precipitation; (2) Mt. Withington precipitation; (3) Langmuir Laboratory and Snake Ranch Flats precipitation; (4) Langmuir Laboratory precipitation; and (5) combined samples from Garcia Canyon Spring and S. Strozzi Windmill. Some of the data from sources (2), (3) and (4) have been taken from Romero and Wilkening (1977). Precipitation is abbreviated as ppt in columns 5 and 6.

Table 2D-2. Spring and well data.

Location	Date Sampled	Tritium activity (TU)	Sample No.
Socorro Spring (22.111)	18 March 1957	4.0 ± 0.5	98
	16 May 1957	2.0 ± 0.4	122
	26 July 1957	4.0 ± 0.3	146
	4 Sept 1957	5.0 ± 0.3	180
	7 Nov 1957	11.0 ± 0.1	177
	16 Jan 1958	2.0 ± 0.5	217
	5 March 1958	3.0 ± 0.4	211
	21 Apr 1958	5.0 ± 0.5	228
	28 May 1958	50.5 ± 3.2	239
	26 July 1958	11.0 ± 0.7	254
	10 Dec 1958	18.8	307
	2 Feb 1959	28.0	310
	28 March 1961	20.0 ± 1.0	450
	11 May 1961	27.0 ± 3.0	454
	5 July 1961	24 or 92? ± 1 or 3	595,602
	11 Sept 1961	39.0 ± 3.0	716
	1 June 1962	15.0	
	2 July 1962	192.0 ± 3.0	(601)
	1 Aug 1962	57.0 ± 2.0	590
	5 Sept 1962	68.0	
	31 Oct 1962	68 or 231? ± 13 or 1	728,611
	3 Dec 1962	135.0 ± 3.0	614

Table 20-2. (continued).

Location	Date Sampled	Tritium activity (TU)	Sample No.
Socorro Spring (22.111)	4 Feb 1977	6.5 ± 0.6	2312
	14 Apr 1977	5.9 ± 0.8	2320
	22 June 1977	9.8 ± 0.9	2348
	25 Oct 1977	1.7 ± 0.8	2384
	19 Jan 1978	3.5 ± 1.0	2423
	14 March 1978	1.5 ± 0.7	2428
Sedillo Spring (22.113)	8 Jan 1962	50.0 ± 6.0	579
	27 April 1962	54.0 ± 6.0	580
	1 June 1962	11.0 ± 2.0	528
	2 July 1962	27.0	
	5 Sept 1962	77.0	
	9 Oct 1962	48.0 ± 3.0	586
	8 Nov 1962	69.0 ± 3.0	589
	3 Dec 1962	165.0 ± 4.0	612
	9 Feb 1963	72.0 ± 4.0	598
	1 May 1963	111.0 ± 3.0	627
	2 June 1963	45.0 ± 37.0	641
	1 July 1963	82.0 ± 25.0	668
	2 Aug 1963	75.0 ± 14.0	678
	4 Sept 1963	27.0 ± 17.0	708
	3 Nov 1963	27.0 ± 2.0	736
	5 Dec 1963	69.0 ± 68.0	752-I
	4 Jan 1964	98.0 ± 26.0	789-I

Table 2D-2. (continued)

Location	Date Sampled	Tritium activity (TU)	Sample No.
Sedillo Spring (22.113) (continued)	31 Jan 1964	45.0 ± 89.0	772-I
	3 March 1964	334.0 ± 7.0	835
	31 March 1964	91.0 ± 14.0	861
	30 April 1964	3.0 ± 20.0	872
	3 June 1964	0	888
	1 July 1964	33.0 ± 6.0	889
	4 Aug 1964	56.0 ± 5.0	893
	1 Oct 1964	10.0 ± 4.0	896
	4 Feb 1977	8.8 ± 0.7	2313
	14 April 1977	11.2 ± 1.0	2321
	22 June 1977	5.9 ± 0.8	2338
	25 Oct 1977	2.0 ± 0.9	2385
	19 Jan 1978	0.2 ± 0.9	2422
	14 March 1978	0.5 ± 0.7	2429
Cook Spring (15.311)	4 Feb 1977	6.5 ± 0.8	2314
	14 April 1977	10.8 ± 1.0	2322
	22 June 1977	6.3 ± 0.7	2349
	25 Oct 1977	1.3 ± 0.9	2386
	19 Jan 1977	0.5 ± 0.5	2424
	14 March 1978	2.6 ± 1.0	2427
Blue Canyon Well (16.323)	1 Aug 1977	12.0 ± 0.8	2350
	6 Feb 1978	3.3 ± 0.8	2425
Lower Nogal Canyon Spring (30.443)	4 March 1977	28.3 ± 1.0	2425

Table 2D-2. (continued).

Location	Date Sampled	Tritium activity (TU)	Sample No.
Lower Nogal Canyon Spring (30.443) (continued)	13 May 1977	31.2 ± 1.2	2350
	3 Aug 1977	37.3 ± 1.4	2425
	29 Oct 1977	24.0 ± 0.8	2411
	19 Jan 1978	21.8 ± 1.3	2420
	14 March 1978	25.1 ± 1.4	2426
Upper Nogal Canyon Spring (31.314)	4 March 1977	24.0 ± 1.0	2315
	13 May 1977	22.8 ± 0.9	2324
	3 Aug 1977	26.6 ± 1.0	2352
	29 Oct 1977	18.3 ± 0.8	2412
	19 Jan 1978	20.8 ± 1.2	2421
Armijo Windmill (33.144)	13 May 1977	54.1 ± 1.8	2325
	5 Aug 1977	52.6 ± 1.1	2353
	25 Oct 1977	47.2 ± i.6	2387
Sedillo Windmill (25.443)	13 May 1977	10.5 ± 0.8	2326
Snake Ranch Windmill (34.432)	16 May 1977	7.9 ± 0.8	2330
	19 Aug 1977	8.4 ± 0.9	2380
	25 Oct 1977	5.7 ± 0.9	2388
Water Canyon Lodge Well (8.432)	4 Mar 1977	4.7 ± 0.7	2319
	13 May 1977	3.4 ± 0.8	2327
	5 Aug 1977	0.8 ± 0.7	2379
	25 Oct 1977	1.5 ± 0.7	2410
B. Kelly Ranch (deep well) (20.311)	16 May 1977	4.3 ± 0.8	2331
	18 Aug 1977	0.0	2381

Table 2D-2. (continued).

Location	Date Sampled	Tritium activity (TU)	Sample No.
B. Kelly Ranch (deep well) (20.311) (continued)	25 Oct 1977	1.0 ± 0.7	2389
Allie Strozzi Well (24.411)	12 March 1977	0.0	2375
	16 May 1977	3.1 ± 0.9	2332
	19 Aug 1977	2.0 ± 0.7	2383
	25 Oct 1977	0.8 ± 0.6	2390
J. B. Kelly Windmill (25.113)	16 May 1977	4.9 ± 0.9	2333
	19 Aug 1977	0.8 ± 0.8	2382
South Canyon Windmill (17.423)	12 March 1977	3.1 ± 0.8	2376
	13 May 1977	4.3 ± 0.8	2329
	5 Aug 1977	0.5 ± 0.7	2378
	29 Nov 1977	1.4 ± 0.7	2418
Upper South Canyon Windmill (20.111)	13 May 1977	2.2 ± 0.7	2328
Snake Ranch Spring (35.324)	29 Nov 1977	1.8 ± 0.6	2417
Garcia Canyon[s]	16 May 1977	47.1 ± 1.5	2334
	5 Aug 1977	43.0 ± 1.6	2354
	29 Nov 1977	34.6 ± 1.3	2419
Nathan Hall Windmill (23.211)	12 March 1977	51.3 ± 3.4	2374
	16 May 1977	55.2 ± 1.7	2335

Table 2D-2. (continued).

Location	Date Sampled	Tritium activity (TU)	Sample No.
Tom Kelly Well (23.342)	4 March 1977	50.9 ± 1.9	2374
	15 May 1977	50.8 ± 1.7	2336
	5 Aug 1977	39.3 ± 1.0	2355
	29 Oct 1977	37.3 ± 1.4	2414
Cibola National Forest Windmill (13.331)	29 Oct 1977	34.1 ± 1.4	2413
Water Canyon Campground Well (26.111)	4 March 1977	46.2 ± 1.6	2318
	16 May 1977	41.4 ± 1.6	2337
	5 Aug 1977	45.0 ± 2.1	2377
	29 Oct 1977	35.4 ± 1.0	2415
Copper Canyon Spring (28.424)	29 Oct 1977	35.2 ± 1.4	2416

Chapter 3

Regional Geothermal Exploration in the Truth or Consequences Area

Part 1

Geological Mapping of the Mud Springs Mountains near Truth or Consequences, New Mexico*

Because the Mud Springs Mountains have been considered as possibly serving as a recharge area for the occurrence of hot water at Truth or Consequences, the mountains were mapped on a topographic base at a scale of 1:24,000. Previous mapping of the area was done by Hill (1956) at a scale of 1"= 0.5 mile, but the mapping was not done on a topographic base and some obvious mapping mistakes were evident. For example, Hill (1956) mapped one low-angle reverse fault, which actually is a high-angle normal fault. Also, one of the mapped dikes is not as continuous and extensive as was described by Hill (1956). Further, reconnaissance work indicates that there were two periods of igneous activity, one in the Quaternary and the other in the Tertiary period. Hill (1956) mapped all intrusive rocks as being in the Tertiary. A 1:24,000 scale geologic map was completed in this phase of the Truth or Consequences study. A reduced version of the map is presented in Figure 3-1.

The Mud Springs Mountains are a fault block tilted to the east at about 20 to 30° with the major fault to the west covered by younger sediments of Tertiary to Quaternary age. At the southwestern face of the mountains, Precambrian and Ordovician rocks are exposed. The range is divided into two

*The principal authors of Chapter 3, Part 1 are Charles J. Zimmerman, Graduate Assistant, Department of Geology, University of New Mexico and Dr. Albert Kudo, Associate Professor of Geology, University of New Mexico.

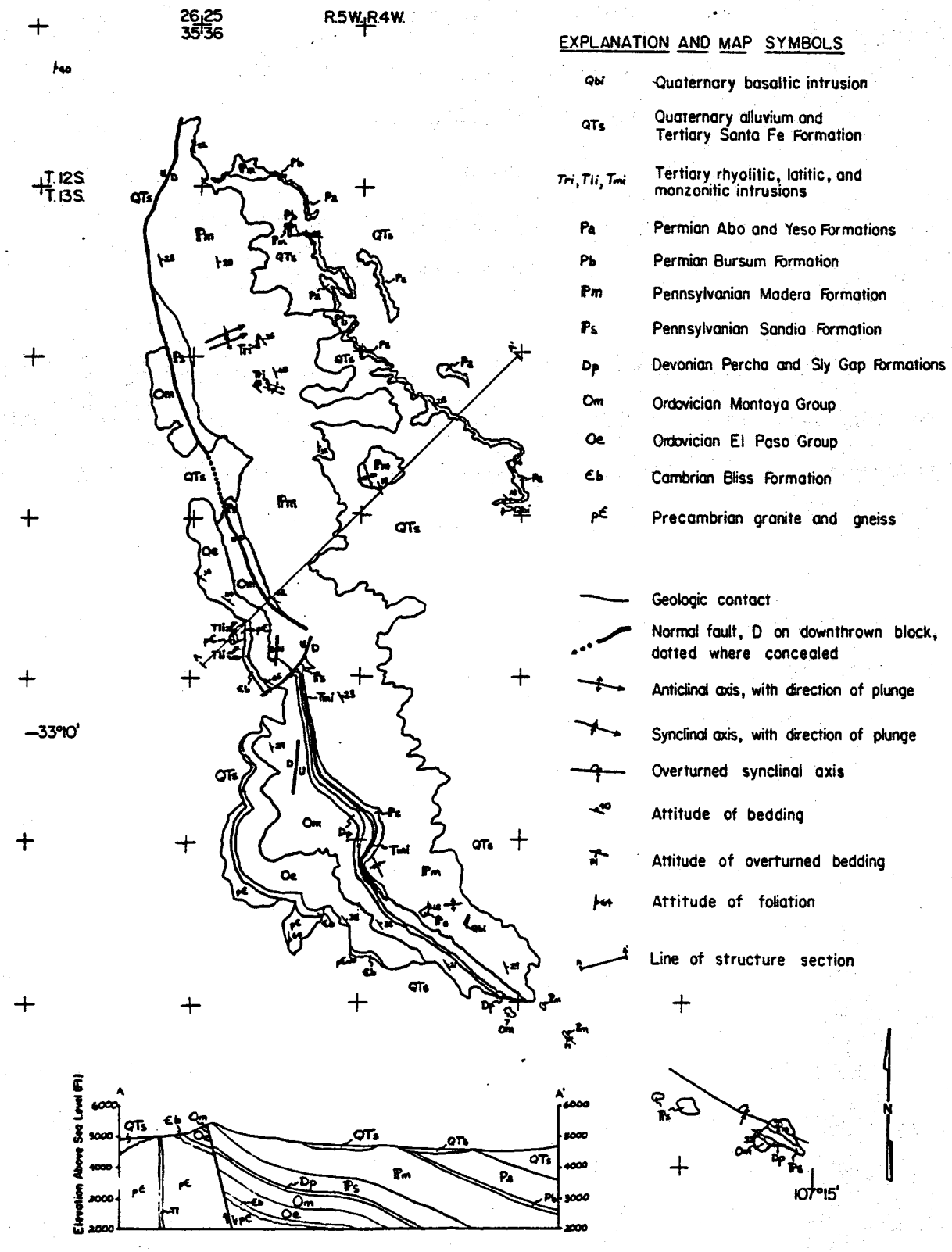

Figure 3-1. Geologic map of the Mud Springs Mountains.

segments by a northeast-trending high-angle fault which cuts the Tertiary latite intrusive sill. From this fault, a major high-angle fault, which was mapped by Hill (1956) as a low-angle reverse fault, can be traced northward to become the main western boundary of the range. This fault brings Ordovician rocks on the west into contact with Pennsylvanian formations on the east. Although the major fault on the west is covered, evidence of its presence may be found in the Cuchillo Negro Creek Valley about 2.4 km (1.5 mi) east of Cuchillo, where the Santa Fe beds are tilted 40° east. The Paleozoic rocks are overturned to the south near Truth or Consequences as mapped by Kelley and Silver (1952).

The extensive limestones in the Ordovician to Pennsylvanian sections probably serve as the aquifer, and their tilting upward at the heights of the mountains serves to provide an excellent recharge potential. The limestones are jointed and may have cavities sufficient to provide porosity and permeability.

Two periods of igneous activity occurred during Tertiary and Quaternary times. The early period saw injection of a latite porphyry sill and a porphyritic rhyolite dike. Because of similarities of these rocks with those found in the San Mateo Mountains to the north, these intrusions may have occurred 30 to 35 m.y. ago. Two Pleistocene (or younger) basaltic intrusions have been mapped. Similar basalts dated at 2.5 m.y. or younger are found on the east side of the Elephant Butte Reservoir (Loeber 1976). If the heat source for the hot springs is igneous in origin, basaltic magma similar to these would be the most likely source of the heat.

References

Hill, J. D., 1956, Paleozoic stratigraphy of the Mud Springs Mountains, Sierra County, New Mexico: University of New Mexico, M.S. thesis, 72 pp.

Kelley, V. C. and Silver, C., 1952, Geology of the Caballo Mountains with special reference to regional stratigraphy and structure, and to mineral resources, including oil and gas: University of New Mexico, Geology Publication 4, 286 pp.

Loeber, K. N., 1976, Geology and igneous petrology of the Truth or Consequences-Engle area, Sierra County, New Mexico: University of New Mexico, unpublished manuscript, 119 pp.

Part 2

Hydrogeology of the Thermal Aquifer near Truth or Consequences, New Mexico*

Introduction

The primary goals achieved during this portion of the geothermal investigation of the Truth or Consequences area include: (1) the definition and description of the thermal and nonthermal aquifers of the study area; (2) elucidation of the discharge-area geology including the age of the fault-controlled springs; and (3) the development of a qualitative model for the thermal-aquifer flow pattern and heat source. Data gathered during this investigation include detailed Cenozoic geologic mapping, detailed field observations, measurements of aquifer characteristics, and aerial photographic analysis. These data were combined with all available data previously published on the thermal springs of the Truth or Consequences area.

The following sections describe the results of this portion of the geothermal investigation. Some of the results are presented in the appendices (e.g., well-temperature data). The first portion of this discussion is devoted to a description of aquifer types and characteristics in the study. Emphasis is given to the thermal groundwater system. This section is followed by a discussion of the major chemical conditions and hydrochemical facies of the study area. Finally, a description of the thermal-aquifer flow pattern

*The principal authors of Chapter 3, Part 2 are Dr. Stephen G. Wells, Assistant Professor of Geology, and Howard Granzow, Research Assistant, Department of Geology, University of New Mexico.

is given, with emphasis on the geology of the discharge area.

Groundwater Occurrences and Aquifer Characteristics

Cox and Reeder (1962) defined three major types of groundwater occurrences in the Rio Grande Valley near Truth or Consequences. In the present study, these major groundwater occurrences are redefined and are classified as three major aquifers: (1) the Mud Springs Mountains carbonate aquifer - artesian and thermal; (2) the Piedmont/Santa Fe Group aquifers - artesian, unconfined, and nonthermal; and (3) the Rio Grande floodplain aquifers - artesian, unconfined, thermal, and nonthermal. Classification of these aquifers is based on regional hydrologic conditions and regional flow patterns in this portion of the Rio Grande Valley. Aquifer nomenclature is based on the dominant geographic or geologic feature related to the aquifer. All three aquifers are related hydrologically to the thermal groundwater conditions near Truth or Consequences; however, the Mud Springs Mountains carbonate aquifer is the major source of thermal waters.

Regional Comparisons

Figure 3-2 illustrates a generalized regional relationship among these aquifers. Boundaries between these aquifers are known only at specific localities and are not accurately portrayed on Figure 3-2. Table 3-1 lists the major hydrologic and geologic characteristics of the three major aquifers. Data provided in Table 3-1 are synthesized from previous studies (Theis et al. 1941; Borton, 1961; Cox and Reeder 1962). Table 3-1 also includes some data gathered during the present investigation.

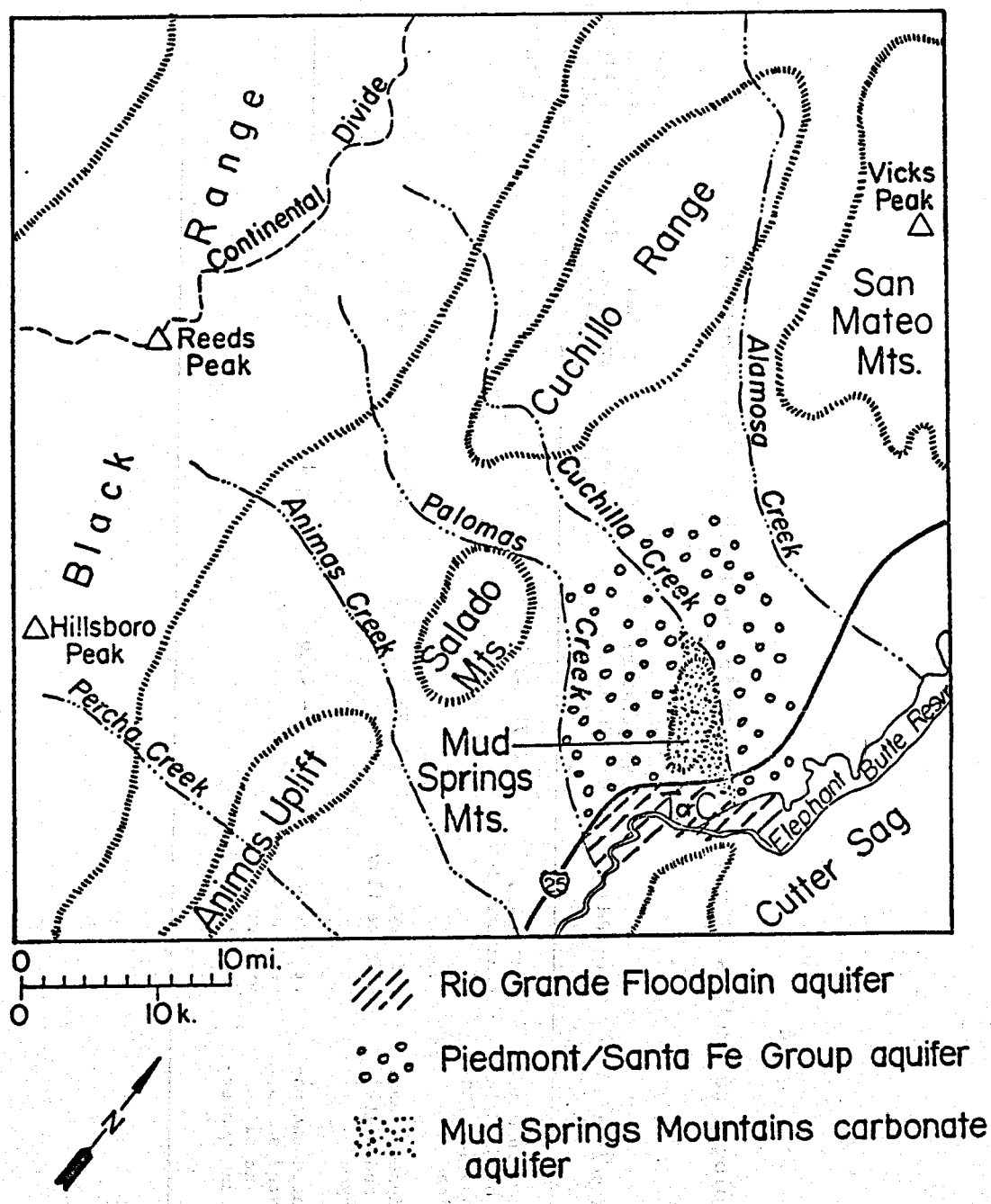

Figure 3-2. Generalized map of major Rio Grande Valley aquifers near Truth or Consequences, New Mexico.

Table 3-1. Hydrogeologic parameters of major aquifers in the Truth or Consequences area.

Aquifer	Rock Type/Age	Permeability	Temperature Range (°C)	Hydraulic Gradient (m/km)	Mean Transmissivity (m^2/s)	Mean Storage Coefficient (dimensionless)	Specific Well Capacity (l/s/m)
Mud Springs Mountain carbonate aquifer	Carbonate with minor clastics of Magdalena Group/Pennsylvanian and Permian	Secondary, fracture flow	36.7 - 45.6	1.6*	6.5×10^{-2}	6.3×10^{-4}	3.9
Rio Grande floodplain aquifers	Unconsolidated sands, gravels, and silts/ Quaternary	Primary, diffuse flow	26.7	0.11	4.7×10^{-3}	3.5×10^{-2}	---
Piedmont/ Santa Fe Group aquifers	Consolidated and unconsolidated sands, gravels, and silts/ Tertiary and Quaternary	Primary and secondary, primarily diffuse flow	17.8 - 43.0	17 - 15	1.6×10^{-3}	----------	---

* inferred

Thermal groundwater is derived from the carbonate aquifers of the Mud Springs Mountains area. These carbonate aquifers are Pennsylvanian-Magdalena Group limestones and dolomites which extend along the dip slope of the Mud Springs Mountains eastward toward Truth or Consequences. Between the Mud Springs Mountains and the city of Truth or Consequences, portions of the carbonate aquifer are exposed as isolated bedrock highs within the Tertiary and Quaternary deposits. The temperature range for groundwater in the Mud Springs Mountains aquifer is 36.7°C (98°F) to 45.6°C (114°F); whereas, temperatures for groundwater in the other two aquifers of the Rio Grande Valley are typically less than 27°C (80°F). Some thermal water exists in the Rio Grande floodplain aquifer due to leakage of the thermal waters from the carbonate aquifer and the vertical movement of the water into the Quaternary alluvium (Theis et al. 1941).

A generalized contour map of the unconfined aquifers of the Rio Grande piedmont and floodplain is given in Figure 3-3. Detailed maps of the water table and potentiometric surface near the city of Truth or Consequences have been published previously (Theis et al. 1941). The flow direction for the Piedmont/Santa Fe Group aquifers is southeast toward the Rio Grande for aquifers on the western side of the Rio Grande. Hydraulic gradients of the aquifers are the steepest and range between 15 and 17 m/km (79 and 90 ft/mi). Flow directions of the Rio Grande floodplain aquifers parallel the channel and floodplain of the river. Hydraulic gradients for these riverine aquifers are the shallowest, approximately 0.11 m/km (0.6 ft/mi). Mean transmissivity for the piedmont and floodplain aquifers range between 1.5 and 5.0 X 10^{-3} m^2/s (1.6 and 5.4 X 10^{-2} ft^2/s). These transmissivities are much less than those for the Mud Springs Mountains carbonate aquifer (6.5 X 10^{-2} m^2/s; 7.0 X 10^{-1} ft^2/s). Higher transmissivities of the carbonate aquifer are due to the fracture, conduit-flow conditions in the limestones.

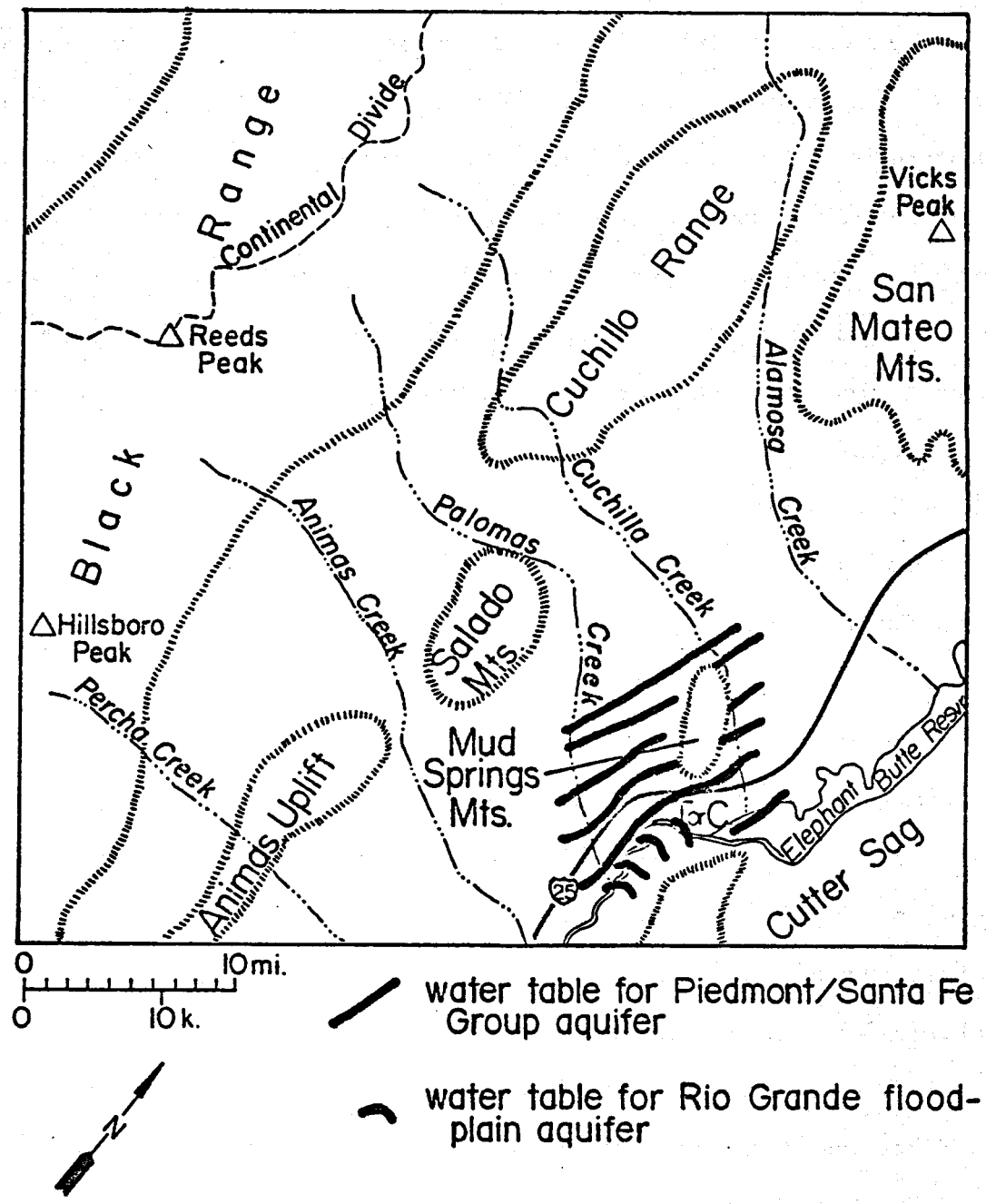

Figure 3-3. Generalized contour map of the water table in unconfined aquifers of piedmont and floodplain.

Permeability conditions for the piedmont and floodplain aquifers are characterized by diffuse flow (i.e., groundwater moving through pore spaces at seepage velocity). The Mud Springs Mountains carbonate aquifer has secondary permeability, or fracture flow (i.e., groundwater moving through integrated fractures and dissolution conduits). Large solutional openings are visible in the Magdalena Group carbonates. These solutional openings occur along the bedding (parallel to the strike) and occur along fractures with orientations of N7°W. These openings are common in the recharge and discharge area for the carbonate aquifer, and they are interpreted as one of the dominant recharge and discharge paths for the thermal water.

Mud Springs Mountains Carbonate Aquifer

The hydrologic properties of the Mud Springs Mountains carbonate aquifer were determined by Theis et al. (1941) (see Table 3-1). The thermal waters are restricted to integrated joints and bedding planes which have been enlarged by solutional activity. Thermal water also occurs in pore spaces of altered limestone and siliceous skeletal frameworks (Theis et al., 1941). High transmissivities and low coefficients of the Mud Springs Mountains aquifer storage are typical of most types of carbonate aquifers (see Table 3-1). These two hydrologic parameters are significantly different for peidmont and floodplain aquifers. The major conclusions drawn by Theis et al. (1941) during their hydrologic investigations of the carbonate aquifer are: (1) groundwater movement is directed along the strike of the Pennsylvanian limestones; (2) movement of groundwater occurs along planes and fractures; and (3) groundwater discharges from these openings by vertical movement from the carbonate aquifer into the overlying Quaternary alluvium of the Rio Grande floodplain.

The strike of the carbonate aquifers lithologies varies between N50°W and N60°W and is aligned with the Mud Springs Mountains. Thus, water moves parallel to the strike and from the Mud Spring Mountains. It is inferred that the Mud Springs Mountains and surrounding area represent the recharge area for the thermal, carbonate aquifer. Little hydrologic or geologic evidence suggests that thermal waters are derived from the piedmont or floodplain aquifers. Rather, groundwater moves down the hydraulic gradient, which is parallel to the Piedmont/Santa Fe Group hydraulic gradient, toward the city of Truth or Consequences. Recharge is supplied to the carbonate aquifer via infiltration of the Cuchillo Negro drainage and the alluvial aquifer of the Cuchillo Negro, as well as via leakage from the Piedmont/ Santa Fe Group aquifers.

Recharge from the Cuchillo Negro into the carbonate aquifer is visible where the limestones are traversed by the stream. Large solutional openings permit the rapid infiltration of surface waters into the aquifer. The Cuchillo Negro drainage is presently ephemeral; however, during the Pleistocene, larger discharges were typical of the stream. It is postulated that recharge of the carbonate aquifer was most effective during the more moist Pleistocene times. A generalized flow chart in Figure 3-4 illustrates the flow patterns for the Mud Springs Mountains carbonate aquifer. The hydraulic gradient of the thermal aquifer is determined by measuring the change of elevation between the recharge and discharge areas and dividing this value by the distance between these two areas. This inferred gradient is approximately 1.6 m/km (8.5 ft/mi).

A discharge of the thermal waters at Truth or Consequences has been measured by Theis et al. (1941) and is 0.099 m^3/s (3.5 cfs). This information is used in conjunction with other hydrologic data to determine the aquifer

FLOW CHART OF HYDROGEOLOGIC THERMAL FLOW SYSTEM

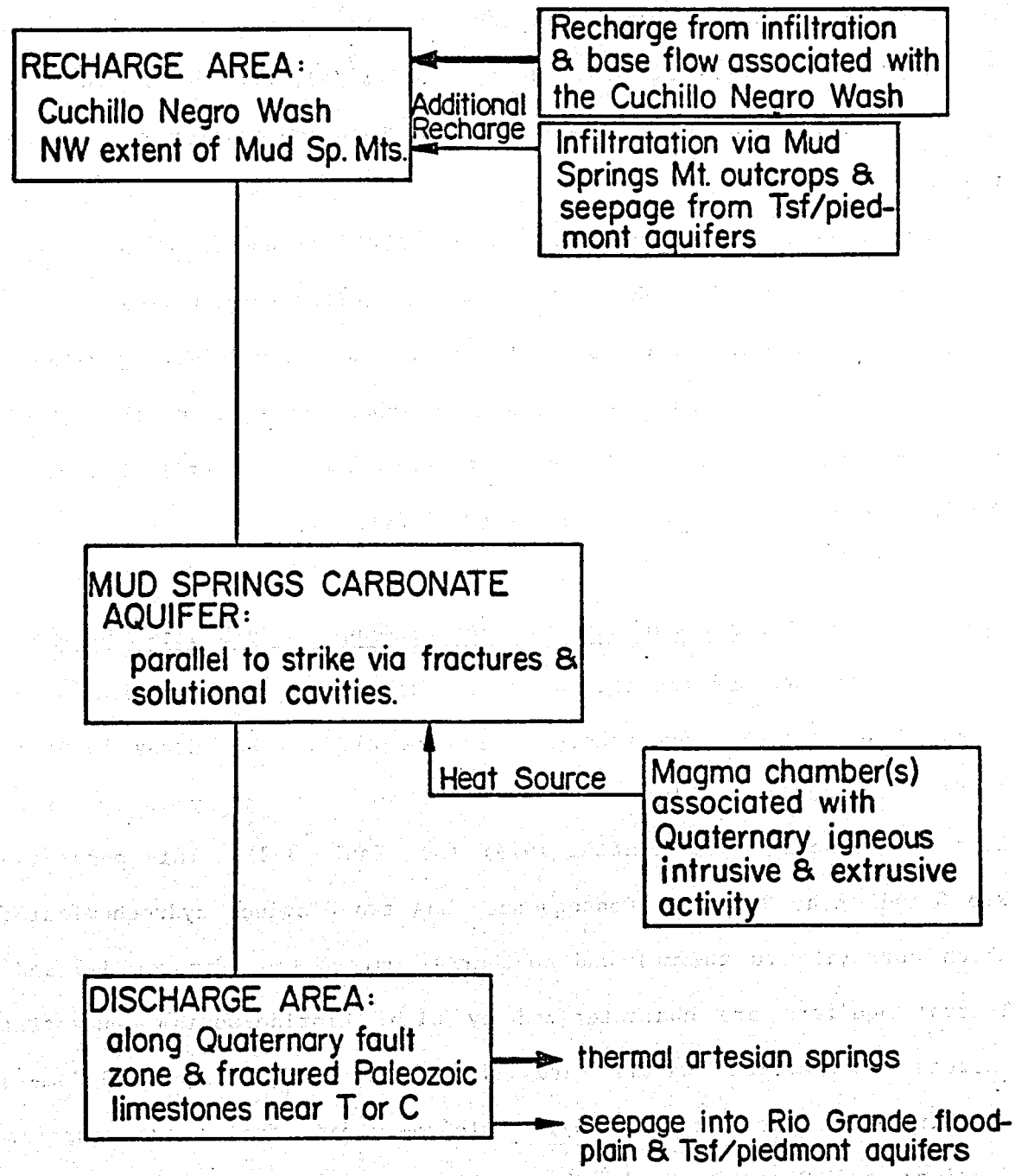

Figure 3-4. Generalized flow chart of the thermal hydrogeologic system of the Mud Springs carbonate aquifer.

width

$$w = Q/\bar{T}i \ ,$$

where w = aquifer width, m; Q = discharge rate, m^3/s; $\bar{T}$ = mean transmissivity, m^2/s; and i = hydraulic gradient, m/m. If a discharge of 0.1 m^3/s (3.5 cfs), a mean transmissivity of 0.065 m^2/s, (0.7 ft^2/s), and the average hydraulic gradient of 1.6 m/km (8.5 ft/mi) are used, then the aquifer width becomes 962 m (3154 ft).

An average aquifer width of 960 m (3150 ft) appears to be a reasonable estimate based on field observations where aquifer widths were determined to range from 800 to 1000 m (2625 to 3281 ft). Thus, the following values appear to be reasonable estimates of the carbonate aquifer characteristics: discharge, 0.1 m^3/s (3.5 cfs); gradient, 1.6 m/km (8.5 ft/mi); transmissivity, 0.065 m^2/s (0.7 ft^2/s); width, 960 m (3150 ft).

Chemical Characteristics of the Mud Springs Mountain Carbonate Aquifer

The chemistry of the thermal waters near Truth or Consequences has been analyzed by several researchers (Theis et al. 1941); Murray 1959; Summers 1965). In addition, data were gathered and were analyzed by Landis and Logsdon (personal communication 1979) (see Table 3-2). This portion of the Rio Grande near Truth or Consequences has two distinct hydrochemical facies which correlate to thermal and nonthermal waters (see Figures 3-5 and 3-6). Thermal aquifers are characterized by high chloride-sodium concentrations; whereas, nonthermal waters are characterized by high calcium-sulfate concentrations (see Figure 3-5). Calcium-sulfate facies are restricted to Tertiary and Quaternary clastic aquifers, and chloride-sodium facies are restricted to the thermal, Pennsylvanian carbonate aquifers.

Table 3-2. Chemistry (in ppm) of selected well, spring, and river water near Truth or Consequences, New Mexico (Logsdon 1979).

Element or Compound	Blackstone (B-9)	Sierra (3-10)	Spring (3-11)	Spring (3-12)	Well (3-15)	Yucca Spring (3-14)	River Water
Ca	143.9	143.9	136.5	110.4	49.5	164.1	15
Mg	18.0	17.9	17.1	9.5	4.5	18.7	4.1
Na	817.5	791.5	764.6	387.4	78.4	785.6	6
K	61.4	63.0	62.6	21.5	3.9	62.6	2.3
CO_3	0	0	0	0	0	0	
HCO_3	164.7	162.3	136.7	211.1	175.7	224.5	58.4
Cl	1285.2	1353.6	1370.3	602.7	80.5	1314.2	7.8
SO_4	196.0	169.1	115.3	138.3	67.2	107.0	11.2
Fe	0.38	< 0.10	< 0.10	< 0.10	0.12	< 0.10	0.50
F	1.49	3.10	3.10	2.46	1.73	3.20	0.10
B	0.38	0.35	0.35	0.20	0.08	0.38	0.012
P	0.01	0.01	0.01	0.05	0.01	0.01	0.020
SiO_2	44.3	44.3	44.3	37.3	32.1	31.3	13.1
NO_3+NO_2	2.12	1.88	2.01	11.14		1.40	1
Pb	0.202	0.200	0.105	0.623		0.257	0.004
Se	0.018	0.017	0.015	0.009		0.029	0.0002
Sr	4.10	4.12	4.19	2.21		4.08	0.060
Zn	0.05	0.07	0.09	0.12		0.10	0.030
Hg	0.0009	0.0003	0.0004	0.0005		0.0005	0.0005
H_2S	< 0.1	< 0.1	< 0.1	< 0.1		< 0.1	
Li	1.21	1.23	1.24	0.42		1.20	0.002
NH_4	0	0	2.01	1.84		0	
As	0.020	0.019	0.018	0.013		0.039	0.002
Br	0.77	0.77	0.75	0.78		0.82	0.020

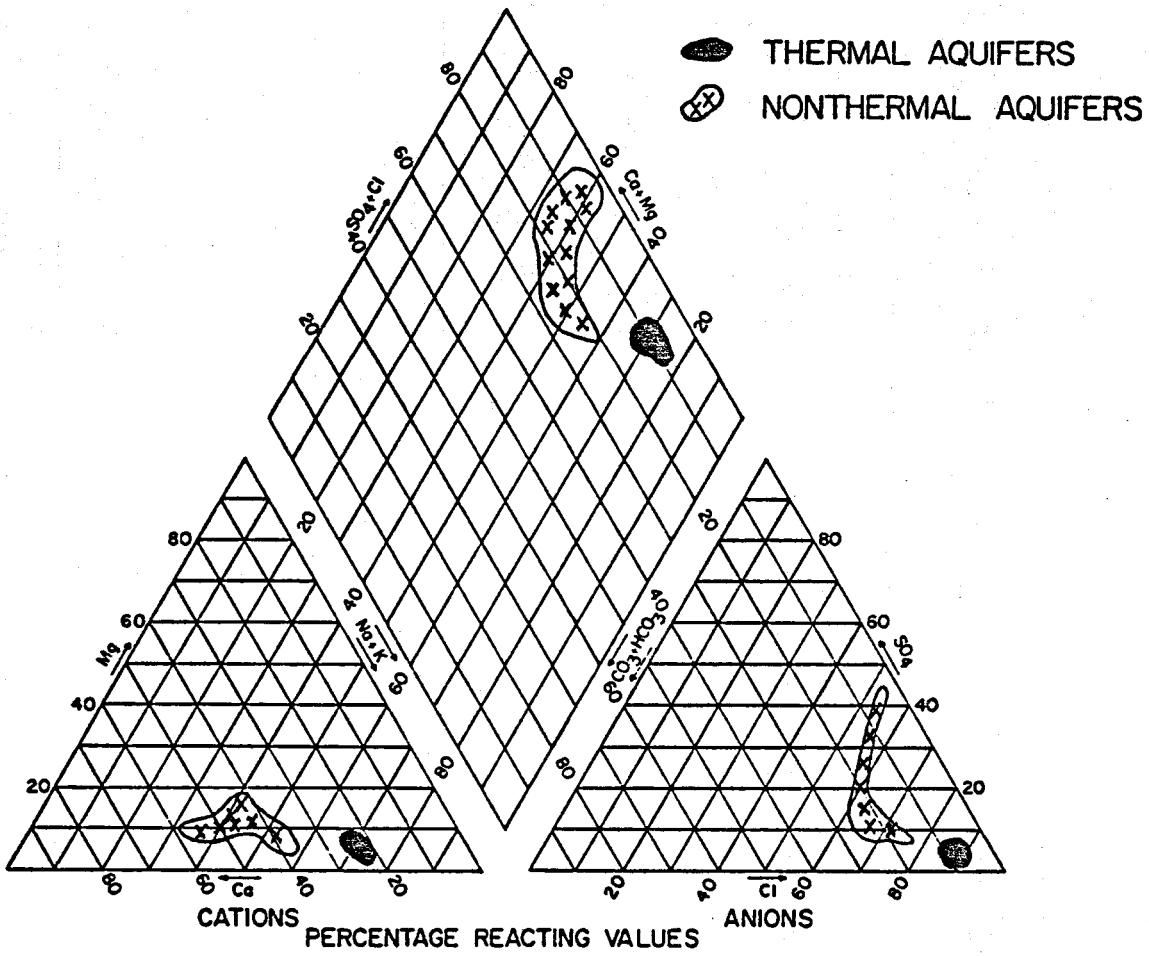

Figure 3-5. Major cation and anion classification of thermal and nonthermal waters.

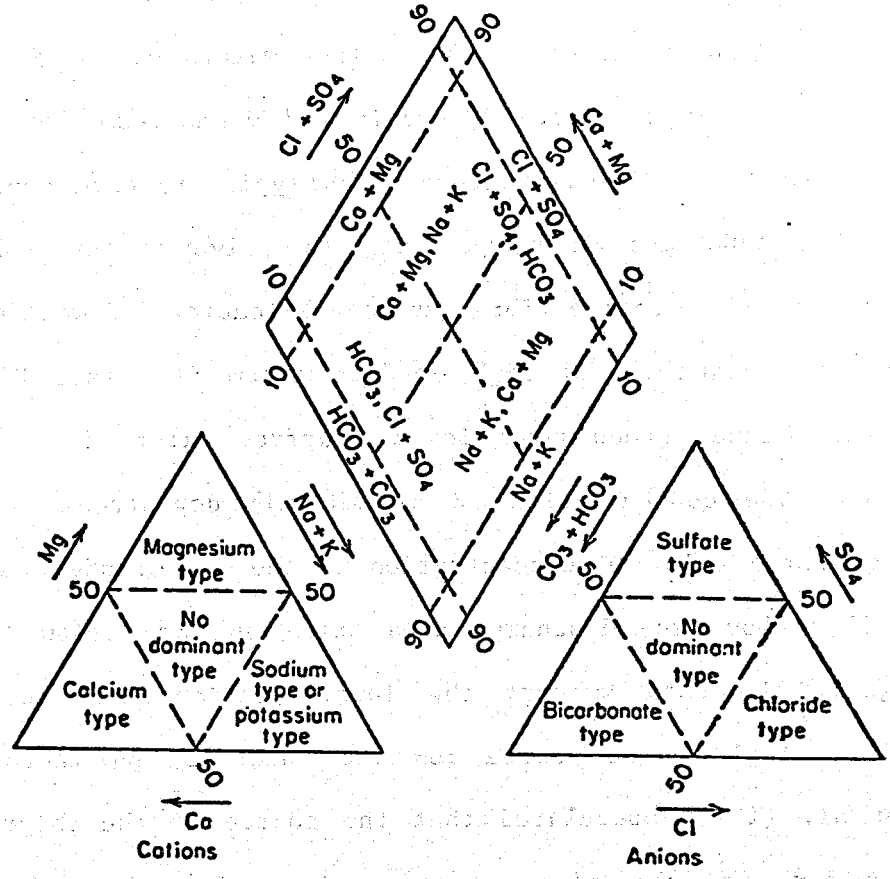

Figure 3-6. Hydrochemical facies-classification diagram for groundwater systems.

Previous researchers have noted the distinct difference in the chemistry between the thermal and nonthermal aquifers and have suggested restricted mixing of the aquifer waters. Higher than normal concentrations of chloride in the nonthermal waters result from leakage of the carbonate aquifer near Truth or Consequences. The data in Figures 3-7 and 3-8 indicate that the carbonate aquifer is the primary source of the high chloride concentrations. An increase in chloride is noted in the surface waters of the Rio Grande as one moves from the Elephant Butte Reservoir and downstream from the spring outlet (see Figure 3-7). Thermal waters which typically have concentrations between 1200 and 1300 ppm discharge into the river water and create a contaminate plume of chloride for several kilometers downstream. This phenomenon occurs regardless of high or low stream flow (see Figure 3-7). Dilution of the thermal groundwater in the surface water of the Rio Grande reduces the chloride concentration 32 km (20 mi) downstream. Figure 3-8 illustrates that the chloride concentration of the Rio Grande does not vary with stream flow above the discharge area but does vary below the thermal springs. Again, the data support the interpretation that the carbonate aquifer is the single point source for the chloride and thermal waters.

Theis et al. (1941) speculated that the source of the chloride in the carbonate aquifer is magnetic vapors mixing with deeply circulating groundwater and concluded that the chloride was not derived from leaching of a high chloride concentration parent material, instead the chloride source was deep-seated igneous activity. This hypothesis is based on the relationship between chloride concentration and temperature. If the source of chloride is magmatic vapors, then a correlation between the temperature of water and the chloride content should be observed. Figure 3-9 illustrates the relationship between these two variables for three thermal or warm springs in the vicinity

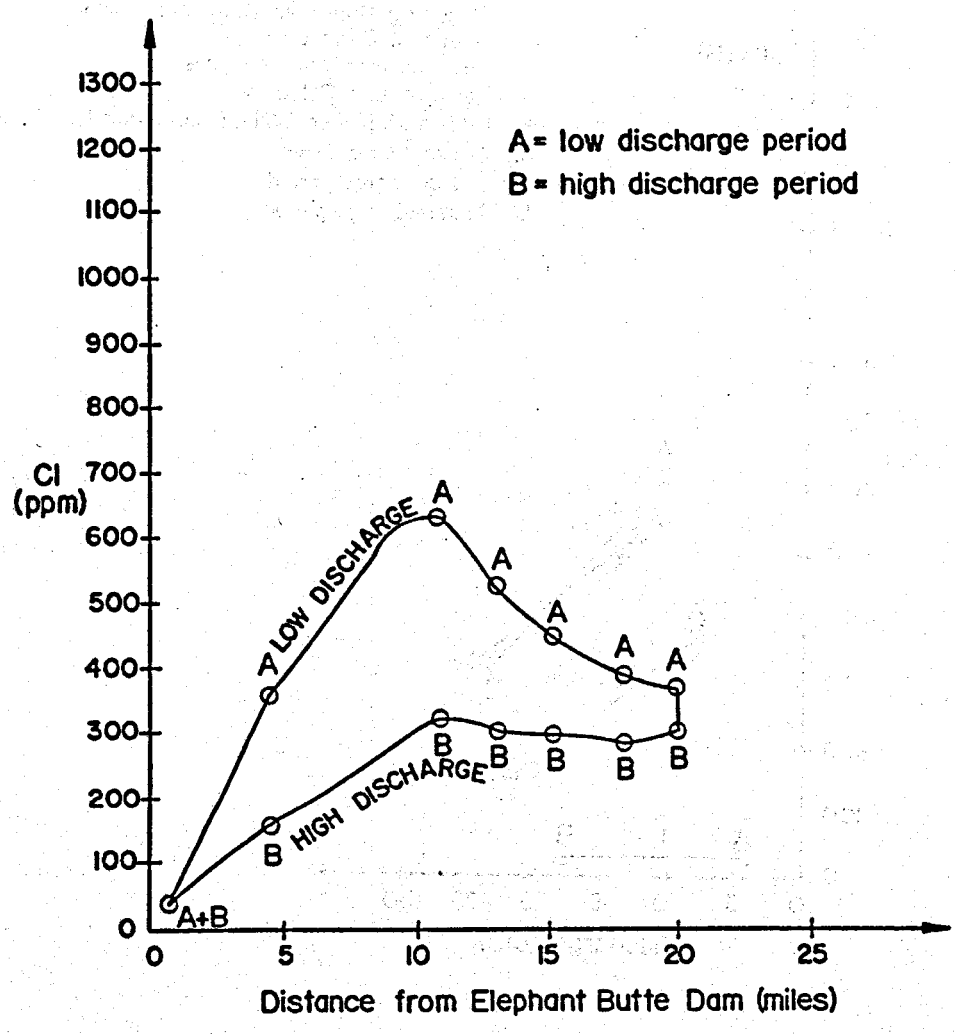

Figure 3-7. Relationship between chloride content and distance along the Rio Grande from Elephant Butte Dam.

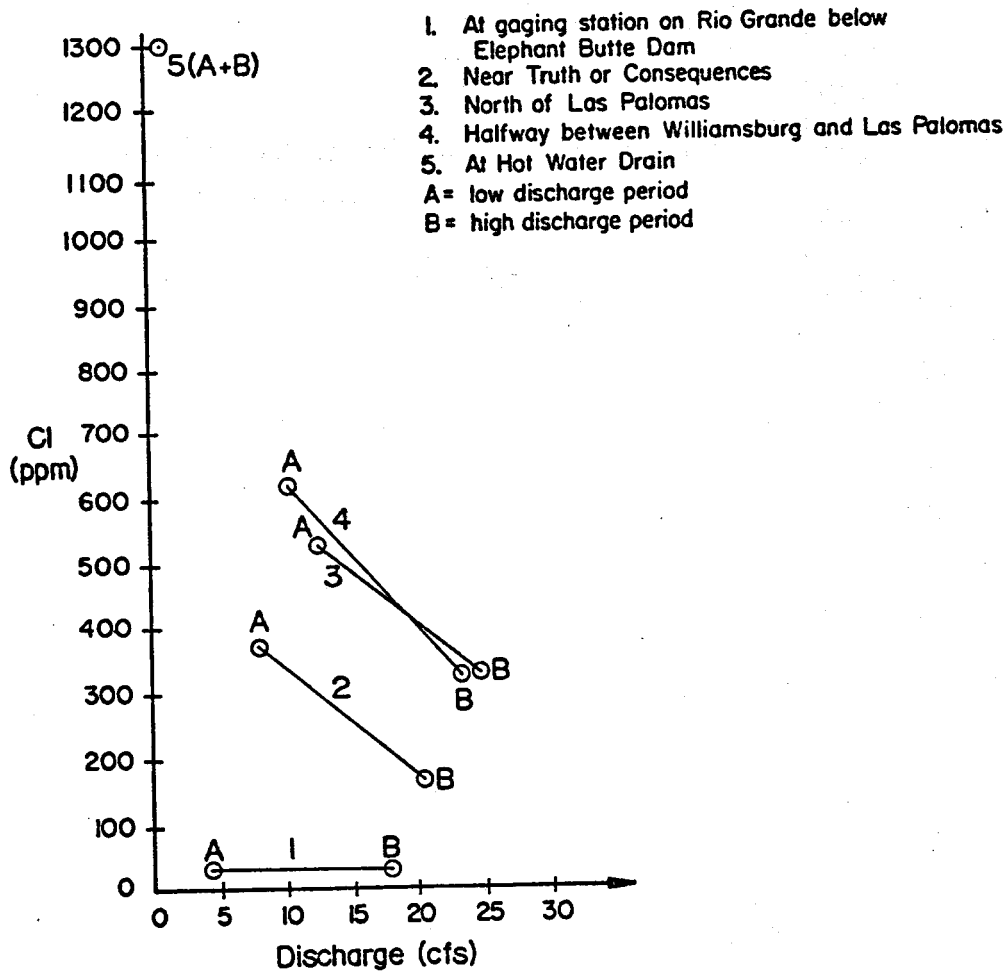

Figure 3-8. Relationship between chloride content and discharge of the Rio Grande below Elephant Butte Dam.

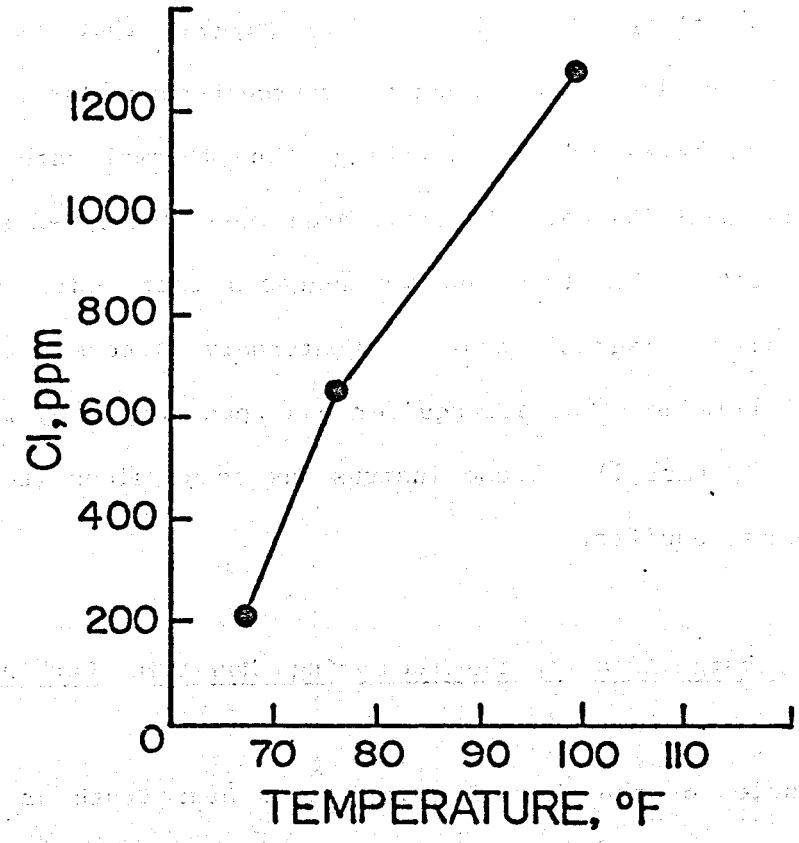

Figure 3-9. Comparison of temperature and chloride content of thermal springs and wells in the area near the Mud Springs Mountains.

of the Mud Springs Mountains. Such chloride-temperature plots are not conclusive evidence of magmatic sources either in the vapor or fluid phase.

Chemical studies on geothermal regions indicate high chloride concentrations in thermal waters result from leaching of parent rock or leaching of parent rock and additional contributions from fluid or vapor magmatic sources (Ellis and Mahon 1964; Ellis and Mahon 1967; White 1970; White 1974). High water/rock ratios (>2:1) suggest that some additional chloride content is supplied from a magmatic source because large rock volumes are required for extensive chloride leaching. The thermal carbonate aquifer of the Mud Springs Mountains covers a small area (see Figure 3-2); thus, a low rock volume associated with this aquifer suggests that additional chloride could be derived from a magmatic source. Quaternary igneous intrusions into the Mud Springs Mountains carbonate aquifer has been mapped by Zimmerman and Kudo (see Chapter 3, Part 1). These instrusions occur along the circulation path of the carbonate aquifer.

Geology of the Discharge Area for the Mud Springs Mountains Carbonate Aquifer

Previous studies of the thermal groundwaters near Truth or Consequences concluded that the thermal waters resurge from the Pennsylvanian-age carbonates along an east-west trending fault zone. The presence of this fault and other geologic structures of the discharge area for the thermal water is obscured by Quaternary and Tertiary sediments. Field investigations conducted during this study elucidated the local, late-Cenozoic geologic features and history of the discharge area and provided new information on the previously hypothesized discharge-area fault.

Results of the Cenozoic geologic mapping conducted during the present study are summarized on Figure 3-10. The major features mapped are:

(1) Quaternary alluvial units: Q_a, Q_{af}, Q_{fp}, and Q_f;

(2) Quaternary age geomorphic surfaces (soils and gravel veneers) truncating the Santa Fe Group units: Q_{s_1}, Q_{s_2}, Q_{s_3}, and Q_{s_4};

(3) Quaternary terraces along the Rio Grande: Q_{t_1} and Q_{t_2};

(4) Camp Rice Formation of the Santa Fe Group and its two major facies: T_{sf_1} and T_{sf_2}; and

(5) late Cenozoic faults.

The majority of the Quaternary alluvial units are either Holocene or very late Pleistocene in age. Surfaces developed on these deposits correlate in age to Fillmore and Leasburg age surfaces near Las Cruces (Hawley 1978). The Quaternary surfaces beveling the Santa Fe Group units range in age from late Pleistocene to mid Pleistocene based on correlations with dated surfaces near Las Cruces, New Mexico (Hawley 1978). Terraces along the Rio Grande are probably late Pleistocene. The major formation of the Santa Fe Group is that of the Camp Rice Formation. Both the piedmont facies (QT_{sf_1}) and the axial drainage facies (QT_{sf_2}) are present in the study area. The age of the Camp Rice Formation is late Pliocene-early Pleistocene. The Camp Rice Formation or its equivalent in this area is faulted. Two of the major Quaternary faults are illustrated on Figure 3-10 and include: (1) a fault directly south of the Mud Springs Mountains which is the easternmost extension of the Mud Springs fault zone; it is a near-vertical normal fault with the north block upthrown; and (2) the T or C fault which is the easternmost fault shown on the map; it is a reverse fault dipping towards the north.

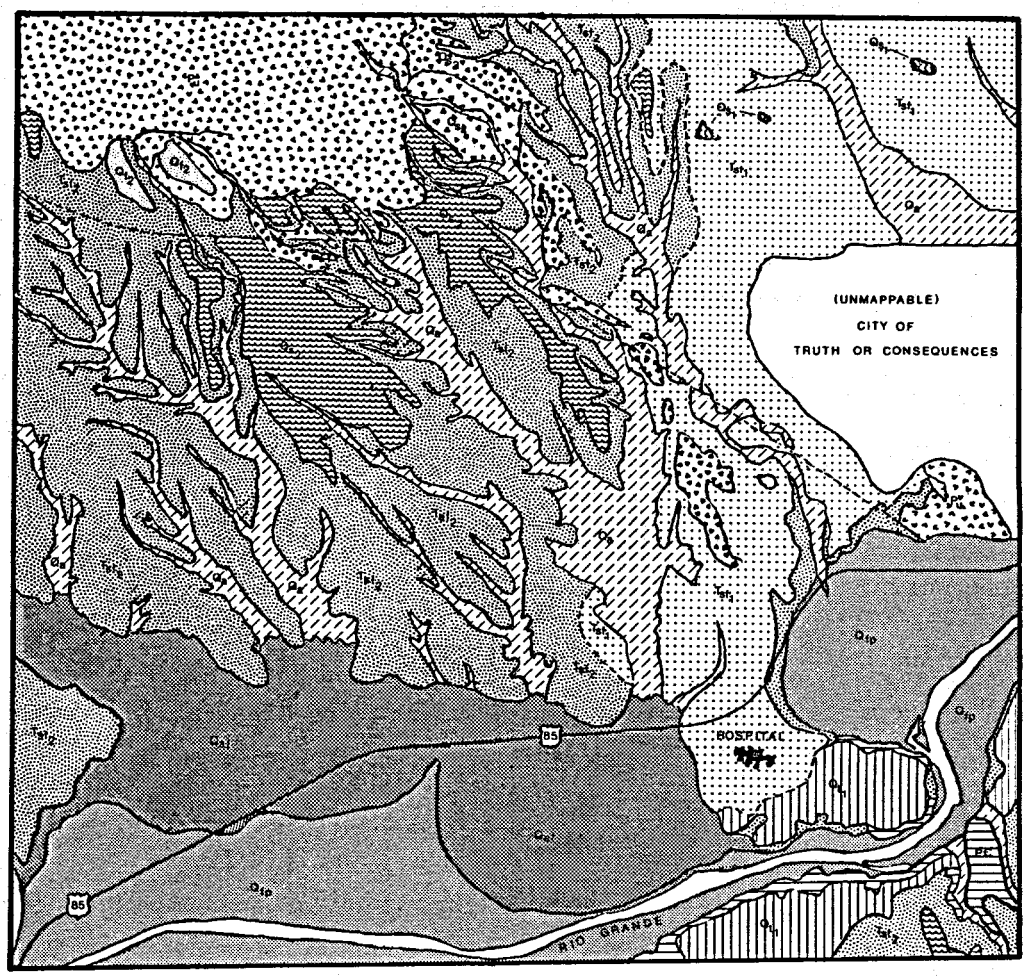

Figure 3-10. Cenozoic geology of the Truth or Consequences, New Mexico area. (See following page for legend.)

Lithologic Symbols

Q_a — Alluvium in active arroyos consisting of unconsolidated silts, sands and lenticular gravels; thickness undetermined.

Q_{af} — Alluvial fans developed on the Rio Grande floodplains consisting of uncemented clays, silts and fine-grained sands; poorly weathered, thickness undetermined.

Q_{fp} — Floodplain deposits of the Rio Grande composed of unconsolidated, fine-grained clays, silts and lenticular gravels; thickness undetermined.

Q_f — Alluvial fans developed at the base of the Mud Springs Mountains composed of indurated, well-cemented, angular to subangular limestone fragments. Medium-grained to 30 cm; minimum thickness is 18 meters.

Q_t — Terrace deposits formed along the Rio Grande consisting of unconsolidated, cemented and uncemented gravels and sands of varying lithologic composition including igneous, metamorphic and sedimentary fragments. Contains silt lenses; thickness varies from 2 to 8 meters. 1 = oldest terrace; 2 = youngest.

Q_s — Erosion surface gravels unconformably resting on Tsf, the erosion surface deposits contain caliche soil horizons developed on angular to subangular, medium- to course-grained limestone fragments; increasing $CaCO_3$ content and induration with age of surface; surface gravels typically 1 to 5 meters thick with the exception of Qs_4. 1 = oldest surface; 4 = youngest.

T_{sf} — Santa Fe Group: poor- to moderately-indurated, reddish to buff siltstone with interbedded gravels (unit 2); intertongued with a white, unconsolidated, subangular to subrounded, medium-grained sand, containing interbedded gravels (unit 1).

P_u — Undifferentiated Paleozoics consisting primarily of limestones and dolomites. Maximum thickness is 1120 meters.

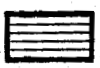

$P\epsilon$ — Granite and gneiss.

Structural Symbols

Strike-dip

Foliation

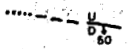

Fault (dashed where inferred; dotted where concealed)

Figure 3-10. (continued).

Structural Control of the Thermal Springs

Several detailed geologic maps of the Mud Springs Mountain carbonate aquifer discharge area have been published (see Figure 3-11). Varied interpretations have resulted from poorly exposed lithologies; however, all previous interpretations agree on three points: (1) the inferred presence of a northwest-southeast trending normal fault between the Paleozoic outcrops in Truth or Consequences and the Precambrain outcrops near Carrie Tingley Hospital; (2) the presence of a north-south trending zone of normal faults between the base of the Sierra Caballo Mountains and the city of Truth or Consequences; and (3) the presence of overturned Paleozoic lithologies forming a series of ridges from Truth or Consequences to the eastern edge of the Mud Springs Mountains.

Summers (1976) discussed the inferred fault south of Truth or Consequences and questioned whether it could be an extension of the Mud Springs fault zone if the fault existed at all. During the current field investigation, this previously inferred fault was located in an exposure along an arroyo wall in the city of Truth or Consequences. Recent gully erosion over the past few years exposed the fault zone which is the T or C fault referred to earlier in this section. The fault is reverse and not normal as previous researchers had speculated. The orientation of the fault is N60°W, and it dips 59° to the north (Figures 3-12 and 3-13). Movement on the fault appears to be episodic in that Pennsylvanian carbonates are faulted against the Camp Rice Formation, and the beds within the Camp Rice Formation have been offset. Additional evidence for reverse motion along this fault zone is visible in displaced chert lenses in the Magdalena Group carbonates. Orientations on the small reverse faults displacing the chert lenses average about N55°W and 66° to the north. These orientations are very similar to the

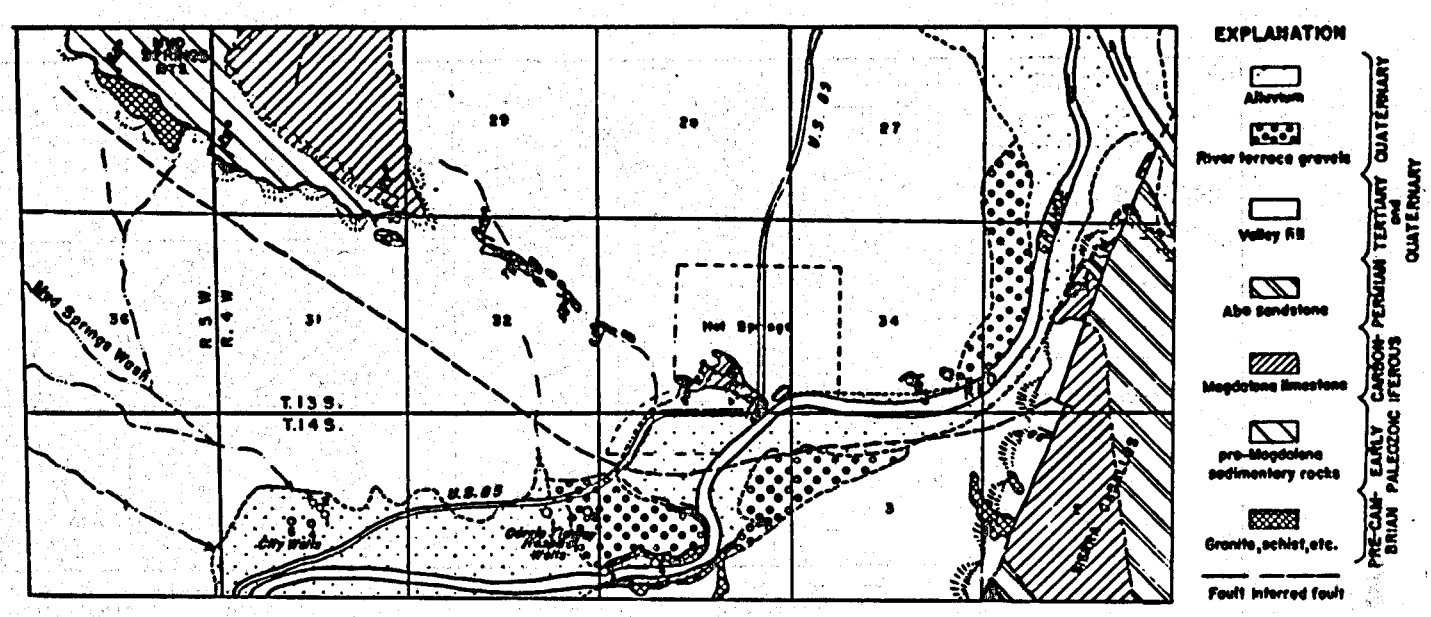

Figure 3-11. Map showing the geology in the vicinity of Truth or Consequences, Sierra County (Theis et al. 1941).

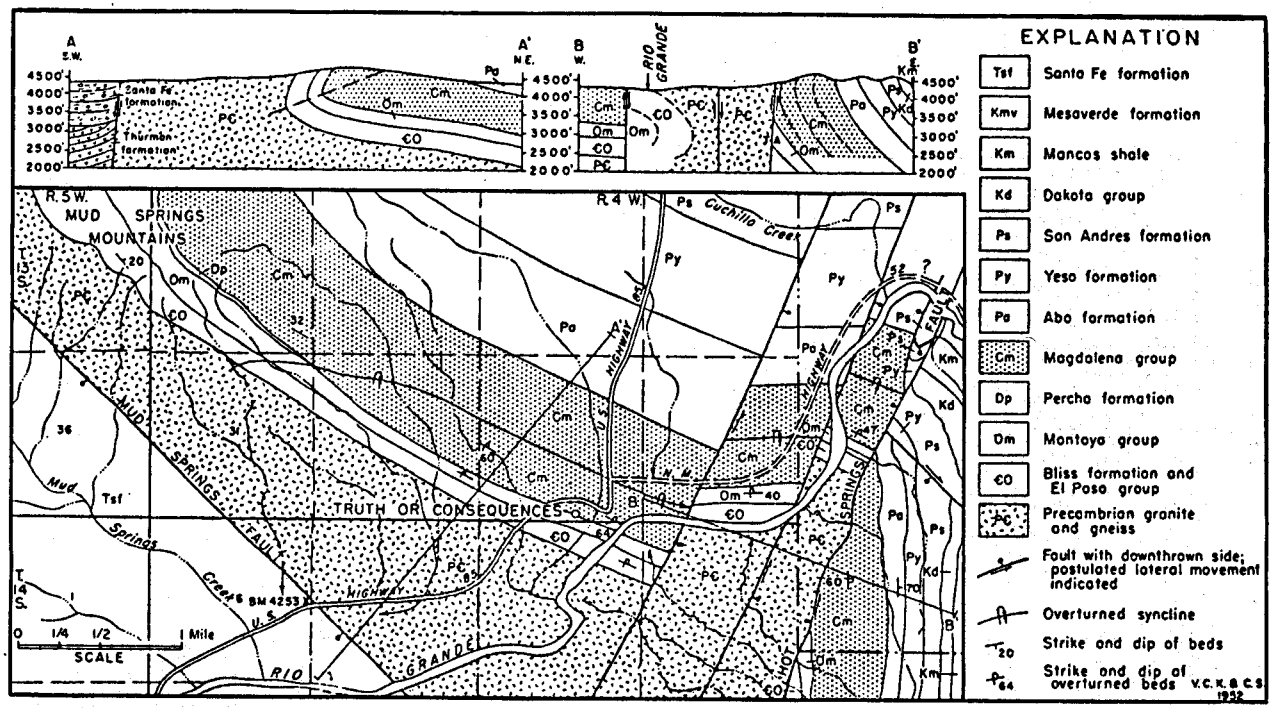

Figure 3-12. Geologic map and cross sections of the Truth or Consequences area with some of the Tertiary rocks removed (Kelly and Silver 1952).

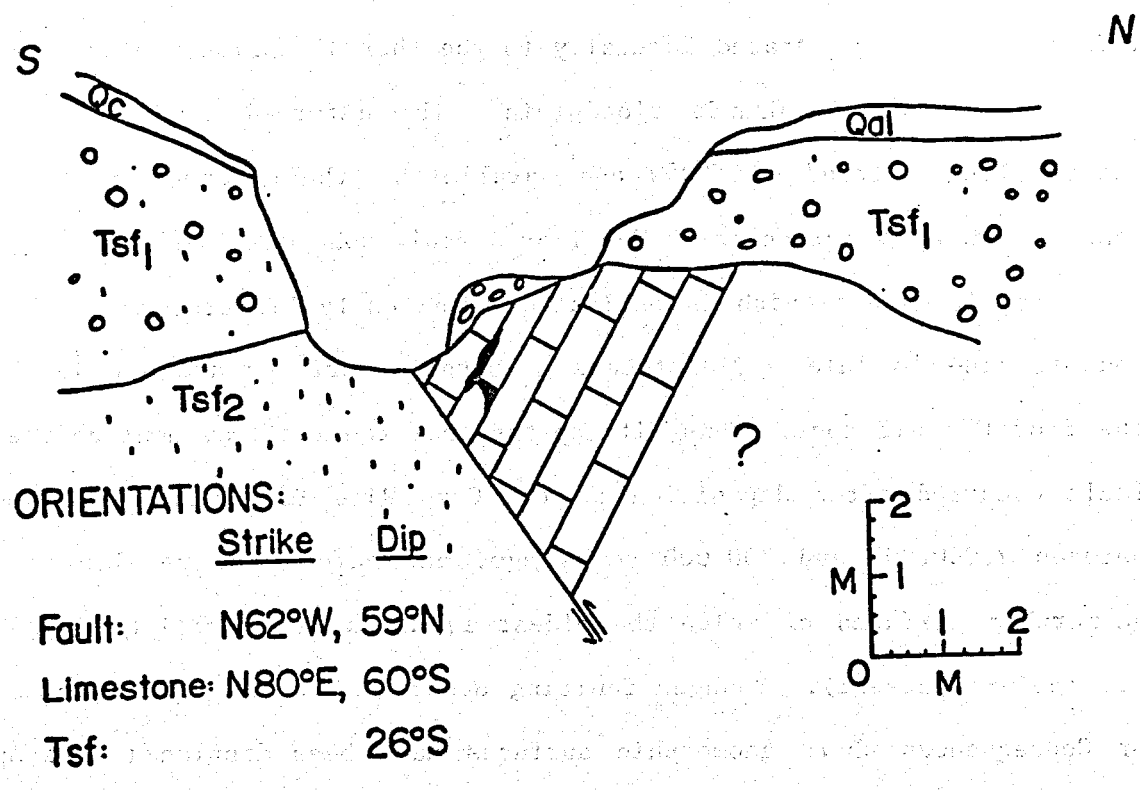

Figure 3-13. Schematic cross sections of the Truth or Consequences fault. The dark area in the limestones indicates solutional openings.

major fault zone mapped as the T or C fault. Reverse faults of this orientation and geographic position are not typical of the Rio Grande Rift but have been noted in the Taos-Picuris mountains area (Muehlberger 1979). Further studies are needed to understand the mechanics and dynamics of the T or C fault zone.

The significant aspect of the T or C fault zone is that it serves as the outlet for thermal waters in the Mud Springs Mountains carbonate aquifer. This fault zone was traced laterally to the thermal springs in the Quaternary alluvium of the Rio Grande floodplain. The deformed Camp Rice Formation occurs along a trend of N60°W and parallel to the outcrops of the faulted Pennsylvanian age carbonates. The T or C fault zone was found to displace the Camp Rice Formation which is estimated to be early Pleistocene in this area. Younger mid- to late - Pleistocene geomorphic surfaces are not displaced by the T or C fault zone. Thus, it appears that the last movement on the T or C fault occurred after deposition of the Camp Rice Formation, which occurred between 2,000,000 and 300,000 years ago, and before the development of the geomorphic surfaces of which the oldest is dated at 200,000 to 25,000 years B.P (before present). Younger faulting occurred 3 km (1.9 mi) west of Truth or Consequences where geomorphic surfaces have been displaced (see Appendix B). This east-west trending fault (part of the Mud Springs fault zone) has been dated by geomorphic techniques at 70,000 to 100,000 years B.P. (see Appendix B). It would appear from these studies that the Mud Springs fault zone is younger than, and therefore truncates, the T or C fault zone. Geomorphic evidence suggests that little faulting has occurred in the study area since movement on the Mud Springs fault zone during the mid to late Pleistocene.

It is concluded that the structure which controls the outlet of thermal groundwater was established by the mid Pleistocene. Uplift of the Mud Springs Mountains along the Mud Springs fault zone in the mid to late Pleistocene probably established the flow path along which the thermal waters presently migrate. The lateral migration of the thermal waters are retarded by another structure zone, the normal faults of the Hot Springs fault zone at the base of the Sierra Caballo Mountains. Precambrian igneous and metamorphic rocks are displaced against the carbonate aquifer. The Precambrian lithologies act as an aquitard; thus, the thermal waters in the carbonate aquifer mound at the intersection of the T or C fault zone and the Hot Springs fault zone. This mound creates some of the artesian conditions and causes the carbonate aquifer to leak vertically into the Rio Grande floodplain aquifer.

Proposed Model for the Thermal Aquifer at Truth or Consequences

Figure 3-4 is a flow chart which qualitatively illustrates the thermal hydrogeologic flow system of the Truth or Consequences area. The recharge area for the carbonate aquifer which supplies thermal waters to the Truth or Consequences area is the northwestern extension of the Mud Springs Mountains. In this area waters enter the aquifer via infiltration from the Cuchillo Negro wash and seepage from aquifers in the Piedmont/Santa Fe Group. Aquifer recharge was most effective during the more moist periods of the late Pleistocene when run-off in the Cuchillo Negro was higher. Groundwater travels through the Mud Springs Mountain carbonate aquifer (Pennsylvanian age Magdalena Group) probably to depths in excess of 700 m (2300 ft). The water travels along a strike through fractures and bedding planes and down the southwest-trending hydraulic gradient. Along this circulation path, heat is provided to the groundwater by Quaternary-age magmatic sources. Then these

thermal waters migrate vertically up fractures and bedding planes as the groundwater mounds near the intersection of two faults (i.e., T or C and Hot Springs faults). Seepage of the thermal waters from the carbonate aquifer into the Rio Grande floodplain aquifer ocurrs along a fault zone which formed around 200,000 to 300,000 years B.P. Thus, the fault zone along which the thermal springs discharge formed by the mid Pleistocene. The heat source for the thermal aquifer appears to be related to early Pleistocene igneous activity.

References

Borton, R. L., 1961, Geology and water resources of the Alamosa-Cuchillo Negro-Palomas Rivers area, Sierra and Socorro counties, New Mexico: New Mexico State Engineer's Office, Open-File Report.

Cox, E. R. and Reeder, H. D., 1962, Ground water conditions in the Rio Grande Valley between Truth or Consequences and Las Palomas, Sierra County, New Mexico: New Mexico State Engineer's Office, Technical Report 25.

Ellis, A. J. and Mahon, W. A. J., 1964, Natural hydrothermal systems and experimental hot-water/rock interactions: Geochimica Cosmochimica Acta, v. 28, p. 1323-1357.

Ellis, A. J. and Mahon, W. A. J., 1967, Natural hydrothermal systems and experimental hot-water/rock interactions (part II): Geochimica Cosmochimica Acta, v. 31, p. 519-538.

Hawley, J. W., ed., 1978, Guidebook to Rio Grande Rift in New Mexico and Colorado: New Mexico Bureau of Mines and Mineral Resources, Circular 163, p. 241.

Kelley, V. C. and Silver, C., 1952, Geology of the Caballo Mountains with special reference to regional stratigraphy and structure and to mineral resources, including gas and oil: University of New Mexico, Geology Publication 4.

Landis, G. and Logsdon, M., 1979, Personal communication, University of New Mexico, Albuquerque, New Mexico.

Muehlburger, W. R., 1979, The Embudo fault between Pilar and Arroyo Hondo, New Mexico, an active intracontinental transform fault, in 13th Field Conference Guidebook: New Mexico Geological Society, p. 77-82.

Murray, C. R., 1959, Ground water conditions in the nonthermal artesian water basin south of Hot Springs, Sierra County New Mexico: New Mexico State Engineer's Office, Report 10.

Summers, W. K., 1965, A preliminary report on New Mexico's geothermal energy resources: New Mexico Bureau of Mines and Mineral Resources, Circular 80.

Theis, C. V., Taylor, G. C., Jr., and Murray, C. R., 1941, Thermal waters of the Hot Springs artesian basin, Sierra County, New Mexico: New Mexico State Engineer's Office, 14-15th Biennial Report.

Wallace, R. E., 1977, Profiles and ages of young fault scarps, north-central Nevada: Geological Society of America, Bulletin, v. 88, p. 1267-1281.

Wallace, R. E., 1978, Geometry and rates of change of fault-generated range fronts, north-central Nevada: U.S. Geological Survey, Journal of Research, v. 6, p. 637-649.

White, D. E., 1970, Geochemistry applied to the discovery, evaluation, and exploitation of geothermal energy resources: United Nations Symposium on the Development and Utilization of Geothermal Resources, Pisa, Proceedings, Geothermics Special Issue 2, v. 1, p. 58-80.

White, D. E., 1974, Diverse origins of hydrothermal ore fluids: Economics of Geology, v. 69, p. 954-973.

Appendix A

Temperature Measurements in Water Wells near Truth or Consequences, New Mexico

Table 3A-1. Temperatures in water wells near Truth or Consequences, New Mexico.

Well # 1 Date August 7, 1979

Location 12.5.27.344 Owner M. Foster

Elevation 4720 ft Well Depth 35 m Depth to water 9 m

Case type metal Case diameter 6 inch

Remarks case extends to bottom of well.

Depth (m)	Water or Air	Temperature (^{o} C)	Depth (m)	Water or Air	Temperature (^{o} C)
9	w	21.03			
10	w	20.88			
11	w	20.86			
12	w	20.87			
13	w	20.87			
14	w	20.88			
15	w	20.92			
16	w	20.98			
17	w	21.05			
18	w	21.10			
19	w	21.15			
20	w	21.21			
21	w	21.28			
22	w	21.35			
23	w	21.42			
24	w	21.49			
25	w	21.57			
26	w	21.68			
27	w	21.75			
28	w	21.81			
29	w	21.91			
30	w	21.95			
31	w	21.99			
32	w	22.05			
33	w	22.10			
34	w	22.15			
35	w	22.18			

Table 3A-1. (continued).

Well # 2 Date August 6, 1979

Location 13.4.28.114 Owner T.J. McNabb

Elevation 4445 Well Depth 45.4 m Depth to Water N/A

Case type metal Case Diameter 2 1/2 inch

Remarks Dry well. Owner states when well was in operation the water level was at 150 ft and the water was warm and contained iron.

Depth (m)	Water or Air	Temperature (° C) 30	1	2	3	4	5	6	7
4	a	31.45	30.89	30.11	29.15	28.28	27.27	26.59	25.87
5	a	23.16	22.74	23.36	22.00	21.73	21.46	21.22	20.99
6	a	20.12	19.99	19.90	19.81	19.70	19.62	19.56	19.49
7	a	19.38	19.32	19.39	19.25	19.21			
8	a	19.18	19.15	19.13	19.11	19.08			
9	a	19.08	19.08	19.08					
10	a	19.11	19.13	19.16	19.19	19.22	19.25	19.26	
11	a	19.29	19.33	19.38	19.42	19.45	19.37	19.49	
12	a	19.50	19.53	19.57	19.60	19.63	19.65	19.66	19.66
13	a	19.68	19.70	19.74	19.76	19.78	19.79	19.80	19.82
14	a	19.83	19.85	19.89	19.91	19.92	19.94	19.94	
15	a	19.96	19.97	20.03	20.04	20.05	20.05		
16	a	20.07	20.08	20.11	20.12	20.13			
17	a	20.15	20.17	20.19	20.20	20.21			
18	a	20.23	20.25	20.27	20.29	20.31			
19	a	20.34	20.36	20.38	20.39	20.40			
20	a	20.40	20.44	20.46	20.48	20.49	20.50	20.50	
21	a	20.40	20.44	20.46	20.48	20.49	20.50	20.50	
22	a	20.51	20.53	20.54	20.56	20.56			
22	a	20.59	20.60	20.61	20.62	20.64	20.64		
23	a	20.67	20.68	20.71	20.72	20.74	20.75	20.76	20.76
24	a	20.77	20.79	20.82	20.83	20.84			
25	a	20.86	20.88	20.90	20.91	20.92			
26	a	20.93	20.93	20.94	20.95	20.95			
27	a	20.96	20.97	20.98	20.99	21.00	21.00		
28	a	21.01	21.02	21.03	21.04	21.04			
29	a	21.04	21.06	21.06					
30	a	21.08	21.08	21.09	21.09				

Table 3A-1. (continued).

Well # 2 (cont.) Date _____

Location _____ Owner _____

Elevation _____ Well Depth _____ Depth to Water _____

Case type _____ Case Diameter _____

Remarks _____

Depth (m)	Water or Air	Temperature (° C) 30	1	2	3	4	5	6	7
31	a	21.10	21.11	21.12	21.13	21.13			
32	a	21.14	21.15	21.16	21.17	21.17			
33	a	21.18	21.19	21.20	21.21	21.21			
34	a	21.22	21.23	21.23	21.23				
35	a	21.24	21.25	21.26	21.26				
36	a	21.27	21.28	21.28	21.28				
37	a	21.30	21.32	21.33	21.33				
38	a	21.34	21.35	21.36	21.36				
39	a	21.37	21.38	21.39	21.40				
40	a	21.41	21.42	21.43	21.44	21.44			
41	a	21.45	21.46	21.46	21.46				
42	a	21.48	21.50	21.50	21.50				
43	a	21.51	21.53	21.53	21.53				
44	a	21.54	21.55	21.56	21.56				
45	a	21.57	21.58	21.59	21.60				
45.4	a	21.61	21.62	21.63	21.63				

Table 3A-1. (continued).

Well # 3 Date August 7, 1979

Location 14.4.33.344 Owner City of Truth or Conseq.

Elevation 4240 Well Depth 18.4 m Depth to Water 0.6 m

Case type metal Case Diameter 12 inch

Remarks Located inside City Civic Center. Water temperature varies during testing possibly indicates movement of water.

Depth (m)	Water or Air	Temperature (° C) 30	1	2	3
5	w	38.52	38.70	38.61	38.61
6	w	39.00	39.00	39.05	39.01
7	w	39.32	39.25	39.29	39.33
8	w	39.47	39.44	39.50	39.50
9	w	39.54	39.76	39.77	39.67
10	w	40.36	40.44	40.48	40.50
11	w	40.69	40.84	40.79	40.75
12	w	41.10	41.10	41.21	41.23
13	w	41.39	41.37	41.52	41.56
14	w	41.55	41.55	41.55	41.55
15	w	41.55	41.55	41.55	41.55
16	w	41.55	41.55	41.55	41.55
17	w	41.55	41.55	41.55	41.55
18	w	41.55			
18.4	w	41.55			

Table 3A-1. (continued).

Well # 4 Date August 16, 1979

Location 14.4.4.124 Owner City of Truth or Con.

Elevation 4235 ft Well Depth 11.8 m Depth to water 2.8 m

Case type metal Case diameter 2 1/2 inch

Remarks Abandoned swimming pool well.

Depth (m)	Water or Air	Temperature (^{o} C)	Depth (m)	Water or Air	Temperature (^{o} C)
2.8	w	31.02			
3	w	31.21			
4	w	31.49			
5	w	31.94			
6	w	32.50			
7	w	33.09			
8	w	33.76			
9	w	34.27			
10	w	34.81			
11	w	35.19			
11.8	w	35.48			

Table 3A-1. (continued).

Well # 5 Date August 15, 1979

Location 13.4.22.333 Owner S. Wilson

Elevation 4360 ft Well Depth 32.5 m Depth to Water 31.7 m

Case type metal Case Diameter 2 1/2 inch

Remarks Located next to Webster residence. Butte City state well.

Depth (m)	Water or Air	Temperature (° C) 30	1	2	3	4	5	6	7
5	a	30.01	29.47	28.78	27.70	26.78	25.81	25.10	23.91
10	a	22.45	22.26	21.86	21.52	21.19	20.94	20.70	20.50
15	a	20.17	20.11	20.03	19.96	19.90	19.84	19.79	19.75
20	a	19.69	19.68	19.67	19.66	19.65	19.63	19.62	19.61
25	a	19.60	19.60	19.61	19.62	19.63	19.64	19.65	19.65
30	a	19.68	19.68	19.70	19.72	19.74	19.76	19.77	19.77
32.5	w	19.89	19.89	19.89					

Table 3A-1. (continued).

Well # 6 Date August 16, 1979

Location 13.4.34.414 Owner Guynn

Elevation 4325 ft Well Depth 28m Depth to Water 24 m

Case type metal Case Diameter 10 inch

Remarks Owner states well water contains too much iron for use.

Depth (m)	Water or Air	Temperature (° C) 30	1	2	3	4	5	6	7
5	a	26.14	26.08	25.81	25.10	24.77	24.43	24.08	23.81
10	a	23.19	23.06	22.82	22.58	22.41	22.26	22.09	21.94
15	a	21.69	21.65	21.59	21.52	21.46	21.41	21.37	21.31
20	a	21.25	21.26	21.28	21.28	21.28			
25	w	21.24	21.25	21.25	21.25				
26	w	21.25							
27	w	21.26							
28	w	21.26							

Appendix B

Fault Age Determination

Introduction

The east-west trending fault scarp located 3 km (1.8 mi) from Truth or Consequences, New Mexico, was analyzed for fault-age determinations by profile measurements. The profile methods developed by Wallace (1977, 1978) were used. Fault-scarp profiles and a geomorphic map were constructed from field measurements. Fault-scarp terminology is shown in Figure 3B-1 (Wallace 1977).

Procedures

Wallace (1977) developed the profile-measurement technique of dating fault scarps. In this study, the procedures outlined by Wallace (1977) were followed and two profiles dating the fault scarp west of Truth or Consequences, New Mexico, were measured (see Figure 3B-2). The profiles were then analyzed to determine the absolute age by the degree and length of crest roundness and the angle of the debris slope.

Results

The degree of roundness measure by the width of the crest was measured at 21 m and 23 m (69 ft and 75 ft). These values, when compared on Figure 3B-3, suggest the age of the fault to be between 70,000 and 100,000 years old. The absence of a well-defined debris slope, when compared to Figure 3B-4, also suggests a possible age range to be between 10,000 and 100,000 years old. The shallow angle of the scarp slope indicates that the age must be much older than 12,000 years. (Wallace 1977).

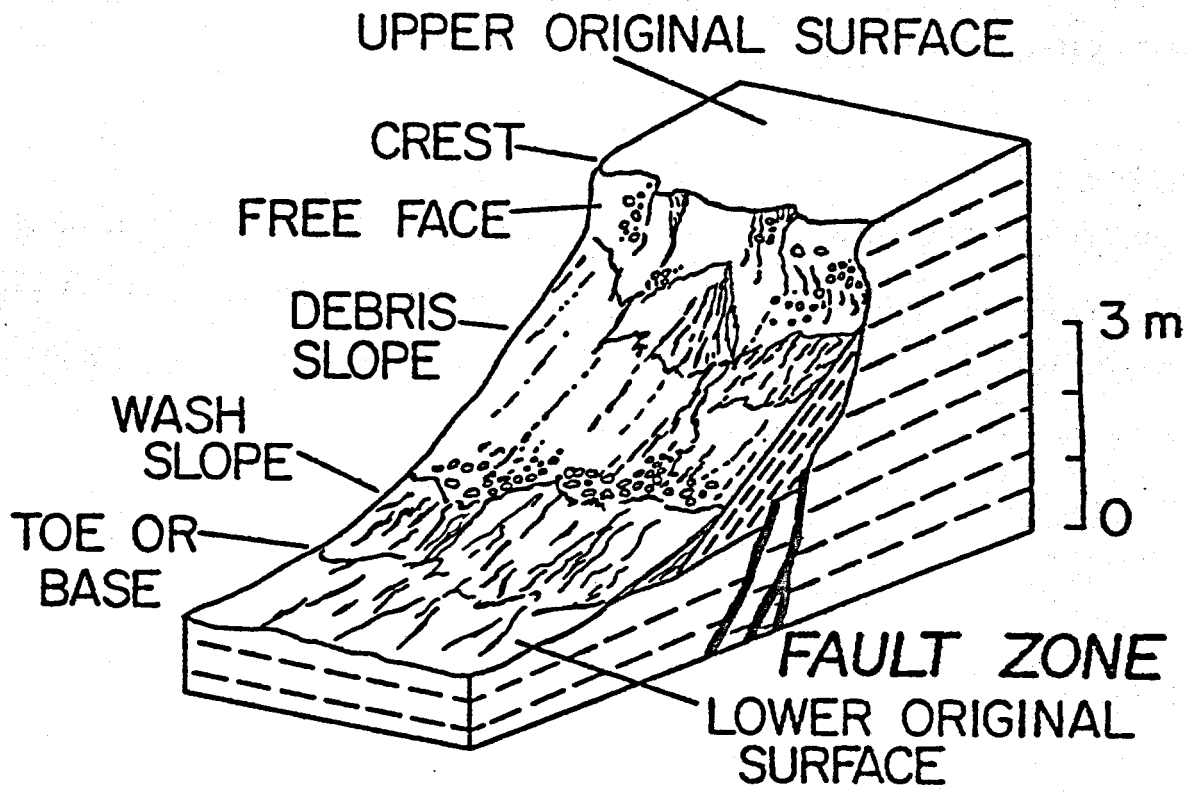

Figure 3B-1. Fault-scarp terminology.

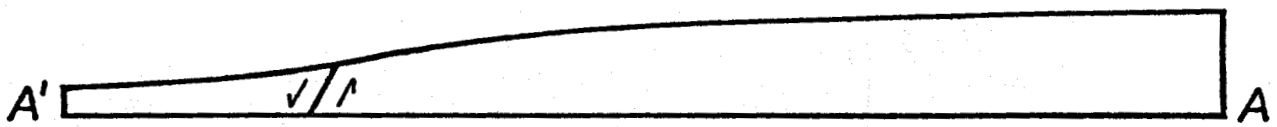

Width of crest 21 meters

Debris slope angle 6.8°

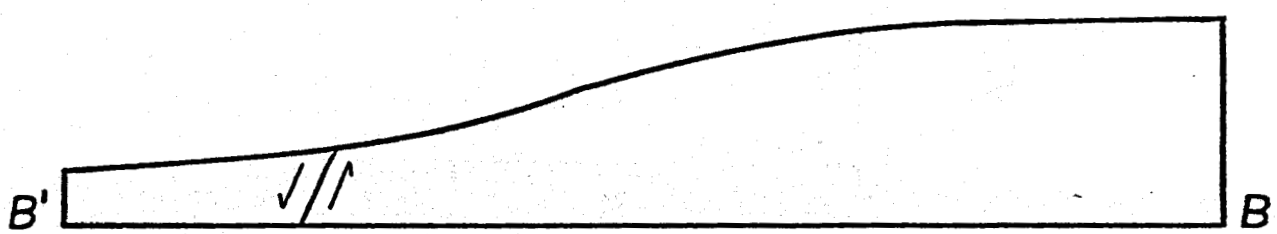

Width of crest 23 meters

Debris slope angle 12°

Figure 3B-2. Fault-scarp profiles near Truth or Consequences, New Mexico. Scale: 2.5 cm = 10 m.

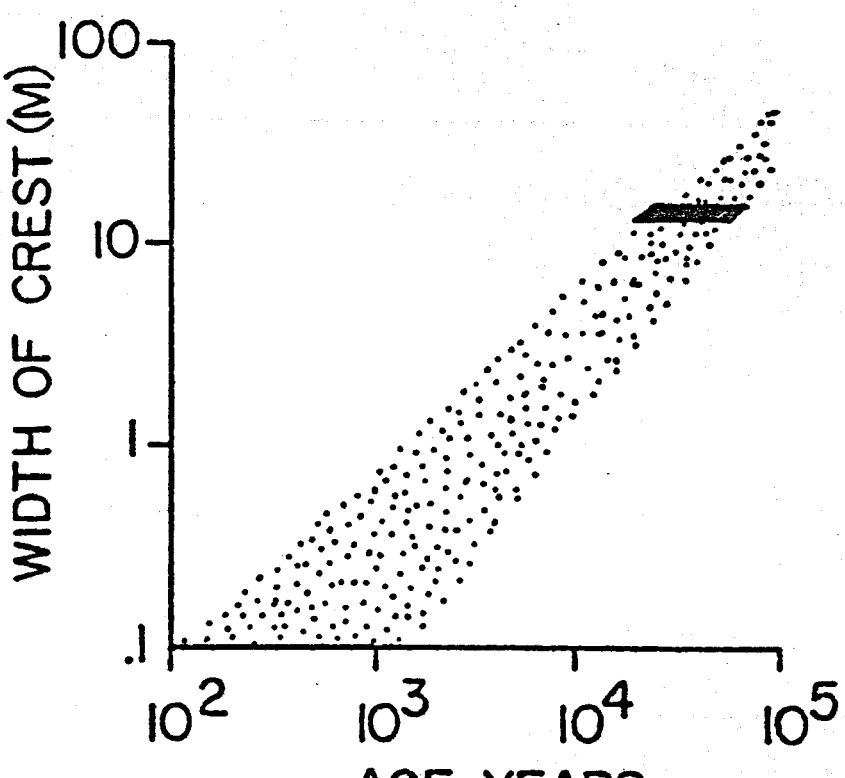

Figure 3B-3. Width of crest plotted against time in years. The darkened area represents T or C data (Wallace 1977).

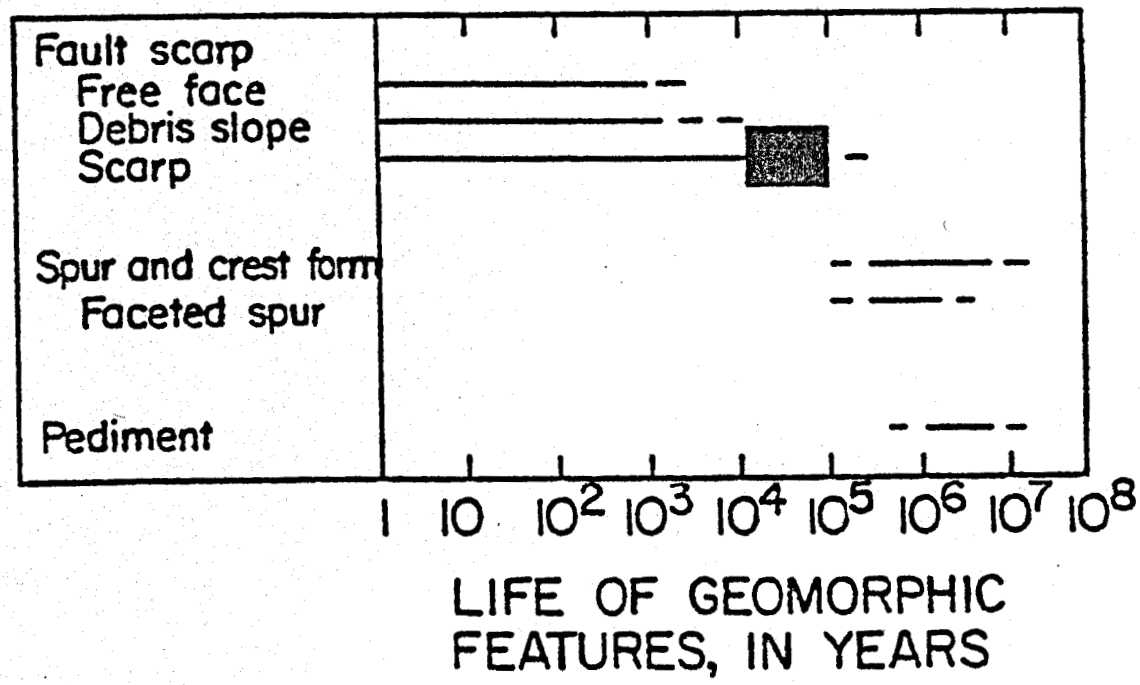

Figure 3B-4. Life of geomorphic features, in years. The darkened area represents T or C data (Wallace 1978).

Part 3

Electrical-Resistivity Investigation of the Geothermal Potential of the Truth or Consequences Area*

Introduction

In conjunction with geological and hydrogeological studies, an electrical-resistivity survey was carried out at Truth or Consequences, New Mexico, during the summer of 1979 by University of New Mexico researchers. The purpose of this project was to better define the characteristics of the geothermal occurrence via a careful examination of the electrical structure of the region. The value of electrical-resistivity investigations in geothermal evaluation has been established in several locations in New Mexico (Jiracek et al. 1976; Jiracek and Smith 1976; Hohmann and Jiracek 1979).

Tests were first performed to determine the geoelectric section west of Truth or Consequences, in the direction of inferred recharge of the thermal waters (Wells and Granzow 1980). Determination of the geoelectric section using Schlumberger soundings enabled the electrical identification of the thermal system flowing in the Mud Springs Mountains carbonate aquifer. This provided estimates of the depth, thickness, and porosity of this thermal aquifer at two locations.

Resistivity mapping of the city of Truth or Consequences and the immediate surroundings was accomplished during a second phase of the resistivity program. Such mapping has elucidated lateral resistivity boundaries such as basin margins and structural uplifts. Conductive

*The principal authors of Chapter 3, Part 3 are Dr. George R. Jiracek, Professor of Geological Sciences, University of New Mexico, and Maureen Mahoney, graduate student, Department of Geology, University of New Mexico.

regions mapped during this activity may be identified, in part, with the shallow alluvial aquifer into which the underlying carbonate aquifer discharges at Truth or Consequences. However, the geothermal component of this shallow aquifer cannot be uniquely separated from the nongeothermal clay or saline portions.

Resistivity Soundings

The first stage of the resistivity survey included three Schlumberger soundings at two locations (see Figure 3-14). The first sounding, S1-TC, was oriented 158° from true north, about 2 km (1.2 mi) east of the Mud Springs Mountains, and approximately parallel to the strike of the mountains. This sounding was expanded to a maximum half spacing (AB/2) of 1000 m (3280 ft). By combination with equatorial soundings (Zohdy 1970) in the directions of 68° and 248°, the effective electrode spacing was expanded to 5700 m (18,700 ft).

The soundings curve for S1-TC and the accompanying interpreted true-resistivity model are plotted in Figure 3-15. This eight-layer geoelectric section was obtained using the inversion program for a layered earth developed by Zohdy (1973). The S1-TC overlies inferred local geology that closely approximates a layered earth. The geologic section is comprised of Quaternary alluvium underlain by a sequence of Paleozoic sediments and Precambrian granites and gneisses. The consolidated sedimentary rocks dip gently to the northeast. The site is also well removed from any mapped faults (Wells and Granzow 1980).

The computed model correlates well with the known geology and hydrology. Water-table contours (Thesis et al. 1941) were used to estimate a depth to the water table of 30 m (98 ft). The model shows a break in resistivity from 730 ohm-m to 8 ohm-m at 33 m (108 ft). This 86-meter thick layer probably

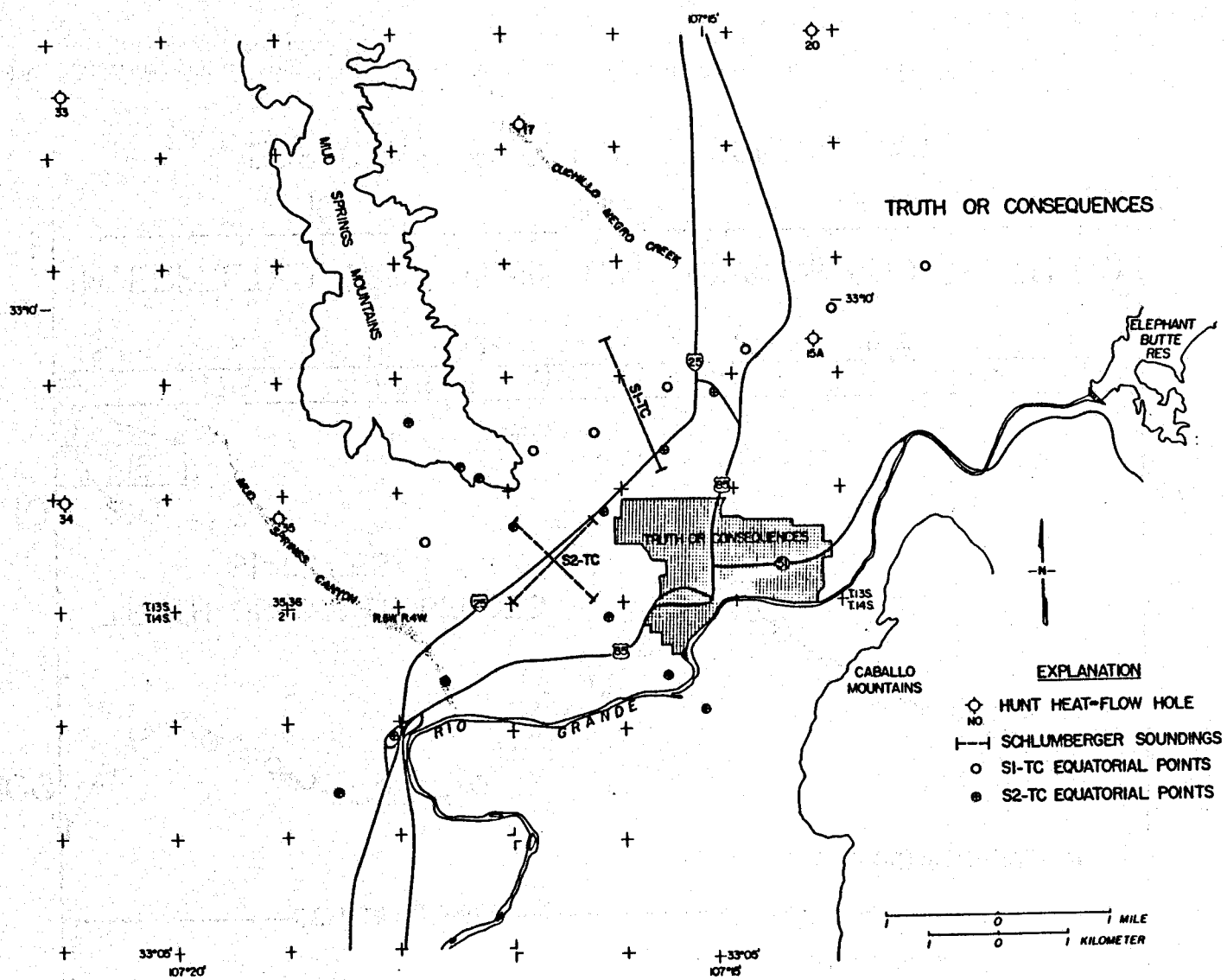

Figure 3-14. Truth or Consequences study area showing locations of Schlumberger soundings and equatorial points.

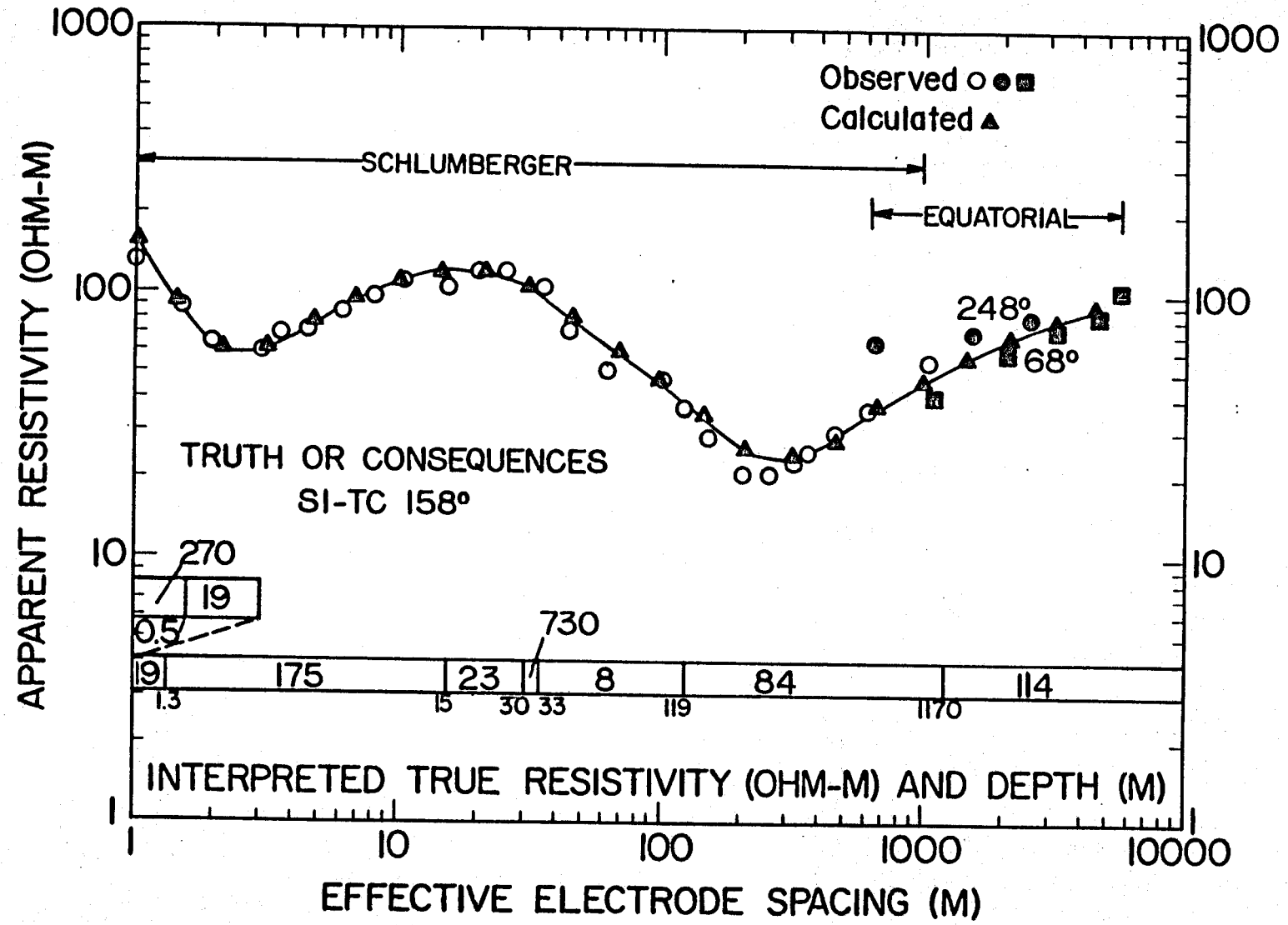

Figure 3-15. Schlumberger sounding SI-TC 158° at Truth or Consequences and the interpreted eight-layer model.

represents the piedmont aquifer into which the thermal carbonate aquifer discharges (Wells and Granzow 1980). Based on the chemistry and temperatures for the shallow thermal waters (Wells and Granzow 1980), an estimate of the porosity of this aquifer was computed using Archie's law (Meidav 1970). The calculation yielded a porosity around 30 percent, which is not unreasonable for an unconsolidated sediment at this depth.

A lithology log from a well near S1-TC records the depth to the top of the Pennsylvanian Madera Limestone as 133 m (436 ft) (Albright et al. 1955). This value is in agreement with the 119-m (390-ft) depth to the top of the 84 ohm-m layer in the geoelectric section. Thus, the well data supports the contention that this 1050-m (3445-ft) thick layer is the fractured, water-filled carbonate aquifer discussed by Wells and Granzow (1980) and Zimmerman and Kudo (1980).

Given a water temperature of about 45°C (113°F) and an equivalent NaCl composition of about 3085 ppm (calculated from the chemistry tabulated by Wells and Granzow (1980)), a porosity of about 14-percent was calculated using a variation of Archie's law suggested for well-cemented, fractured limestones (Keller and Frischknecht 1966). Normally, 14 percent porosity would be considered high for Paleozoic limestones; however, this formation exhibits extensive secondary porosity in the form of fractures and dissolution cavities, resulting in high permeability and porosity. The porosity estimate would decrease if a higher than 45°C (113°F) temperature at depth was assumed.

Finally, the model in Figure 3-15 defines a 114 ohm-m basement at a depth of 1170 m (3840 ft). What this result represents geologically is uncertain; however, this basement may well be unsaturated Paleozoic limestones or sandstones. On the other hand, an inspection of a gravity model developed by Loeber (1966) and the geology map of Zimmerman and Kudo (1980) suggest that

this formation may be a Precambrian basement. Estimated depth is around 1100 m (3610 ft), coincident with the 1170-m (3840-ft) depth.

The second Schlumberger sounding site, S2-TC, was located about 1 km (0.62 mi) west of the city and around 1 km (0.62 mi) southeast of the southern extension of the Mud Springs Mountains (see Figure 3-14). A crossed-Schlumberger array was completed here at orientations of 135° and 45° from true north. Both arrays were expanded to a maximum AB/2 spacing of 800 m (2625 ft) (i.e., shorter spacing than S1-TC due to terrain conditions). Equatorial points increased the effective electrode spacing of the 135° sounding to 4500 m (14,765 ft), while the 45° sounding was expanded to 3000 m (9845 ft).

Figure 3-16 presents the S2-TC 135° sounding curve and interpreted true resistivity with depth. This array is nearly parallel to the one at S1-TC, but overlies a different geologic structure. While lithologies at both sites are similar, the limestones and sandstones underlying the alluvium at S2-TC are dipping steeply at 71°SW. This structural change has been described as an overturned syncline (Zimmerman and Kudo 1980). In addition, two major fault zones lie within a few kilometers of S2-TC. In fact, the equatorial points at 225° (see Figure 3-14) cross over the Mud Springs Fault about 1 km (0.62 mi) from the center point. For this reason, the equatorial points in this direction were not used in the layered inversion (see Figure 3-16). In spite of the obvious departure from horizontal layers, the inversion of the 135° sounding curve yields a nine-layer model which bears important similarities to the one at S1-TC.

Figure 3-16 shows an 8 ohm-m layer at a depth of 40 m (131 ft). Again, the water-table contours of Theis et al. (1941) were used to estimate the water-table depth at this site. The 40-m (131-ft) estimate is in excellent

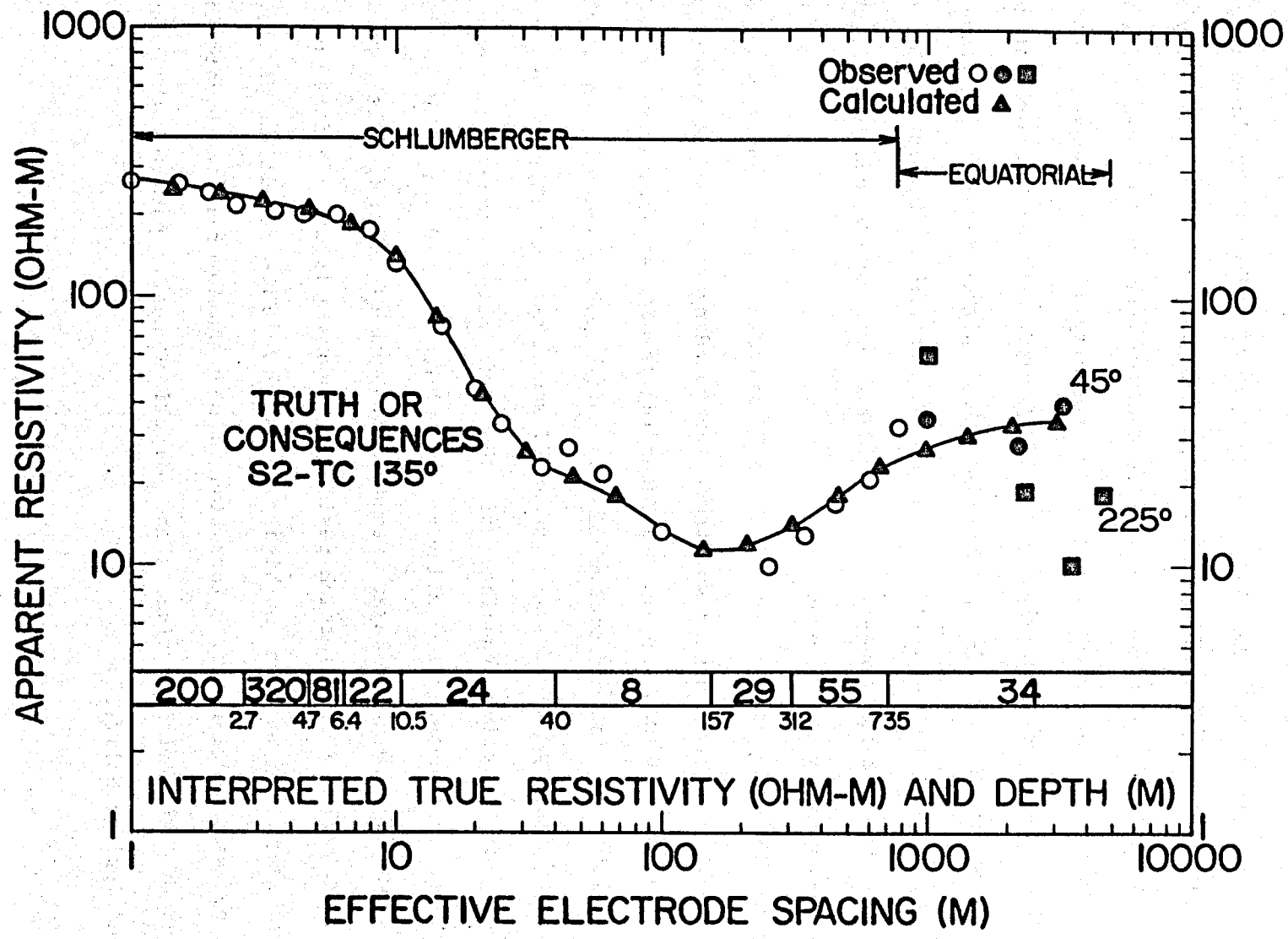

Figure 3-16. Combined Schlumberger-equatorial sounding S2-TC 135° at Truth or Consequences and the interpreted nine-layer model.

agreement with the geoelectric section. Using the water chemistry and temperatures of Wells and Granzow (1980), the aquifer is again assigned a porosity of around 30 percent. The 8 ohm-m layer is underlain by three layers with resistivities of 29, 55, and 34 ohm-m, respectively. All three layers below 157 m (515 ft) at S2-TC are more conductive than the 84 ohm-m layer at S1-TC. This observation could mean that the porosity of the carbonate aquifer beneath S2-TC is higher than that of the S1-TC layer. Given the more intense structural deformation at S2-TC, the existence of higher porosity (i.e., more fracturing and dissolution cavities) is not unreasonable. Interpretation of the results from S2-TC, however, is considered unreliable, considering the lateral heterogeneity of the area.

Figure 3-17 illustrates the S2-TC 45° sounding curve. Both sets of equatorial points were used to construct the sounding curve to an electrode spacing of 3 km (1.86 mi). Again, this sounding is over structurally- complex geology, making an interpretation of the model ambiguous. However, the surprising similarity between the two S2-TC soundings (see Figures 3-16 and 3-17) out to effective spacings of 100s of meters warrants several observations. The unsaturated alluvium is modeled to a depth of 60 m (197 ft). A conductive 10 ohm-m layer extends to a depth of 228 m (748 ft) and is underlain by a 77-m (253-ft) thick resistive 170 ohm-m layer. In fact, below 228 m (748 ft), the section is highly resistive. This result is probably observed because the Precambrian formation is much shallower in the equatorial directions of 135° and 315° since these directions nearly parallel the trend of the Mud Springs Uplift.

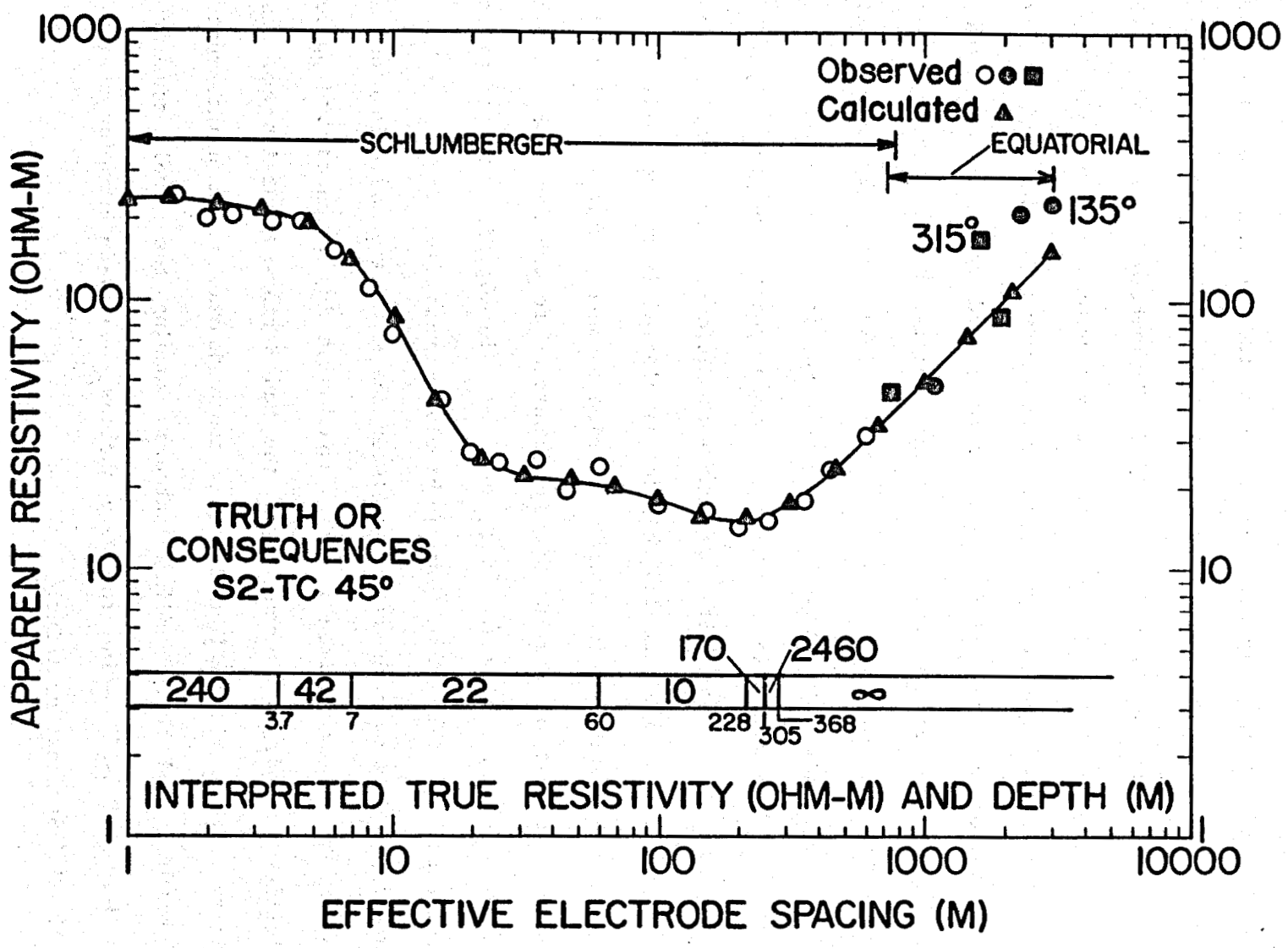

Figure 3-17. Combined Schlumberger-equatorial sounding S2-TC 45° at Truth or Consequences and the interpreted seven-layer model.

Resistivity Mapping

Phase two of the electrical resistivity investigation consisted of bipole-dipole mapping. Figure 3-18 depicts the location of the 800-m (2626-ft), L-shaped source array and the receiver locations. The two sources were coincident with portions of the S2-TC Schlumberger array (see Figure 3-14). Areal coverage obtained with 62 receiver points was approximately 59 km^2 (22 mi^2). The resistivity mapping concentrated in the region of the southern portion of the Mud Springs Mountains and the city of Truth or Consequences. Receiver stations, in general, consisted of two 100-m (328-ft) dipoles orthogonal to each other. Figures 3-19 and 3-20 present the total-field apparent-resistivity maps generated from the bipole sources oriented at 315° and 225° from the common point, respectively. The total-field apparent resistivity computed mathematically for a bipole joining the end points of the 315° and 225° bipoles is plotted in Figure 3-21.

The area immediately surrounding the bipole source array is dominated by the resistive effect of the Mud Springs Mountains to the west-northwest and the water-saturated alluvial fill of the Rio Grande Valley to the east-southeast. The two most western bipole sources (see Figures 3-19 and 3-21) are apparently over the contact between the resistive mountain block and the conductive valley sediments. This conclusion is evidenced by apparent resistivities exceeding 100 ohm-m over the Mud Springs Mountains and sharp resistivity gradients straddled by the bipole sources. The uninterrupted, steep gradients and corresponding contours crossing the bipole sources in Figures 3-19 and 3-21 define the very shallow, nearly-outcropping resistive toe of the Mud Springs Mountains.

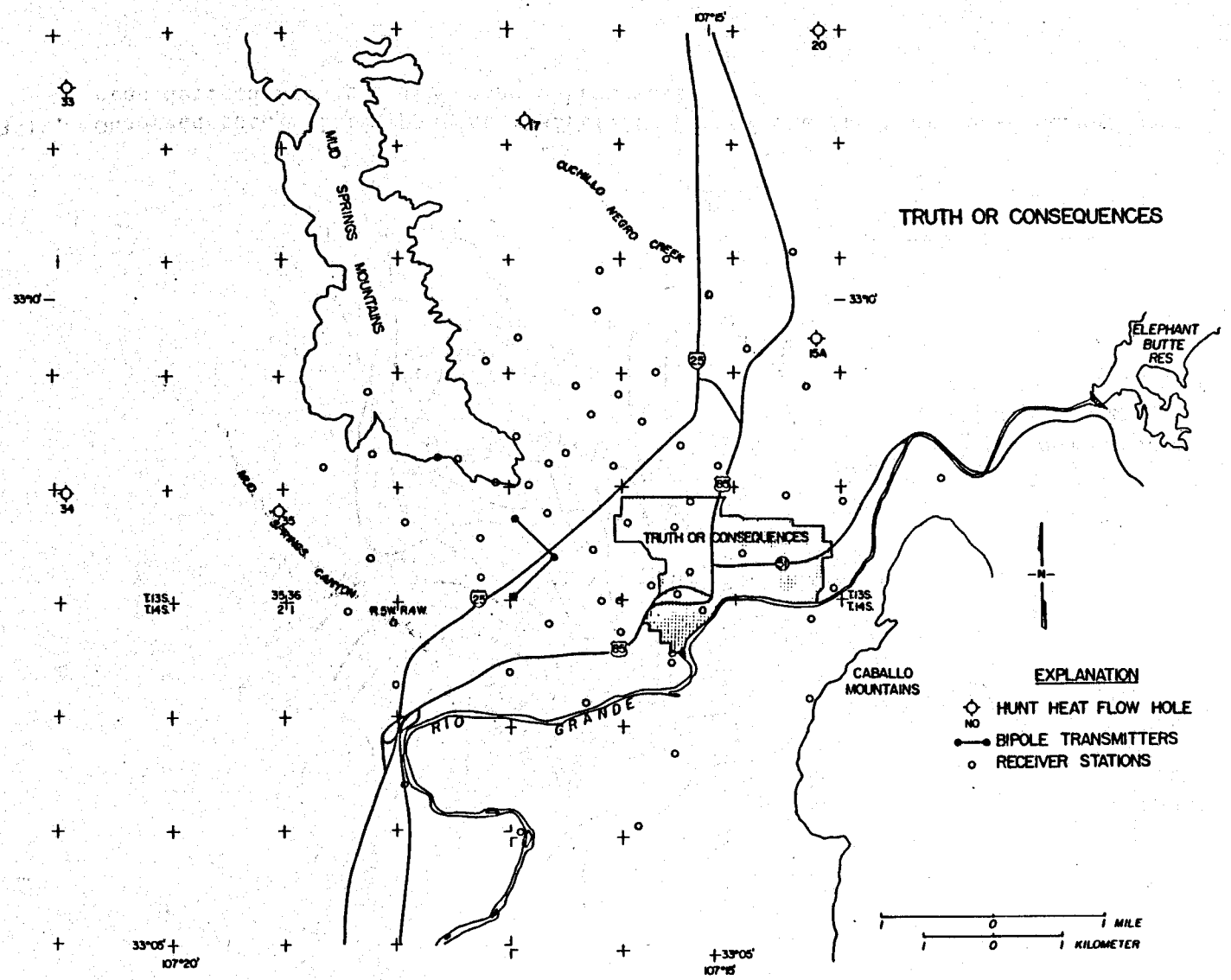

Figure 3-18. Truth or Consequences study area showing locations of bipole transmitter and receiver stations.

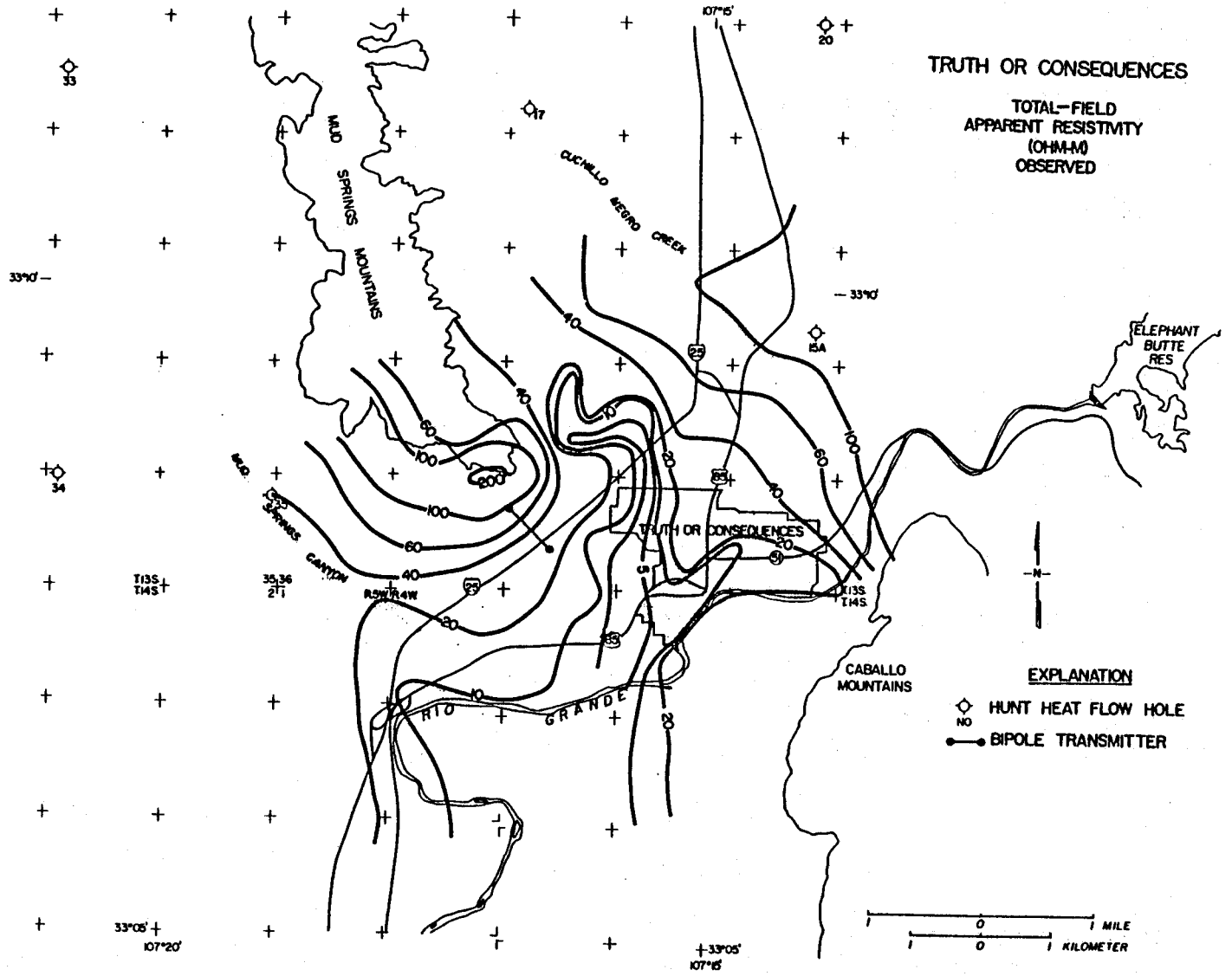

Figure 3-19. Observed total-field apparent resistivity map of the Truth or Consequences study area derived from the 315° bipole transmitter.

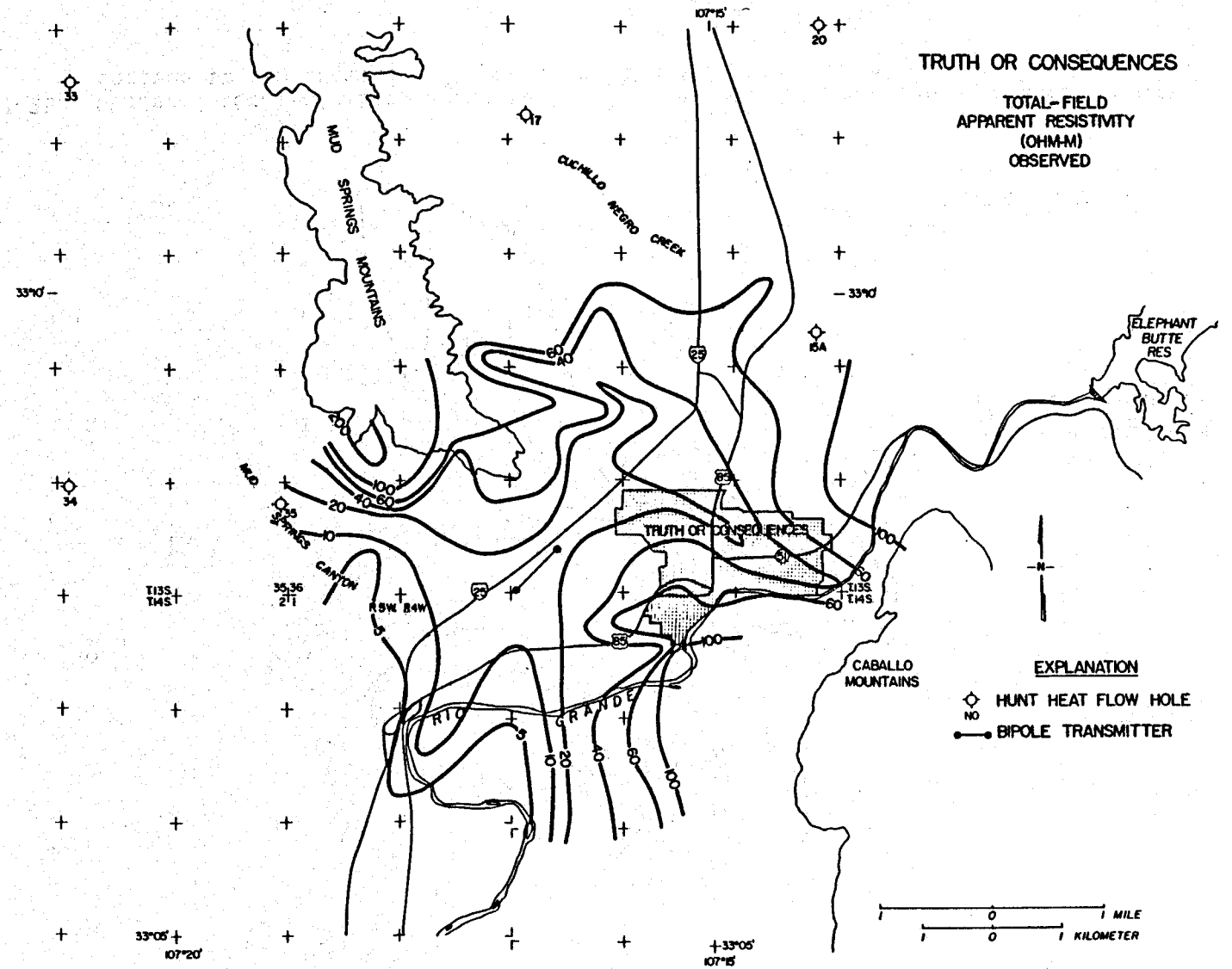

Figure 3-20. Observed total-field apparent resistivity map of the Truth or Consequences study area derived from the 225° bipole transmitter.

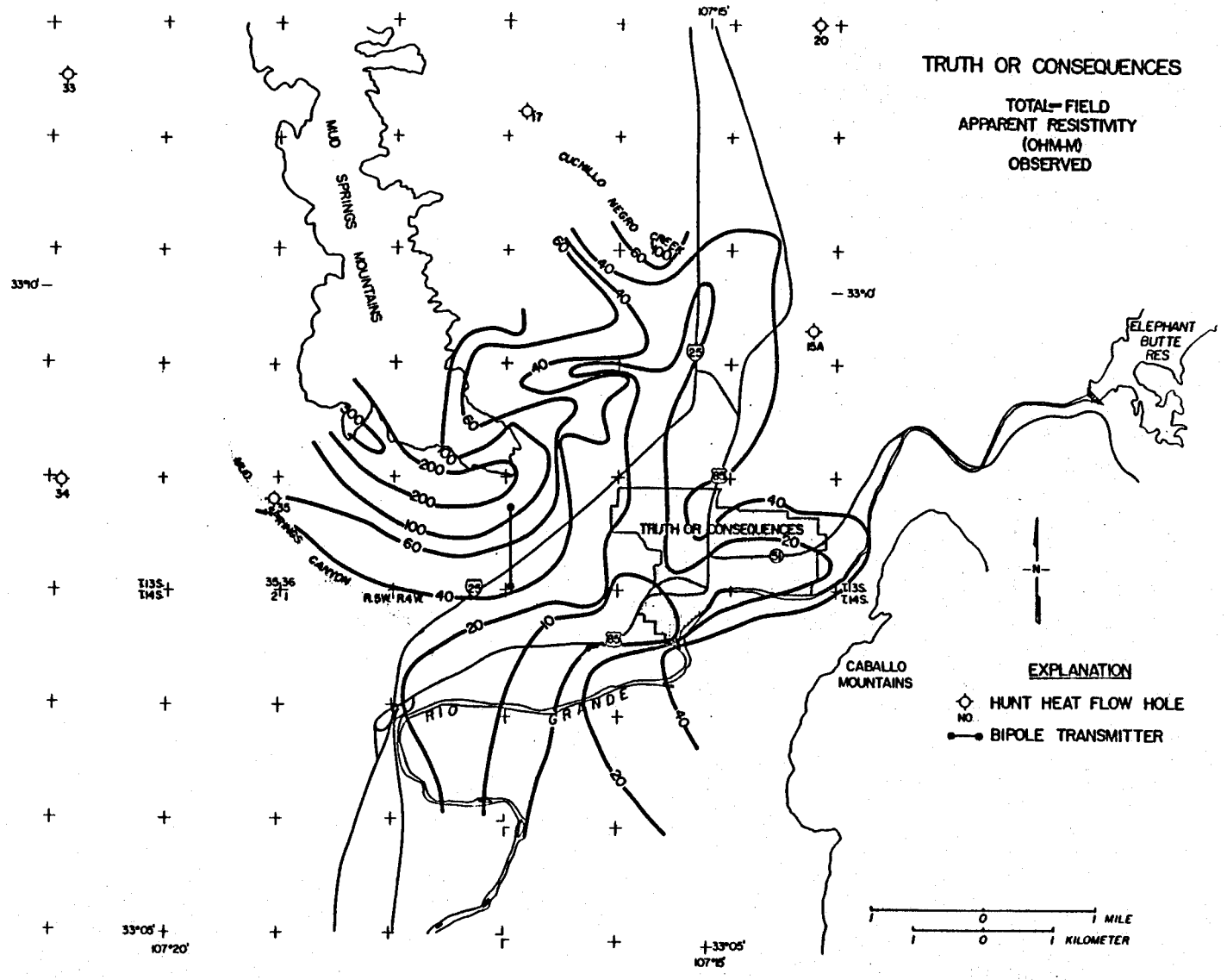

Figure 3-21. Observed total-field apparent resistivity map of the Truth or Consequences study area derived from mathematically combining the 315° and 225° bipole transmitters.

The bipole source in Figure 3-20 is, by contrast, entirely over shallow, conductive valley fill. The symmetry of the apparent-resistivity patterns about this bipole source in Figure 3-20 defines a clear saddle-like structure between the resistivity highs of the Mud Springs and the Caballo mountains. Increasingly-thick conductive sediments of the Palomas Basin are apparent in the south-polar direction of the bipole where resistivities of less than five ohm-m are mapped (see Figure 3-20). In the north-polar direction from the bipole in Figure 3-20 the trace of the 20 ohm-m contour defines a conductive zone partially identifiable with the thermal waters leaked into the shallow neogene sediments. The eastern lobe of this conductive pattern is undoubtedly influenced by the Rio Grande flow as evidenced by the obvious coincidence with the river in each of Figures 3-19, 3-20, and 3-21. The western lobe, however, appears to mark the shallow alluvial thermal waters in the vicinity of Schlumberger sounding S1-TC (see Figure 3-14). This zone is only indirectly related to the deeper, more resistive carbonate-source aquifer; bipole-dipole detection of this layer (calculated to be at a 119 to 1170-m (390 to 3839-ft) depth beneath S1-TC) is probably seen as increased apparent resistivity on the north end of the survey area. Conductive sediments, presumably present in the Engle Basin further to the north, are not sensed by the northern extent of the survey.

Conclusions

To address the geothermal resource implications of our resistivity mapping and sounding results, it is useful to consider appropriate heat-flow data collected by Geothermal Services, Incorporated. Table 3-3 contains data presented by Sanford et al. (1979) for the six drillholes in the mapped areas

Table 3-3. Selected heat-flow data in the Truth or Consequences, New Mexico area (Sanford et al. 1979).

Hole No.	Total Depth (m)	Geothermal Gradient (°C/km)	Gradient Interval (m)	Heat Flow (HFU)
15A	148	17.7	67-146	1.0
17	134	35.0	73-131	1.9
20	152	40.8	76-152	2.5
33	147	51.4	30-137	2.5
34	152	65.6	85-152	2.5
35	152	60.9	91-152	2.6

the mapped areas of Figures 3-19, 3-20, and 3-21. Heat-flow values were calculated using thermal conductivity measurements made on a minimum of four drill cuttings from each hole.

It is quite evident that, upon excluding data from holes 15A and 17, the heat flow from the remaining holes is almost exactly the regional background heat flow of 2.5 HFU in this section of the Rio Grande Rift (Reiter et al. 1975). Jarzabek and Combs (1978) consider the temperature gradients in holes 15A and 17, as well as those in 34 and 35, to be disturbed by shallow groundwater; however, they believe the lower portion of holes 34 and 35 to not be seriously disturbed. The lack of any anomalous heat flow in the sixteen holes logged for Hunt Energy Corporation by Geothermal Services, Incorporated resulted in Hunt dropping its geothermal leases because they were searching for a high-temperature resource. Even so, the possibility of an economic low- to moderate-temperature resource in the Truth or Consequences area still bears consideration.

To this end we identify two potential geothermal areas worthy of further evaluation by drilling. First, the area surrounding our Schlumberger sounding S1-TC is defined by bipole-dipole mapping as a shallow conductive region probably produced, in part, by leakage of thermal waters from the limestone-source aquifer below. From Schlumberger sounding S1-TC, we estimate the shallow alluvial aquifer to be 86-m (282-ft) thick beginning at a depth of 33 m (108 ft). The carbonate aquifer immediately below may be over 1-km (0.62-mi) thick. Porosities of the two zones are estimated to be 30 percent and 14 percent, respectively.

A second area of interest is defined south and southwest of the Mud Springs Mountains, roughly along the trend of Hunt heat-flow holes 34 and

35. These two holes recorded the highest temperature gradients in the exploration program carried out by Hunt (i.e., 65.6°C/km and 60.0°C/km, 3.6°F/100 ft and 3.3°F/100 ft, respectively) and are situated on, or in line with, steep bipole-dipole resistivity gradients (see Figures 3-19, 3-20, 3-21). The gradients are thought to mark a recently (70,000 yr. B.P.) active fault (Wells and Granzow 1980) separating the Mud Springs Mountains from the Palomas Basin to the south. Such a basin-bounding fault could provide deep hydrothermal circulation and a correspondingly enhanced surface thermal anomaly. Our resistivity mapping and previous gravity modeling (Loeber 1976) indicates a pronounced deepening of the Palomas basin fill in this vicinity; thus, ample reservoir potential is present. Recent regional gravity modeling by Birch (1980) provides an estimate of over 0.5 km (0.31 mi) of low-density, high-porosity rift (Neogene) sediments in this vicinity. Both of the areas described above are considered possible economic low- to moderate-temperature resource areas near the city of Truth or Consequences.

Acknowledgements

We would first like to thank the other members of the University of New Mexico field crew: J. Cooney, M. Gerety, M. Hermann, M. Parker, T. Summers, Jr., M. Vaughn, and R. Wasserman. H. T. Holcombe assisted in the numerical computations. We also acknowledge the assistance of the Truth or Consequences Chamber of Commerce and the cooperation of several local landowners. R. L. Bowers of Hunt Energy Corporation very kindly provided us with the results of their exploration program. P. Morgan of New Mexico State University, as well as our co-investigators, A. M. Kudo and S. G. Wells from the University of New Mexico, provided timely discussions.

References

Albright, J. L., Alcorn, and H. S. Cave, 1955, Oil and gas possibilities of the basins of the Sierra County region, in 6th Field Conference Guidebook: New Mexico Geological Society, p. 124-135.

Birch, F. S., 1980, Three-dimensional gravity modeling of basin hydrologic parameters in New Mexico: U.S. Geological Survey, unpublished report, Contract 14-08-0001-17899, 27 pp.

Hohmann, G. W. and G. R. Jiracek, 1979, Bipole-dipole interpretation with three-dimensional models (including a field study of Las Alturas Estates, New Mexico): University of Utah Research Institute, Earth Science Laboratory Report ESL-20, Salt Lake City, 20 pp.

Jarzabek, D. and J. Combs, 1978, Hunt Energy Corporation, Elephant Butte Prospect, New Mexico: Geothermal Services, Inc., Job no. 16-76, 12 pp.

Jiracek, G. R. and C. Smith, 1976, Deep-resistivity investigations at two known geothermal resource areas (KGRAs) in New Mexico, Radium Springs and Lightning Dock: New Mexico Geological Society, Special Publication 6, p. 71-76.

Jiracek, G. R., C. Smith, and G. A. Dorn, 1976, Deep geothermal exploration in New Mexico using electrical resistivity: Second United Nations Symposium on the Development and Use of Geothermal Resources, Proceedings, v. 2, p. 1095-1102.

Keller, G. V., and Frischknecht, F. C., 1966, Electrical methods in geophysical prospecting: Permagon Press, New York, 517 pp.

Loeber, K. N., 1976, Geology and igneous petrology of the Truth or Consequences-Engle area, Sierra County, New Mexico: University of New Mexico, unpublished manuscript, 119 pp.

Meidav, T., 1970, Application of electrical resistivity and gravimetry in deep geothermal exploration: United Nations Symposium on the Development and Utilization of Geothermal Resources, Pisa, Proceedings, Geothermics Special Issue 2, p. 303-310.

Reiter, M., C. L. Edwards, H. Hartman, and C. Weidman, 1975, Terrestrial heat flow along the Rio Grande Rift, New Mexico and southern Colorado: Geological Society of America Bulletin, v. 86, p. 811-818.

Sanford, R. M., R. L. Bowers, and J. Combs, 1979, Rio Grande Rift geothermal exploration case history, Elephant Butte prospect, south central New Mexico: Geothermal Resources Council, Transactions, v. 3, p. 609-612.

Theis, C. V., G. C. Taylor, Jr., and C. R. Murray, 1941, Thermal waters of the Hot Springs Artesian Basin, Sierra County, New Mexico: New Mexico State Engineer's Office, 14th-15th biennial report, p. 419-492.

Wells, S. R. and H. Granzow, 1980, Hydrogeology of the thermal aquifers near Truth or Consequences, New Mexico, in Icerman, L., Starkey, A. and Trentman, N., eds., State-coupled low temperature geothermal resource assessment program, fiscal year 1980: New Mexico Energy Institute at New Mexico State University, p. 3-5 - 3-52.

Zimmerman, C. J. and A. M. Kudo, 1980, Geological mapping of the Mud Springs Mountains, near Truth or Consequences, New Mexico, in Icerman, L., Starkey, A., and Trentman, N., eds, State-Coupled Low Temperature Geothermal Resource Assessment Program, Fiscal Year 1980, New Mexico Energy Institute at New Mexico State University, p. 3-1 - 3-4.

Zohdy, A. A. R., 1970, Geometric factors of bipole-dipole arrays: U.S. Geological Survey, Bulletin 1313-B, 26 pp.

Zohdy, A. A. R., 1973, A computer program for the automatic interpretation of Schlumberger sounding curves over horizontally stratified media: National Technical Information Service, Springfield, Virginia, Report PB-232 703, 25 pp.

Chapter 4

Geothermal Exploration with Electrical Methods near Vado, Chamberino, and Mesquite, New Mexico*

Introduction

The area near Vado, Chamberino, and Mesquite, New Mexico, may contain a low-temperature resource similar to the Las Alturas field adjacent to Las Cruces. A reconnaissance d.c.-resistivity survey was made in the area. The results show low-resistivity zones, which may be due to hot water, and abrupt variations in bedrock depth, which may be due to faulting. The faults may be conduits for the circulation of hot water.

Geologic Setting

The general geology and hydrogeology of the southern Rio Grande Valley, in which our study area is located, is discussed in King and Hawley (1975) and Seager (1975), and is summarized here.

The Rio Grande Valley consists of a series of deep basins oriented approximately north-south. The valley is punctuated by uplifts and bounded by faults. In Dona Ana County, one of the main basins is the Mesilla Valley, which begins a few kilometers north of El Paso, Texas, in the south and extends north to a few kilometers north of Las Cruces.

Our study area is shown as a rectangle on a map of New Mexico in Figure 4-1. Figure 4-2 shows the main geological landmarks in the survey area; the study area is in the eastern half of the Mesilla Valley between alluvium to the west and the uplifted Franklin Mountains to the east.

*The principal author of Chapter 4 is Dr. Charles T. Young, Assistant Professor of Physics, New Mexico State University.

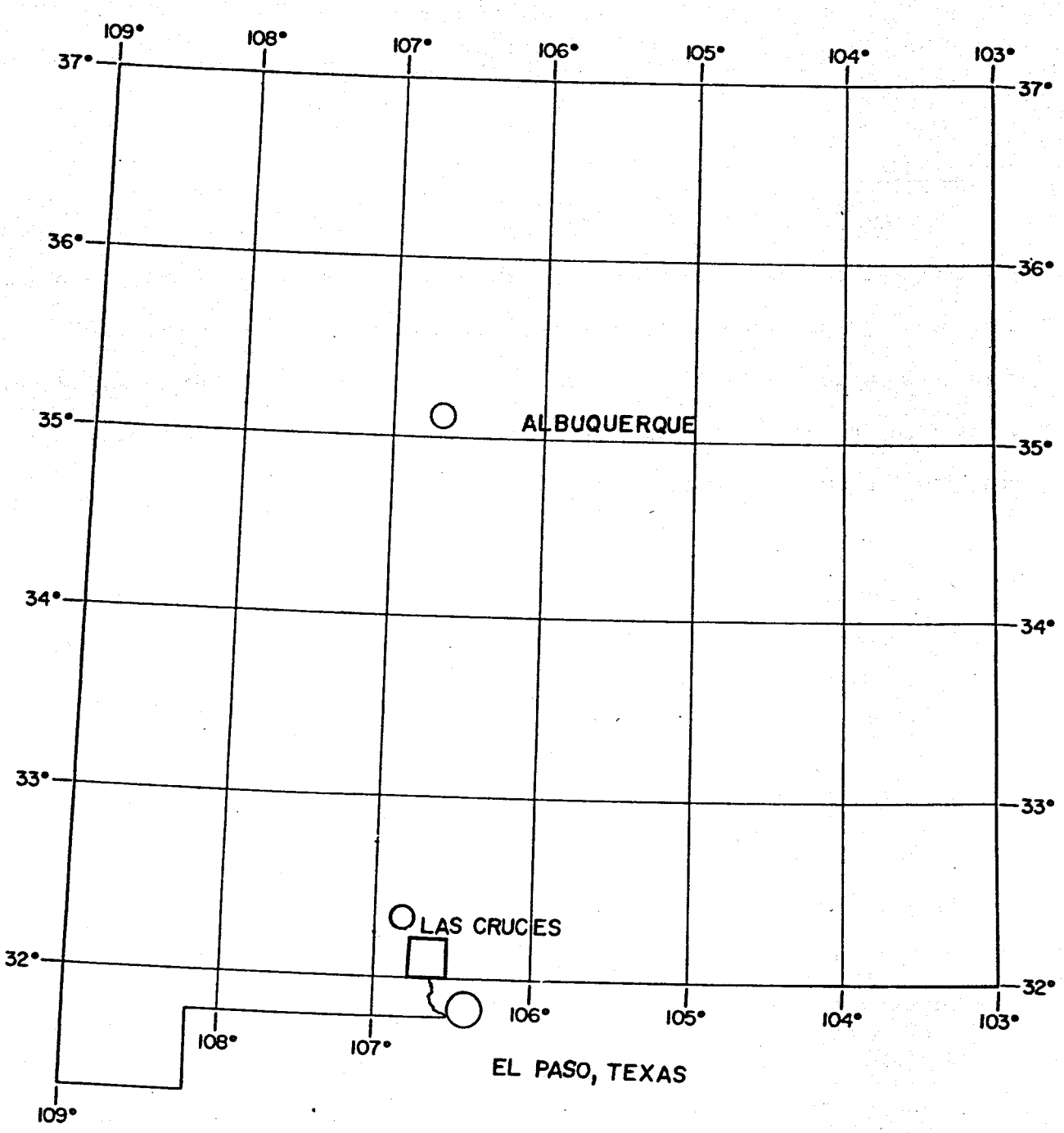

Figure 4-1. Study area on background map of New Mexico.

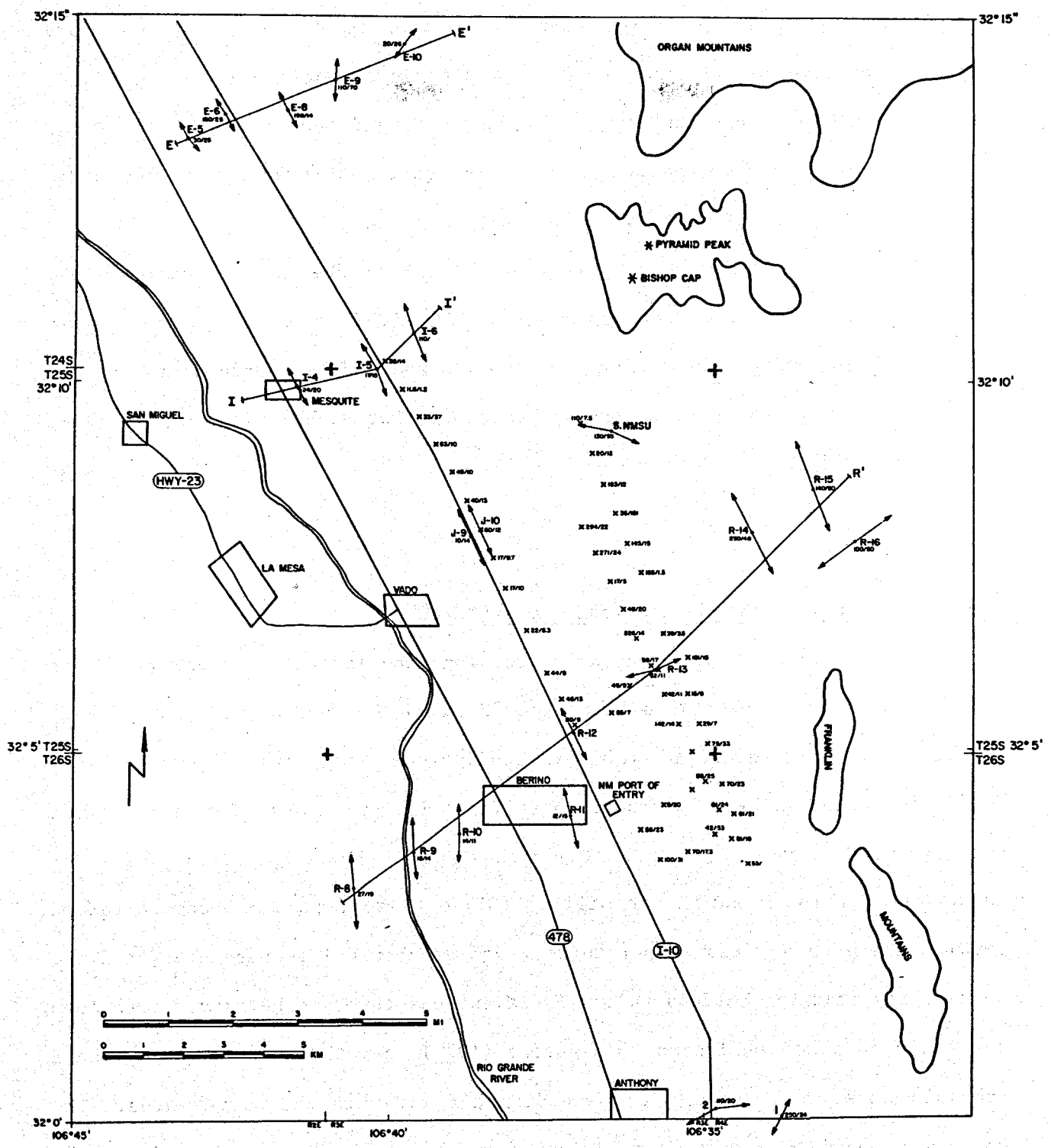

Figure 4-2. Map of study area. Double-ended arrows are locations of Schlumberger soundings of Jackson (1976), except for the double arrow marked NMSU, which is a sounding by the author. Light crosses are profile stations. Numbers by the profile stations are the apparent resistivities in ohm-m at AB/2 = 100 m and 800 m on the left and right of the slash mark, respectively. The AB/2 = 800 m data are contoured on Figure 4-6.

North-south running faults near Las Cruces extend south to the study area. These faults run along Interstate Highway 10 along the east and west sides of Tortugas Mountain, and along the east and west sides of the Organ Mountains. Gravity measurements show a high east-west gradient in the study area, supporting the concept of north-south faulting.

There may be a buried north-south volcanic ridge in the survey area. Andesite hills near the Vado Interstate exit within the survey area and a buried volcanic ridge, known from drill holes and located north of the survey area just east of Las Cruces, provide evidence that such a ridge exists (King and Hawley 1975).

Groundwater Quality and Geochemical Temperatures

The only wells in the study area are along the interstate highway. These wells have water temperatures between 25°C and 30°C. Geochemical analysis of these wells gives maximum estimated equilibrium temperatures greater than 200°C for the Na-K-Ca geothermometer and 100 to 150°C for the silica geothermometer (Swanberg 1975). The highest total dissolved solids value for these wells is 4500 parts per million (Clyde Wilson, personal communication 1980). These warm water temperatures, high geochemical temperatures, and the possibility that the Mesilla Valley Fault extends through the survey area form the basis for the conclusion by Swanberg (1975) that the Mesilla Valley Fault probably acts as a conduit for ascending hot water in the survey area. The hot water would then move down the water table cooling and mixing with water from rainfall.

Electrical Resistivity Measurements

There are two sets of electrical resistivity data reported here. The first set is Schlumberger soundings, from which layer thicknesses and resistivities can be determined. These data were obtained by Jackson (1976). Clyde Wilson, USGS geologist in Las Cruces, prepared hydrogeologic and geologic interpretations of these data.

The second set of data is Schlumberger profiling. In this method the apparatus is moved along a survey line at a constant electrode spacing. These data, obtained by NMSU personnel under this research contract, are used to locate regions of high and low resistivity and to obtain a rough estimate of the depth to the anomalies.

Schlumberger Soundings

Figure 4-2 shows the location of parts of Schlumberger sounding lines E, I, J, and R from Jackson (1976). The author has reinterpreted the original data and the resulting models are presented as profiles in Figures 4-3, 4-4, 4-5, and 4-6. In general, this group of soundings shows:

1. Surface layers that differ in thickness and resistivity, from one station to the next. Typically, high resistivities, between 100 and 500 ohm-meters occur near the surface. The dry, loose material conducts electricity poorly. These layers are not important to the present study.

2. Intermediate layers with resistivities from 3 to 35 ohm-meters, usually interpreted as an aquifer. Lower values of resistivity are due to high dissolved solids, high temperatures, or high clay content. Even though layers like these are usually interpreted as an aquifer, water wells in the Mesilla Valley have shown that the top of the water table is not coincident with the top of the low-resistivity layer. This discordance is probably due

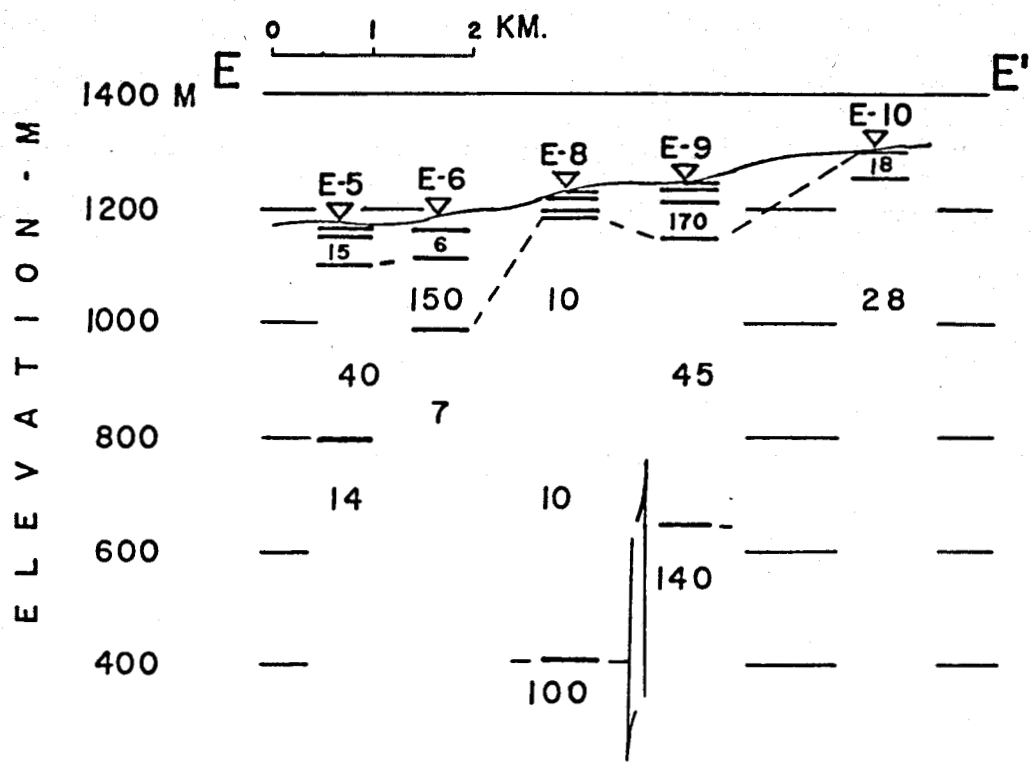

Figure 4-3. East end of profile E. Data from Jackson (1976). Modeling and fault interpretation by the author. The layer resistivities are given in ohm-m. Layer boundaries are indicated by short, heavy, horizontal lines. Dashed lines are inferred correlations of layers between models.

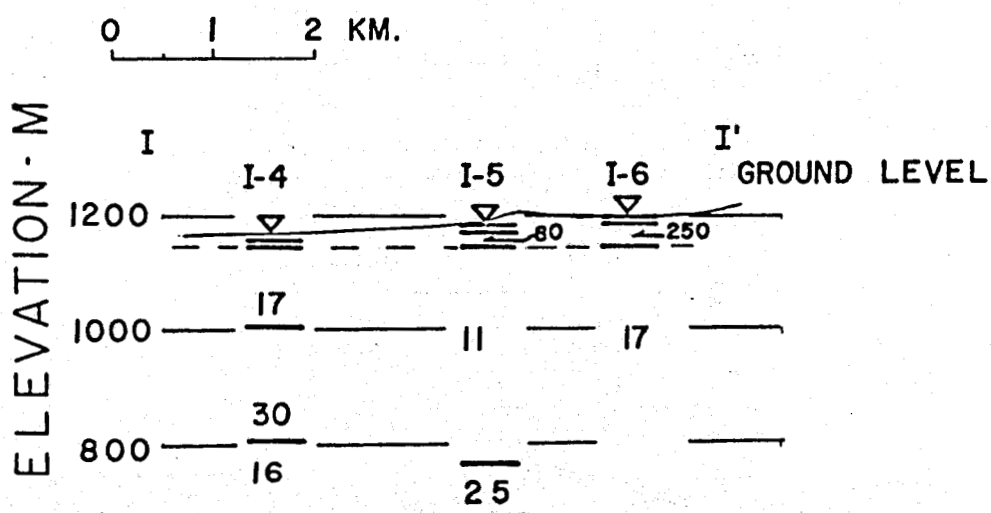

Figure 4-4. East end of profile I. Data from Jackson (1976). Modeling and fault interpretation by the author. The layer resistivities are given in ohm-m. Layer boundaries are indicated by short, heavy, horizontal lines. Dashed lines are inferred correlations of layers between models.

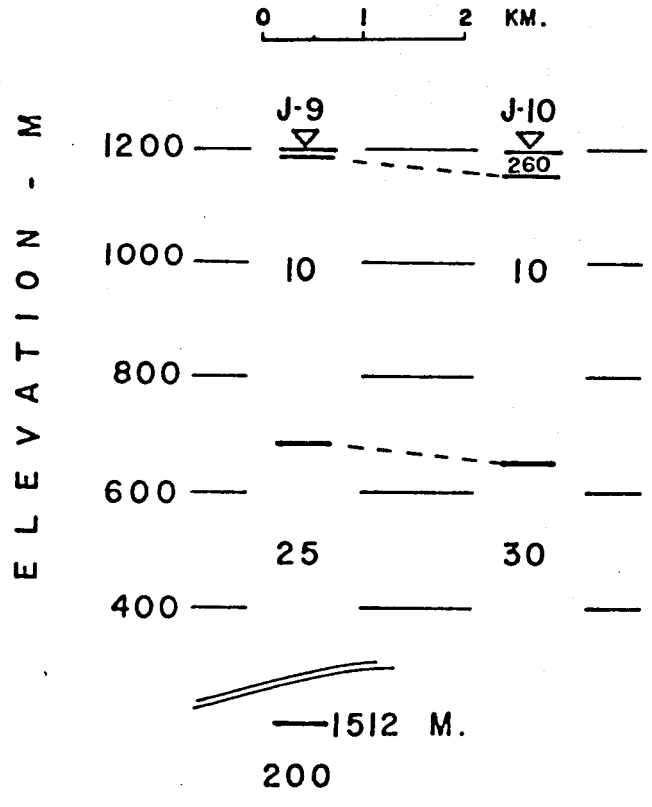

Figure 4-5. East end of profile J. Data from Jackson (1976). Modeling and fault interpretation by the author. The layer resistivities are given in ohm-m. Layer boundaries are indicated by short, heavy, horizontal lines. Dashed lines are inferred correlations of layers between models.

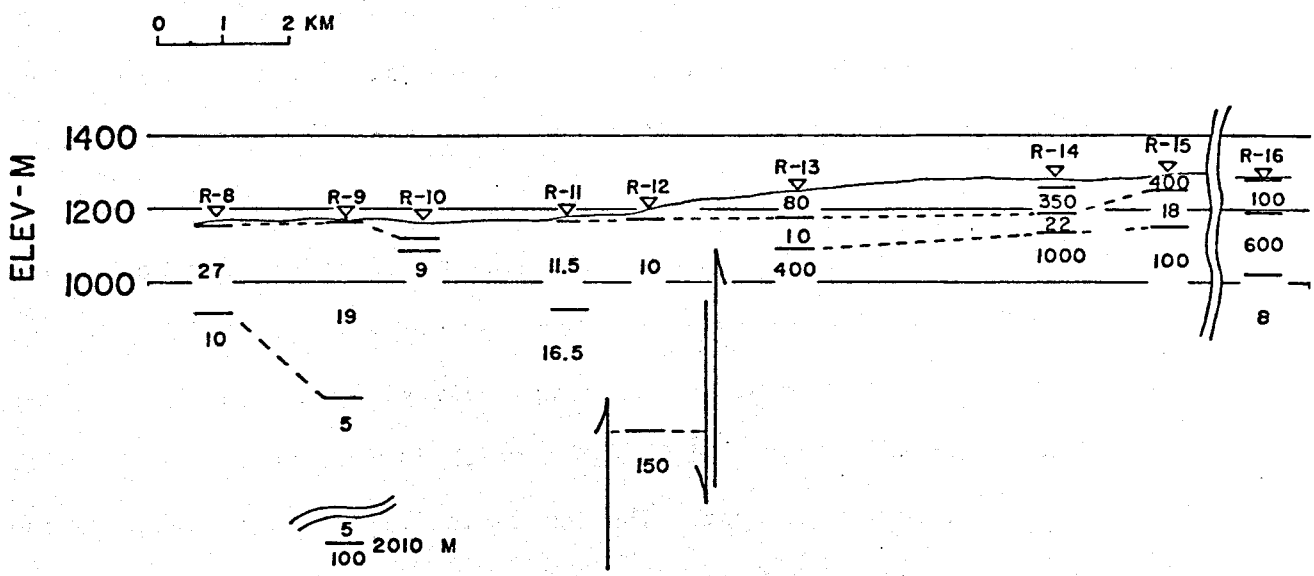

Figure 4-6. East end of profile R. Data from Jackson (1976). Modeling and fault interpretation by the author. The layer resistivities are given in ohm-m. Layer boundaries are indicated by short, heavy, horizontal lines. Dashed lines are inferred correlations of layers between models.

to the fact that the top of the water table is not an exact depth, but a broad zone. There could be an unsaturated zone of soil moisture that conducts electricity well, but does not yield water to wells. In fact, the water table generally falls roughly in the middle of this conductive zone.

3. A resistive electrical basement, a layer usually interpreted as the bottom of the aquifer. The resistivity of this layer is often difficult to resolve from the sounding data. For the Mesilla Valley, electrical-basement resistivities from 50 to 200 ohm-meters are interpreted as volcanics. Higher resistivities, 500 to 1000 ohm-meters, are interpreted as limestones. The differences are due more to the differences in water content than to rock type.

Profile E (see Figure 4-3) shows thick layers of moderately conductive material to the east. The layers at stations E-5 and E-6 are probably valley fill saturated with ground water of varying quality; soundings E-8 and E-9 show an abrupt change of electrical basement which is interpreted as a fault, with the upthrown block to the east. The low resistivities to the west of the inferred fault, at station E-8, suggest geothermal potential.

The I profile (see Figure 4-4) shows thick layers of moderately conductive material to the west at station I-4. This sounding is in the part of the Mesilla Valley which contains the deepest sediments. The lowest resistivity in the profile occurs at station I-5, 11 ohm-m in a layer 370 m thick. This possible warm or hot water layer covers 25 ohm-m material interpreted as volcanic. This electrical basement may be the same composition as Vado Hill, five km to the south. The abrupt rise in basement at station I-5 may be due to faulting or a broad dyke.

At station I-6 the aquifer has higher resistivity. The electrode array was not extended as far out here as elsewhere and did not detect an electrical basement.

Stations J-9 and J-10, profile J from Jackson (1976), are within our survey area. The models for these data, shown in Figure 4-5, show layers of 10 ohm-m material several hundred meters thick, overlying moderately resistive material 25 to 30 ohm-m. The 10 ohm-m material is probably an aquifer containing warm or saline water. The underlying 25 to 30 ohm-m layer may be volcanic rock. Soundings J-9 and J-10 are situated between two andesite hills (not shown on the map) which may form an underground saddle. It is not possible to tell from these two soundings whether or not there are faults along the profile.

Profile R from Jackson (1976) is shown in Figure 4-6; stations R-10, R-11, R-12, and R-13 are in or near the survey area and show low-resistivity aquifers, from 9 to 11.5 ohm-m. In between soundings R-11, R-12, and R-13 there are abrupt changes in depth to electrical basement which are interpreted as faults. The faults and the low-aquifer resistivities suggest the circulation of geothermal fluids.

Soundings R-14 and R-15 to the east indicate higher aquifer resistivities, suggesting lower geothermal potential. The easternmost sounding, R-16, is about 1.5 km south of R-14 and R-15 and shows a very different structure, including an eight ohm-m layer below 300 meters. The rapid change in geologic structure indicates a probable fault between stations R-16 to the south and R-14 and R-15 to the north. The fault could be an extension of a fault along the east or west face of the Organ Mountains.

Stations R-8, R-9, and R-10 to the west have low resistivities as low as three ohm-m (R-10); however, water wells there have lower temperatures, and geothermometry calculations do not show high geochemical temperatures.

Data from the NMSU sounding, not shown, are too erratic to model as

layers. The data indicate near-surface inhomogeneities such as faults, possibly superimposed on a three-layer structure. Other nearby soundings are needed for a structural interpretation.

Content AB/2 Profiling

Sounding data by Jackson (1976) show resistivities as low as 10 ohm-m at stations E-8, I-5, R-12, and R-13 located near a probable extension of the Mesilla Valley Fault. To determine the extent of these low-resistivity layers, NMSU personnel made Schlumberger resistivity measurements at constant electrode spacings. The measurements, located by light crosses on Figure 4-2, are 800 m or one-half mile apart. There are two data sets for each station, made with AB/2 spacings of 800 m and 100 m. The reason for choosing the 800-m spacing is that in almost all of the soundings by Jackson (1976), a deep, low-resistivity layer would show up as a low-resistivity anomaly at AB/2 = 800 m.

Apparent resistivity data for each station are tabulated on Figure 4-2. The apparent resistivities for AB/2 = 800 m are contoured on Figure 4-7. Two principles of resistivity measurement should be kept in mind when interpreting these contours: (1) any apparent resistivity value represents a weighted average of true resistivities; and (2) the greatest weight is always less than the AB/2 electrode separation, so that the effective depth of investigation is always less than AB/2.

The contours on Figure 4-7 represent regions of high and low resistivity at depths less than 800 m. The contours show a region in the survey area with resistivities less than 10 ohm-m, running parallel to the interstate highway, approximately 10 kilometers long by five kilometers wide. The low-resistivity zone terminates abrupty near the New Mexico Port of Entry terminal.

The fault detected between sounding stations R-11 and R-12 lies

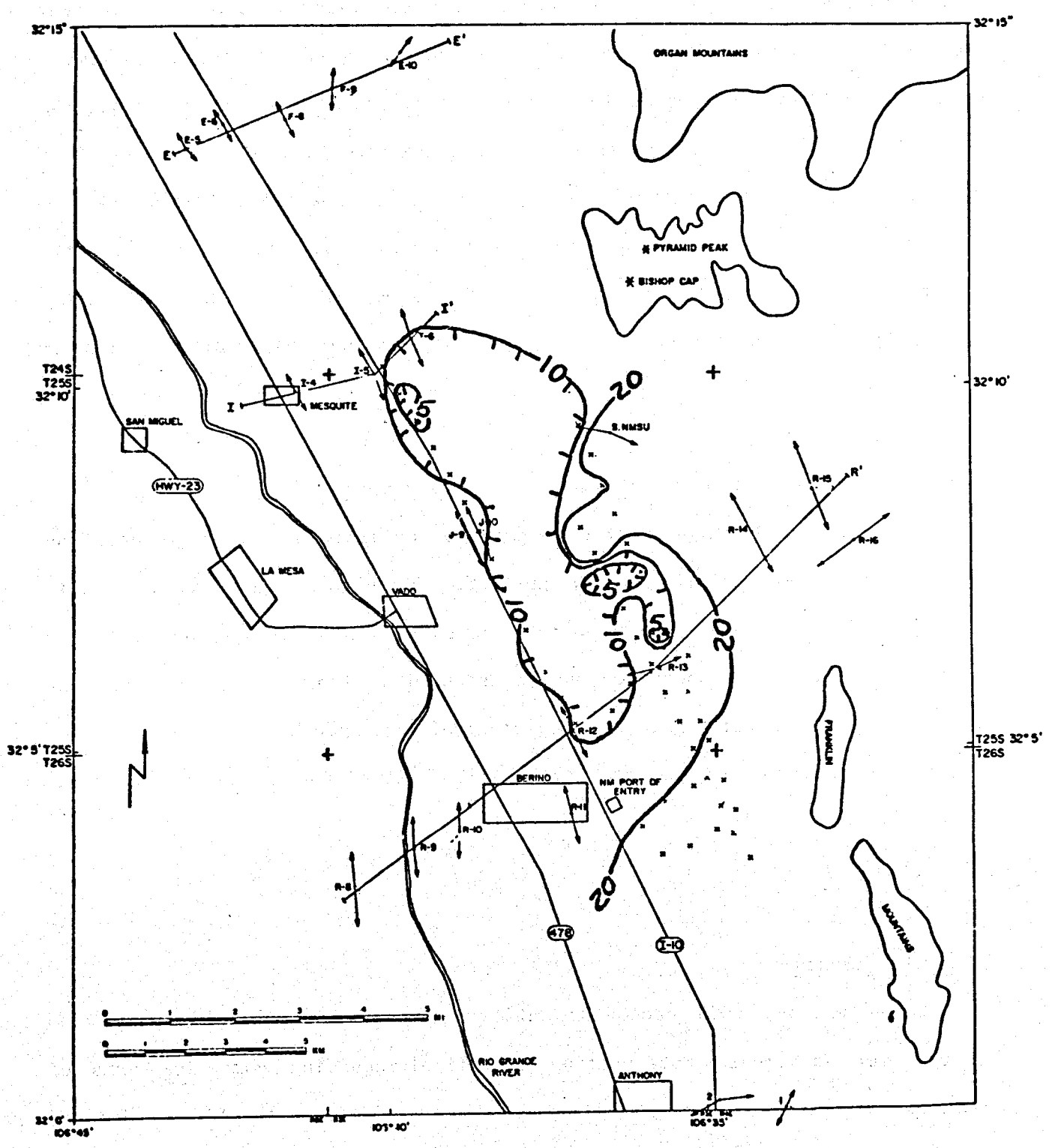

Figure 4-7. Apparent resistivity contours for AB/2 = 800 m data of Figure 4-2.

approximately under the 10 ohm-m contour in the eastern half of the survey area. The 10 ohm-m contour has additional twists in it due to the two lowest apparent resistivities, which are less than five ohm-m, just north of sounding R-12. These contours suggest that the structure here is more complicated than may be explained solely by a fault running across line R-R'. There could be cross-faulting, or plumes of geothermal fluids, or both. The author's interpretation, showing faults inferred from high lateral-resistivity gradients and abrupt changes in depth to electrical basement, is shown in Figure 4-8.

Interpretation of Geothermal Potential of Survey Area

The electrical resistivity data suggest faulting in the survey area and updwelling of geothermal fluids along certain faults. There are no wells, measured temperatures, or geochemical geothermometer calculations directly over the resistivity anomalies or interpreted faults. To verify the high temperatures inferred from these geological and geophysical data, it is recommended that the low-resistivity zones be drilled for temperature gradient measurements.

Acknowledgements

Clyde Wilson, USGS geologist, allowed use of data from his files and shared his experience interpreting electrical sounding data in terms of geologic structure and water quality. Robert Sanders was the field chief and technician for the project. Other students and staff members who helped were Justine Gilkey, Sandra Adams, Kevin Suter, Dave Lynch, James Pratt, and Dave Price.

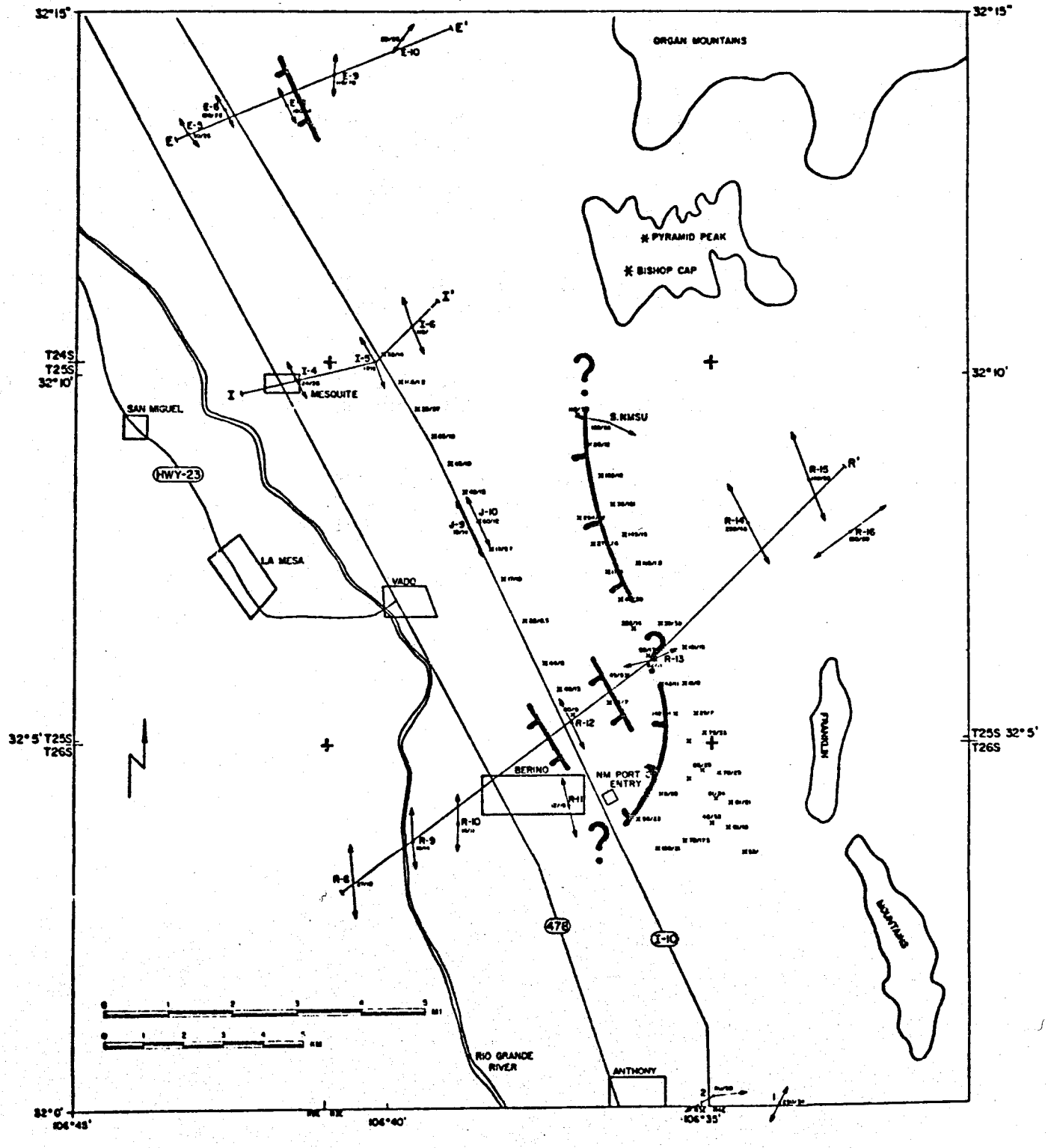

Figure 4-8. Inferred faults in survey area plotted as heavy bars and superimposed on Figure 4-2.

References

Jackson, D., 1976, Schlumberger soundings in the Las Cruces, New Mexico area: U.S. Geological Survey, Open-File Report 76-231.

King, W., and Hawley, J., 1975, Geology and groundwater resources of the Las Cruces area, New Mexico, in 26th Field Conference Guidebook: New Mexico Geological Society, p. 195-204.

Seager, W., 1975, Cenozoic tectonic evolution of the Las Cruces area, New Mexico, in 26th Field Conference Guidebook: New Mexico Geological Society, p. 241-250.

Seager, W. R., Clemons, R. E., and Callender, J., 1975, Guidebook of the Las Cruces country; 26th Field Conference Guidebook: New Mexico Geological Society, 376 pp.

Swanberg, C., 1975, Detection of geothermal components in groundwaters of Dona Ana County, Southern Rio Grande Rift, New Mexico, in 26th Field Conference Guidebook: New Mexico Geological Society, p. 175-180.

Wilson, Clyde, 1980, Personal communication, U. S. Geological Survey, Las Cruces, New Mexico.

Chapter 5

Geothermal Investigations in Southcentral New Mexico Counties

Part 1

A Heat-Flow Study of Dona Ana County, Southern Rio Grande Rift, New Mexico*

Introduction

Dona Ana County is located between the Basin and Range and Great Plains physiographic provinces in southcentral New Mexico (see insert, Figure 5-1; stippled area is the approximate boundary of the Rio Grande Rift in New Mexico as defined by Chapin and Seager (1975)). Figure 5-1 also shows the location of wells logged in this study and the hot springs and wells used for lithologic control.

The main physiographic features of the county are the entrenched valley of the Rio Grande, which crosses the area from northwest to southeast, and two large intermountain basins, the Jornado del Muerto and the Mesilla Bolson. The basic geomorphic setting is one of mountain uplifts alternating with broad structural basins. Many of the mountains are uplifted fault blocks of Paleozoic strata with a general north-south trend. Other mountain types are broad domal uplifts and igneous intrusive and extrusive bodies. King et al. (1971) report that the Santa Fe Group basin fill of Miocene to middle Pleistocene age and the Rio Grande and tributary arroyo valley fills of late Quaternary are the two major groundwater reservoirs in the area.

---

*The principal authors of Chapter 5, Part 1 are Richard L. Lohse, Staff Engineer, New Mexico Energy Institute at New Mexico State University, Dr. Paul Morgan, Staff Scientist, Lunar and Planetary Institute, Houston Texas, and Dr. Chandler Swanberg, Associate Professor of Earth Sciences and Physics, New Mexico State University.

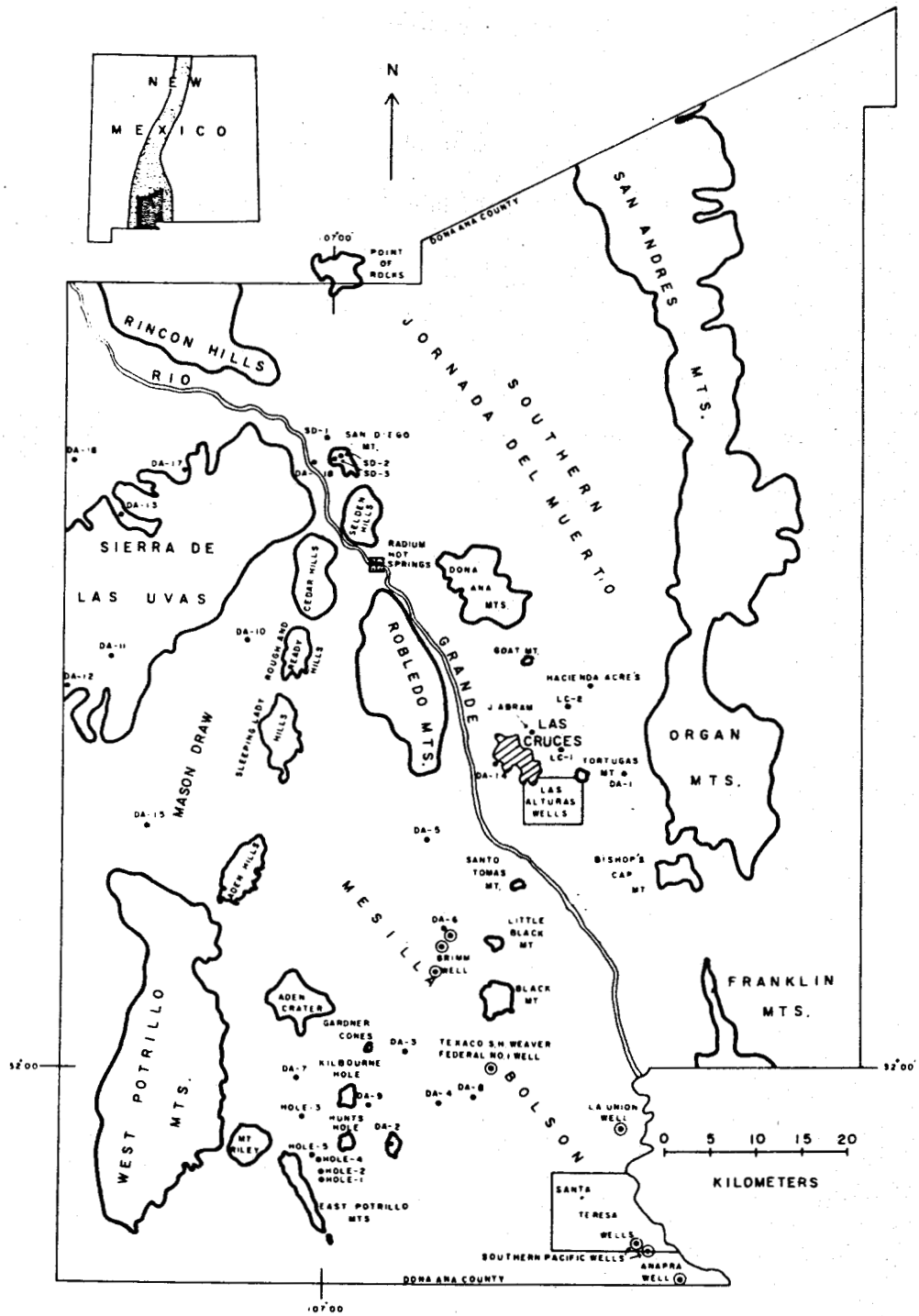

Figure 5-1. Location map for wells in Dona Ana County. Solid dots are wells that were temperature-logged. Circles surrounding solid dots are wells used for lithologic control (Lohse 1980).

Tectonically, the county sits within the southern Rio Grande Rift system as defined by Chapin (1971) and modified by Chapin and Seager (1975) and Seager and Morgan (1979). The present topography is dominated by intrarift uplifts and basins of late Cenozoic age, which are superimposed upon late Cretaceous and early Cenozoic features and a variety of very different tectonic features of middle Tertiary age (Seager 1975). Reiter et al. (1978), based on a limited amount of heat-flow values throughout southcentral New Mexico, have placed the study area within an envelope of heat-flow values greater than 105 mWm^{-2} (2.5 HFU).

Other geological and geophysical data for the area comes from a complete Bouguer gravity anomaly map (Cordell et al. 1978), late Cenozoic fault maps (Callender and Seager 1980), geochemistry (Swanberg 1975), electrical resistivity work (Jackson and Bisdorf 1975; Hoover and Tippens 1975; O'Donnell et al. 1975; Young 1979, 1980), and magnetic surveys (Cordell 1975; Seager 1978; Keller 1979).

Temperature Gradients

In order to obtain a better understanding of the heat flow throughout the county, a search was conducted for abandoned boreholes suitable for temperature logging. Approximately 60 wells have been logged (see Figure 5-1).

The method of least squares was used to calculate the temperature gradients from the temperature-depth data. Obviously disturbed sections and the uppermost 10 meters of the boreholes (dominated by annual temperature effects) were neglected. Temperature gradients were calculated for depth intervals both above and below the water table. Depth intervals, temperature

gradients, and standard deviations of temperature gradients are summarized in Table 5-1. The standard deviations generally show the magnitude of the non-linearity of the temperature gradients.

Thermal Conductivity

Thermal conductivity values were estimated using empirical data from Robertson (1978) (see Figures 5-2 and 5-3) by assuming a thermal conductivity model of a horizontally-stratified earth composed of two homogeneous layers separated by the water table. Because thermal conductivity values may change appreciably over short horizontal distances due to facies changes and the heterogeneity of the individual lithologic units, the boreholes for which thermal conductivies had to be estimated were divided into groups according to locality. The average composition of the layers for each area were estimated from the nearest boreholes to each group with sufficiently detailed lithologic logs for adequate thermal conductivity values to be determined.

Estimated thermal conductivity values are presented in Table 5-2. Table 5-2 also contains the names of the lithologic logs used to estimate the conductivity values for each group of wells. The location of the wells from which the lithologic logs came are shown in Figure 5-1. Estimating a minimum uncertainty of ±5 percent for porosity values and ±10 percent for relative-percentage values of clay and/or quartz content, Robertson's (1978) method gives an uncertainty of at least 20 percent of the estimated thermal conductivity values. The cross-hatched areas in Figures 5-2 and 5-3 are believed to be representative of the range of most conductivity values to be found in this area.

Table 5-1. Temperature gradients and estimated heat-flow values for Dona Ana County wells (Lohse 1980).

Name	Long.	Lat.	Elev. (m)	D.I. (m)	T*** (°C/km)	Kest.*	H.F.**
Hole-1	107°00.1'	31°53.3'	1233	10-95	40.6±4.2	1.9	77±8
				95-130	24.4±0.6	3.2	78±2
Hole-2	107°00.1'	31°53.8'	1235	10-90	44.2±2.2	1.9	84±4
Hole-3	107°01.5'	31°57.0'	1254	10-30	38.6±5.2	1.9	73±10
Hole-4	107°00.3'	31°54.5'	1235	30-100	35.1±0.5	1.9	67±1
				110-130	17.4±0.5	3.2	56±2
Hole-5	107°00.8'	31°54.8'	1248	15-60	41.7±0.6	1.9	79±1
DA-1	106°39.0'	32°17.4'	1380	20-50	56.2±2.8	2.1	118±6
				55-65	15.0±2.9	3.5	53±10
DA-2	106°55.4'	31°55.4'	1227	20-25	54.0±0.1	3.2	173±10
DA-3	106°54.3'	32°00.8'	1257	10-85	88.2±15.3	1.9	168±29
				85-115	76.1±5.8	1.9	145±7
DA-4	106°52.2'	31°57.8'	1253	30-110	70.2±0.6	1.9	133±1
DA-5	106°52.9'	32°13.5'	1263	35-100	17.6±0.6	1.7	30±1
DA-6	106°51.8'	32°08.2'	1257	25-105	38.4±0.4	1.7	65±1
				110-260	15.9±0.3	2.5	40±1
NMSU-3	106°43.9'	32°17.3'	1218	10-100	51.7±0.7	2.1	109±1
				105-150	20.6±4.0	3.5	72±14
NMSU-4	106°43.0'	32°16.2'	1230	10-30	415.8±9.4	2.1	873±20
NMSU-5	106°42.9'	32°15.9'	1236	10-30	396.8±6.1	2.1	812±13
NMSU-6	106°44.1'	32°16.7'	1206	10-30	87.6±2.6	2.1	184±5
NMSU-7	106°43.6'	32°16.8'	1224	10-30	320.2±12.3	2.1	672±26
NMSU-8	106°43.2'	32°17.0'	1248	10-30	445.8±14.8	2.1	936±31
NMSU-9	106°42.8'	32°17.2'	1266	10-30	433.0±5.6	2.1	909±12
NMSU-10	106°43.6'	32°17.0'	1242	10-70	221.2±10.7	2.1	465±22
				85-145	112.9±3.0	3.5	395±11
DT-1	106°43.1'	32°17.0'	1254	10-75	302.9±8.3	2.1	636±17
				80-300	74.1±29.8	3.5	259±104
DT-2	106°43.5'	32°16.9'	1230	10-75	256.8±11.5	2.1	539±24
				80-360	7.7±2.5	3.5	27±9
LC-2	106°43.1'	32°21.2'	1310	10-125	220	2.1	462
				125-265	142	3.5	498
Hacienda Acres	106°42.5'	32°22.8'	1344	10-130	39.6±0.6	2.1	83±1
				135-340	40.3±0.0	3.5	141±0
J. ABRAM	106°45.0'	32°19.7'	1230	35-130	1.8±0.2	3.5	6±1
ST-3	106°40.7'	31°50.7'	1227	15-95	85.1±2.9	1.7	145±5
				100-180	37.9±1.3	2.5	95±3
ST-5	106°41.6'	31°51.2'	1226	15-95	45.0±3.7	1.7	77±6
				100-175	37.2±1.4	2.5	93±4
ST-6	106°41.4'	31°51.8'	1232	15-105	62.7±1.2	1.7	107±2
				105-175	29.5±1.4	2.5	74±4
ST-7	106°38.4'	31°51.4'	1140	10-20	164.0±31.2	1.7	279±53
				20-70	42.5±1.3	2.5	106±3
ST-9	106°41.4'	31°50.7'	1223	15-90	68.7±1.8	1.7	117±3
				95-170	32.5±3.0	2.5	81±8

*Units are W $m^{-1}K^{-1}$; uncertainty is about 20%. (1 W $m^{-1}K^{-1}$ = 2.39 mcal cm^{-1} sec^{-1} K^{-1})

**Units are mW m^{-2}; errors presented are due entirely to errors in temperature gradients and do not include errors in thermal conductivity values (41.8 mW m^{-2} = 1 HFU = 1 ucal cm^{-2} sec^{-1})

***Errors are standard deviations of least squares fit to temperature data over specified depth intervals.

++Thermal conductivities from Reiter, M., Shearer, C., and Edwards, C.L., Geothermal anomalies along the Rio Grande rift in New Mexico, Geology, 6, 85-88, 1978.

Table 5-1. (continued).

Name	Long.	Lat.	Elev. (m)	D.I. (m)	T*** (°C/km)	Kest.*	H.F.**
DA-7	107°01.8'	31°59.4'	1263	50-105	71.2±1.1	1.9	135±2
DA-8	106°49.8'	31°58.2'	1250	50-110	75.8±0.4	1.9	144±1
DA-9	106°56.9'	31°57.7'	1250	20-90	66.7±0.5	1.9	127±1
DA-10	107°05.3'	32°25.4'	1434	40-230	50.0±0.2	1.9	95±0
				235-250	44.1±2.8	3.2	141±9
DA-11	107°14.8'	32°24.4'	1446	10-30	74.0±3.4	1.9	141±6
				30-85	49.7±0.4	1.9	94±1
				90-115	36.6±2.6	3.2	117±8
DA-12	107°17.7'	32°22.7'	1398	10-60	84.5±6.9	1.9	161±13
				60-80	12.6±1.8	3.2	40±6
DA-13	107°14.1'	32°32.9'	1491	10-50	102.8±6.5	1.9	195±12
DA-14	106°48.1'	32°17.9'	1169		neg. gradient		
DA-15	107°12.3'	32°14.4'	1290	10-30	102.2±11.2	1.9	194±21
				30-70	46.2±1.1	3.2	148±4
DA-16	107°17.5'	32°36.2'	1353	10-25	86.4±11.6	1.9	164±22
DA-17	107°09.8'	32°35.7'	1410	10-15	42.0±0.1	3.2	134±0
DA-18	107°00.9'	32°36.1'	1200	10-15	60.0±0.1	3.2	192±0
SD-1	106°59.9'	32°37.6'	1260	10-55	277.1±18.5	1.9	526±35
				80-175	70.4±0.6	3.2	225±2
SD-2	106°58.9'	32°36.5'	1373	10-150	213.6±1.1	3.15++	673±3
SD-3	106°59.1'	32°36.3'	1388	10-150	219.8±0.9	2.93++	643±3
LA-1	106°43.6'	43°15.8'	1200	10-50	51.2±2.3	2.1	108±5
				50-85	26.1±1.4	3.5	91±5
LA-2	106°43.2'	32°16.1'	1226	10-65	322.3±7.7	2.1	677±16
				65-75	105.9±1.3	3.5	371±5
LA-3	106°43.1'	32°15.9'	1218	10-60	297.9±3.3	2.1	626±7
				60-95	129.8±4.6	3.5	454±16
[illegible]-1	106°45.0'	32°16.6'	1176		neg. gradient		
[illegible]-2	106°45.3'	32°16.2'	1178		neg. gradient		
ST-10	106°41.6'	31°49.8'	1223	10-105	66.8±1.9	1.7	114±3
				105-170	35.8±2.6	2.5	90±7
ST-12	106°39.4'	31°52.7'	1149	10-25	100.8±18.2	1.7	171±31
				25-40	48.4±1.5	2.5	121±4
ST-14	106°42.7'	31°51.3'	1233	20-100	54.7±3.3	1.7	93±6
				100-145	29.9±0.6	2.5	75±2
ST-15	106°39.1'	31°52.1'	1146	10-25	160.0±23.1	1.7	272±39
				25-35	32.0±0.0	2.5	80±0
ST-21	106°37.3'	31°50.3'	1143	10-25	194.6±10.2	1.7	331±17
				25-85	36.1±1.4	2.5	90±4
ST-23	106°36.8'	31°50.1'	1137	15-25	171.0±5.2	1.7	291±9
				25-85	34.9±1.1	2.5	87±3
ST-25	106°41.8'	31°52.1'	1233	15-105	69.7±2.1	1.7	118±4
				105-175	31.3±1.1	2.5	78±3
ST-26	106°42.3'	31°52.3'	1233	10-105	79.2±2.4	1.7	135±4
				105-140	35.6±0.5	2.5	89±1
ST-27	106°40.9'	31°51.5'	1226	10-100	67.4±0.8	1.7	115±1
				100-160	21.6±0.8	2.5	54±2
ST-28	106°39.7	31°51.7'	1191	10-40	124.6±4.2	1.7	212±7
				40-65	36.9±1.5	2.5	92±4
ST-29	106°41.2'	31°51.1'	1224	10-95	66.6±0.9	1.7	113±2
				95-140	33.5±0.8	2.5	84±2
ST-30	106°40.4'	31°50.4'	1224	10-100	87.0±1.5	1.7	148±3
				100-170	32.8±1.9	2.5	82±5
ST-31	106°39.8'	31°50.2'	1218	20-100	71.5±0.8	1.7	122±1
				100-120	25.2±4.2	2.5	63±11

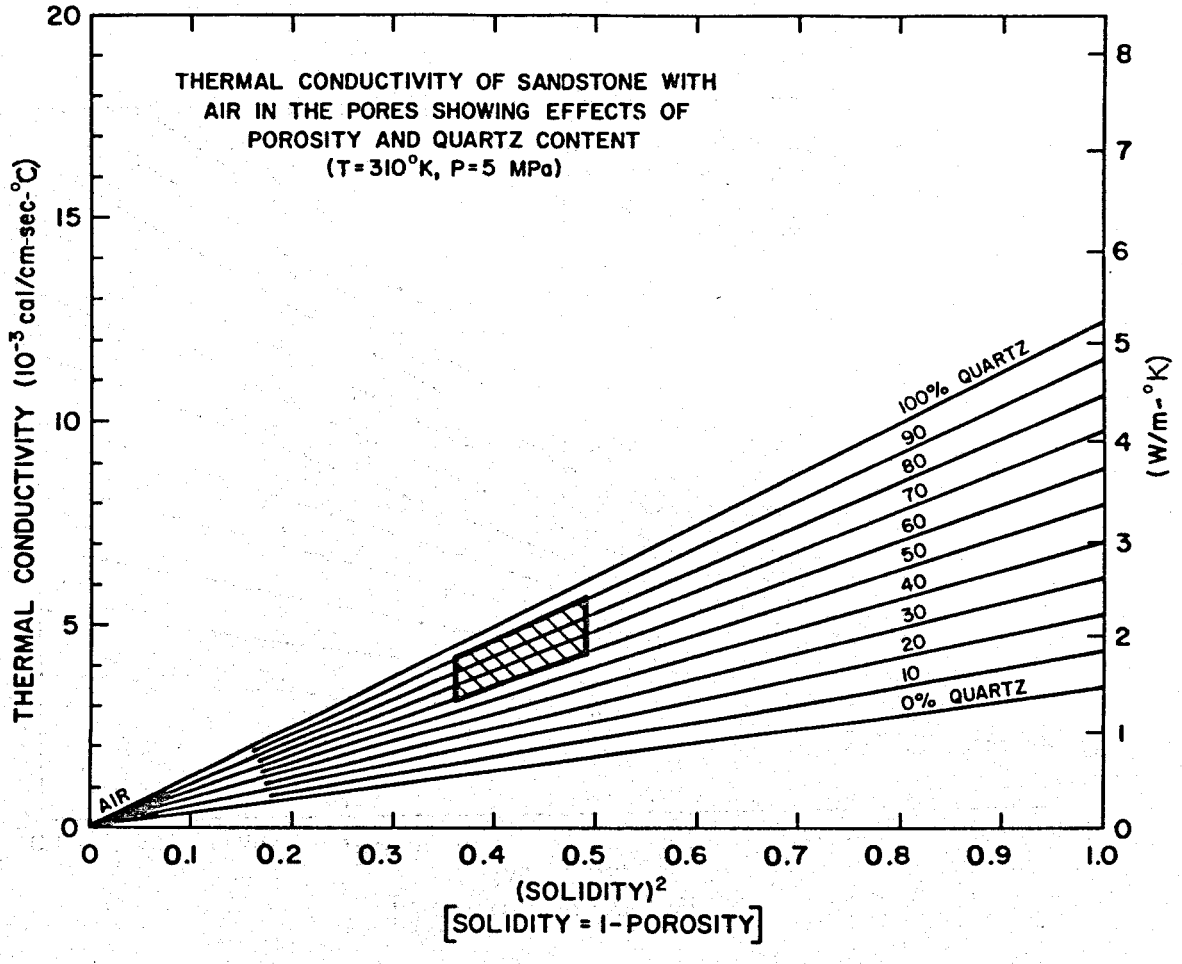

Figure 5-2. Figure constructed from empirical data by Robertson (1978) used for the purpose of estimating thermal conductivities above the water table. Cross-hatched area shows range of most values thought to exist in Dona Ana County.

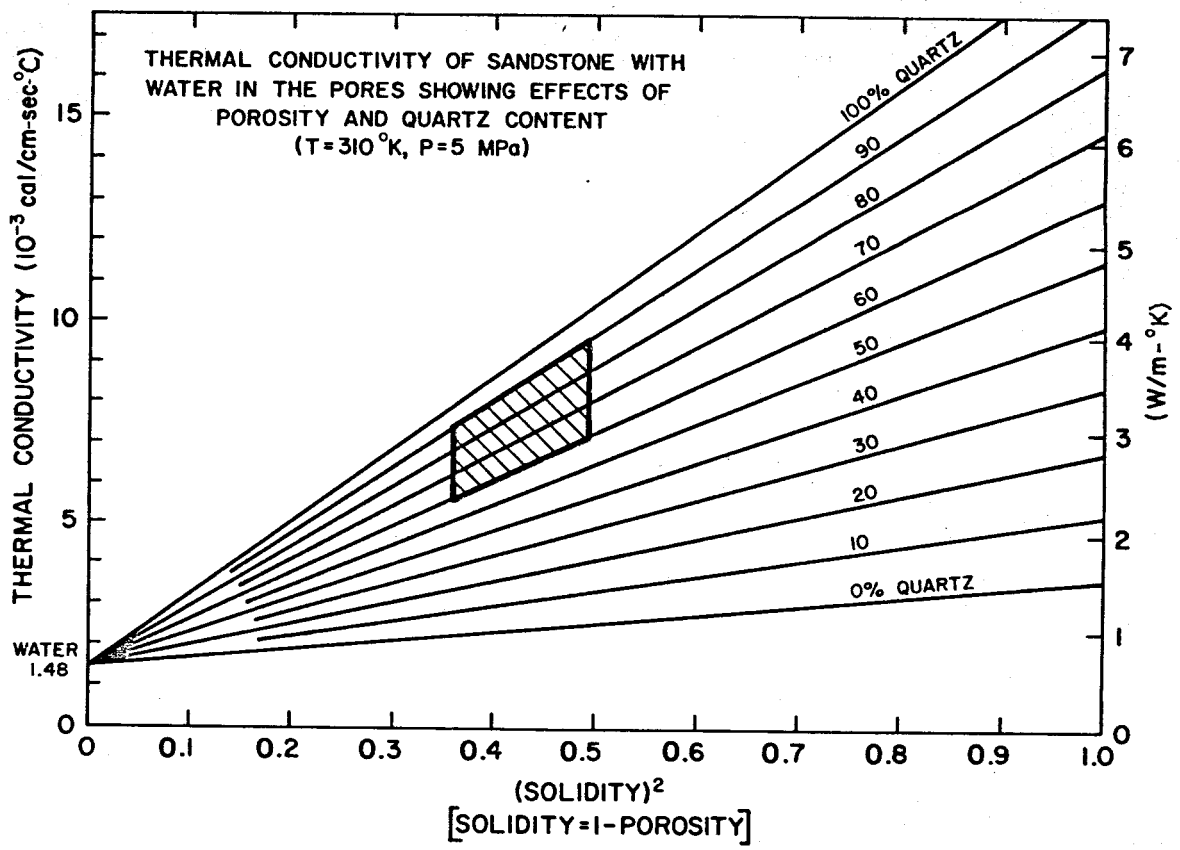

Figure 5-3. Figure constructed from empirical data by Robertson (1978) used for the purpose of estimating thermal conductivities below the water table. Cross-hatched area shows range of most values thought to exist in Dona Ana County.

Table 5-2. Estimated thermal-conductivity values (Lohse 1980).

Wells	Thermal Conductivity (mWm^{-2}) (above water table)	(below water table)	Well Logs Used
Hole-1	1.9	3.2	Texaco S.H. Weaver Federal no. 1
Hole-2	1.9	3.2	
Hole-3	1.9	3.2	
Hole-4	1.9	3.2	
Hole-5	1.9	3.2	
DA-2	1.9	3.2	
DA-3	1.9	3.2	
DA-4	1.9	3.2	
DA-7	1.9	3.2	
DA-8	1.9	3.2	
DA-9	1.9	3.2	
DA-10	1.9	3.2	
DA-11	1.9	3.2	
DA-12	1.9	3.2	
DA-13	1.9	3.2	
DA-15	1.9	3.2	
DA-16	1.9	3.2	
DA-17	1.9	3.2	
DA-18	1.9	3.2	
SD-1	1.9	3.2	
SD-2	3.15*		Reiter et al. (1978)
SD-3	2.93*		
J. ABRAM	2.1	3.5	DT-1 DT-2
DA-1	2.1	3.5	
DA-14	2.1	3.5	
LA-1	2.1	3.5	
LA-2	2.1	3.5	
LA-3	2.1	3.5	
NMSU-1	2.1	3.5	
NMSU-2	2.1	3.5	

*Actual measured values.

Table 5-2. (continued).

Wells	Thermal Conductivity (mWm^{-2}) (above water table)	(below water table)	Well Logs Used
NMSU-3	2.1	3.5	
NMSU-4	2.1	3.5	
NMSU-5	2.1	3.5	
NMSU-6	2.1	3.5	
NMSU-7	2.1	3.5	
NMSU-8	2.1	3.5	
NMSU-9	2.1	3.5	DT-1
NMSU-10	2.1	3.5	DT-2
DT-1	2.1	3.5	
DT-2	2.1	3.5	
Hacienda Acres	2.1	3.5	
LC-2	2.1	3.5	
ST-3	1.7	2.5	
ST-5	1.7	2.5	
ST-6	1.7	2.5	La Union 700
ST-7	1.7	2.5	
ST-9	1.7	2.5	Anapra 450
ST-10	1.7	2.5	
ST-12	1.7	2.5	Southern Pacific
ST-14	1.7	2.5	RR Company Lizard
ST-15	1.7	2.5	Well
ST-21	1.7	2.5	
ST-23	1.7	2.5	Southern Pacific
ST-25	1.7	2.5	RR South Lizard
ST-26	1.7	2.5	Well
ST-27	1.7	2.5	
ST-28	1.7	2.5	
ST-29	1.7	2.5	
ST-30	1.7	2.5	
ST-31	1.7	2.5	
DA-5	1.7	2.5	El Paso Natural Gas Well
DA-6	1.7	2.5	Asarco La Mesa Test Well

Heat Flow

Conductive heat-flow values (see Table 5-1) were calculated as simple products of temperature gradients and thermal-conductivity values. Heat-flow values were determined for depths above and below the water table. Heat-flow values above the water table are shown in Figure 5-4. A histogram (see Figure 5-5) of the heat-flow values above the water table shows a modal class of 100 to 150 mWm^{-2} (2.4 to 3.6 HFU) and a range from less than -42 to 672 mWm^{-2} (-1 to 16 HFU). In areas of high-density data, average values are used so as not to bias the regional heat-flow values towards certain localities. Comparison of conductive heat-flow values from above and below the water table at individual sites show that the Las Alturas and San Diego Mountain areas have an appreciable convective component of heat-flow below the water table.

Some anomalously low heat-flow values and all negative heat-flow values (wells DA-14, NMSU-1, and NMSU-2) are located in or near the Rio Grande drainage system. Low heat-flow values of 30 and 65 mWm^{-2} (0.75 and 1.5 HFU) are associated with wells DA-5 and DA-6, respectively, and are located in the north end of the Mesilla Bolson. Very high heat-flow values (400 mWm^{-2} = 9.5 HFU) are found in the San Diego Mountain and in the Las Alturas areas. A recent city well, LC-2 (see Figure 5-1), drilled by the City of Las Cruces, located roughly 7 km (4.5 miles) north of the Las Alturas geothermal wells, has a high heat-flow value (450 mWm^{-2} = 10.8 HFU) and has a bottom-hole temperature of 67.9°C at 265 m (154°F at 883 ft).

Because of the density of data in the Las Alturas and Santa Teresa area, blow-ups of each area are shown. Figures 5-6 and 5-7 show the well positions and heat-flow values above the water table (based on Table 5-3) for the Las Alturas area. Figures 5-8 and 5-9 show the well positions and heat-flow values above the water table for the Santa Teresa area. There is a definite

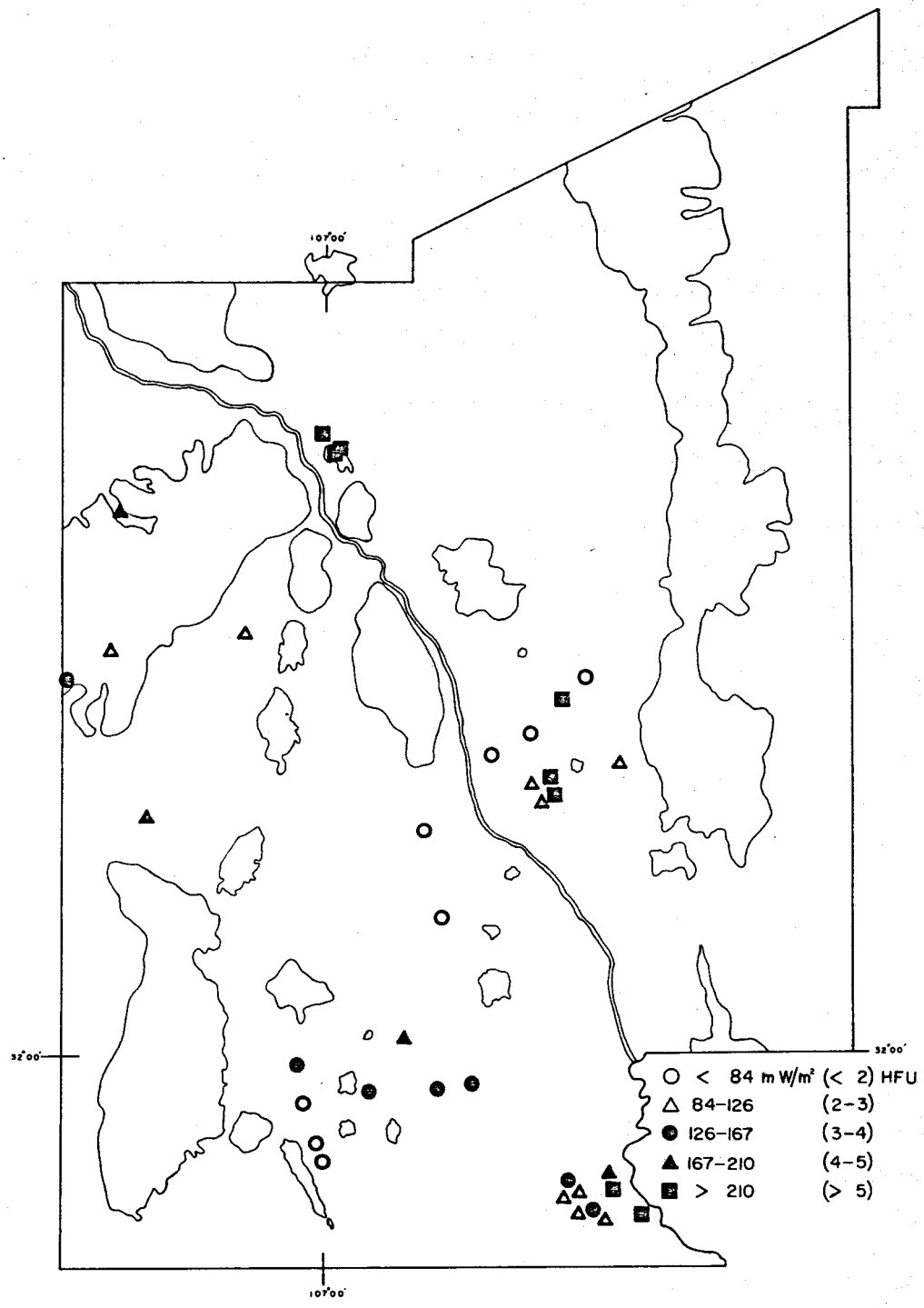

Figure 5-4. Locations and magnitudes of heat-flow values from above the water table in Dona Ana County (Lohse 1980).

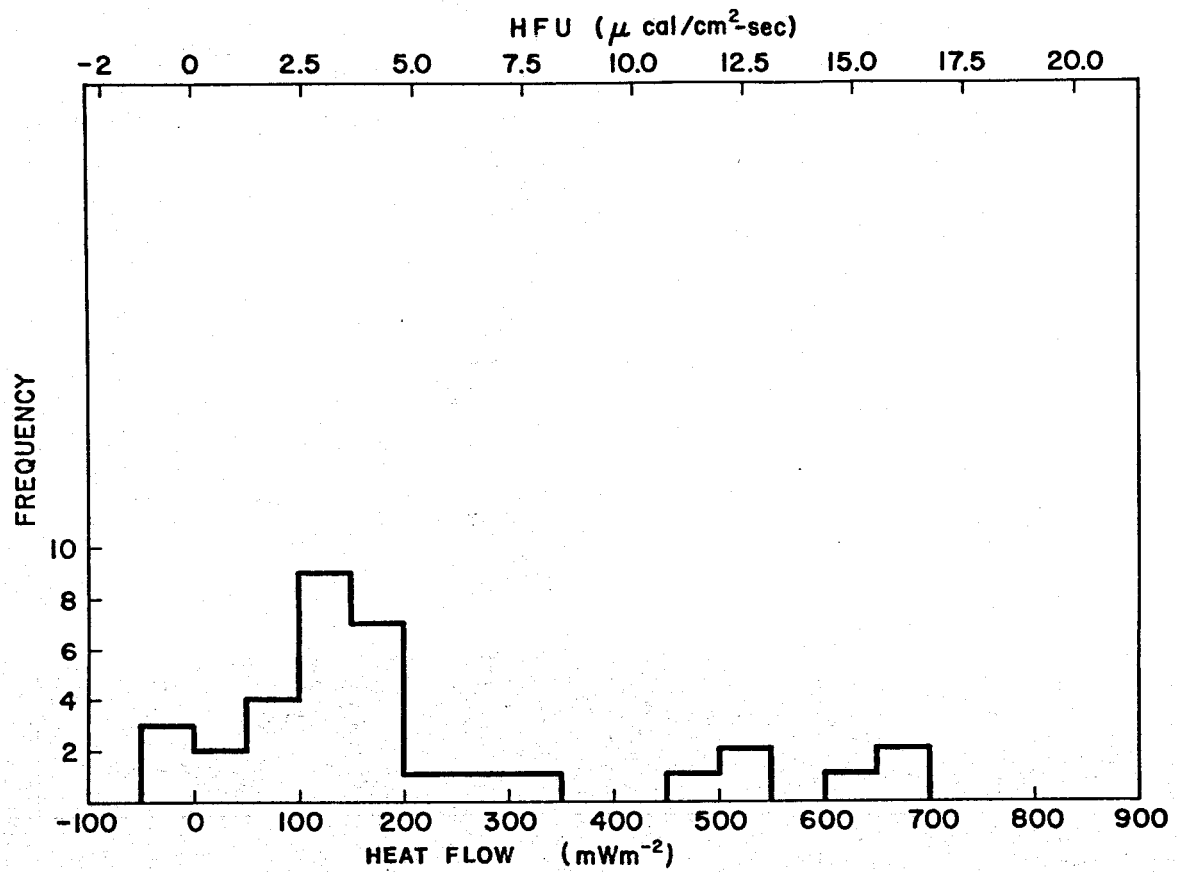

Figure 5-5. Histogram of heat-flow values from above the water table in Dona Ana County (Lohse 1980).

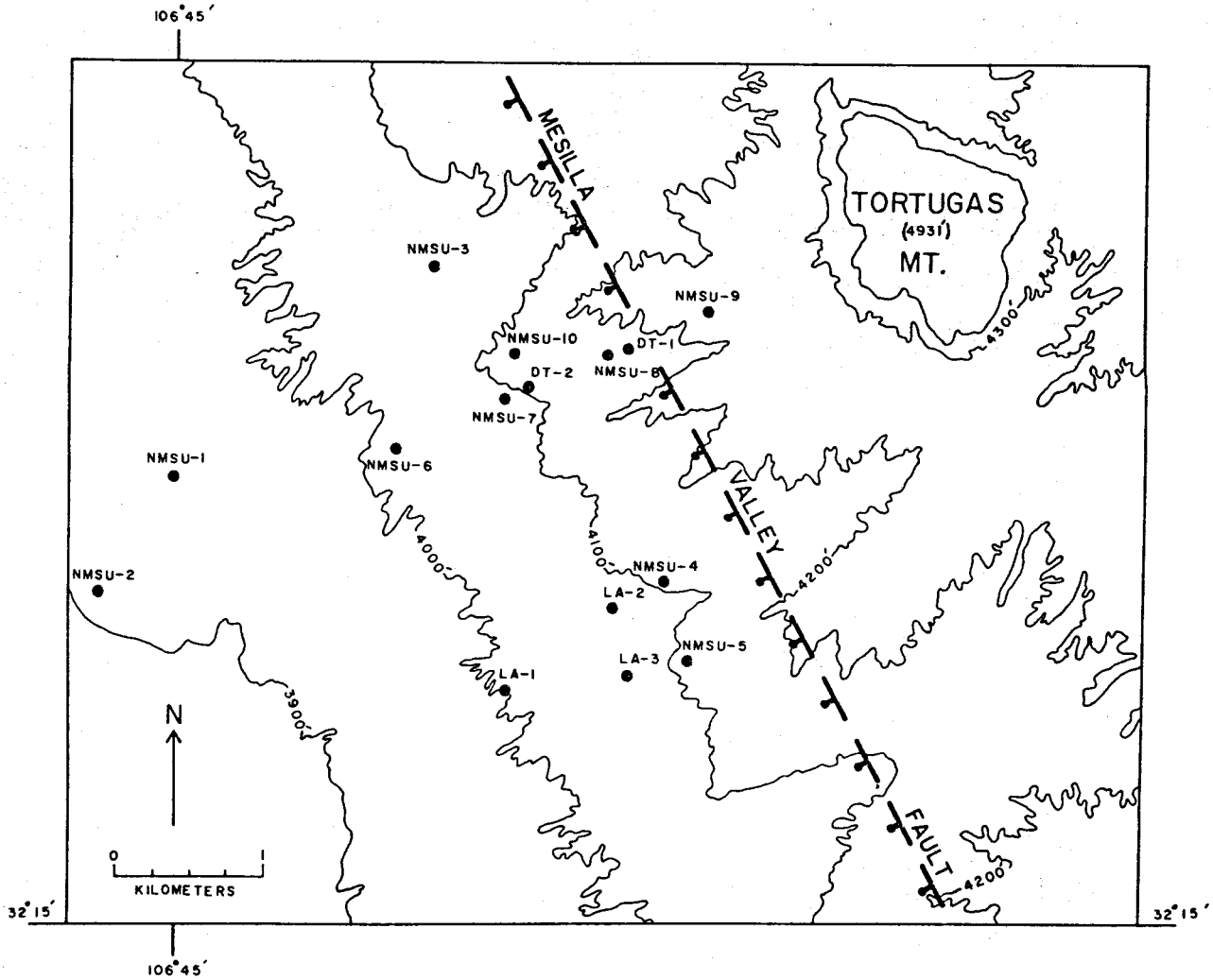

Figure 5-6. Location of temperature-logged wells in the Las Alturas area (Lohse 1980).

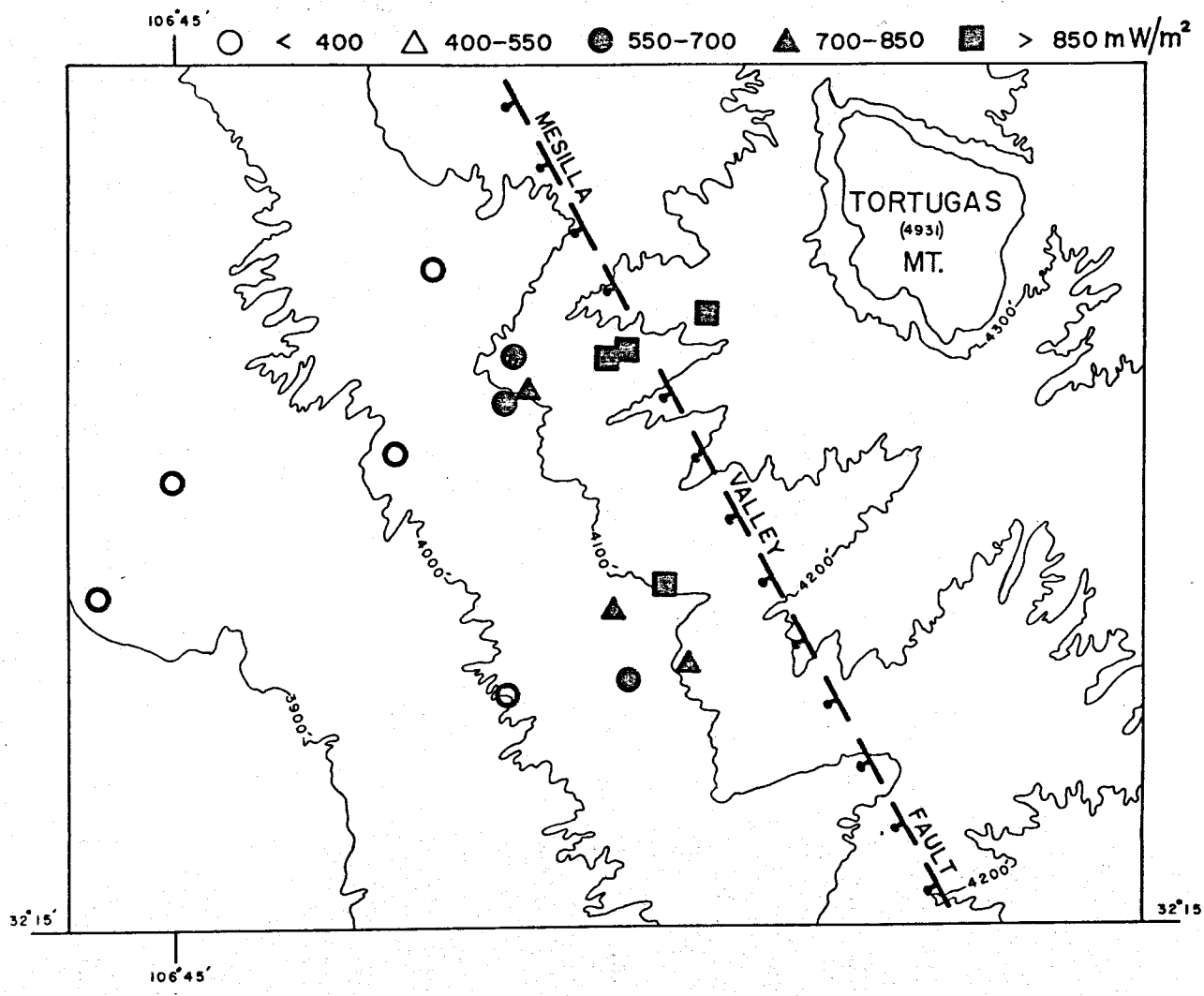

Figure 5-7. Heat-flow values from above the water table in the Las Alturas area. For comparison, only the upper 30 to 40 meters of the deeper holes were used (see Table 5-3) (Lohse 1980).

Table 5-3. Near-surface heat-flow values used for the Las Alturas area (Lohse 1980).

Well	Depth Interval (m)	Temperature Gradient (°C/km)	Thermal Conductivity* ($Wm^{-1}K^{-1}$)	Heat Flow** ($mW\ m^{-2}$)
LA-1	10 - 35	44	2.1	92
LA-2	10 - 30	378	2.1	794
LA-3	10 - 40	275	2.1	578
NMSU-1	-------	†	---	neg
NMSU-2	-------	†	---	neg
NMSU-3	10 - 35	53	2.1	111
NMSU-4	10 - 30	416	2.1	874
NMSU-5	10 - 30	387	2.1	813
NMSU-6	10 - 30	88	2.1	185
NMSU-7	10 - 30	320	2.1	672
NMSU-8	10 - 30	446	2.1	937
NMSU-9	10 - 30	433	2.1	909
NMSU-10	10 - 30	324	2.1	680
DT-1	10 - 30	411	2.1	863
DT-2	10 - 30	393	2.1	825

*1 $Wm^{-1}K^{-1}$ = 2.39 mcal $cm^{-1}sec^{-1}K^{-1}$ (thermal-conductivity values estimated)

**41.8 $mW\ m^{-2}$ = 1 $\mu cal\ cm^{-2}\ sec^{-1}$ = 1 HFU

†Wells have negative gradients.

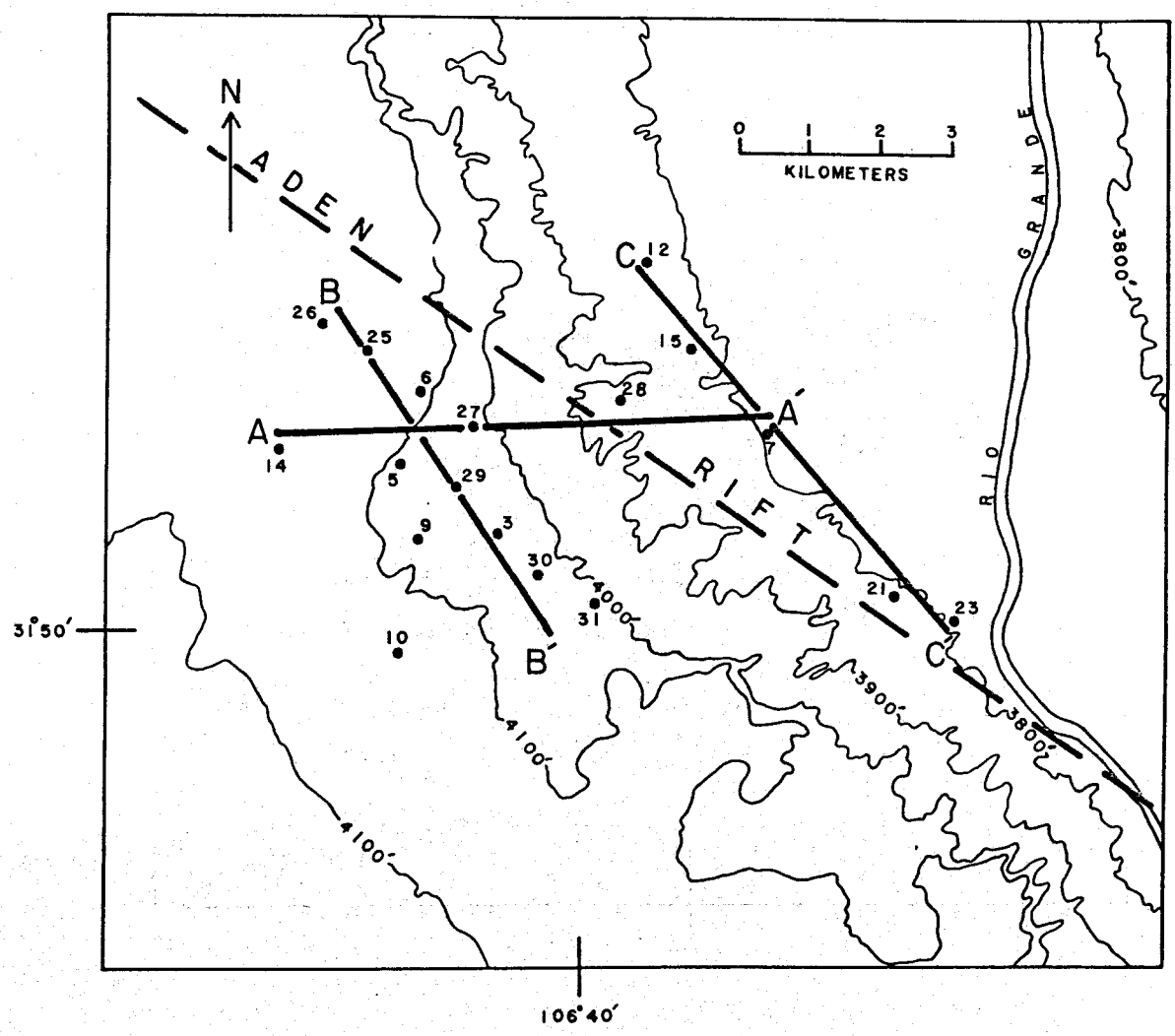

Figure 5-8. Locations of temperature-logged wells in the Santa Teresa area. The numbers refer to the ST series of wells tabulated in Table 5-2. Also shown are the profiles along which the simple geologic section of Figure 5-15 were taken and the approximate location of the Aden Rift (Hoffer 1975).

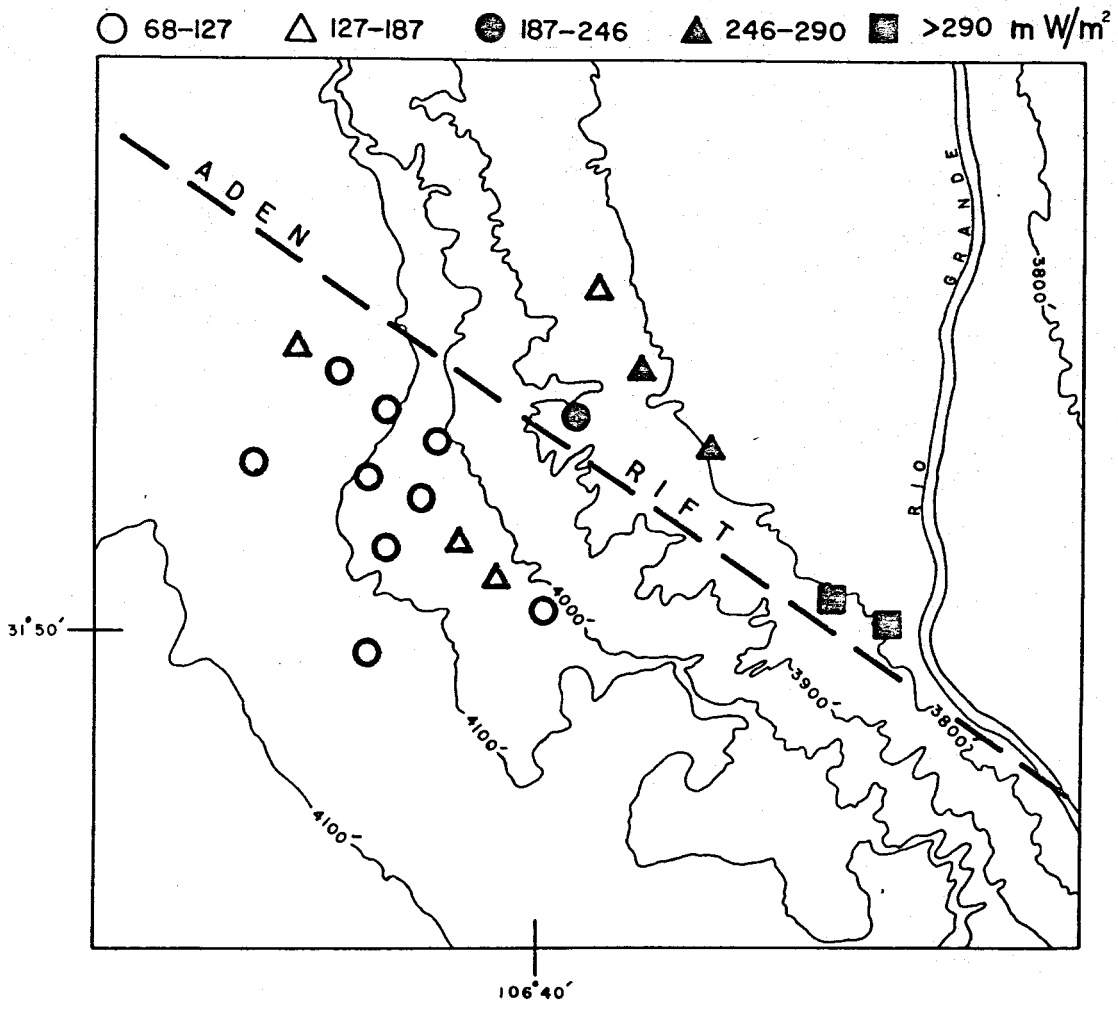

Figure 5-9. Heat-flow values from above the water table in the Santa Teresa area (Lohse 1980).

increase in heat-flow values in the Las Alturas area (see Figure 5-7) as one approaches the suspected position of the valley fault. The increase in heat-flow values in the Santa Teresa area (see Figure 5-9) from west to east may be misleading. The increase in heat-flow values is believed to be due to a large decrease in the thickness of the overburden above the water table which is at a near constant temperature. This situation causes an increase in the temperature gradient and, hence, an increase in heat flow.

Bottom-Hole Temperature Gradients

An effort was made to supplement the heat-flow data with bottom-hole temperature data in order to better understand the thermal regime of the county. An estimated surface temperature and measured bottom-hole temperatures and depth were used to calculate bottom-hole temperature gradients (see Figure 5-10). Temperature-depth profiles suggest that a large discrepancy exists between the regional mean air temperature (15.6°C) and near-surface (five meters) temperatures. Consequently, a surface temperature of 20°C was estimated by projecting temperature gradients back to the surface. The surface temperature has an estimated accuracy of about one or two degrees Centigrade. The bottom-hole temperatures and depths come from three sources: (1) the USGS Water Quality File, WATSTORE, evaluated by Swanberg (1980), (2) bottom-hole oil well data compiled by Chaturvedi (1980), and (3) data collected for this study. The data from the first and third sources are tabulated in Tables 5-4 and 5-5, respectively. Only the positive gradients are tabulated from the USGS WATSTORE File. All the negative gradients (i.e., all the wells with bottom-hole temperatures less than 20°C) are associated with the cold under flow of the Rio Grande. No tabulation of the precise locations of the data from Chaturvedi (1980) is presently available, although the locations are plotted on base maps from which they were taken.

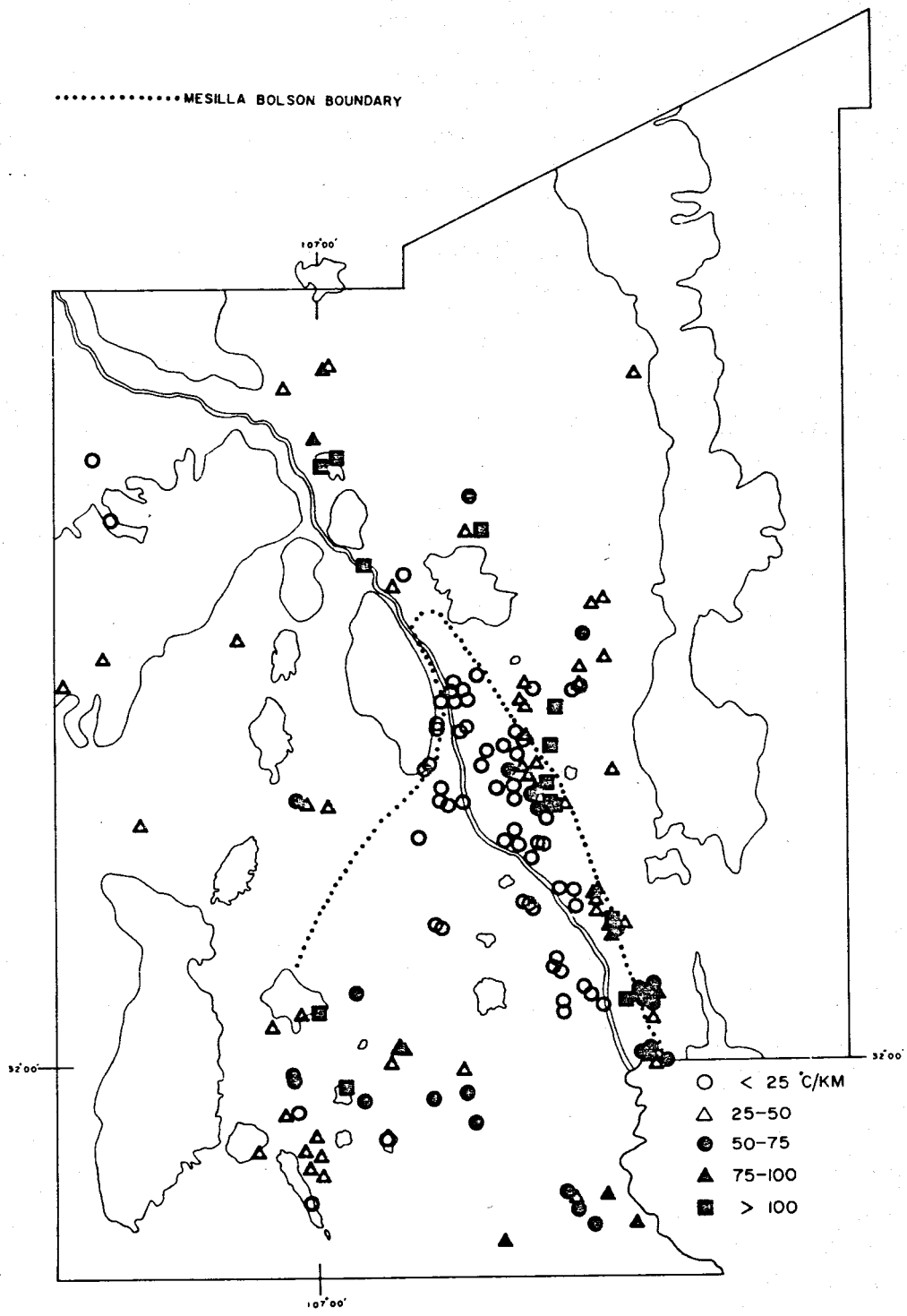

Figure 5-10. Bottom-hole temperature gradient map of Dona Ana County. A surface temperature of 20°C has been used and, with the exception of a few wells, most wells are less than 300 meters deep (Lohse 1980).

Table 5-4. Wells from the USGS WATSORE file # (Swanberg 1980).

Longitude	Latitude	Depth to Bottom-Hole Temperature * (m)	Bottom-hole Temperature (BHT)* (°C)	Gradient from BHT** (°C/km)
106°51'	31°54'	138	27.0	51
107°00'	31°56'	183	28.0	44
106°36'	32°00'	64	24.5	70
106°44'	32°14'	73	20.5	7
106°45'	32°19'	223	24.0	18
106°44'	32°18'	128	25.0	39
106°43'	32°16'	148	27.0	47
107°01'	32°16'	320	36.0	50
106°40'	32°10'	122	25.0	41
106°39'	32°09'	76	31.5	151
106°39'	32°08'	79	27.5	95
106°36'	32°04'	171	27.0	41
106°40'	32°04'	186	22.0	11
106°36'	32°00'	123	24.0	33
106°37'	32°04'	153	31.0	72
106°38'	32°49'	306	31.0	36
106°48'	32°18'	610	21.0	2
106°59'	32°42'	116	25.0	43
106°45'	32°10'	213	21.5	7
106°49'	32°23'	99	21.5	15
106°45'	32°24'	213	25.0	23
106°36'	32°02'	82	23.5	43
106°49'	32°23'	215	20.5	2
106°47'	32°18'	52	21.5	29
106°47'	32°18'	24	22.0	83
106°59'	32°42'	118	25.0	43
106°45'	32°18'	152	24.0	26
107°02'	32°42'	79	23.0	38
106°54'	32°29'	284	23.5	12
106°41'	32°23'	358	28.0	22
106°45'	32°23'	305	26.0	20
107°15'	32°37'	101	22.0	20
106°40'	32°28'	161	25.0	31
106°55'	32°29'	32	21.0	31

Only the wells with bottom-hole temperatures above 20°C appear in this table.

*The measured temperature of the flowing water at the well head is assumed to be the same as the temperature of the water at the depth from which it came. The depth of the wells is usually obtained from casing records.

**Bottom-hole gradients were calculated using a surface temperature of 20°C.

Table 5-5. Water-table temperatures and bottom-hole temperature gradients for Dona Ana County (Lohse 1980).

Name of Well	Depth to Water Table (m)	Temperature of Water Table (°C)	Depth to Bottom-Hole Temperature (m)	Bottom-Hole Temperature (BHT) (°C)	Gradient (BHT)* (°C/km)
Hole-1	95	24.79	130	25.63	43
Hole-2	90	24.25	95	24.31	45
Hole-3	ǂ	>20.00	30	20.29	10
Hole-4	105	25.70	130	26.13	47
Hole-5	ǂ	>22.00	60	22.50	42
DA-2	20	19.99	25	20.26	10
DA-3	ǂ	>28.00	115	31.20	97
DA-4	ǂ	>23.00	110	27.15	65
DA-7	ǂ	>23.00	110	27.04	64
DA-8	ǂ	>28.00	115	28.55	74
DA-9	ǂ	>23.00	90	26.79	75
DA-5	110	21.55	110	21.55	14
DA-6	110	23.88	260	26.17	24
DA-10	230	29.97	250	30.77	43
DA-11	90	22.87	115	23.71	32
DA-12	60	23.69	80	23.93	49
DA-13	ǂ	>19.00	50	19.83	†
DA-15	30	21.16	70	22.94	42
DA-16	ǂ	>19.00	25	19.19	†
DA-17	10	19.10	15	19.31	†
DA-18	10	17.33	15	17.63	†

Table 5-5. (continued).

Name of Well	Depth to Water Table (m)	Temperature of Water Table (°C)	Depth to Bottom-Hole Temperature (m)	Bottom-Hole Temperature (BHT) (°C)	Gradient (BHT)* (°C/km)
SD-1	60	28.56	175	35.98	91
SD-2	ǂ	>52.00	150	51.76	212
SD-3	ǂ	>53.00	150	52.70	218
LA-1	55	23.76	80	24.49	56
LA-2	65	40.26	80	41.42	268
LA-3	60	37.59	100	42.18	222
NMSU-1	25	21.26	90	20.32	4
NMSU-2	25	18.26	25	18.26	†
NMSU-3	70	24.26	150	28.09	54
NMSU-4	ǂ	>32.00	30	32.11	404
NMSU-5	ǂ	>32.00	30	32.31	410
NMSU-6	ǂ	>22.00	30	22.37	79
NMSU-7	ǂ	>30.00	30	30.27	342
NMSU-8	ǂ	>34.00	30	34.07	469
NMSU-9	ǂ	>33.00	30	33.37	446
NMSU-10	75	38.70	145	47.62	190
DT-1	80	48.04	300	62.43	141
DT-2	80	42.93	360	49.61	82
DA-1	55	22.86	65	23.01	46
DA-14	10	20.77	100	17.80	†
J. ABRAM	45	21.13	130	21.33	10
HACIENDA ACRES	120	24.54	340	33.39	39
LC-1	130	53	235	54	145
LC-2	125	48.00	265	67.90	181
ST-3	100	26.55	175	29.33	53
ST-5	100	26.43	175	29.16	52

Table 5-5. (continued).

Name of Well	Depth to Water Table (m)	Temperature of Water Table (°C)	Depth to Bottom-Hole Temperature (m)	Bottom-Hole Temperature (BHT) (°C)	Gradient (BHT)* (°C/km)
ST-6	105	26.52	175	28.71	50
ST-7	20	24.43	70	26.60	94
ST-9	95	26.33	165	28.67	53
ST-10	105	26.85	165	29.02	55
ST-12	25	24.93	55	25.92	108
ST-14	100	27.01	160	28.43	53
ST-15	25	24.95	80	26.06	76
ST-21	25	24.98	85	27.34	86
ST-23	25	25.04	85	27.24	85
ST-25	105	27.32	175	29.66	55
ST-26	105	27.67	140	28.90	64
ST-27	100	26.64	155	27.90	51
ST-28	40	25.52	65	24.40	98
ST-29	95	26.77	150	28.41	56
ST-30	100	26.75	170	29.34	55
ST-31	100	27.17	115	27.53	65

*Bottom-hole gradients were calculated using a surface temperature of 20°C.

†Bottom-hole gradients are negative.

‡Wells did not penetrate the water table.

There are several trends in the geographical distribution of bottom-hole temperature gradients which can be seen in Figure 5-10: (1) abnormally low and/or negative temperature gradients associated with the northern part of the Mesilla Bolson; (2) a north-northwesterly trend of abnormally high temperature gradients along the eastern boundary of the Mesilla Bolson; (3) a west-northwesterly trend of high gradients bounded by more normal gradients across the southern part of the Mesilla Bolson; and (4) anomalously high gradients associated with San Diego Mountain, Radium Springs, and the Las Alturas known geothermal areas.

Discussion

Suspected large groundwater flow, flow patterns, and permeabilities suggest that the abnormally low or negative bottom-hole temperature gradients and heat-flow values in and the northern part of the Mesilla Bolson may be due to local recharge and intrabasin groundwater flow. Figure 5-11 shows the probable direction of groundwater flow based on the water-table contour map of King et al. (1971). Groundwater moves in the direction of least hydraulic head from areas of recharge to areas of discharge (i.e., perpendicular to the water-table contours). Also included in Figure 5-11 are the groundwater divides (resulting mainly from the groundwater reservoirs, the Miocene to Middle Pleistocene basin fill, being uplifted above the present water table), groundwater barriers (uplifted bedrock), and the temperature of the water level encountered in the boreholes (see Table 5-5). Groundwater in the Mesilla Bolson is recharged from the north end of the basin and generally flows south. King et al. (1971) report that permeabilities are greatest in the north and generally decrease to the south and with depth. They also report internal drainage in the basin and that, although most of the

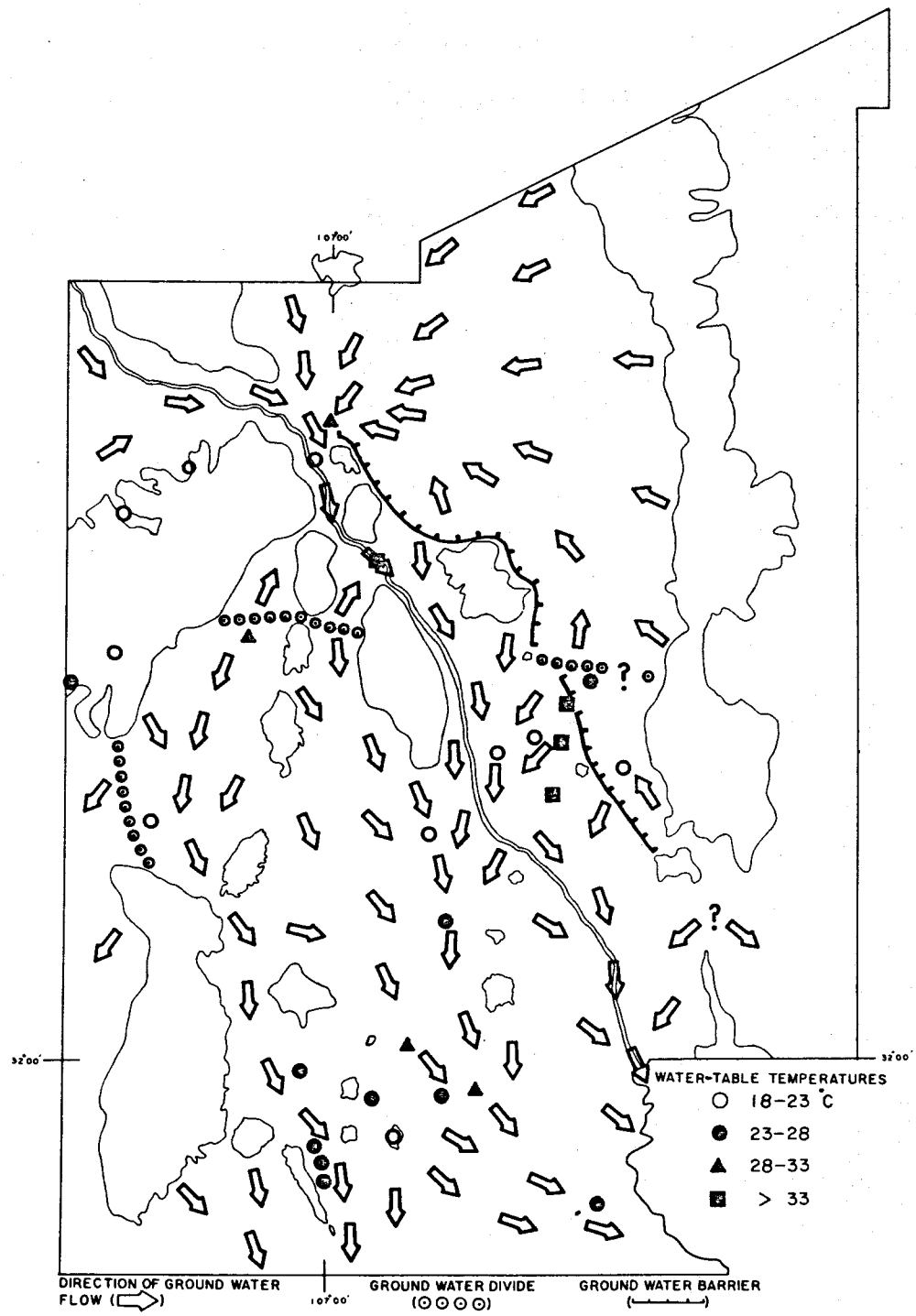

Figure 5-11. Hydrologic map of Dona Ana County (after King et al. 1971).

natural recharge to the groundwater reservoirs in the county come from only a few percent of the annual percipitation, it is generally sufficient to cause groundwater movement from the basin towards the Rio Grande Valley drainage system. The reversals of temperature gradients for wells DA-14, NMSU-1, and NMSU-2 and the abnormally low-temperature gradients of wells DA-5, DA-6, and J. ABRAMS suggest that groundwater movement and/or recharge is sufficient to cause significant temperature disturbances in the boreholes.

Figure 5-12 is a complete Bouguer gravity anomaly map of the county based on the Bouguer gravity anomaly map by Cordell et al. (1978). There is a strong correspondence between positive anomalies (-140 to -115 mgals) and mountains and/or uplifts and negative anomalies (-160 to -180 mgals) and deep sedimentary basins (compare Figures 5-1 and 5-12). There is a zone of moderate gravity values (-150 mgals) between the basins which could reflect suspected elevated bedrock in this area with respect to the deep basins. The negative gravity anomaly (see Figure 5-12) which corresponds to the Mesilla Bolson suggests that the deepest part of the basin is in the more permeable north end. King et al. (1971) report as much as 1150 meters of sandy-to-gravelly Santa Fe basin fill in the central part of the Mesilla Bolson (based on data from the Grimm Well shown in Figure 5-1).

Gravity profiles and late Pliocene-Pleistocene and late Quaternary fault patterns (see Figure 5-13) suggest that the mountains and/or uplifts and deep basins are bounded by faults. The fault patterns in Figure 5-13 are based on Callender and Seager (1980) and show where faults cut late Pliocene-Pleistocene and late Quaternary surfaces. Figure 5-13 also includes the approximate boundaries of the Mesilla Bolson and southern Jornada del Muerto intrarift basins based on gravity data (see Figure 5-12) and on data by Seager and Morgan (1979).

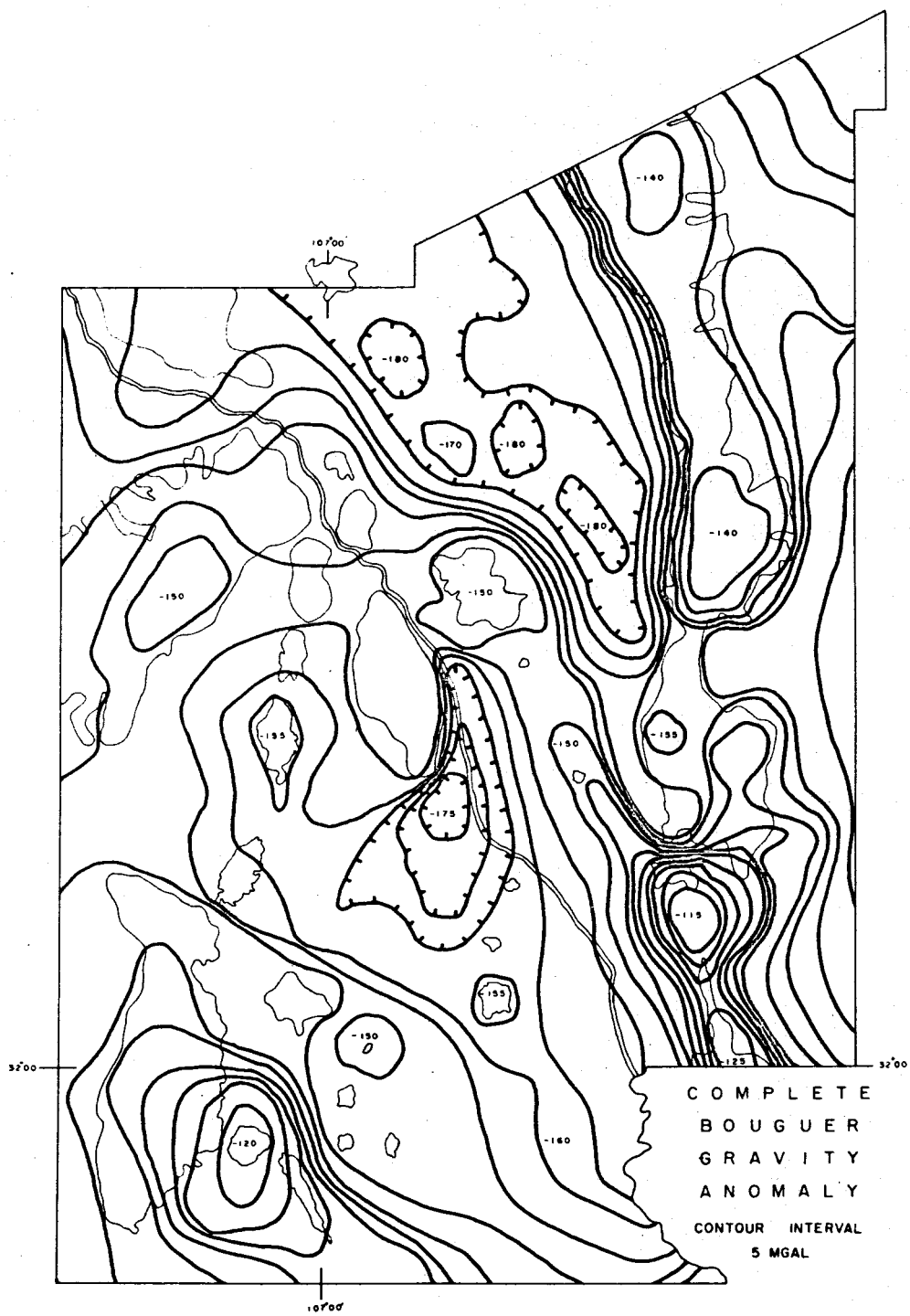

Figure 5-12. Complete Bouguer gravity anomaly map of Dona Ana County (after Cordell et al. 1978).

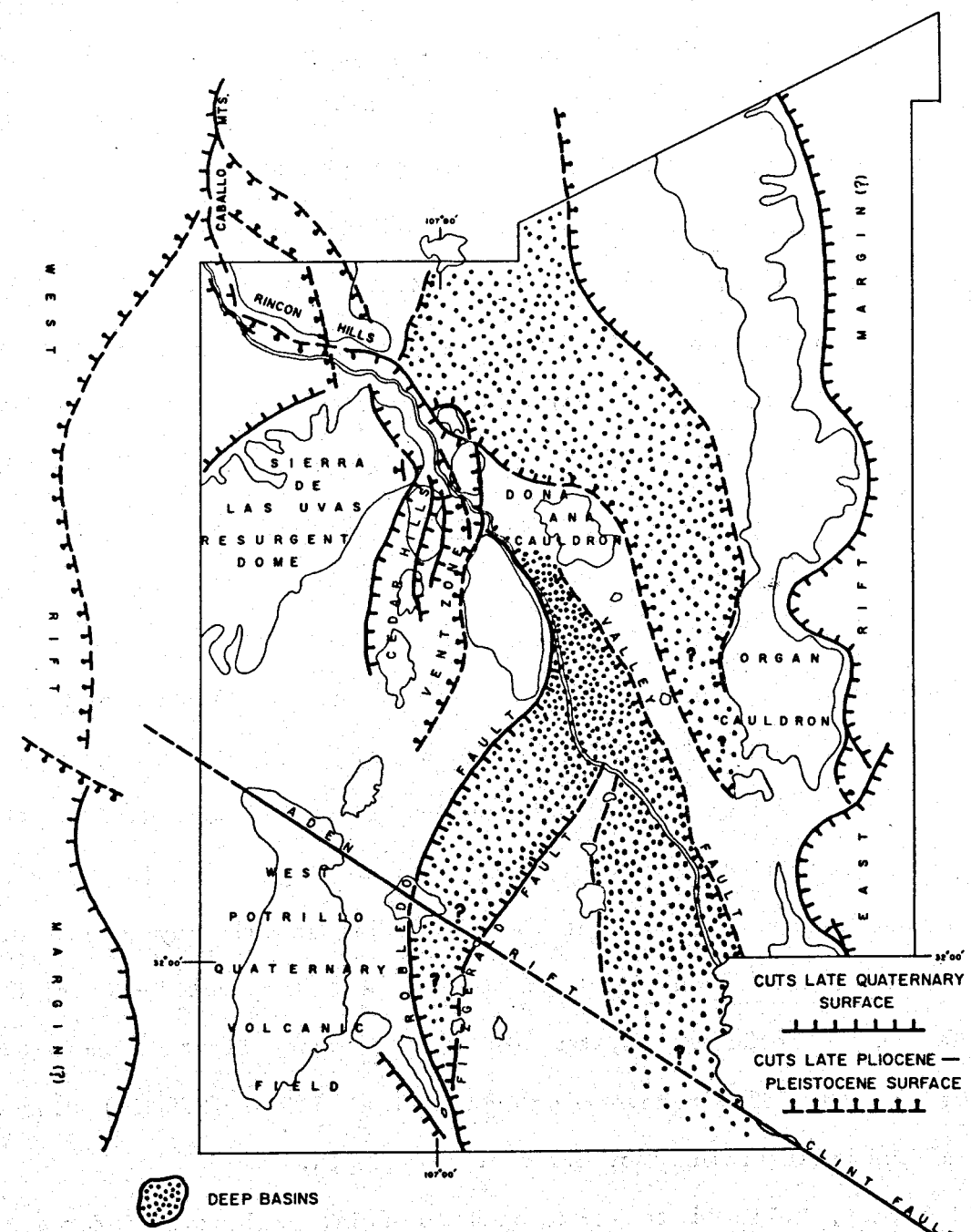

Figure 5-13. Tectonic map of Dona Ana County (late Pliocene to Pleistocene and late Quaternary faults (Callender and Seager 1980)). Aden Rift is after Hoffer (1975).

It appears there exists a spatial relationship between high heat-flow values (see Figure 5-4), the north-northwesterly trend of high bottom-hole temperature gradients (see Figure 5-10), a steep gravity gradient associated with a north-northwesterly trending positive gravity anomaly (see Figure 5-12), and the valley fault (see Figure 5-13). This spatial relationship is also supported by anomalous geochemical data (Swanberg 1975) and other geophysical data (see Figure 5-14). Figure 5-14 shows the areas in the county which are characterized by high subsurface temperatures predicted by SiO_2 and Na-K-Ca geothermometers, low electrical-resistivity anomalies, and high magnetic anomalies. The geochemical data are from Swanberg (1975); the electrical-resistivity data are from Jackson and Bisdorf (1975), Hoover and Tippens (1975), O'Donnell et al. (1975), and Young (1979, 1980); the magnetic data are from Cordell (1975), Seager (1978), and Keller (1979).

The valley fault is thought to pass through the Las Alturas geothermal anomaly (see Figure 5-6). Swanberg (1975) and Morgan et al. (1979) suggest that the geothermal anomaly is due to a fault-controlled hydrothermal system. The geographic location of a recently drilled and temperature logged well, LC-2 (see Figure 5-1), suggests that the geothermal anomaly may be somewhat larger in areal extent than first estimated, and temperature-depth data suggest that the geothermal system is warmer than first anticipated. Temperatures of 68°C (155°F) have been obtained at 265 m (885 ft) with no indication of the well turning isothermal at this depth.

The Aden Rift, believed to be related to a late Paleozoic deformation along the Clint Fault (see Figure 5-13), is located across the southwest corner of the county (Hoffer 1975; Uphoff 1978). The extension of this structural feature across the southern part of the Mesilla Bolson is suggested by a west-northwesterly trend of high bottom-hole temperature gradients

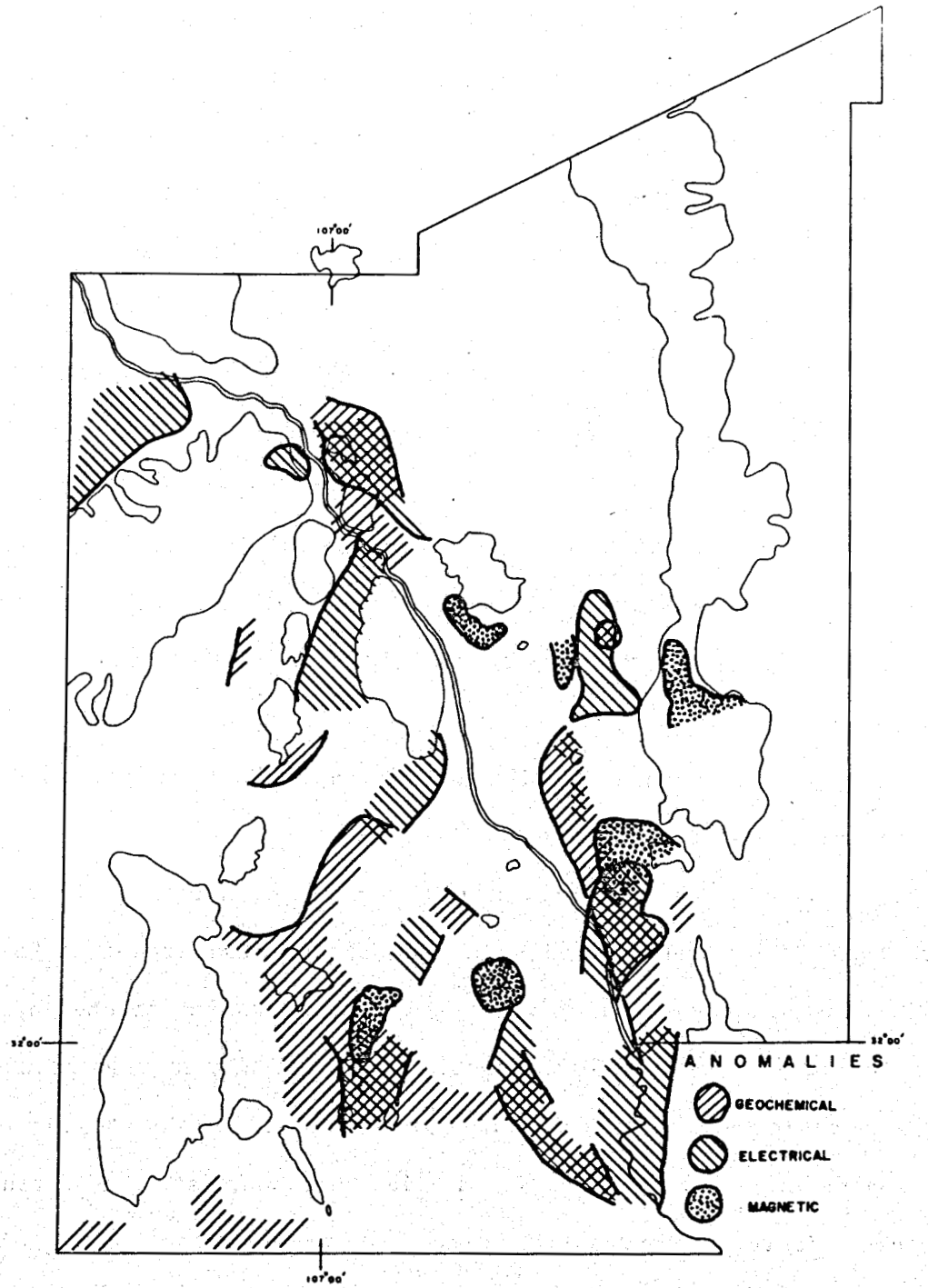

Figure 5-14. Geophysical anomaly map of existing data for Dona Ana County. Geochemical anomalies show high subsurface temperatures; electrical anomalies show highly conductive zones; and magnetic anomalies show areas with relatively higher magnetic values than surrounding areas (Lohse 1980).

bounded by more normal values (see Figure 5-10). This anomalous trend runs parallel to and on-line between the Clint Fault and Aden Rift. The existence of this structural feature is also suggested by anomalous geochemical data (see Figure 5-14). There is high heat flow (see Figure 5-4) in the Gardner Cones area (see Figure 5-1), which is situated at the intersection of the Fitzgerald Fault and the Aden Rift (see Figure 5-13). Low electrical resistivity and high magnetic anomalies (see Figure 5-14) are also associated with this area, although the electrical anomaly is more closely associated with the Fitzgerald Fault. Aden Crater, a middle-to-late Pleistocene basalt flow (Seager 1980), is located at the intersection of the Robledo Fault and the Aden Rift (see Figure 5-13). A low electrical-resistivity anomaly is associated with the Robledo Fault (see Figure 5-14) in this area. Additional evidence comes from gravity data (see Figure 5-12), which suggest that a west-northwesterly, positive gravity anomaly across the southwest corner of the county may be structurally related to the Aden Rift. Gravity data also show a wedging out of the Mesilla Bolson basin fill to the south in the general vicinity of the Aden Rift.

Some interesting observations should be noted with respect to the well at Gardner Cones (DA-3) and the wells in the Santa Teresa area (see Figures 5-1 and 5-8). The upper portion of well DA-3 appears to be affected by recharge and, at the same time, the lower portion exhibits higher temperatures and a linear temperature gradient. This observation could be due to the existence of an impermeable layer, such as a clay horizon, at the depth of the temperature increase preventing the recharge water from disturbing temperatures below this horizon. The Aden Rift is also thought to pass through the Santa Teresa area (see Figures 5-8 and 5-9).

An apparent dropping off of the temperature gradients seen in wells ST-14, ST-29, ST-31, ST-12, and ST-28 appears to be associated with an impermeable clay layer(s). This layer is shown in Figure 5-15 which shows the cross sections along the three profiles indicated in Figure 5-8. The cross sections show the present topography, water table, and a distinguishable clay horizon seen in the lithologic logs from the Santa Teresa wells. The data used for the construction of Figure 5-15 are tabulated in Table 5-6. The profiles from wells ST-6, ST-9, ST-25, ST-15, ST-21, and ST-23 show temperature gradients which correspond to the clay horizon. It is believed that this disturbance of the temperature gradients is due to a grouting problem associated with the water wells (i.e., there seems to be communication of groundwater between individual water-bearing strata).

Wells in the San Diego Mountain area (SD-1, SD-2, and SD-3 of Figure 5-1) have abnormally high heat flow (see Figure 5-4) and bottom-hole temperature gradients (see Figure 5-10). Temperatures greater than 50°C have been reported (Summers 1976) at the Radium Springs hot springs (see Figure 5-1). Travertine deposits are reported by Seager (1975) in the San Diego Mountain area. The deposits have been estimated by Seager (1980) to be late Pleistocene to early Holocene.

The main tectonic features in this northwestern part of the county are the Sierra de Las Uvas resurgent dome and the Cedar Hills Vent Zone (see Figure 5-13). Seager (1975) reported there is evidence from the stratigraphy of the bottom deposits of the Miocene intrarift basins (displayed in the uplifted blocks of the San Diego Mountain, the Rincon Hills, and the East and West Selden Hills areas) and from the structure itself to suggest that the Sierra de Las Uvas and the Cedar Hills Vent Zone areas have undergone intermittent uplift throughout the Miocene and Pliocene. Fault patterns (see

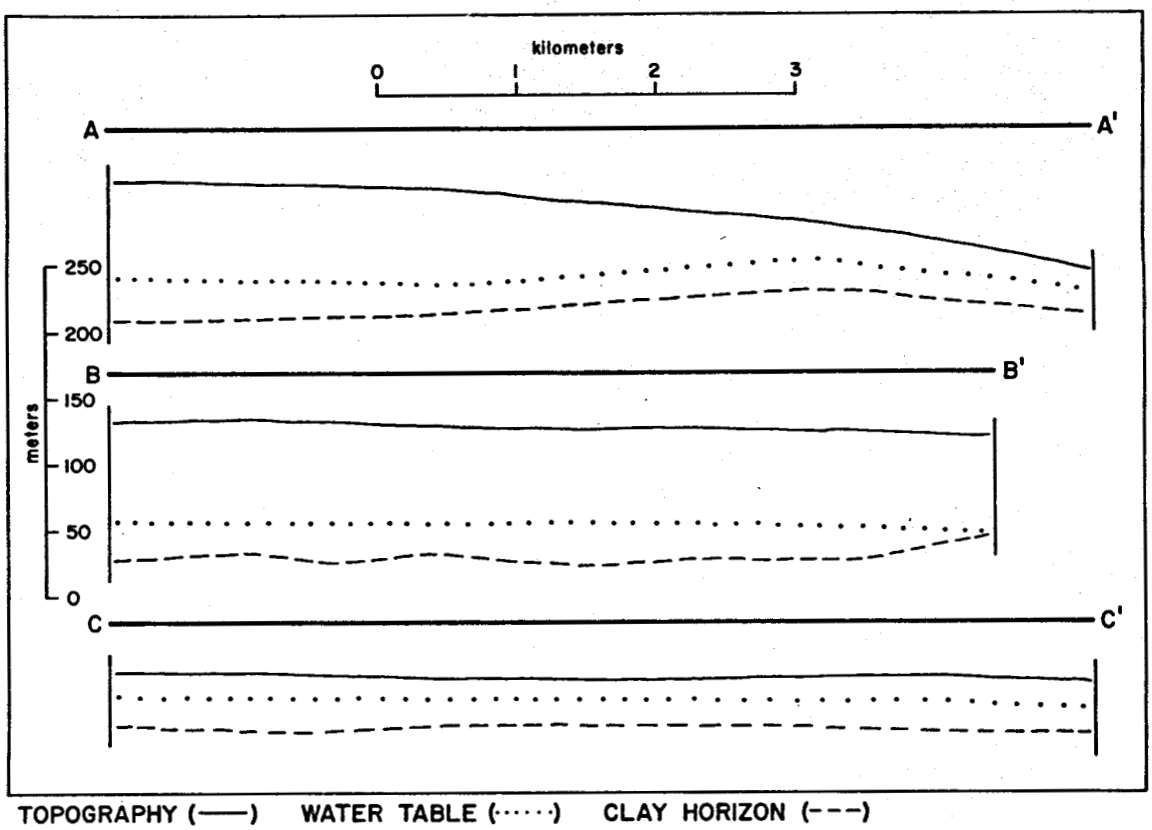

Figure 5-15. Simple geologic cross sections of the Santa Teresa area showing topography, water table, and a clay horizon.

Table 5-6. Depths to the water table and a particular clay horizon for the Santa Teresa area (Lohse 1980).

Borehole	Depth to the Water Table* (m)	Depth to the Clay Horizon* (m)
ST-3	106	141
ST-5	107	137
ST-6	106	146
ST-7	113	138
ST-9	105	135
ST-10	105	130
ST-12	109	139
ST-14	100	145
ST-15	112	147
ST-21	115	145
ST-23	121	146
ST-25	105	135
ST-26	105	>140
ST-27	107	137
ST-28	82	112
ST-29	104	149
ST-30	109	144
ST-31	115	115

*Measured from a datum of 1233 meters above sea level.

Figure 5-13) suggest that uplift of these areas and the Caballo Mountain-Rincon Hills continued throughout the late Pliocene-Pleistocene and late Quaternary. Faults cutting late Quaternary surfaces (see Figure 5-13) suggest that subsidence of the Mesilla Bolson, contemporaneous with uplift of the Sierra de Las Uvas and Cedar Hills Vent Zone areas, may have occurred into the late Pleistocene and Holocene.

Geophysical data (see Figure 5-14) show a possible relation between faults (see Figure 5-13) and low electrical-resistivity anomalies and anomalously high subsurface temperatures predicted by SiO_2 and Na-K-Ca geothermometers in the San Diego Mountain area.

Conclusion

Conductive heat-flow values from above the water table have a modal class of 100 to 150 mWm^{-2} (2.4 to 3.6 HFU) and a range from less than -42 to +672 mWm^{-2} (-1 to +16 HFU). The large range in heat-flow values is believed attributed to cool groundwater recharge and lateral groundwater flow, which causes a reduction in heat flow, and upward convecting warm and hot water, which increases surface heat flow.

The geographic distribution of bottom-hole temperature gradients shows a strong spatial relationship between abnormally low bottom-hole temperature gradients and the interior of the Mesilla Bolson, an intrarift basin, and also between abnormally high bottom-hole temperature gradients and the boundaries of the Mesilla Bolson.

Large groundwater flow, flow patterns, and large permeabilities suggest that the abnormally low heat-flow values and bottom-hole temperature gradients associated with the interior of the Mesilla Bolson are due in part to groundwater recharge, but mostly are due to a large volume of intrabasin

groundwater flow, which enters the basin in the north from the Rio Grande and generally flows in a southernly direction throughout the basin.

Early-to-late Quaternary faults generally have a spatial relationship with intrarift basin boundaries, abnormally high heat-flow values and bottom-hole temperature gradients, and anomalous geophysical data. Because of this spatial relatonship, a fault-controlled hydrothermal system(s) is favored as the mechanism and cause of the anomalous data.

Early-to-late Quaternary fault patterns plus ongoing fault-controlled hydrothermal activity suggest that a downwarping of the Mesilla Bolson is occurring with respect to adjacent lands (in particular, the Sierra de Las Uvas and Robledo Moutain areas) and is structurally controlled by the Mesilla Valley Fault, Robledo Fault, and the Aden Rift.

References

Callender, J., and Seager, W., 1980, Quaternary and late Pliocene geology, in Icerman, L., Starkey, A., and Trentman, N., eds., State-coupled low-temperature geothermal resource assessment program, fiscal year 1979: New Mexico Energy Institute at New Mexico State University, p. 6-1 - 6-4.

Chapin, C. E., 1971, The Rio Grande Rift, Part I: Modifications and additions, in 22 Field Conference Guidebook: New Mexico Geological Society, p. 191-202.

Chapin, C. E., and Seager, W., 1975, Evolution of the Rio Grande Rift in the Socorro and Las Cruces areas, in 26th Field Conference Guidebook: New Mexico Geological Society, p. 297-321.

Chaturvedi, L., 1980, Geothermal hydrology, in Icerman, L., Starkey, A., and Trentman, N., eds., State-coupled low-temperature geothermal resource assessment program, fiscal year 1979: New Mexico Energy Institute at New Mexico State University, p. 8-1 - 8-22.

Cordell, L., 1975, Combined geophysical studies at Kilbourne Hole maar, New Mexico, in 26th Field Conference Guidebook: New Mexico Geological Society, p. 269-271.

Cordell, L., Keller, G. R., and Hildenbrand, T. G., 1978, Complete Bouger gravity anomaly map of the Rio Grande Rift: U.S. Geological Survey, unpublished report.

Hoffer, J. M., 1975, A note on the volcanic features of the Aden Crater area, southcentral New Mexico, in 26th Field Conference Guidebook: New Mexico Geological Society, p. 131-134.

Hoover, D. B., and Tippens, C. L., 1975, A reconnaissance audio-magnetotelluric survey at Kilbourne Hole, New Mexico, in 26th Field Conference Guidebook: New Mexico Geological Society, p. 277-278.

Jackson, D. B., and Bisdorf, R. J., 1975, Direct-current soundings on the La Mesa surface near Kilbourne and Hunt's holes, New Mexico, in 26th Field Conference Guidebook: New Mexico Geological Society, p. 273-275.

Keller, G. R., 1979, Aeromagnetic map of Tortugas Mountain, Dona Ana County, New Mexico: New Mexico Bureau of Mines and Mineral Resources, Open-File Report 110.

King, W. E., Hawley, J. W., Taylor, A., and Wilson, R., 1971, Geology and groundwater resources of central and western Dona Ana County, New Mexico: New Mexico Bureau of Mines and Mineral Resources, Hydrologic Report 1.

Lohse, R. L., 1980, Heat-flow study of Dona Ana County, southern Rio Grande Rift, New Mexico: New Mexico State University, Las Cruces, New Mexico, M. S. thesis, 101 pp.

Morgan, P., Swanberg, C. A., and Lohse, R. L., 1979, Borehole temperature studies of the Las Alturas Geothermal Anomaly, New Mexico: Geothermal Resources Council, Transactions, v. 3, p. 79-288.

O'Donnell, J. E., Martinez, R., and Williams, J., 1975, Telluric current soundings near Kilbourne and Hunt's holes, New Mexico, in 26th Field Conference Guidebook: New Mexico Geological Society, p. 279-280.

Reiter, M., Shearer, C., and Edwards, C., 1978, Geothermal anomalies along the Rio Grande Rift in New Mexico: Geology, v. 6, p. 85-88.

Robertson, E., 1978, Thermal conductivities of rocks: U.S. Geological Society, Open-File Report.

Seager, W., 1975, Cenozoic tectonic evolution of the Las Cruces area, New Mexico, in 26th Field Conference Guidebook: New Mexico Geological Society, p. 241-250.

Seager, W., 1978, Supplemental log no. 2: Organ and Dona Ana calderas, in Field guide to selected cauldrons and mining districts of the Datil-Mogollon volcanic field, New Mexico: New Mexico Geological Society, Special Publication No. 7, p. 73-82.

Seager, W., 1980, Personal communication, New Mexico State University, Las Cruces, New Mexico.

Seager, W., and Brown, L., 1978, The Organ Caldera, in Field guide to selected cauldrons and mining districts of the Datil-Mogollon volcanic field, New Mexico: New Mexico Geological Society, Special Publication No. 7, p. 139-149.

Seager, W., and Morgan, P., 1979, The Rio Grande Rift in southern New Mexico, west Texas, and northern Chihuahua, in Riecker, R. E., ed., Rio Grande Rift, Tectonics and magmatism: American Geophysical Union, Washington, D.C., p. 87-106.

Summers, W., 1976, Catalog of thermal waters in New Mexico: New Mexico Bureau of Mines and Mineral Resources, Hydrologic Report 4, 80 pp.

Swanberg, C. A., 1975, Detection of geothermal components in groundwaters of Dona Ana County, southern Rio Grande Rift, New Mexico, in 26th Field Conference Guidebook: New Mexico Geological Society, p. 175-180.

Swanberg, C. A., 1980, Subsurface temperatures of geothermal resources, Catalog of thermal waters, in Icerman, L., Starkey, A., and Trentman, N., eds., State-coupled low-temperature geothermal resource assessment program, fiscal year 1979: New Mexico Energy Institute at New Mexico State University, p. 1-18 - 1-30.

Uphoff, T., 1978, Subsurface stratigraphy and structure of the Mesilla and Hueco bolsons, El Paso region, Texas and New Mexico: University of Texas at El Paso, M.S. thesis, 66 pp.

Young, C., 1979, Electrical exploration for geothermal resources near San Diego Mountain, New Mexico: New Mexico Energy Institute at New Mexico State University, NMEI Report 48.

Young, C., 1980, Geothermal exploration with electrical methods near Vado, Chamberino, and Mesquite, New Mexico, in Icerman, L., Starkey, A., and Trentman, N., eds., State-coupled low-temperature geothermal resource assessment program, fiscal year 1980: New Mexico Energy Institute at New Mexico State University, p. 4-1 - 4-18.

Part 2

Preliminary Heat-Flow Assessment of Southeast Luna County, New Mexico*

Luna County, New Mexico, (see insert, Figure 5-16) lies adjacent to Dona Ana County on the west. Characteristically, Luna County has the same tectonics and geomorphology as Dona Ana County (see Chapter 5, Part 1). Northwesterly-trending faults are late Pliocene or Pleistocene. There are also late Quaternary north-south faults present. These two sets of faults control the structure of the basins and uplifts. The basins are deep and filled with Quaternary alluvium. The basin fill is generally permeable and, as is also the case in Dona Ana County, lateral-groundwater flow is believed to be substantial, especially in well-pumped areas.

Six wells were temperature logged in the southeastern portion of Luna County (see Figure 5-16). A comparison of bottom-hole temperature gradients (see Table 5-7) shows an increase toward the east and decrease to the west. The temperature profiles (see Figure 5-17) indicate that the subsurface temperatures are the warmest for the wells to the east, Luna-1 and Luna-2. Luna-3 has the coolest near-surface temperatures. The temperature-log data and the curvature of the temperature profiles suggest that wells Luna-3, Luna-4, and Luna-5 are influenced by lateral groundwater flow. These wells are temporarily abandoned water wells and Luna-3 and Luna-5 are situated in the center of large irrigation areas. Because irrigation areas are

*The principal authors of Chapter 5, Part 2 are Richard L. Lohse, Staff Engineer, New Mexico Energy Institute at New Mexico State University, Dr. Paul Morgan, Staff Scientist, Lunar and Planetary Institute, Houston, Texas, and Dr. Chandler A. Swanberg, Associate Professor of Physics and Earth Sciences, New Mexico State University.

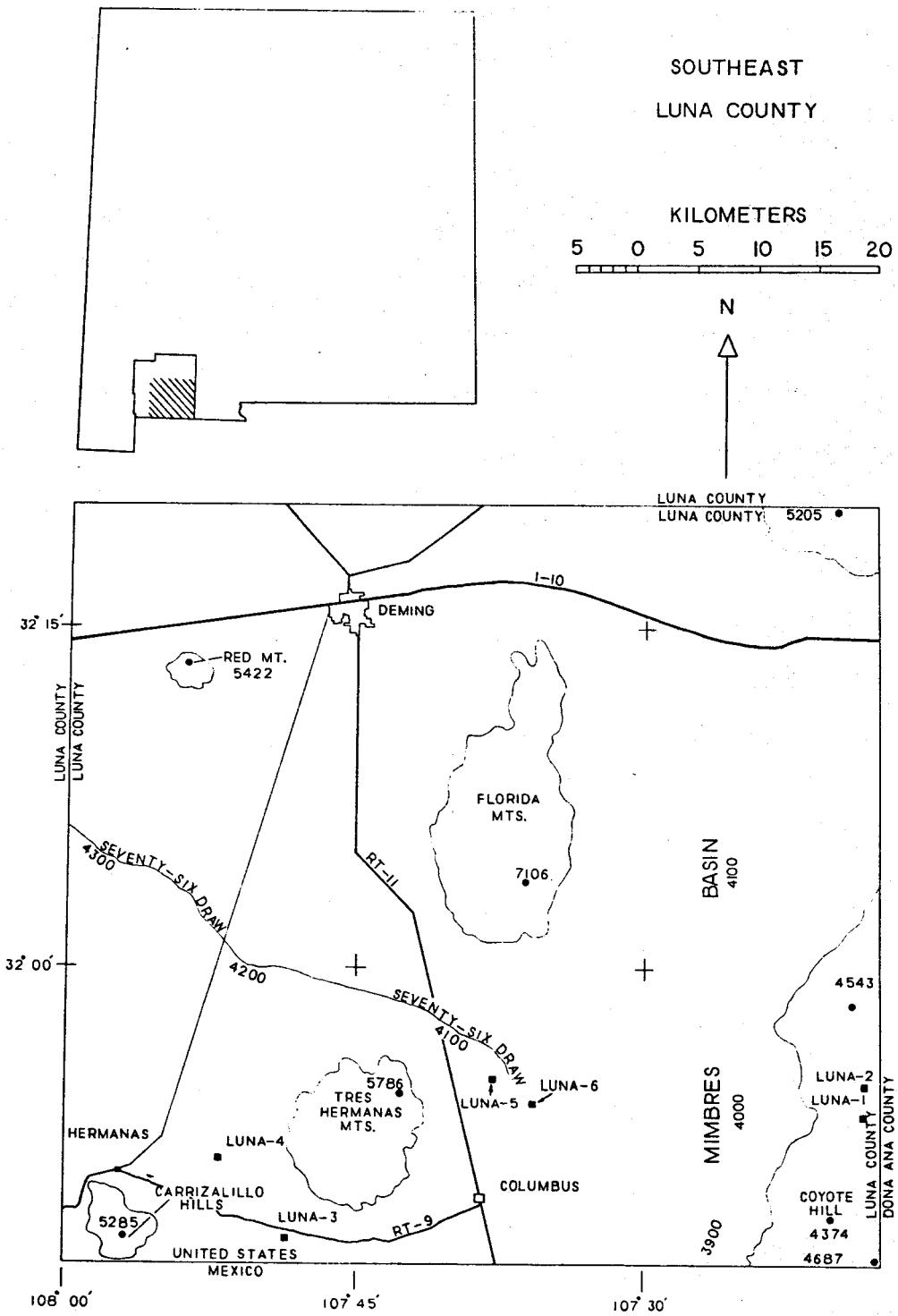

Figure 5-16. Location map for southeast Luna County and the locations of the six temperature-logged wells.

Table 5-7. Water-table and bottom-hole temperature data for southeast Luna County.

Well Name	Depth to Water Table (m)	Bottom-hole Depth (m)	Bottom-hole Temperature (°C)	Bottom-hole Temperature Gradient* (°C/km)
Luna-1	85	175	28.9	51
Luna-2	80	85	25.6	66
Luna-3	80	95	22.4	25
Luna-4	>70	70	21.6	22
Luna-5	80	90	23.3	37
Luna-6	90	185	26.1	33

*A surface temperature of 20°C was assumed.

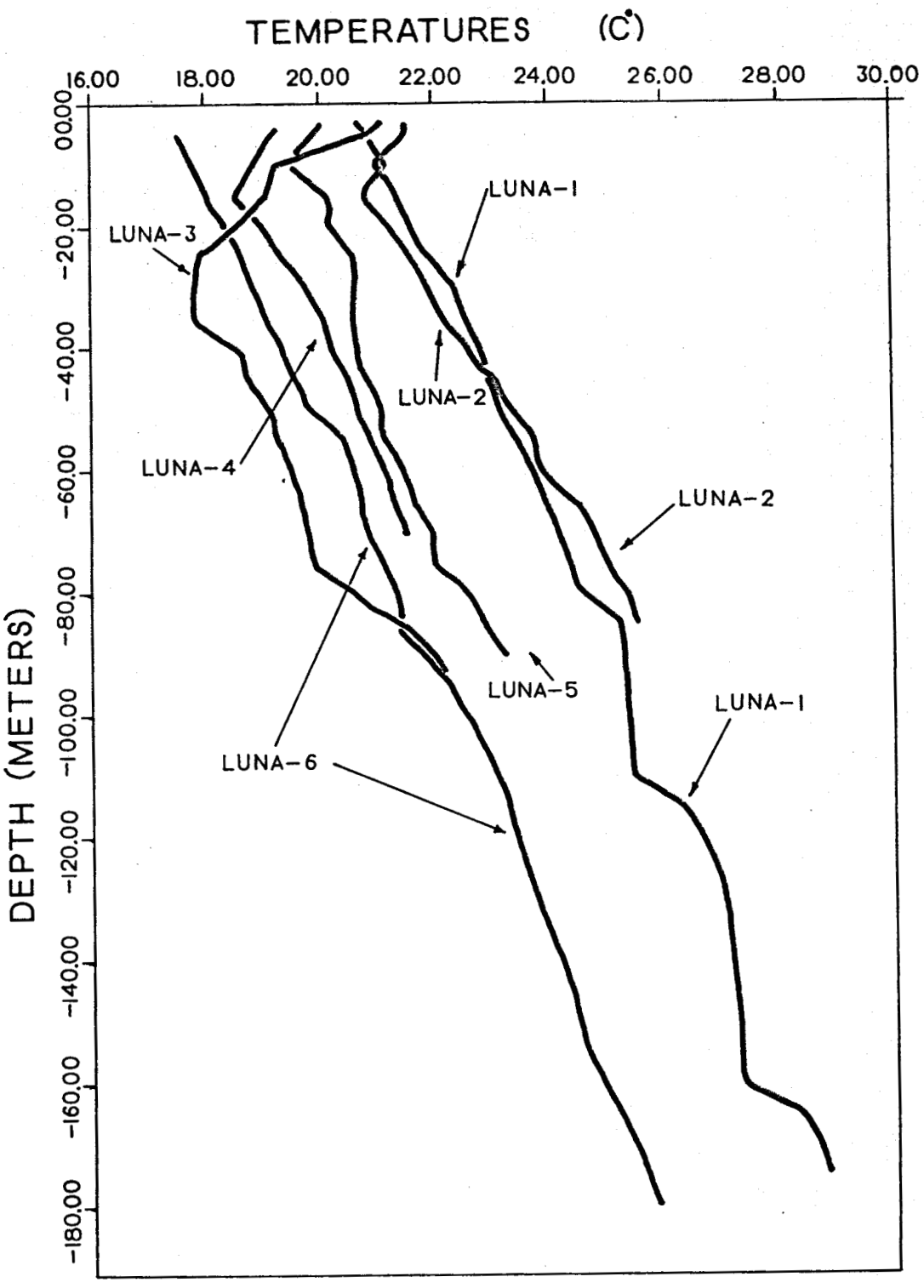

Figure 5-17. Temperature profiles of wells logged in southeast Luna County.

characteristically located in permeable aquifers and because induced recharge is caused by pumping, lateral groundwater flow is expected in these areas. Wells Luna-1 and Luna-2 do not seem to be disturbed by groundwater flow, although Luna-1 appears to have a grouting problem (i.e., communication of groundwater between aquifers outside the non-cemented casings). Neither of these two wells are located in an irrigation area.

Temperature gradients, the depth intervals over which the gradients were calculated, estimated thermal conductivities, and best-guess heat-flow values from above the water table are given in Table 5-8 along with the well locations. Depth intervals were based on depth to water table estimates and apparent breaks in the linearity of the temperature gradients due to lithologic variations.

Depths to the water table shown in Table 5-7 could be in error since it is not known whether the head in the well is the water table or a deeper confined aquifer under a slightly higher or lower head. Generally the wells are cased and screened in such a manner that the head in the well is the same or very nearly the same as the water table. Also, characteristically the near-surface aquifers near the center of the basins throughout this region are not subject to very significant confining pressures.

The temperature gradient and estimated thermal conductivity were used to estimate the heat flow. The values range from abnormally low values of 48 mWm^{-2} and 74 mWm^{-2} (1.2 HFU and 1.8 HFU, respectively) for Luna-3 and Luna-5 to values representative of the modal class (2.4 to 3.6 HFU) for the region (see Chapter 5, Part 1), namely, 105 mWm^{-2} (2.5 HFU) for Luna-1 and 132 mWm^{-2} (3.1 HFU) for Luna-2. An average temperature gradient was used for Luna-1 and the 15 to 30 meter section of Luna-4 was disregarded due to suspected groundwater disturbance. Because of the similiarity in lithologies between

Table 5-8. Locations and heat-flow values for temperature-logged wells in southeast Luna County.

Well Name	Geographical Location	Estimated Thermal Conductivity ($Wm^{-1}K^{-1}$)	Interval (m)	Temperature Gradient (°C/km)	Best Guess Heat Flow Above Water Table (mWm^{-2})
Luna-1	28S.5W.12.123	1.9	10 - 30	65 ± 1.0	105 (2.5 HFU)
		1.9	30 - 80	45 ± 1.0	
	107°18.5' 31°51.8'	3.1	85 - 175	39 ± 1.0	
Luna-2	27S.5W.36.313	1.9	15 - 85	69 ± 1.0	131 (3.1 HFU)
	107°20.5' 31°54.8				
Luna-3	29S.10W.12.244	1.9		25*	48 (1.2 HFU)
	107°48.7' 31°49.5'				
Luna-4	28S.10W.21.124	1.9	15 - 30	83 ± 1.0	82 (2.0 HFU)
	107°52.3' 31°51.7'	1.9	35 - 70	43 ± 1.0	
Luna-5	27S.8W.35.124	1.9	15 - 90	39 ± 1.0	74 (1.8 HFU)
	107°38.4' 31°55.1'				
Luna-6	28S.7W.6.133	1.9	20 - 50	48 ± 1.0	91 (2.2 HFU)
	107°36.2' 31°54.2'	3.1	55 - 185	44 ± 1.0	

*Bottom-hole temperature gradient taken from Table 5-7.

Luna County and Dona Ana County, and because accurate values for thermal conductivities were not available, the values used for Luna County are the averages of the values used for Dona Ana County (see Chapter 5, Part 1). Heat-flow values were calculated for both above and below the water table. The error in these values is probably greater than 20 percent and is attributed mostly to the uncertainty in thermal-conductivity values.

Chapter 6

Active Fault Analysis and Radiometric Dating of Young Basalts in Southern New Mexico*

Introduction

The two major objectives of the work summarized here were: (1) to compile a map showing the location of all known faults in southcentral New Mexico which have been active within the last 0.4 m.y.; and (2) to determine by radiometric dating the age of 15 basaltic volcanic rocks in four areas with geothermal potential. This work was conducted during the summer of 1979.

Active Faults

Figure 6-1 shows the location of all known faults in southcentral New Mexico which have been active within the last 0.4 m.y. This map was compiled from (1) unpublished field studies made by the senior investigator over the last fourteen years, (2) published data, and (3) field work and aerial photo studies completed in 1979.

Dating of the faults is based on determination of the age of the youngest geomorphic surfaces displaced by the faults. The surfaces have been dated by means of soil studies, radiocarbon dating of caliche, and K/Ar dating of volcanic ash associated with the surfaces (e.g., Hawley et al. 1976; Gile and Hawley 1968; Seager and Hawley 1973; Hawley 1978). All of the faults mapped displace surfaces at least as young as 0.4 m.y. and some, such as the Organ Mountains fault along the eastern side of that range, have been active within

*The principal authors of Chapter 6 are Dr. William R. Seager, Professor of Earth Sciences, New Mexico State University, Muhammad Shafiquallah, Research Associate, Department of Geosciences, University of Arizona, and Dr. Russell E. Clemons, Professor of Earth Sciences, New Mexico State University.

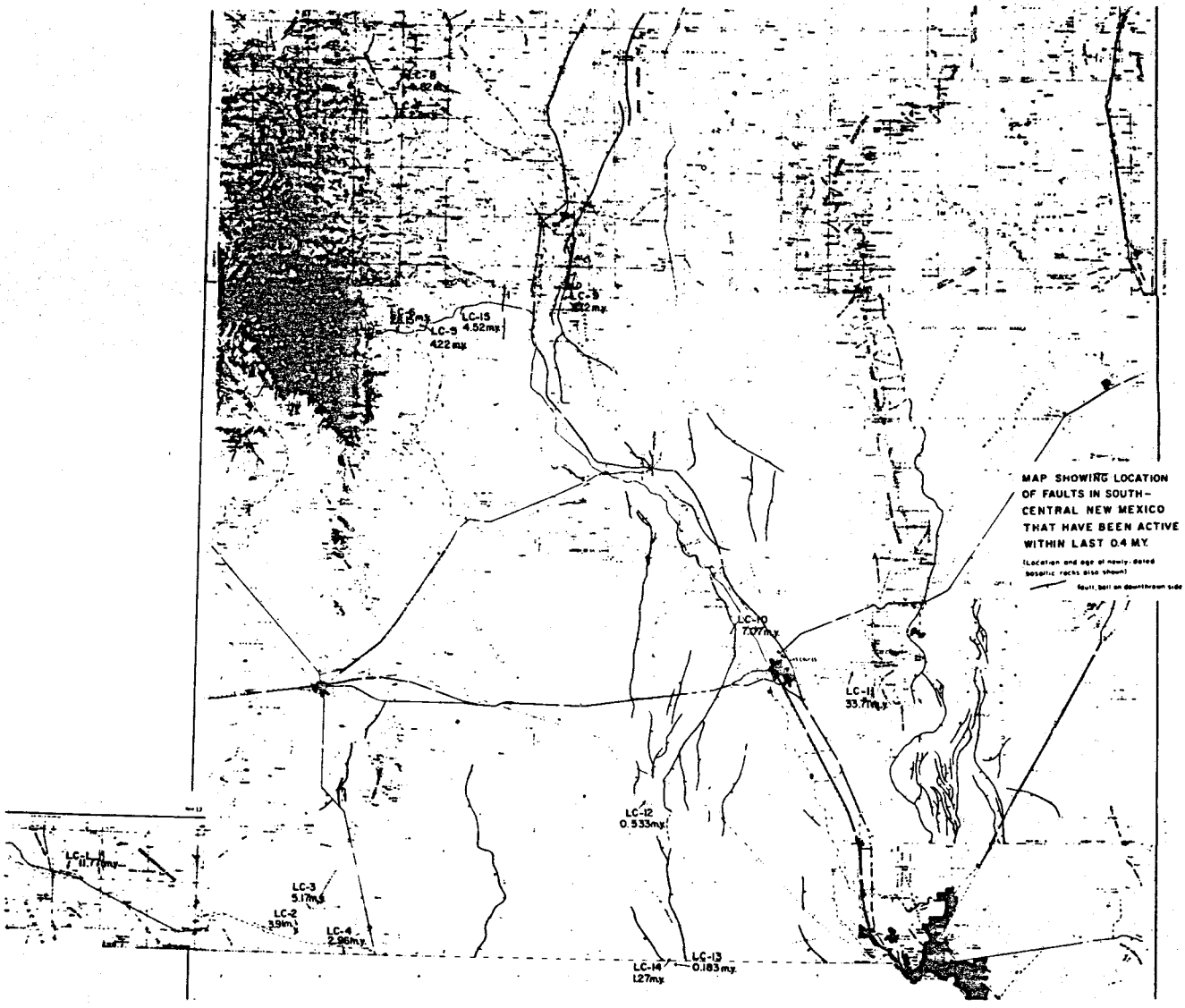

Figure 6-1. Map showing the location of faults in southcentral New Mexico that may have been active within the last 0.4 m.y.

the last 4,000 years (L. Gile, personal communication 1979). The highest density of young faults in the mapped region is in the southern Tularosa Basin and the west mesa, located southwest of Las Cruces between the Potrillo Maar and Interstate 10. Major active faults also exist in the Truth or Consequences area and along the western side of the Florida Mountains southeast of Deming. The southern Tularosa Basin, the Las Cruces west mesa (especially the Kilbourne Hole-Aden Crater region), and the Truth or Consequences area have been investigated as sites of known or potential geothermal activity. It seems likely that circulation of groundwaters in these areas is controlled to a large extent by permeable, fractured rock on or adjacent to recently active fault systems.

Age and Mineralogy of Fifteen Basalts in Southcentral New Mexico

Fifteen basaltic rocks were selected to date by the K/Ar method and 14 of these were analyzed for their mineralogical composition. The samples were selected from four areas of known or suspected geothermal potential: (1) the eastern Potrillo Mountains, including the Aden Volcano-Kilbourne Hole-Potrillo Maar area, (2) the Columbus-Hachita area, (3) the Truth or Consequences-Winston area, and (4) the eastern Black Range area. The present result of dating and the location of samples is shown on the fault map to be published as part of the New Mexico Scientific Geothermal Resource Map.

The objective in obtaining these dates was to determine whether the basaltic lavas and volcanoes in the four areas were young enough to be associated with magmatic heat sources at depth. Volcanoes in the Columbus area appear to be about three to five m.y. old and volcanic rocks in the Truth or Consequences area also range from about three to five m.y. Basalts at Aden Crater, however, are about 0.5 m.y. and the 180,000 year date at Potrillo Maar

shows that it along with Hunt's and Kilbourne holes are the youngest volcanic features in the region. These features clearly could be associated with modern magmatic heat sources at shallow depth as in the Socorro, New Mexico, area.

Whether volcanoes three to five m.y. old still have hot bodies of rock beneath them is uncertain. If the magmas moved directly to the surface from a mantle source as suggested by xenolith studies at Kilbourne Hole (Padovani and Carter 1977), then little associated heat will remain in the shallow crust. However, if the magma accumulated within a shallow chamber, say less than 10 km beneath the surface, it will probably still be contributing heat to geothermal systems above it. This condition appears to be the origin of geothermal waters in the Socorro area (Chapin et al. 1978).

Mineralogical studies were done in order to help classify the basalts. This classification is important because it allows one to judge whether the magmas are related to the Rio Grande Rift volcano-tectonic structure or to an earlier or unrelated episode of magmatic activity. Most of the geothermal waters in New Mexico are being heated within the Rio Grande Rift; the rift is the primary thermal engine for geothermal waters in the state. As far as their mineralogy is concerned, all of the basalts are typical of rift basalts except 79-125, 79-124, and possibly 79-119. The two former basalts (79-125 and 79-124) are calc-alkaline basalts typical of early rift or back-arc basalts reported from several places along the rift.

Table 6-1 shows the detailed locations and ages of the basaltic rocks sampled. Table 6-2 describes the petrographic characteristics of the basaltic rock samples.

Table 6-1. Locations and ages of basaltic rocks sampled from southcentral New Mexico.

Sample No.	LC-1(79WS12) 79-119	LC-2(79WS13) 79-120	LC-3(79WS14) 79-121	LC-4(79WS16) 79-122	LC-5(79WS16) 79-123	LC-6(79WS17) 79-124
Location	S½,SE¼, Sec 29 T.27S, R.14W Hachita, NM 31°55.4'N.Lat 108°17.16'W.Long	NW¼, Sec 6 T.29S, R.9W Palomas Field, NM 31°49.04'N.Lat 107°48.07'W.Long	NE¼,NW¼, Sec 21 T.28S., R.9W Black Top Mt., NM 31°51.71'N.Lat 107°46.10'W.Long	SW¼,NE¼, Sec 18 T.29S., R.8W Palomas Field at Mexico border, NM 31°47.15'N.Lat 107°41.67'W.Long	SE¼, Sec 9 T.16S., R.7W Hillsboro Mesa, NM 32°55.97'N.Lat 107°34.13'W.Long	E½, Sec 3 T.16S, R.7½W Percha Narrows, NM 32°55.04'N.Lat 107°36.55'W.Long
Age	11.77±0.26 m.y.	3.91±0.18 m.y.	5.17±0.11 m.y.	2.96±0.07 m.y.	4.22±0.01 m.y.	28.13±0.6 m.y.
Sample No.	LC-7(79WS18) 79-125	LC-8(79WS19) 79-126	LC-9(79WS20) 79-127	LC-10(79WS21) 79-128	LC-11(79WS22) 79-129	LC-12(79WS23) 79-130
Location	NW¼,SW¼, Sec 14 T.11S, R.8W Winston, NM 33°20.96'N.Lat 107°38.45'W.Long	NW¼,SE¼, Sec 12 T.11S, R.8W Table Top Mt., NM 32°21.82'N.Lat 107°37.12'W.Long	NW¼,SE¼, Sec 21 T.15S, R.4W Caballo Mt., NM 32°59.25'N.Lat 107°15.00'W.Long	SW¼,NE¼, Sec 19 T.22S., R1E Robledo Mts., NM 32°22.95'N.Lat 106°52.88'W.Long	SW¼,SE¼, Sec 15 T.23S., R3E Organ Mts., NM 32°18.42'N.Lat 106°37.24'W.Long	SW¼,SW¼, Sec 4 T.26S., R.2W Aden Crater, NM 32°04.21'N.Lat 107°03.28'W.Long
Age	18.27±0.5 m.y.	4.81±0.08 m.y.	3.12±0.08 m.y.	7.07±0.15 m.y.	33.65±0.71 m.y.	0.533±0.04 m.y.
Sample No.	LC-13(79WS24) 79-131	LC-14(79WS25) 79-132	LC-15 79-139			
Location	Potrillo Maar central cinder and lava, Chihuahua, Mexico 31°46.51'N.Lat 106°59.87'W.Long	T.29S, R.2W Potrillo Maar, NM 31°47.52'N.Lat 106°59.91'W.Long	NW¼,NW¼, Sec 33 T.15S., R.6W NM Highway 90, east of Hillsboro 32°57.31'N.Lat 107°27.32'W.Long			
Age	0.183±0.03 m.y.	1.23±0.06 m.y.	4.52±0.1 m.y.			

Table 6-2. Petrographic descriptions of "basalt" thin sections

79-119=79WS12: Hachita Mesa finger flow

Olivine basalt, or basaltic andesite

Microphenocrysts of olivine (0.3 to 1.4 mm) occur in a groundmass of plagioclase, pale-brown augite, olivine, and opaques ranging in size from 0.5 to 0.3 mm. The groundmass is subophitic to inter-granular and microvesicular. The augite is probably titaniferous as suggested by the pale-brown color. Plagioclase ranges from andesine to labradorite (Anorthite45 to 55). Bright reddish material iddingsite (?) occurs around the borders and along fractures of the olivine. Minor carbonate occurs in irregular patches.

79-120=79WS13: Cinder cone flow, outlier of Palomas field, west of Columbus

Olivine basalt

Olivine (0.2 to 4.0 mm) and minor hypersthene (0.2 to 0.7 mm) and augite (0.2 to 1.0 mm) microphenocrysts occur in an intergranular matrix of plagioclase, pyroxene, olivine, and abundant opaques. The plagioclase laths (0.55 to 0.2 mm) are labradorite. A few corroded, angular fragments of more sodic plagioclase are probably xenocrysts.

79-121=79WS14: Black Top Mesa, southwest corner Tres Hermanas Mountains

Olivine basalt

Phenocrysts of plagioclase (0.5 to 2.1 mm) and microphenocrysts of olivine (0.2 to 0.6 mm) and pyroxene (0.2 to 0.8 mm) occur in an intergranular groundmass of plagioclase, pyroxene, olivine, and abundant opaques. The pyroxene phenocrysts are predominantly hypersthene whereas the groundmass pyroxene appears to be mostly clinophyroxene. The plagioclase phenocrysts are zoned and most have corroded margins. They are probably xenocrysts as suggested by their more sodic composition (Anorthite40) whereas the aligned, blocky, groundmass laths are laboradorite (Anorthite65).

Table 6-2. (continued).

79-122=79WS15: Flow near Mexico-New Mexico border, north edge of Palomas field

Olivine basalt

Microphenocrysts of olivine (0.2 to 1.0 mm) and pyroxene (0.2 to 0.8 mm) occur in an intergranular matrix of plagioclase, pyroxene, olivine, and abundant opaques. The plagioclase laths (0.2 mm long) are sodic labradorite. One xenocryst of quartz (1.4 mm) has corroded borders with prominent reaction corona.

79-123=79WS16: Basalt capping mesa, north of Hillsboro

Olivine-bearing basaltic andesite

Microphenocrysts of olivine (0.2 to 0.8 mm) and minor augite (0.2 to 0.4 mm) occur in a slightly vesicular, intergranular to pilotaxitic ground-mass of plagioclase laths, olivine, pyroxene, and abundant opaque grains. Much of the olivine is altered to iddingsite. The plagioclase laths are andesine and vary in length from 0.5 to 1.0 mm; the larger ones are zoned, ranging from An40 to An50. Some of the microvesicles are filled with carbonate.

79-124=79WS17: Narrows of Percha Canyon, west of Hillsboro

Pyroxene andesite

Sparse microphenocrysts of plagioclase (0.4 to 1.3 mm), augite (0.1 to 0.3 mm) and pyroxene (?) replaced by chloride and serpentine (0.3 to 0.8 mm) occur in a pilotaxitic groundmass consisting of dominant plagioclase laths and lesser amounts of pyroxene and opaque microlites. Plagioclase phenocrysts are sodic labradorite and the groundmass plagio-clase is calcic andesine. Several quartz xeno-crysts with thick coronas of pyroxene grains are present.

79-125=79WS18: Beneath Santa Fe Group, east of Winston

Pyroxene andesite

Sparse plagioclase microphenocrysts (0.5 to 1.5 mm) occur in a pilotaxitic matrix of andesine laths, pyroxene, and opaques. Abundant bright-red, translucent microlites (0.01 to 0.04 mm) also are part of the groundmass. Carbonate partially replaces some of the plagioclase phenocrysts and also fills most of the vesicles.

Table 6-2. (continued).

79-126=79WS19: Table Top Mountain, above Santa Fe Group, east of Winston

Olivine basalt (as determined by labradorite extinction angles) Olivine basaltic andesite (by chemical analysis)

Abundant olivine (0.3 to 2.0 mm) and sparse plagioclase (0.7 to 3.0 mm) phenocrysts occur in a micro-vesicular, intergranular matrix of plagioclase (0.03 to 0.3 mm), pyroxene, olivine, and abundant opaque grains. Plagioclase phenocrysts are corroded, embayed, and partially replaced by carbonate. They may be xenocrysts. Olivine is mostly fresh but some phenocrysts have thin red rims and are altered to iddingsite along fractures. All the microvesicles are filled with carbonate.

79-127=79WS20: Along Caballo Fault

Olivine basalt

Abundant olivine (0.4 to 2.0 mm) and sparse hypersthene (0.4 to 2.0 mm) phenocrysts occur in a groundmass of plagioclase, olivine, pyroxene, and opaques. The groundmass is vesicular and inter-granular to pilotaxitic. Thin iddingsite rims many of the olivine phenocrysts and olivine (?) in the groundmass is largely replaced by iddingsite. The narrow plagioclase laths (0.05 to 0.15 mm) are labradorite. A few vesicles are partly filled with carbonate.

79-128=79WS21: Robledo plug

Olivine basalt or olivine basaltic andesite melilite basanite

Anhedral to subhedral olivine microphenocrysts (0.1 to 0.4 mm), opaque-rich xenocrysts(?) (0.3 to 4.0 mm), and sparse plagioclase xenocrysts (?) occur in a "dirty" matrix of olivine, pyroxene, plagioclase, opaques, and glass. Several small (0.2 to 0.7 mm), anhedral, gray phenocrysts filled with rod-shaped inclusions may be melilite. The groundmass is generally intergranular, ranging to intersertal in places. Plagioclase laths are sodic labradorite to calcic andesine.

Table 6-2. (continued).

79-129=79WS22: West side of Organ Mountains

Dacite

Oligoclase (0.3 to 3.5 mm), biotite (0.3 to 0.7 mm), and hornblende (0.5 to 1.5 mm) phenocrysts occur in a reddish-brown groundmass of glass, sparse plagioclase microlites, and curved brown flakes. Oligoclase is replaced by kaolin(?) in patches, veins along fractures, and along cleavage planes. Some biotite is fresh appearing and some biotite and the hornblende is oxidized. One augite phenocrysts (0.4 mm) is present. Flow banding is prominantly displayed around the phenocryst.

79-130=79WS23: Aden Crater lava lake

Olivine basalt or olivine basaltic andesite

Microphenocrysts or olivine (0.3 to 1.5 mm) and plagioclase (0.3 to 0.5 mm) occur in a very vesicular, intersertal to subophitic groundmass. The groundmass is composed of brown glass with abundant translucent brown microlites, pyroxene, plagioclase, olivine, and opaques. Plagioclase phenocrysts are zoned labradorite whereas the groundmass laths range from sodic labradorite to calcic andesine. Very little alteration is present.

79-131=79WS24: Cone flow, center of Potrillo Maar

Olivine basalt

Microphenocrysts of olivine (0.3 to 1.5 mm), minor plagioclase (0.5 to 1.2 mm) and pyroxene occur in a groundmass of mostly pyroxene and plagioclase with lesser amounts of opaques, glass, and olivine. Glomerporphyritic aggregates of olivine are common. The groundmass is vesicular and inter-sertal to intergranular. The glass contains abundant brown translucent rod-shaped microlites. Plagioclase is calcic labradorite, present as subparallel-aligned, euhedral to subhedral laths.

79-132=79WS25: Northwest edge of Potrillo Maar

Olivine basalt

Subhedral microphenocrysts of olivine (0.5 to 1.8 mm) occur in a vesicular, intersertal groundmass of mostly pale-brownish pyroxene and slender plagioclase laths with lesser amounts of opaques and olivine. Minor patches of intersitial brownish glass containing rod-shaped microlites are present. Several xenocrysts of quartz and feldspar are present and have been deeply corroded.

Acknowledgements

All dates were obtained by M. Shafiqullah at the University of Arizona Geochronology Laboratory. R. E. Clemons described the petrography of the basalts. We also want to acknowledge the NSF grant EAR-78-11535 to Paul E. Damon and M. Shafiqullah since it supported part of this study.

References

Chapin, C. E., Chamberlin, R. M., Osburn, G. R., Sanford, A. R., and White, D. W., 1978, Exploration framework of the Socorro geothermal area, New Mexico: New Mexico Geological Society, Special Publication 7, p. 115.

Gile, L. H., 1979, Personal communication, Soil Conservation Service, Las Cruces, New Mexico.

Gile, L. H. and Hawley, V. W., 1968, Age and comparative development of desert soils at the Gardner Spring radiocarbon site, New Mexico: Soil Scientific Society American, Proceedings, v. 32, p. 709-716.

Hawley, J. W., 1978, Guidebook to the Rio Grande Rift: New Mexico Bureau Mines and Mineral Resources, Circular 163, 241 pp.

Hawley, J. W., Bachman, G. O., and Manley, K., 1976, Quaternary stratigraphy in the Basin and Range and Great Plains provinces, New Mexico and western Texas, in Quaternary stratigraphy of North America: Dowden, Hutchinson and Ross, Stroudsburg, Pennsylvania, p. 235-274.

Seager, W. R. and Hawley, J. W., 1973, Geology of Rincon quadrangle, New Mexico: New Mexico Bureau Mines and Mineral Resources, Bulletin 101, 42 pp.

Padovani, E. R. and Carter, J. L., 1977, Aspects of the deep crustal evolution beneath south central New Mexico, in The Earth's Crust: American Geophysical Union, Washington, D.C., Geophysical Monograph 20, 754 pp.

Chapter 7

Evaluation of the Geothermal Potential of the San Juan Basin in Northwestern New Mexico*

Introduction

The San Juan Basin is a relatively stable and less deformed geological region in northwest New Mexico. It is situated in the eastern part of the Colorado Plateau physiographic province and is surrounded by several uplifts, arches, monoclines, and thrusts. Figure 7-1 shows the boundary of the San Juan Basin in relation to other regional geologic features. Because of the structural stability, lack of geothermal manifestation on the surface, and relatively low heat-flow values calculated from limited observations, the geothermal potential of the San Juan Basin area has generally been regarded as low or even non-existent.

A systematic evaluation of the geothermal potential of the San Juan Basin has been undertaken to fill the existing gap in the data. This chapter summarizes the results of the first stage of this study. The San Juan Basin contains several producing horizons of oil and gas. A large number of exploratory and producing wells have, therefore, been drilled in this area during the past seventy years. Well logs and bottom-hole temperatures recorded during logging are available for most of the wells drilled. Bottom-hole temperature data were collected for 12,243 of these wells and analyzed to determine the areas of high geothermal potential.

*The principal author of Chapter 7 is Dr. Lokesh Chaturvedi, Associate Professor of Earth Sciences and Civil Engineering, New Mexico State University.

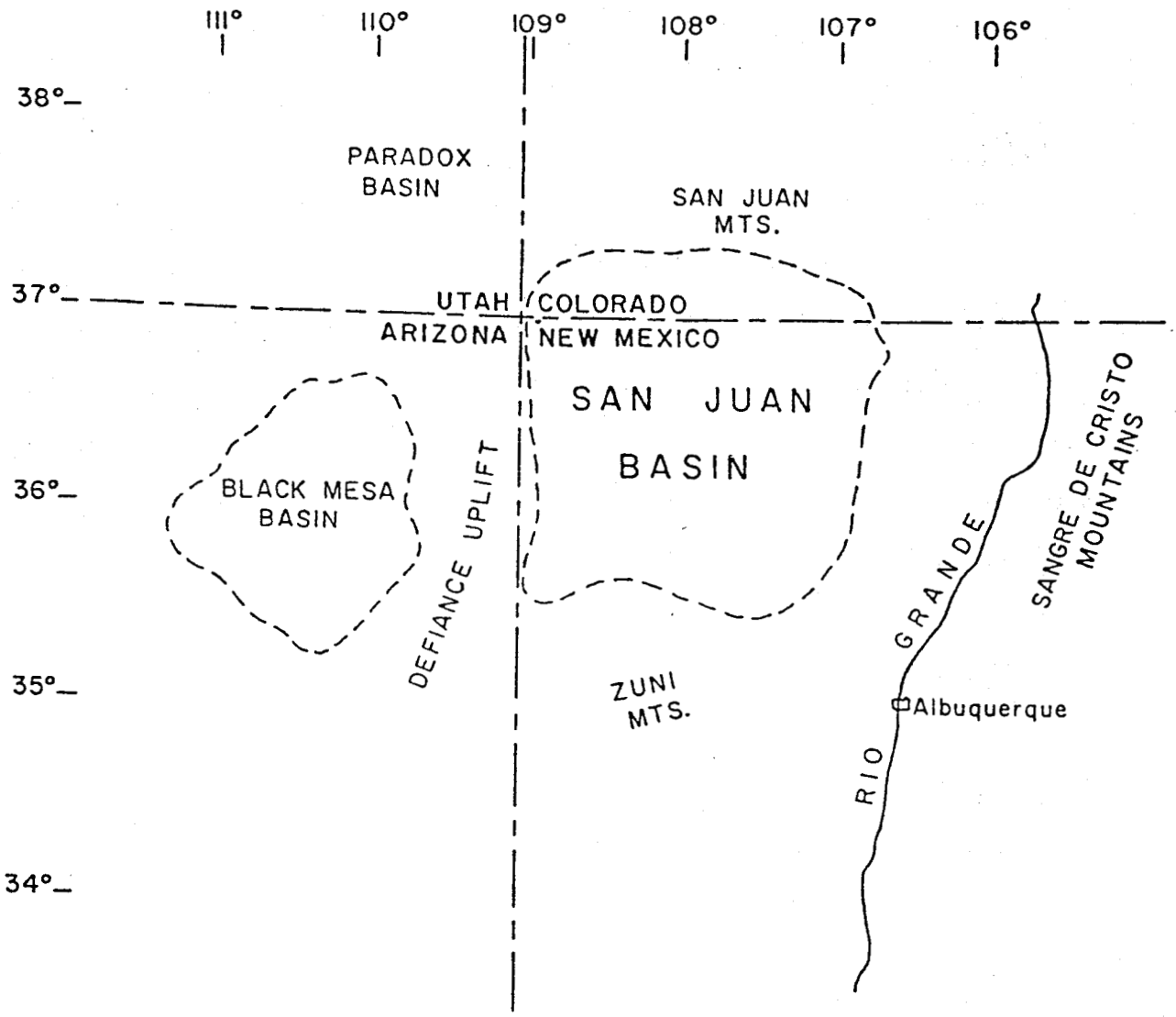

Figure 7-1. Location of San Juan Basin with respect to surrounding physiographic features.

Geologic Setting

The central part of the basin is covered by continental sediments of Late Cretaceous or Tertiary age. These sediments are surrounded by marine and continental formations of Cretaceous age. Paleozoic and Mesozoic formations are found along the rim of the basin. The total thickness of the sedimentary rocks in the center of the basin ranges from 10,000 to 15,000 feet. The central part of the basin is broadly downwarped. Defiance and Zuni uplifts flank the basin to the west and south, respectively. The Nacimiento Uplift to the east, the Galliana-Archuleta Arch to the northeast, and the Hogback Monocline to the north, flank the San Juan Basin. Oil and gas is located in domal, faulted, and stratigraphic traps in the basin.

Bottom-Hole Temperatures

There has been some concern about using bottom-hole temperature readings to estimate the correct formation temperature at depth and to use these values to estimate the approximate thermal gradients. However, the results obtained by Jaeger (1961), Schoeppel and Gillaranz (1966), Tanner (1976), and Hodge et al. (1979) have shown that bottom-hole temperatures may be used as reliable data to estimate the regional variations in temperature gradients. These data have been used to outline the areas of anomalous geothermal gradients and, therefore, areas of high geothermal potential in the San Juan Basin.

The temperature gradient for each location was calculated by using the bottom-hole temperature at a given depth obtained from the well log, minus the estimated surface temperature, divided by the well depth. The mean air temperature for northwest New Mexico is reported to be 12°C. However, in

order to keep the computed gradient values on the conservative side, a value of 15°C was used for the surface temperature.

The calculated gradients from 12,243 wells, ranging in depth from 113 m to 2300 m yield a low value of 15°C/km and a high value of 110°C/km. Approximately 0.5 percent of the wells show temperatures which result in a gradient of 15°C/km, which may be caused by unusual depths of flow of cold groundwater or by inaccurate data. More than 95 percent of the wells recorded have a total depth greater than 500 m. The data from shallower wells were used in the analysis, especially since several of these have an obviously anomalous recorded temperature. These wells can be easily used to confirm the accuracy of the data. The average gradient computed from the entire data set is 26.9°C/km.

Figure 7-2 shows the locations (to the nearest quarter township) of the wells where the bottom-hole temperature data were recorded. Figure 7-3 shows the locations of all wells with computed gradients more than 45°C/km. This value was arbitrarily chosen to represent more than 1.5 times the average computed gradient. Figure 7-4 shows the locations of wells with computed gradients more than 50°C/km. Seven wells show computed gradients which are over 90°C/km.

Conclusions

The use of bottom-hole temperatures to locate the areas of geothermal potential is an inexpensive and time-saving technique which appears to work for reconnaissance of large areas. It is especially useful in areas where a large number of well-log records are available. In northwest New Mexico, the area around Shiprock appears to have the highest geothermal potential. Several relatively shallow wells in this area (300 to 600 m deep) have a

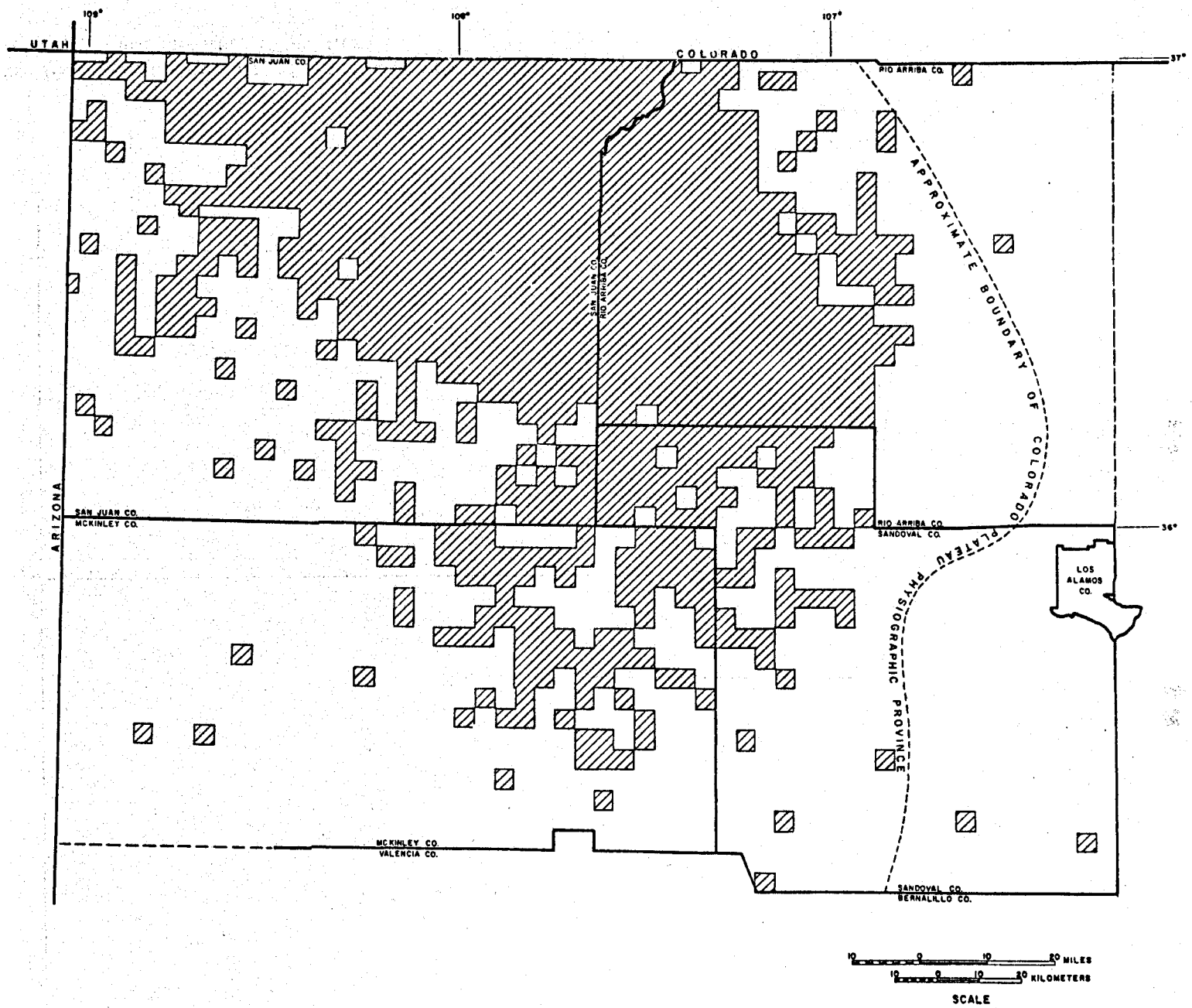

Figure 7-2. Locations (to the nearest quarter township) of oil and gas wells where bottom-hole temperatures were recorded in northwestern New Mexico.

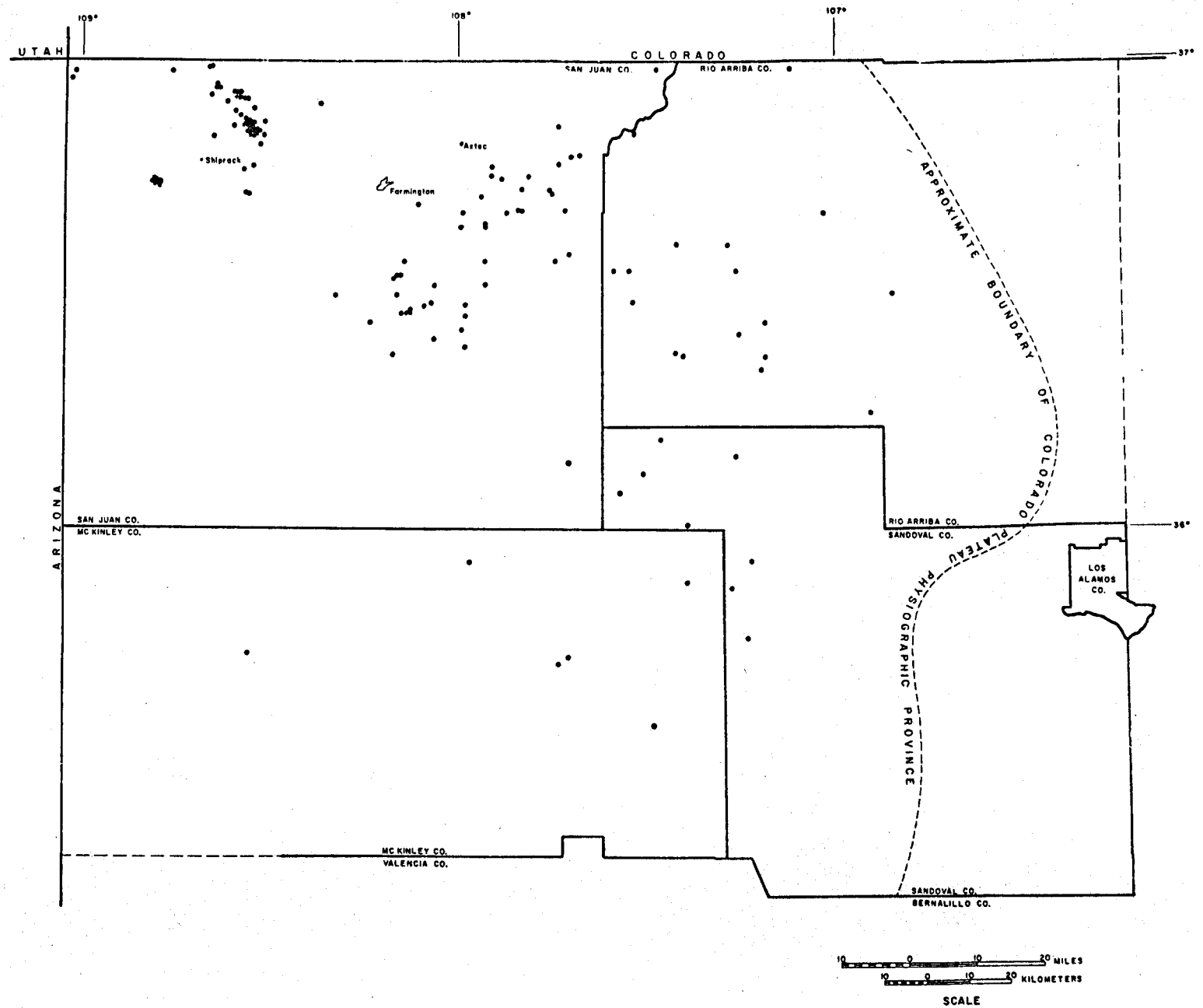

Figure 7-3. Locations of oil and gas wells with computed gradients greater than 45°C/km in northwestern New Mexico.

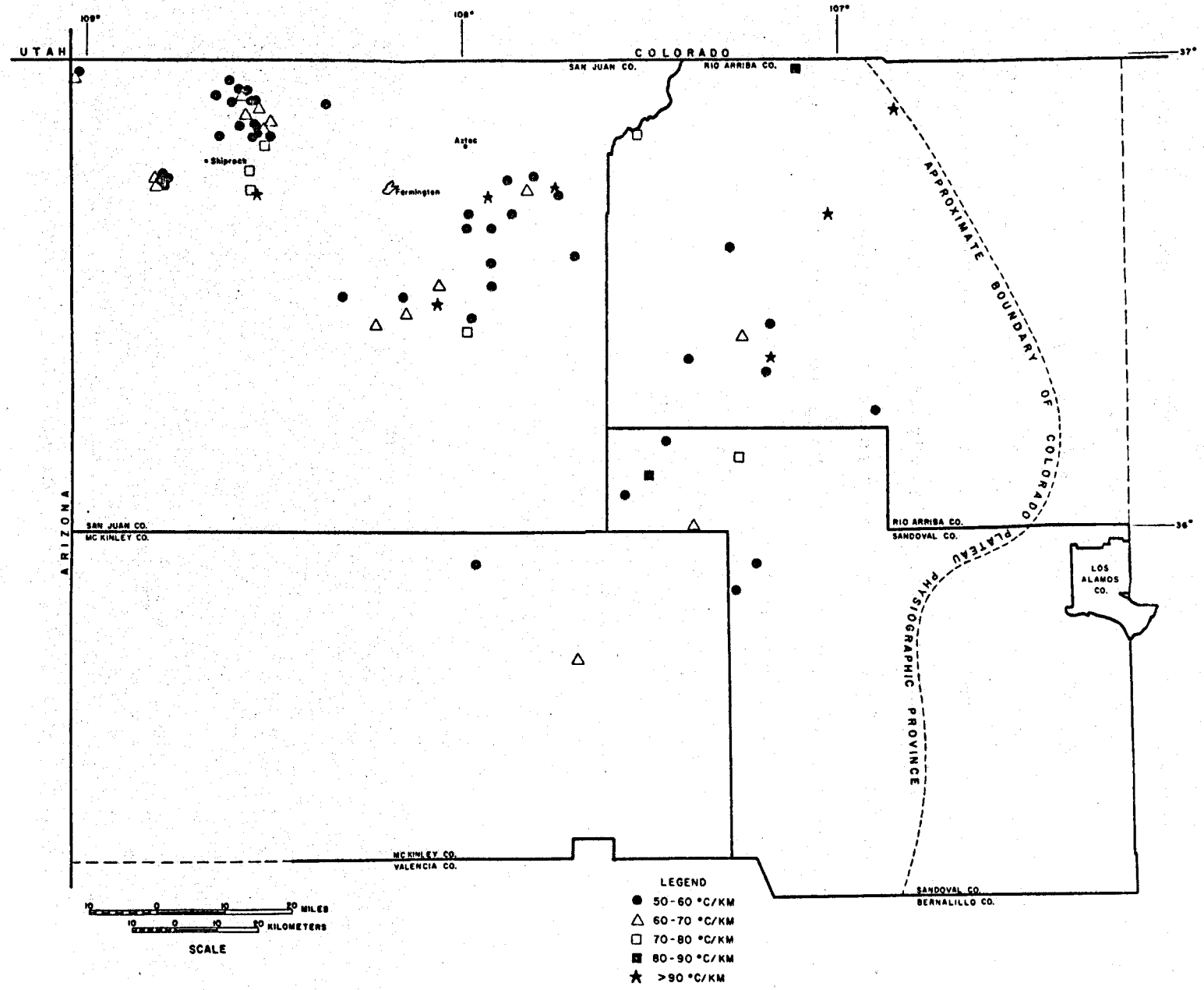

Figure 7-4. Northwestern New Mexico locations of oil and gas wells with computed gradients greater than 50°C/km.

recorded bottom-hole temperature ranging from 32°C to 55°C. There are a number of outcrops of igneous intrusives of Tertiary age in this area besides the famous Shiprock. It is conceivable that the anomalous recorded temperatures are related to this igneous activity.

The center of the basin, located 10 to 20 miles south and southeast of the Farmington-Aztec area, shows a number of computed anomalous gradient locations. Similarly, a number of wells in Rio Arriba and Sandoval counties and some in McKinley County show significantly anomalous temperatures (see Figures 7-3 and 7-4). Field checking of these wells, correlation with the detailed geologic setting, and the geohydrologic assessment of these areas will form the contents of future studies.

References

Hodge, D. S., Hilfiker, K., Morgan, P., and Swanberg, C. A., 1979, Preliminary geothermal investigations in New York: Geothermal Resources Council, Transactions, v. 3, p. 317-320.

Jaeger, J. C., 1961, The effect of the drilling fluid on temperatures measured in bore holes: Journal of Geophysical Research, v. 66, p. 563-569.

Schoeppel, R. J., and Gillaranz, S., 1966, Use of well-log temperatures to evaluate regional geothermal gradients: Journal of Petroleum Technology, June 1966, p. 667-673.

Tanner, W. F., 1976, Geothermal exploration from deep-well data: Gulf Coast Association of Geological Societies, Transactions, v. 26, p. 65-68.